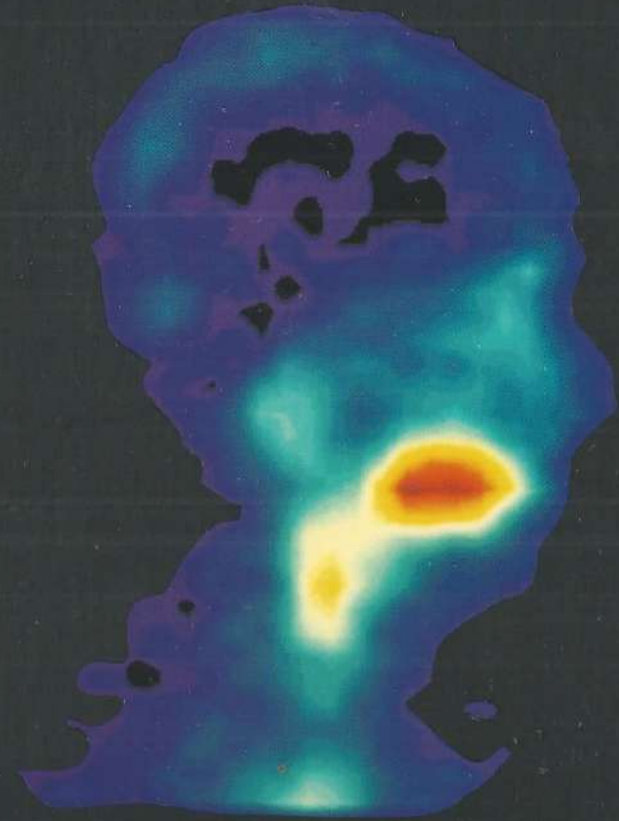


**CLINICAL TARGETING OF  
HEAD AND NECK CANCER WITH  
RADIOLABELED MONOCLONAL ANTIBODIES**



**Remco de Bree**

CLINICAL TARGETING OF HEAD AND NECK CANCER WITH RADIO-LABELED MONOCLONAL ANTIBODIES

Remco de Bree

**CLINICAL TARGETING OF  
HEAD AND NECK CANCER WITH  
RADIOLABELED MONOCLONAL ANTIBODIES**

**Remco de Bree**

VRIJE UNIVERSITEIT

**CLINICAL TARGETING OF HEAD AND NECK CANCER WITH  
RADIOLABELED MONOCLONAL ANTIBODIES**

ACADEMISCH PROEFSCHRIFT

ter verkrijging van de graad van doctor aan  
de Vrije Universiteit te Amsterdam  
op gezag van de rector magnificus  
prof.dr E. Boeker,  
in het openbaar te verdedigen  
ten overstaan van de promotiecommissie  
van de faculteit der geneeskunde  
op vrijdag 16 juni 1995 te 13.45 uur  
in het hoofdgebouw van de universiteit,  
De Boelelaan 1105

door

Remco de Bree

geboren te Utrecht

This thesis was sponsored by: Astra Pharmaceuticals BV, Electro Medical Instruments BV, Entarmed BV, GN Danavox Nederland BV, Mallinckrodt Medical BV, Pfizer BV Barlett Divisie producent van o.a. Zithromax, Roussel BV, Sopha Medical BV, Johan Vermeij Stichting.

Promotor: prof.dr G.B. Snow

Copromotoren: dr G.A.M.S. van Dongen  
dr J.C. Roos

Referent: prof.dr E.K.J. Pauwels

*Aan mijn ouders*



## CONTENTS

Chapter 1.	General introduction	9
Part A.	Squamous cell carcinoma of the head and neck	11
Part B.	Monoclonal antibodies for tumor targeting	25
Part C.	Aim of the study	36
Addendum.	Remarks om analysis of data	38
Chapter 2.	Clinical imaging of head and neck cancer with $^{99m}\text{Tc}$ -labeled monoclonal antibody E48 IgG or F(ab') <sub>2</sub>	39
Chapter 3.	Biodistribution of radiolabeled monoclonal antibody E48 IgG and F(ab') <sub>2</sub> in patients with head and neck cancer	55
Chapter 4.	Clinical screening of monoclonal antibodies 323/A3, cSF-25, and K928 for suitability of targeting tumors in the upper aerodigestive and respiratory tract	73
Chapter 5.	Radioimmunosintigraphy and biodistribution of $^{99m}\text{Tc}$ -labeled monoclonal antibody U36 in patients with head and neck cancer	93
Chapter 6.	Selection of monoclonal antibody E48 IgG or U36 IgG for adjuvant therapy in head and neck cancer patients	109
Chapter 7.	Summary	131
Chapter 8.	Samenvatting	135
	Dankwoord	139
	Curriculum vitae	141

---

## Chapter 1

### General Introduction

## PART A. SQUAMOUS CELL CARCINOMA OF THE HEAD AND NECK

Head and neck cancer traditionally refers to malignant tumors that arise in the mucosa of the upper aerodigestive tract including the oral cavity, pharynx, larynx, nasal cavity, and paranasal sinuses (Fig. 1). More than 90% of these tumors are squamous cell carcinomas (SCC) <sup>1</sup>. Malignant tumors arising in adjacent structures including the salivary glands, thyroid gland, soft tissues, and bone are relatively infrequent.

### I. Epidemiology

Squamous cell carcinoma of the head and neck (HNSCC) is a disease predominantly of males and has a peak incidence in the seventh decade of life. World-wide, more than 500,000 new cases are projected annually, and this incidence is rising <sup>2,3</sup>. HNSCC accounts for approximately 5% of all newly diagnosed malignant neoplasms in North Western Europe and the United States <sup>1,2,4</sup>. During 1994, approximately 42,100 U.S.A. citizens developed head and neck cancer and 11,725 died from head and neck cancer <sup>2</sup>. In the Netherlands the incidence of HNSCC is about 14 per 100,000 persons a year. In 1991, 1996 Dutch people developed HNSCC and 663 died from it <sup>5</sup>. About one-third of the patients presents with early stage disease (stage I and II), while two-third presents with advanced disease (stage III and IV) <sup>6</sup>.

### II. Extension

#### II-1. The primary tumor

Spread at the primary site is dictated by the local anatomy, and each anatomic site has its own spread pattern <sup>7,8</sup>.

#### II-2. Lymph node metastases

Lymphatic dissemination is an important mechanism in the spread of HNSCC. After penetration in the basement membrane of the epithelium, cancer cells enter the lymphatics partly by active movement, partly by hydrostatic pressure. These cells pass through the lymphatic vessels and settle in the subcapsular sinus of the first echelon of lymph nodes. Clinical practice reveals that lymph nodes provide a very good soil for tumor growth. After local proliferation and infiltration into the lymph node, the capsule of the lymph node can ultimately be destroyed. A tumor infiltrated lymph node itself can act as a focus for further dissemination into the surrounding lymphatics or the blood stream <sup>9</sup>.

The incidence of lymph node involvement depends mainly on the site and size of the primary tumor. The distribution of lymphatic metastases is mainly explicable in anatomical terms and depends on the site of the primary tumor <sup>10,11</sup>.

Several methods for describing the various clusters of the lymph nodes in the neck are in use. The original nomenclature of lymph nodes is based on the classical work of Rouvière <sup>12</sup>, who defined lymph node clusters according to their location relative to other structures of the neck. A practical classification system of the lymph nodes in the neck has been developed by head and neck surgeons from the Memorial Sloan-Kettering Center <sup>13</sup> and this has found widespread acceptance. In this system which is depicted in Figure 2, five levels are distinguished. Level I includes the content of the submental and submandibular triangles. Levels II, III, and IV include the lymph nodes adjacent to the internal jugular vein and the lymph nodes contained within the fibroadipose tissue located



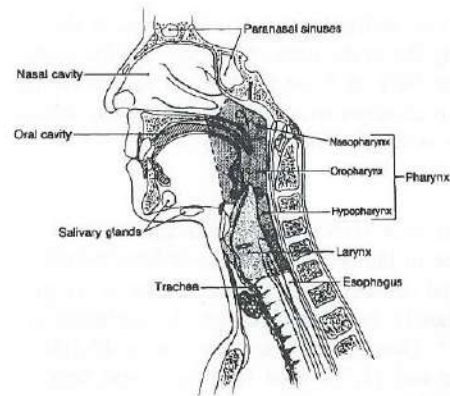


Figure 1. Sites of the upper aerodigestive tract.

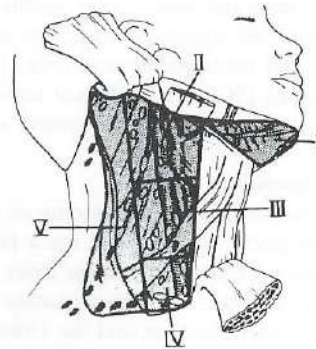


Figure 2. Lymph node levels of the neck.

medial to the sternocleidomastoid muscle. This area is arbitrarily divided into equal thirds, in which level II is the highest and level IV the lowest. Level V includes the contents of the posterior triangle of the neck. As an addition to this classification, clinical and surgical landmarks are described for the boundaries of the three jugular levels (II, III, and IV): the hyoid bone and the carotid bifurcation between levels II and III, and the cricothyroid notch and the omohyoid muscle between regions III and IV <sup>14</sup>.

The status of the lymph nodes in the neck is one of the most important prognostic factors in head and neck cancer <sup>15-18</sup>. The presence of lymph node metastasis in the neck cuts the expected survival in half. In addition, among patients with involved nodes, survival is significantly lower if more nodes are involved <sup>19-25</sup>, if there is nodal involvement at multiple levels <sup>21</sup>, or if extranodal spread is present <sup>20,21,26-29</sup>. Survival worsens as lower lymph node levels are involved <sup>30-32</sup>.

### II-3. Distant metastases

Distant metastases usually occur late in the disease. The overall incidence of clinically detected distant metastases in HNSCC is 10-24% <sup>19,33-35</sup>. The actual incidence may even be higher as autopsy studies report on an incidence of 37-47% <sup>36-38</sup>. Eighty percent of the distant metastases become manifest within 2 years after the appearance of lymph node metastasis <sup>19,33</sup>. The lungs are the most frequent initial site of distant metastases (52-60%), followed by the skeletal system (19-35%). Other localizations of metastatic deposits are the liver, mediastinum, skin, and brain <sup>19,33,39</sup>.

The rate of distant metastases correlates more with the appearance of cervical node metastases than with the primary tumor stage <sup>20,33,34,40</sup>. The number of histopathologically positive lymph nodes, extra nodal spread, and lymph node metastases at multiple levels in the neck have been shown to be risk factors for the development of distant metastases <sup>19,20,35,40</sup>. Patients with more than three lymph node metastases have a risk of almost 50% to develop distant metastases <sup>19</sup>.

### III. Staging

Staging of cancer is a method of gathering groups of classified patients for the purpose of analysis: to aid the clinician in the planning of treatment, to give some indication of prognosis, to assist in the evaluation of the results of treatment, and to facilitate the exchange of information. Fortunately, since 1988 the rules of classification and stage grouping according to the International Union Against Cancer (Union Internationale Contre le Cancer, UICC) <sup>41</sup> correspond with those of the American Joint Committee on Cancer (AJCC) <sup>42</sup>. The TNM system for describing the anatomic extent of disease is based on the assessment of three components: T, extent of the primary tumor; N, status of regional lymph nodes; M, presence or absence of distant metastases. The addition of numbers to these three components indicates the extent of the disease. The clinical classification is based on evidence acquired from physical examination, imaging, endoscopy, biopsy, surgical exploration, or other relevant examinations. Apart from pretreatment clinical classification, pathological classification can be carried out postsurgically, designated as pTNM. This is based on the evidence acquired before treatment, supplemented or modified by the additional evidence acquired from surgery and from histopathological examination. The T classification is dependent on the size of the tumor and its extension into adjacent structures, like cartilage and bone. Different criteria are operative for each tumor site. The definitions for tumor involved regional lymph nodes (N categories) are based on size, number, and neck side (Table 1). If distant metastasis is present (M1) the site is recorded. After T, N, and M categories are assigned, these may be grouped into stages. Stage grouping is identical for all primary tumor sites. Stages I and II refer to small tumors without lymph node or distant metastases, whereas stages III and IV consist of large tumors or tumors with lymph node or distant metastases (Table 2).

Although the histological grade of the tumor does not enter into staging of the tumor, it should be determined. The definitions of the tumor grade (G) are as follows: G1, well differentiated; G2, moderately differentiated; G3, poorly differentiated; G4, undifferentiated.

Table 1. N-Classification of regional lymph nodes according to the UICC.

Nx	Regional lymph nodes can not be assessed
N0	No regional lymph node metastasis
N1	Metastasis in a single ipsilateral lymph node, 3 cm or less in greatest dimension
N2a	Metastasis in a single ipsilateral lymph node, between 3 cm and 6 cm in greatest dimension.
N2b	Metastasis in multiple ipsilateral lymph nodes, none more than 6 cm in greatest dimension
N2c	Metastasis in bilateral or contralateral lymph nodes, none more than 6 cm in greatest dimension
N3	Metastasis in a lymph node more than 6 cm in greatest dimension

Table 2. Stage grouping for all head and neck sites according to the UICC.

Stage I	T1,N0,M0
Stage II	T2,N0,M0
Stage III	T3,N0,M0
	T1 or T2 or T3, N1, M0
Stage IV	T4, N0 or N1, M0
	any T, N2 or N3, M0
	any T, any N, M1



#### IV. Assessment

Because HNSCC arises from mucosal surfaces, most tumors can be detected by physical examination. In almost all patients an endoscopic evaluation is performed. The major objectives of endoscopy are confirmation of the diagnosis by biopsy and determination of the extent of the lesion<sup>43,44</sup>. The tumor stage can be assessed more accurately if endoscopic findings are used in conjunction with imaging techniques, like computed tomography (CT) and magnetic resonance imaging (MRI)<sup>45,46</sup>.

The assessment of the status of the neck lymph nodes is essential for optimal treatment planning. In many institutions, this is mainly based on palpation. However, palpation is not reliable for the detection of lymph node metastasis<sup>30,47,48</sup>. Histopathological studies have demonstrated that both the false positive rate and the false negative rate are unsatisfactory high<sup>49,50</sup>. The overall error of palpation is about 20-30%<sup>31,48,49,51</sup>. Modern imaging techniques, like CT, MRI, ultrasound (US), and US-guided fine needle aspiration cytology (FNAC) are more reliable than palpation, but still leave much to be desired<sup>51-58</sup>. At our department radiological criteria for the optimal assessment of cervical lymph node metastases with CT or MRI were defined: nodes with necrosis, or nodes with a minimal diameter in the axial plane of 11 mm or more for nodes located in the subdigastric level and 10 mm or more for all other nodes, or groups of three or more borderline lymph nodes (1-2 mm smaller)<sup>59</sup>. Using these criteria, the overall error of CT and MRI in the preoperative detection of lymph node metastases in neck sides is about 20%. For US-guided FNAC, this figure is about 10%. However, the accuracy of this method is fully dependent on the skill and the motivation of the ultrasonographer and the cytopathologist<sup>50,53,59</sup>. Furthermore, US-guided FNAC and other conventional imaging techniques provide only locoregional information, while no information on systemic dissemination is obtained.

For further refinement of staging a number of (experimental) radiopharmaceuticals have been evaluated in conventional scintigraphy and positron emission tomography (PET). Where CT and MRI provide anatomical information, radionuclide scintigrams can provide functional information. Radionuclide scintigrams generally have a resolution of 8 mm at best<sup>60</sup>, but can easily be used for investigation of the whole body. Scintigraphy, using intramucosal injection of technetium (<sup>99m</sup>Tc) labeled colloids has been used for the assessment of lymph node metastases in the neck<sup>61</sup>. Scintigraphy using intravenous injection of <sup>99m</sup>Tc-labeled (V) DMSA or glutathione, has been used for the detection of lymph node and distant metastases<sup>62-67</sup>. Other experimental methods for evaluation of the neck include scintigraphy using radiolabeled bleomycin<sup>68,69</sup> and <sup>67</sup>gallium citrate<sup>70</sup>. PET relies on the use of radionuclides which decay with emission of positively charged particles with the mass of an electron. In comparison to conventional scintigraphy, PET provides superior sensitivity, resolution, and allows absolute quantification. Depending on the radionuclide, different aspects of cellular metabolism can be measured, such as oxygen utilization, protein synthesis, and glucose consumption<sup>71</sup>. For imaging of head and neck cancer, <sup>11</sup>carbon-methionine and <sup>18</sup>fluorine-fluorodeoxyglucose (FDG) have been used<sup>72-77</sup>. However, all experimental radiopharmaceuticals mentioned above also accumulate to some extent in inflammatory processes, like reactive lymph nodes, which limit their role in tumor detection and delineation<sup>66,73</sup>. Other disadvantages of conventional scintigraphy and PET are the lack of anatomical information and poorer resolution as compared to CT and MRI.

The capability of all the above mentioned techniques to detect small tumor deposits is limited. Moreover, these imaging techniques very often can not discriminate between normal lymph nodes, reactively enlarged lymph nodes, and tumor infiltrated lymph nodes. Because of these problems with the pretreatment assessment of the status of the neck, it may be difficult to decide whether the neck should be treated or not and this may lead to over- or undertreatment of the neck. Also the presence of distant metastases has impact on the choice of the treatment. Thus, there is a great demand for a specific method to detect small metastases in the lymph nodes in the neck as well as at distant sites.

#### V. Treatment

Therapy usually consists of surgery, radiotherapy, or a combination of these modalities. Generally, patients with stage I and II disease undergo either surgery or radiotherapy with curative intent<sup>78</sup>. This goal will be achieved in 80% of the patients with stage I disease and in more than 60% of patients with stage II disease. For patients with local or regional advanced disease (stage III and IV), the prognosis is much worse. Frequently, a planned combination of surgery and radiotherapy is used<sup>79,80</sup>. Less than 30% of these patients are cured<sup>81</sup>.

It is disappointing that the survival rates of patients with advanced stage head and neck cancer have not been increased much over the last decades<sup>2</sup>. Although many studies have observed a decrease of local and particularly regional failures by the widespread use of planned combined surgery and radiation therapy<sup>18,22</sup>, this has not been reflected in a proportional increase of the five-year survival rates. As fewer patients die from uncontrolled disease in the head and neck, more are exposed to the risk of disseminated disease below the clavicles<sup>82,83</sup>. It is obvious that there is a great demand for a systemic treatment effective in destroying micrometastases at distant sites and minimal residual disease at the local or regional level. Initially hope was high for chemotherapy to play this role, but unfortunately these expectations have not been materialized<sup>39,84-86</sup>. Clearly, a more tumor specific systemic therapy is needed.

#### PART B. MONOCLONAL ANTIBODIES FOR TUMOR TARGETING.

Based on the assumption that tumors possess specific antigens, Ehrlich proposed the concept of the 'magic bullet'<sup>87</sup>. At the beginning of this century he envisioned that antibodies, being part of individual's natural anti-tumor surveillance system, can deliver toxic reagents to tumor cells to detect or eradicate these cells. In 1975, Köhler and Milstein<sup>88</sup> introduced the hybridoma technology. This technology made it possible to develop monoclonal antibodies (MAbs) specifically directed against each particular cellular antigen. However, tumor specific antigens (TSA), antigens exclusively restricted to tumor tissue, are found in experimentally induced tumors, but evidence is still lacking that TSAs are also present on so-called spontaneous tumors<sup>89</sup>. Most identified antigens in human tumors represent tumor associated antigens (TAAs), present on tumor tissue but also detectable on normal tissues<sup>90</sup>. Despite this shortcomings, the accessibility of TAAs can make a MAb 'operationally' selective for tumor targeting. The barrier offered by the normal capillary endothelial cells varies greatly between tissues. In the liver, spleen, and bone marrow there is virtually no barrier as there is a discontinuous endothelium with numerous gaps between the cells, fenestrations in the cells, and no basement membrane



beneath the cells. At the other end of the scale, the endothelium of, for example, the lung and skin is particularly poorly permeable to MABs and passage across the endothelial cells is generally believed to occur by intracytoplasmic vesicles and transendothelial cell channels. Intermediate permeability is seen in organs such as intestine, endocrine and exocrine glands, and kidney, where the endothelial cells have fenestrations and a basement membrane. In contrast to normal tissues, tumor tissue can be characterized by the presence of fenestrated endothelium and a frequently defective basement membrane<sup>91</sup>. These histological features are likely to facilitate the access of MABs to tumor cells more than to normal tissues.

The distribution of injected MAB is likely to vary between tumors and within an individual tumor. Heterogeneity of TAA expression alone cannot account for heterogeneous distribution of antibodies throughout tumors. Three physiological barriers responsible for the poor localization of MABs in tumors have been identified: heterogeneous blood supply, elevated interstitial pressure, and large transport distances in the interstitium. Also less obvious structural differences in blood vessel walls and biochemical differences in the extracellular matrix may play a role. Strong antigen-antibody binding at the periphery of a tumor may prevent deeper penetration. However, these physiological barriers may not be a problem for radioimmunodetection and treatment of leukemia, lymphomas, and small tumors (e.g. micrometastases) in which the interstitial pressure is low and diffusion distances are short<sup>91-93</sup>.

Anticancer MABs have a long history in the management of cancer, with major applications in the immunohistochemistry and immunoassays to TSA or TAA markers. Later, diagnostic and therapeutic strategies were explored whereby MABs are used as carriers of radionuclides for in vivo localization of or radiation to tumors. The underlying principle is that when these radiolabeled MABs are introduced into the bloodstream of patients with certain tumors, the MABs are passively carried to the tumor, whereby they specifically bind to tumor at tumor-antigen binding sites. The MABs bypass the normal tissues, because there are no specific binding sites in these tissues or these binding sites are not or less accessible. Gradually, over the course of several hours to a few days, a progressive higher amount of radiolabeled MAB accumulates in the tumor as compared to normal tissue. When tracer doses of radionuclides are used to label the MABs, the location of the primary tumor, recurrence, and metastases can be detected using a gamma camera; this general procedure has been termed radioimmunosintigraphy (RIS). When larger amounts of radiation are employed, antitumor therapy is possible; this process is termed radioimmunotherapy (RIT).

## I. Radioimmunoconjugates

### I-1. Size of monoclonal antibodies

A smaller molecular size has been shown to have better accessibility to tissue, to distribute more homogeneously throughout tumor and to clear faster from blood and tissues<sup>94</sup>. Controlled proteolytic cleavage of a purified intact MAB can be used to obtain several smaller fragments which can be separated chromatographically:  $F(ab')_2$  and Fab. Using recombinant DNA technology even smaller derivatives of the MABs can be produced: Fv fragments<sup>95,96</sup> (Fig. 3). For radioimmunosintigraphy better results are reported using MAB fragments instead of intact MABs, probably due to higher tumor to blood ratios obtained shortly after injection<sup>97,98</sup>. However, tumor to non-tumor ratios can be similar as

shown by a study of Buist et al.<sup>99</sup> in which ovarian cancer patients were simultaneously injected with both IgG and its  $F(ab')_2$  fragment. For radioimmunotherapy intact MAB may be preferable, because of higher and prolonged uptake in tumor tissues. In comparison to their intact MAB all the MAB fragments mentioned above lack the Fc domain needed for antibody dependent cellular cytotoxicity (ADCC) and complement binding. MAB fragments usually show lower immunogenicity.

### I-2. Genetically modified monoclonal antibodies

Besides the use of MAB fragments, other strategies to avoid human anti-mouse antibody (HAMA) responses, which can lead to anaphylactic shock and rapid clearance of the injected MAB, are the development of chimeric, humanized, and human MABs (Fig. 3)<sup>100</sup>. Chimeric antibodies, made by genetic manipulation, possess murine variable domains and human constant regions. If the antigenicity of a MAB is resided in the variable domains, HAMA responses will still occur. To prevent HAMA responses, other MAB types have been developed. Structural analysis of antigen-antibody complexes shows that the antigen binding surface of the antibody is formed by six hypervariable loops of amino acids called complementarity determining regions (CDRs). These loops are mounted on relatively constant framework regions and by genetic manipulation can be transplanted from a murine antibody on to a human framework. This results in a CDR grafted or humanized antibody with the same specificity as the murine MAB from which the loops were grafted. This process may reduce the affinity of the antibody. In vitro gene amplification and genetic engineering of bacteriophage have resulted in the production of human monoclonal antibodies with high specificity<sup>95,96</sup>.

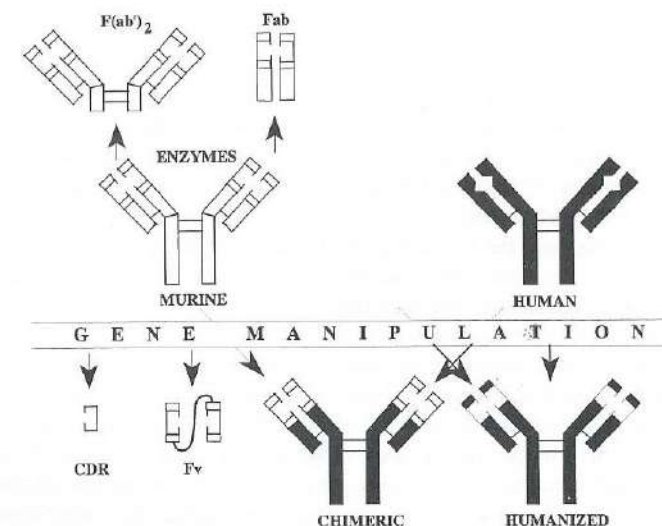


Figure 3. Modifications of monoclonal antibodies.



### I-3. Selection of monoclonal antibodies

Selection of appropriate MAbs is of paramount importance for successful clinical use of MAbs. The first step in the selection of MAbs is an extensive immunohistochemical screening of tumors and normal tissues. The MAbs have to show minimal reactivity with normal tissues, with special emphasis on normal tissues lacking the physiological barriers mentioned above. Ideally, the MAb reacts with all tumors and with all cells within these tumors. However, the heterogeneity of antigen expression in tumors is a major problem. Several MAb characteristics may influence tumor targeting *in vivo*. MAbs should be preferentially of the IgG subclass rather than of the IgM subclass, because extravasation and penetration into tumor will be better for the smaller IgG molecules. The recognized epitope should have a surface domain rather than a cytoplasmic localization. Less absolute criteria are: the MAb should not react with an antigen shed into the blood and the MAb should bind the antigen with high affinity<sup>101</sup>.

Experiments in an animal model are a prerequisite in evaluating the properties of a radiolabeled MAb. In preclinical testing, nude mice bearing human tumor xenografts receive intravenous injections of radiolabeled MAbs. When in this animal model localization in tumor tissue occurs in a satisfactory way, clinical studies will have to determine the localization characteristics in patients. Practice has learned that many of the MAbs with favorable characteristics in immunohistochemical selection as well as in xenograft bearing nude mice, show unexpected and unwanted localizations when administered to patients<sup>102</sup>.

Requirements for tumor selectivity may be more strict when MAbs are used for therapeutic approaches than when used for diagnosis.

### I-4. Radionuclides

Different radionuclides were used and investigated in clinical radioimmunodetection studies. Several comments can be made on the applicability of these radionuclides in radioimmunotargeting of HNSCC. 131-Iodine (<sup>131</sup>I)- and 123-Iodine (<sup>123</sup>I)-labels are not favorable because of dehalogenation of MAbs, which may result in radionuclide uptake in the thyroid hampering interpretation of the images. Similar considerations can be made for detached 111-Indium (<sup>111</sup>In) which may accumulate in reticuloendothelial organs, particularly the liver. High costs (<sup>123</sup>I and <sup>111</sup>In), high radiation exposure to the patient (<sup>131</sup>I and <sup>111</sup>In), limited availability (<sup>123</sup>I), long half-life (<sup>131</sup>I), and poor imaging qualities (<sup>131</sup>I) are other drawbacks. 99m-Technetium (<sup>99m</sup>Tc) has many advantages over the previous mentioned radionuclides because the low radiation delivery to the patient, its ideal properties for gamma cameras, low costs, and good availability. Its short physical half-life of 6.02 h, however, limits its use for late imaging.

Unlike radionuclides used for diagnostic imaging which are  $\gamma$ -emitters, therapeutic radionuclides by definition emit radiation that has high linear energy transfer and an appropriate range in order to destroy tumor tissue. Concomitant  $\gamma$ -emission in high abundance merely contribute to the whole body radiation burden and may cause problems in the radiation protection of medical personnel, other patients, and relatives. In contrast, the use of therapeutic radionuclides with some  $\gamma$ -emission makes radioimmunoscintigraphy possible and might confirm tumor targeting. Low-dose experiments may determine the biodistribution prior to the administration of a therapeutic dose of the same preparation. This is a real advantage because it has been observed that the biodistribution can be influenced by the choice of the radionuclide alone, even with the same chelate-antibody complex<sup>103</sup>. Radioimmunoconjugates with  $\alpha$ -emitters are limited in that they can only kill

cells from close proximity, that is, only those cells that are directly targeted by the radioimmunoconjugate. Because Auger electron-emitters, like 125-Iodine, can only damage DNA, when they are in the vicinity of the nucleus, the radioimmunoconjugate should be bound and internalized. Until now, the  $\beta$ -emitters <sup>131</sup>I and 90-yttrium (<sup>90</sup>Y) are the most widely used radionuclides in clinical radioimmunotherapy studies. However, <sup>131</sup>I is not the radionuclide of choice for clinical application because of the low percentage of  $\beta$ -emission, the high  $\gamma$ -energy, and because of the rapid dehalogenation of the <sup>131</sup>I-labeled conjugates. Disadvantages of <sup>90</sup>Y are its high particle energy accompanied by a path length which may be too long for treatment of minimal residual disease, the lack of  $\gamma$ -emission which makes it impossible to monitor the localization of the radioimmunoconjugate, and sequestration of the radionuclide in organs like spleen, liver, and bone marrow as a result of the instability of the antibody-chelate-radionuclide complex<sup>104</sup>. 186-Rhenium (<sup>186</sup>Re) may be a better candidate for radioimmunotherapy<sup>105,106</sup>. Its physical half-life of 3.7 days seems appropriate, its 9%  $\gamma$ -emission which has an energy of 137 KeV is ideal for imaging, and its  $\beta$ -energy and path length (1.8 mm) seems to be favorable for treatment of minimal residual disease<sup>103,107</sup>. Stable coupling of a MAb with <sup>186</sup>Re was the major problem limiting its clinical application. However, recently a solid state synthesis of <sup>186</sup>Re-MAG3 for reproducible and aseptical production of stable <sup>186</sup>Re-MAb conjugates was developed at our department<sup>108</sup>.

Clinically it may be necessary to image each patient prior to radioimmunotherapy in order to assess antigenic status and to calculate the absorbed radiation doses in tumor and sensitive tissue doses from the observed biodistribution. However, even though imaging photons in <sup>186</sup>Re can be used particularly at therapeutic dose levels, the 'matched pair' approach using <sup>99m</sup>Tc and <sup>186</sup>Re, the former for imaging and the latter for therapy is a very attractive option. These radionuclides can both be attached to antibodies via similar chemistry and the thus obtained radioimmunoconjugates generally show a similar biodistribution<sup>103,109</sup>.

### I-5. Routes of administration

In general, radioimmunoconjugates are administered intravenously. However, in some cases regional administration is advocated. In the treatment of central nervous system malignancies MAbs were directly injected into the primary tumor<sup>110,111</sup>. The rationale for this type of administration is that brain tumors are only locally invasive and gross metastatic disease is uncommon<sup>110</sup>. For diagnosis and treatment of brain gliomas and liver metastases, MAbs have been infused intra-arterially<sup>109,112</sup>.

An alternative route is the intracavitary administration. Intracavitary disease such as pleural effusions, ascites, peritoneal implants, or intrathecal tumors are fairly common manifestations of carcinoma. The most extensively investigated intracavitary route is the intraperitoneal injection<sup>113-117</sup>. For example, the peritoneal cavity is the primary disease site of ovarian carcinoma, and metastases originating from the breast and colon. Administration of diagnostic or therapeutic tumor targeting agents via an intracavitary route provides the theoretical advantages of increasing the concentration of the agent present at the tumor site and decreasing toxicity to normal organs such as bone marrow, as well as those organs that may be involved in immunoglobulin catabolism. The radiolabeled MAbs have a more direct contact with the tumor cells. As soon as the tumor exceeds 5-10 mm in diameter, however, locally injected MAbs penetrate less well than intravenously injected ones<sup>118</sup>. Intravenous and intracavity injections can be complementary<sup>118</sup>. For the



treatment of pleural effusions MABs have been injected into the thoracic cavity <sup>119</sup>. In leptomeningeal tumors MABs have been administered intrathecally <sup>120</sup>. In superficial bladder carcinoma intravesical administration of radiolabeled MAB can achieve selective tumor targeting of malignant cells <sup>121,122</sup>.

When the objective is to detect tumor in regional lymph nodes, subcutaneous injections may prove more effective. After subcutaneous injection, MABs enter local lymphatic capillaries, pass to the draining lymph nodes, and bind to the target cells. A major disadvantage of local injections in general, however, is that distant metastases are not reached adequately. Subcutaneous radioimmunotherapy may result in a high radiation dose at the injection site <sup>123</sup>.

## II. Clinical applications

### II-1. Monoclonal antibodies in diagnosis

Detection of tumors by radioimmunoscinigraphy, even of lesions of <0.5 cm in diameter, has been achieved with MABs of different species, isotypes, and forms, even when they were not truly specific for the neoplasm targeted. Many antigen targets, although merely quantitatively increased in certain cancers, are suitable for antibody targeting. In the case of imaging small lesions, a tumor to non-tumor ratio larger than 10 results in sufficient contrast in single photon emission computed tomography (SPECT) imaging, but not in planar images. In fact, independent of the size of the lesion, contrast on radioimmunoscinigrams is visible for an experienced investigator when the uptake ratio of two related pixels is at least 1.2. Performing RIS, spatial resolution is most important, since specific MAB uptake is often superimposed by non-specific uptake in non-target organs (liver, spleen, kidneys, bladder) and blood pool. Thus, SPECT imaging delineates lesions better than planar imaging by improving lesion to background ratios. Therefore, SPECT may be useful to increase diagnostic accuracy of RIS <sup>124</sup>. Some studies suggest that a combination of planar and tomographic RIS are necessary to provide most information <sup>125</sup>. In general, the limit of resolution appears to be about 1 cm <sup>93</sup>. This does not mean that the size of a single lesion has to be 1 cm or more, but that its size on the radioimmunoscinigrams looks like 1 cm, at the cost of lower intensity. Still, lesions of a few millimeters can be detected if the difference in uptake between the lesion and its environment is high enough.

RIS studies have been performed in patients with many common tumors, including solid tumors, such as colorectal, melanoma, breast, ovarian, prostate, and lung, and lymphomas, such as cutaneous T-cell lymphoma <sup>98,125,126-132</sup>. In melanoma, lymphoma, neuroblastoma, and colorectal cancer, RIS has demonstrated occult tumors, which were not found by conventional methodologies <sup>133</sup>. At the present time, RIS has been successfully employed to assess the extent of disease in patients being evaluated for different therapy options, to assess the location of tumor deposits in patients suspected for recurrent disease, and to discriminate whether a lesion is malignant or a scar following radiation therapy or surgery <sup>134</sup>. Despite these observations, a clear positive impact of routinely used RIS on the management of the cancer patients has not been demonstrated yet <sup>93</sup>. However, when used in selected clinical situations RIS detects more tumors in comparison to state of the art diagnostic procedures and alters patient management in some cases <sup>133</sup>.

In contrast to external scintigraphic examinations a gamma probe can be used intra-operatively for the detection of tumor deposits <sup>135</sup>. The use of positron-emission

tomography (PET) to detect MABs labeled with positron-emitting radionuclides should increase the sensitivity and specificity for tumor detection and should allow more precise dosimetry estimations <sup>136</sup>.

### II-2. Monoclonal antibodies in therapy

Presently, much interest is focussed on the potential of MABs in the treatment of cancer. Research on the therapeutic utility of MABs is characterized by its great diversity. In some approaches unconjugated antibodies are being used for elimination of tumor cells. The rationale for their use is that immunological effector mechanisms like antibody dependent cellular cytotoxicity (ADCC), complement dependent cytotoxicity (CDC), and induction of anti-anti-idiotypic MABs can serve as cytotoxic modality, or that MABs block tumor-associated processes, like proliferation and dissemination, by binding to receptors directly involved in these processes <sup>137</sup>. Anti-idiotypic antibodies can be used in active immunotherapy approaches <sup>138</sup>. In other approaches, MABs are used as targeting agents for selective delivery of radionuclides, chemotherapeutics, toxins, enzymes, photosensitizers, and biologic response modifiers to tumor cells <sup>138-145</sup>.

Unmodified MABs have demonstrated efficacy in some tumor types. The best results, including complete remissions, have been observed in patients with hematological malignancies <sup>144</sup>. MABs having the human  $\gamma_1$  constant region of the IgG molecule were the most effective in ADCC experiments <sup>146</sup>. Tumors in lymph nodes and solid tumors were generally found refractory to treatment <sup>146-151</sup>. However, in most of these trials, the patients had an advanced stage disease and immunodeficiencies. Therapy with unconjugated MABs may be considerably more effective in cases of minimal disease than in cases of well established tumor <sup>152</sup>. In colorectal cancer adjuvant treatment with repeated injections of unlabeled MAB resulted in significantly less relapses at distant sites and higher 5-year survival rates <sup>153</sup>. Even when the MAB can be delivered, simple binding of immunoglobulin to the tumor-cell surface will not necessarily inhibit tumor growth. With the exception of MABs directed against peptide growth factor receptors or other critical growth-regulating molecules, the lysis of tumor cells by immunologic mechanisms requires complement components or cellular effectors that may not function optimally in patients with cancer <sup>154,155</sup>. Enhancement of patients immune status by cytokines, like IL-2, and colony-stimulating-factors (CSF), like GM-CSF, may support the therapeutic efficacy of unconjugated MABs <sup>151,156</sup>. In experiments with blood from healthy donors the lytic capacity of peripheral blood mononuclear cells (PBMC) and granulocytes on tumor cells in ADCC was enhanced when in addition to MABs a CSF was added <sup>145</sup>.

An argument in favor of radiolabeled MABs is related to heterogeneity in antigen expression and the heterogeneous penetration of MABs in solid tumors. It is not necessary for radiolabeled MABs to bind to each single tumor cell to achieve maximal therapeutic effects, because most radionuclides in use are cytotoxic at a distance of several cell diameters. Cells not targeted by the MAB can thus be eliminated by 'cross-fire' of radiation from a radioimmunoconjugate molecule bound to an adjacent tumor cell. The nonuniform distribution of MABs will certainly limit the efficacy of MAB-drug and MAB-toxin conjugates, because for these approaches every cell must be directly exposed to the therapeutic agent. Therefore, radionuclide linked MABs may have a clear advantage over drug and toxin conjugates <sup>93,141</sup>.

From a radiobiological perspective, it appears that RIT alone is unlikely to cure many tumors and that combination with other treatment modalities will be essential in



which RIT is used as an adjuvant treatment <sup>157</sup>. It is expected that the most probable areas of success for this approach in solid tumors would be in tumors of the head and neck and metastatic ovarian and prostate cancer <sup>158</sup>.

In clinical radiomunotherapy trials, remissions were observed in patients with hepatoma, Hodgkin's and Non-Hodgkin's lymphoma, cutaneous T-cell lymphoma, melanoma, ovarian cancer, colorectal cancer, brain gliomas, and leptomeningeal tumors <sup>112,117,120,130,159-165</sup>. Trials in patients with B-cell lymphoma have been the most promising. Response rates of greater than 90% with many complete remissions have been reported by several groups using radiolabeled MAb against B-cell antigens <sup>160,161,166</sup>.

### II-3. Limitations of MAb in clinical applications

A homogeneous expression of the antigen, recognized by the MAb, is preferable for all clinical applications, although it is not fully required for RIT. There are only a few detailed reports on the antigen expression pattern in tumors. In most papers the terms 'homogeneous' and 'heterogeneous' are not defined. In colorectal cancer antigen expression by more than 50 % of the tumor cells was found for CEA in 59 %, for B72.3 in 33 %, for 19.9 in 54 %, and for 29-1 in 85 % of the tumors <sup>167</sup>. This figure was for OKB7 in Non-Hodgkin's lymphoma 74 % <sup>168</sup>, for PD41 in prostate adenocarcinoma 26 % <sup>169</sup>, and for G250 in renal cell carcinoma 85 % <sup>170,171</sup>. In adenocarcinomas of colon, stomach, pancreas, breast, ovarian, and lung the percentage of the tumor biopsies in which 50 % of the tumor cells showed expression of the B72.3 antigen ranged from 29 to 67 %, while the percentage positive tumor cells never exceeded 95 % <sup>172</sup>.

A major limitation for the therapeutic application of MABs may be the low uptake of the MAb in the tumor. In general, the tumor uptake is 1 to 15 % of the injected MAB dose per kilogram (%ID/kg) <sup>133</sup>. For instance, the mean uptake was for AUA1 IgG and HMFG2 IgG in breast, ovarian, and gastrointestinal cancer 1 day p.i. 15 %ID/kg <sup>173</sup>, for OC 125 IgG in large ovarian cancer 2 days p.i. 3.1 %ID/kg <sup>174</sup>, for 81C6 IgG in intracranial malignancies 29-77 h p.i. 1.6 %ID/kg <sup>175</sup>, for OKB7 IgG in Non-Hodgkin's lymphomas 3-5 days p.i. 1.8 %ID/kg <sup>176</sup>, for B72.3 IgG in colon cancer 4-14 days p.i. 7.5 %ID/kg <sup>177</sup>, for BW431 IgG in colorectal cancer 4-14 days p.i. 7.7 %ID/kg <sup>178</sup>, for G250 IgG in renal cell carcinoma 8 days p.i. 14 %ID/kg <sup>179</sup>, for chimeric MOv18 IgG in ovarian cancer 2 days p.i. 8.7 %ID/kg <sup>99</sup>, for human 16.88 IgM in colorectal carcinoma 0.2 %ID/kg <sup>180</sup>, and for HMFG1 IgG in HNSCC 1 day p.i. 5.0 %ID/kg <sup>181</sup>.

The tumor uptake of radiolabeled MABs in animals and humans, is generally a function of tumor mass: the smaller the mass, the higher the uptake. In ovarian cancer uptake in small tumor nodules and malignant cell clusters is even up to 100 times higher than in large tumors. Therefore, it can be expected that radioimmunotherapy may be more effective in minimal residual disease than in bulky tumors <sup>182,183</sup>. Extrapolation of murine to human data can be used to estimate the amount of radioactivity needed to achieve therapeutic doses in humans. In an animal model small metastases are a preferential target for MABs, especially in the absence of primary tumor masses and at subsaturating MAB concentrations. Therefore, RIT may be especially suitable in a postoperative adjuvant setting <sup>184</sup>.

### II-4. Improvement of tumor targeting

The strength of radiolabeled monoclonal antibodies include their high degree of specificity for TAAs. Their clinical limitation, however, results from their low uptake and

heterogeneous distribution. Therefore, several attempts were made to improve tumor targeting.

Several physical (e.g., radiation, heat) and chemical stimuli (e.g., vasoactive agents) may lead to an increase in tumor blood flow. A key problem with this approach is that the increase in blood flow is short-lived and usually confined to well vascularized regions. Lytic enzymes, fractionated radiation, and osmotic agents (e.g., mannitol) may lower the interstitial pressure <sup>185</sup>.

There are numerous other factors that can effect the pharmacology of MABs in tumor targeting. Some of these factors are intrinsic, such as size and location of the tumor mass, while others can be manipulated. Most of these manipulations are aiming to increase the percentage of the injected dose taken up by the tumor or to increase the tumor to non-tumor ratios. Higher tumor to non-tumor ratios have also been seen with the use of second antibodies to clear the blood pool of primary MABs <sup>185-187</sup>.

Two-step pre-targeting has been explored as a method to reduce the delivery of radiolabeled MABs to normal tissues. First a non-radiolabeled bispecific MAB with one arm directed against a tumor associated antigen and the second arm directed against a radiolabeled hapten is injected. After a few days, when the bispecific MAB has localized in the tumor, the low-molecular-weight radiolabeled hapten is injected in large excess <sup>118,188</sup>. Similar approaches have been developed using MABs conjugated with avidin or biotin and radiolabeled biotin or avidin, MABs conjugated with an oligonucleotide and a radiolabeled antisense oligonucleotide, and finally using MABs conjugated with an enzyme and a radiolabeled enzyme inhibitor.

Injection of unlabeled MAB prior to the administration of the labeled MAB may result in saturation of antigen at non-tumor sites, while due to excess of the antigen in the tumor the tumor targeting becomes more specific.

Besides the use of smaller MAB fragments, a more homogeneous distribution can also be obtained by MAB dose escalation <sup>189</sup>. Increase of MAB dose may also result in saturating uptake at non-tumor sites and higher tumor uptake <sup>190</sup>. As a consequence, improvement of imaging is reported using higher MAB doses <sup>128,191</sup>.

To overcome the heterogeneous distribution of MABs within tumor tissue caused by heterogeneous antigen expression, cocktails of different MABs directed against the same tumor type may be of benefit. Another method to overcome the dose heterogeneity in RIT is to combine antibody treatment with other modalities depending upon the tumor type <sup>92</sup>. By using RIT to provide a substantial proportion of the treatment to a defined volume, a modest reduction in the external beam total dose may lead to significantly less complications <sup>157,181</sup>.

### III. Monoclonal antibodies directed against squamous cell carcinomas

So far, only a limited number of MABs directed against HNSCC have been produced <sup>192-208</sup>. Many of these MABs and the antigens recognized by these MABs are poorly characterized, e.g. Ig6 <sup>192</sup>, A1 16 <sup>198</sup>, and 1/A to 1/E <sup>205</sup>. Almost all of the more extensively described MABs have drawbacks for tumor targeting in patients. Therefore, most MABs have been used for immunohistochemical purposes only. MABs B10 <sup>200</sup>, 1H5 <sup>200</sup>, 174H.64 <sup>202</sup>, and 3H1 <sup>206</sup> recognize antigens which are predominantly intracellular and thus less accessible for these MABs as compared to an antigen on the outer cell surface. Almost all MABs directed to HNSCC, recognize an antigen with restricted expression. The 174H.64 <sup>202</sup>, 3F8E3 <sup>203</sup>, 3H1 <sup>206</sup>, and G6K12 <sup>208</sup> antigens are not expressed in all



grades of tumor cell differentiation. Positive immunohistochemical staining of more than 50 % of the HNSCC cells was observed for MAbs SQM1<sup>195</sup>, 3H1,<sup>206</sup> and 1/A to 1/E<sup>205</sup> in 60 % or less of the tumor biopsies. MAbs G10<sup>193</sup>, SQM1<sup>195</sup>, LAM2<sup>196</sup>, 17.13.<sup>199</sup>, 3H1<sup>206</sup>, BM2<sup>207</sup>, and G6K12<sup>208</sup> are large molecules of the IgM isotype, and thus less suitable for in vivo tumor targeting. MAb 3F8E3<sup>203</sup> showed a low affinity binding. Finally, some MAbs show considerable reactivity with normal tissues: MAb G10 reacts with a precursor blood group antigen<sup>192</sup>, MAbs A9 and SQM1 with normal blood vessels<sup>194,195</sup>, MAb LuCa2 with several normal tissues like thyroid, kidney, colon, and other epithelia<sup>197</sup>, and MAb B10 with connective tissue, striated muscle, and nerve fiber<sup>199</sup>.

Based on these data the development of new MAbs directed against HNSCC was pursued<sup>209</sup>. As a result, a panel of 5 high affinity MAbs of the IgG subclass directed against antigens at the outer cell surface of HNSCC was generated: MAbs E48, U36, K928, K931, and K984. MAbs E48 and U36, the latter being developed only recently, are selectively reactive with squamous and transitional epithelia and their malignant counterparts<sup>210,211</sup>. MAb K928 is reactive with HNSCC and with suprabasal keratinocytes in normal stratified squamous epithelia<sup>212</sup>. This MAb recognizes a so called pan-carcinoma marker expressed by squamous cell carcinoma (SCC), small cell lung carcinoma, and adenocarcinomas of lung, breast, and ovary. MAbs with similar features to MAb K928 have not been described before. K931 is reactive with HNSCC but not with normal stratified epithelia<sup>213</sup>. This MAb recognizes a pan-carcinoma marker expressed by SCC, small cell lung carcinoma, and adenocarcinomas of lung, breast, colon, and ovary. Biochemical characterization revealed that the antigen recognized by MAb K931 is similar to the one recognized by MAb 17-1A, a MAb produced by the group of Koprowski<sup>214</sup>, and by MAb 323/A3, a MAb developed by Edwards et al.<sup>215</sup>. MAb K984 is reactive with HNSCC and basal keratinocytes in normal stratified squamous epithelia<sup>212</sup>. This MAb recognizes also a pan-carcinoma marker expressed by SCC, small cell lung carcinoma, and adenocarcinomas of lung, breast, and ovary. Biochemical characterization indicated that the antigen recognized by MAb K984 is similar to the antigen recognized by MAb SF-25, a MAb produced by the group of Wands<sup>216</sup>.

Because of the drawbacks mentioned above only a few MAbs have been administered to HNSCC patients. Until now, a limited number of clinical RIS studies in head and neck cancer patients have been described<sup>217-221</sup>. Results obtained in clinical RIS studies are difficult to compare. Firstly, in almost all studies only a small proportion of the 5-21 patients included in these studies had lymph node involvement, thus limiting accurate calculation of sensitivity and specificity. Secondly, studies differ considerably with respect to (a) patient selection, (b) control of tumor deposits for antigen expression, (c) scintigraphic methods, (d) the way of topographical evaluation of the diagnostic findings, and (e) the way to confirm scintigraphic findings. In the study of Tranter et al.<sup>217</sup> 5 patients were included who received <sup>131</sup>I-labeled sheep IgG to carcinoembryogenic antigen (CEA). In this study tumor masses above 2 cm were detected by RIS as confirmed by CT or surgery. Soo et al.<sup>218</sup> have reported on the use of an <sup>111</sup>In-labeled MAb directed against the epidermal growth factor receptor (EGFR) for localizing HNSCC tumors. Positive images were obtained in 8 of 11 patients with tumors larger than 3 cm diameter. All five neck node metastases (diameter > 4 cm) were detected. Anti-EGFR MAbs, however, accumulate to a high level in the liver, hampering their applicability for RIT<sup>222</sup>. Kairemo et al.<sup>219</sup> used an <sup>111</sup>In-labeled F(ab')<sub>2</sub> directed against CEA. Without using SPECT imaging they visualized 17 out of 19 tumor sites in 13 patients. From the 19 sites,

7 comprised lymph node metastases which were all larger than 2 cm in size. Timon et al.<sup>220</sup> have presented a study on 7 patients with 5 primary tumors and 3 lymph node metastases. All deposits except one lymph node metastasis were detected by RIS using an <sup>111</sup>In-labeled anti-CEA antibody. Unfortunately, in this study no tumor sizes are mentioned and it is not clear how the scintigraphic findings were confirmed. Disadvantages of MAbs directed against CEA may be that they are not specifically directed against HNSCC which may result in false-positive scintigrams<sup>223</sup> and limited applicability for therapy. Despite the intracellular localisation of the antigen Baum et al.<sup>221</sup> recently reported on a RIS study in which <sup>99m</sup>Tc-labeled MAb 174H.64 showed good tumor targeting. Unfortunately, tissue uptake levels were not determined for this MAb. For RIT the intracellular localization of the 174H.64 antigen may be a serious problem. From all forementioned studies it is not clear whether the examiner for RIS was blinded to the results of the other diagnostic examinations.

Maraveyas et al.<sup>181</sup> performed a biodistribution study with iodine-labeled HMFG1 in HNSCC patients. The mean tumor uptake of this MAb was low: 5.0 %ID/kg one day after injection. Another limitation of this MAb is its heterogeneous reactivity pattern in HNSCCs. Since MAb HMFG1 was raised against the human milk fat globule, this MAb may react with normal tissues as well. Because RIS was not performed, uptake of the MAb at non-tumor sites can not be excluded. For these reasons MAb HMFG1 does not seem to be the MAb of choice for RIT.

Until now, there are no clinical RIT studies in HNSCC patients. In ferritin-positive human HNSCC xenograft bearing nude mice injection of 90-yttrium labeled antiferritin polyclonal antibodies resulted in tumor reduction<sup>224</sup>. In this study polyclonal antibodies were used, which implicates limitations with respect to antibody availability and excludes the possibility of humanization or chimerization. These factors will certainly limit its applicability in HNSCC patients.

Using rhenium-186 labeled MAb E48 tumor growth delay and complete remissions occurred in HNSCC xenograft bearing nude mice<sup>225</sup>. In mice bearing small HNSCC tumors even 100% complete remissions could be obtained after one single injection of <sup>186</sup>Re-labeled MAb E48<sup>226</sup>. In experimental models also MAbs linked to drugs or photosensitizers have been tested<sup>227,228</sup>. The group of Mach investigated the feasibility of MAb E48 labeled with a fluorescent dye for immunophotodiagnosis and therapy in squamous cell carcinoma xenograft bearing nude mice<sup>229</sup>.

## PART C. AIM OF THE STUDY.

The major aim of the present study is to investigate the perspectives of promising candidate monoclonal antibodies for diagnosis and therapy of head and neck cancer.

As stated previously, the assessment of lymph node metastases in the neck is of major importance. Pre-treatment assessment of the status of the lymph nodes is essential for optimal treatment planning. Since the current staging techniques are not fully reliable, the management of the clinical negative neck remains a problem. Radioimmunoscintigraphy (RIS) using radiolabeled monoclonal antibodies (MAbs) against tumor associated antigens has been successful in the detection of metastases from several tumor types. In chapter 2, 4, and 5 the diagnostic value of RIS with MAb E48, 323/A3, cSF25, K928, and U36 in head and neck cancer is investigated.



From these kind of studies one can also obtain information about the feasibility of these MABs for RIT. In fact, there is a great demand for a systemic adjuvant therapy effective in destroying both micrometastases at distant sites as well as minimal residual disease at the locoregional level. From radioimmunosintigrams in combination with biopsy measurements from the surgical specimen extensive information on tumor targeting and biodistribution can be obtained. In chapter 3, 4, 5, and 6 the feasibility of several MABs for therapy of head and neck cancer is examined and finally the most suitable MAB is selected.

## REFERENCES

1. Muir C, Weiland L. Upper aerodigestive tract cancers. *Cancer* 1995;75:147-53.
2. Boring CC, Squires TS, Tong T, Montgomery, S. Cancer statistics 1994. *CA Cancer J Clin* 1994;44:7-26.
3. Blitzer PH. Epidemiology of head and neck cancer. *Semin Oncol* 1988;15:2-9.
4. Parkin DM, Laara E, Muir CS. Estimates of worldwide frequency of sixteen major cancers in 1980. *Int J Cancer* 1988;41:184-97.
5. Coordinating council of comprehensive cancer in the Netherlands 1991. Third report of the Netherlands Cancer Registry. Utrecht: LOK, 1994.
6. Verham GA, Crowther JA. Head and neck carcinoma - stage at presentation. *Clin Otolaryngol* 1994;19:120-4.
7. Carter RL, Tanner NSB, Clifford P, Shaw HJ. Perineural spread in squamous cell carcinomas of the head and neck; a clinicopathological study. *Clin Otolaryngol* 1979;4:271-81.
8. Poleksic S, Kalwaic HJ. Prognostic value of vascular invasion in squamous cell carcinoma of the head and neck. *Plast Reconstr Surg* 1978;61:234-40.
9. Carr I. Lymphatic metastases. *Cancer Metastasis Rev* 1983;2:307-17.
10. Lindberg RD. Distribution of cervical lymph node metastases for squamous cell carcinoma of the upper respiratory tract. *Cancer* 1972;29:1446-9.
11. Shah JP. Patterns of cervical lymph node metastases from squamous carcinomas of the upper aerodigestive tract. *Am J Surg* 1990;160:405-9.
12. Rouvière H. Anatomie des lymphatiques de l'homme. Paris: Masson et Cie, 1932.
13. Shah JP, Strong E, Spiro RH, Vikram B. Neck dissection: Current status and future possibilities. *Clin Bulletin* 1981;11:25-33.
14. Robbins KT, ed. Pocket guide to the neck dissection classification and TNM staging of head and neck cancer -Subcommittee for neck dissection terminology and classification. American Academy of Otolaryngology-Head and Neck Surgery Foundation Inc. Rochester: Custom Printing Inc., 1991:9-10.
15. Jones AS. Prognosis in mouth cancer: tumour factors. *Oral Oncol*, *Eur J Cancer* 1994;30B:8-15.
16. Regueiro CA, Aragon G, Millan I, Valcarcel FJ, De la Torre A, Magallon R. Prognostic factors for local control, regional control and survival in oropharyngeal squamous cell carcinoma. *Eur J Cancer* 1994;30A:2060-7.
17. Gamel JW, Jones AS. Squamous carcinoma of the head and neck: cured fraction and median survival time as function of age, sex, histologic type and node status. *Br J Cancer* 1993;67:1071-5.
18. Snow GB. The N0 neck in head and neck cancer patients. *Eur Arch Otorhinolaryngol* 1993;250:423.
19. Leemans CR, Tiwari R, Nauta JJP, van der Waal I, Snow GB. Regional lymph node involvement and its significance in the development of distant metastases in head and neck carcinoma. *Cancer* 1993;71:452-6.
20. Cerezo L, Millan I, Torre A, Aragon G, Otero J. Prognostic factors for survival and tumor control in cervical lymph node metastases from head and neck cancer. A multivariate study of 492 cases. *Cancer* 1992;69:1224-34.
21. O'Brien CJ, Smith JW, Soon S-J, Urist MM, Maddox WA. Neck dissection with and without radiotherapy: prognostic factors, patterns of recurrence, and survival. *Am J Surg* 1986;152:456-63.
22. Snow GB, Annys AA, Slooten EA van, Bartelink H, Hart AAM. Prognostic factors of neck node metastasis. *Clin Otolaryngol* 1982;7:185-92.
23. Richard JM, Sancho-Garnier H, Mischeau C, Saravane D, Cachin Y. Prognostic factors in cervical lymph node metastasis in upper respiratory and digestive tract carcinomas: a study of 1,713 cases during a 15-year period. *Laryngoscope* 1987;97:97-101.
24. Stell PM. Prognosis in laryngeal carcinoma: tumour factors. *Clin Otolaryngol* 1990;15:69-31.
25. Mantravadi RVP, Skolnik EM, Haas RE, Applebaum EL. Patterns of cancer recurrence in the postoperatively irradiated neck. *Arch Otolaryngol* 1983;109:753-6.
26. Tannock IF, Browman G. Lack of evidence for a role of chemotherapy in the routine management of locally advanced head and neck cancer. *J Clin Oncol* 1986;4:1121-6.



27. Som PM. Lymph nodes of the neck. *Radiology* 1987;165:593-600.
28. Johnson JT, Barnes EL, Myers EN, Schramm VL, Borochovit D, Sigler BA. The extracapsular spread of tumors in cervical node metastasis. *Arch Otolaryngol* 1981;107:725-9.
29. Carter RL, Bliss JM, Soo K-E, O'Brien CJ. Radical neck dissections for squamous cell carcinomas: pathological findings and their clinical implications with particular reference to transcapsular spread. *Int J Radiat Oncol Biol Phys* 1987;13:825-32.
30. Spiro RH, Alfonso AE, Farr HW, Strong EW. Cervical node metastases from epidermoid carcinoma of the oral cavity and oropharynx. A critical assessment of current staging. *Am J Surg* 1974;128:562-7.
31. Grandi C, Alloisio M, Moglia D, Podrecca S, Sala L, Salvatori P, Molinari R. Prognostic significance of lymphatic spread in head and neck carcinomas: therapeutic implications. *Head Neck Surg* 1985;8:67-73.
32. Jones AS, Roland NJ, Field JK, Phillips DE. The level of cervical lymph node metastases: their prognostic relevance and relationship with head and neck squamous carcinoma primary sites. *Clin Otolaryngol* 1994;19:63-69.
33. Merino OR, Lindberg RD, Fletcher GH. An analysis of distant metastases from squamous cell carcinoma of the upper respiratory and digestive tracts. *Cancer* 1977;40:145-51.
34. Berger DS, Fletcher GH. Distant metastases following local control of squamous cell carcinoma of the nasopharynx, tonsillar fossa and base of tongue. *Radiology* 1971;100:141-3.
35. Vikram B, Strong EW, Shah JP, Spiro R. Failure at distant sites following multimodality treatment for advanced head and neck cancer. *Head Neck Surg* 1984;6:730-3.
36. Dennington ML, Carter DR, Meyers AD. Distant metastases in head and neck carcinoma. *Laryngoscope* 1980;90:196-201.
37. Nishijima W, Takooda S, Tokita N, Takayama S, Sakura M. Analyses of distant metastases in squamous cell carcinoma of the head and neck and lesions above the clavicle at autopsy. *Arch Otolaryngol Head Neck Surg* 1993;119:65-68.
38. Zbären P, Lehmann W. Frequency and site of distant metastases in head and neck squamous cell carcinoma. An analysis of 101 cases at autopsy. *Arch Otolaryngol Head Neck Surg* 1987;113:762-4.
39. Head and Neck Contracts Program. Adjuvant chemotherapy in advanced head and neck squamous carcinoma. Final report of the Head and Neck Contracts Program. *Cancer* 1987;60:301-11.
40. Ellis ER, Mendenhall WM, Rao PV, Parsons JT, Sprangler AE, Million RR. Does node location affects the incidence of distant metastases in head and neck squamous cell carcinoma? *Int J Radiat Oncol Biol Phys* 1989;17:293-97.
41. Hermanek P, Sobin LH, eds. International Union Against Cancer. TNM classification of malignant tumours, 4th edition. New York: Springer Verlag, 1987.
42. Beahrs OH, Henson DE, Hutter RP, Meyers MH, eds. American Joint Committee on Cancer (AJCC). Manual of staging of cancer, 3rd edition. Philadelphia: JB Lippincott Company, 1988.
43. Snow JB. Surgical management of head and neck cancer. *Semin Oncol* 1988;15:20-8.
44. Haughey BH, Gates GA, Arfken CL, Harvey J. Meta-analysis of second malignant tumors in head and neck cancer: the case for an endoscopic screening protocol. *Ann Otol Rhinol Laryngol* 1992;101:1051-2.
45. Madison MT, Remley KB, Latchaw RE, Mitchell SL. Radiologic diagnosis and staging of head and neck squamous cell carcinoma. *Radiol Clin North Am* 1994;32:163-81.
46. Muraki AS, Mancuso AA, Harsberger HR, Johnson LP, Meads GB. CT of the oropharynx, tongue base, and floor of mouth: normal anatomy and range of variations, and applications in staging carcinoma. *Radiology* 1983;148:725-31.
47. Watkinson JC, Johnston D, Jones N, Coady M, Laws D, Allen S, Hibbert J. The reliability of palpation in the assessment of tumours. *Clin Otolaryngol* 1990;15:405-9.
48. Sako K, Pradier RN, Marchetta FC, Pickren JW. Fallibility of palpation in the diagnosis of metastases to cervical nodes. *Surg Gyn Obst* 1964;113:989-90.
49. Ali S, Tiwari RM, Snow GB. False positive and false negative neck nodes. *Head Neck Surg* 1985;8:78-82.
50. Brekel van den MWM, Castelijns JA, Croll GA, Stel HV, Valk J, Waal van der I, Golding RP, Meijer CJLM, Snow GB. Magnetic resonance imaging vs palpation of cervical lymph node metastasis. *Arch Otolaryngol Head Neck Surg* 1991;117:66-73.
51. Brekel van den MWM, Castelijns JA, Stel HV, Golding RP, Meijer CJLM, Snow GB. Lymph node staging in patients with clinically negative neck examinations by ultrasound and ultrasound-guided aspiration cytology. *Am J Surg* 1991;162:362-6.
52. Castelijns JA, Brekel van den MWM. Magnetic resonance imaging evaluation of extracranial head and neck tumors. *Magn Res Q* 1993;9:113-28.
53. Brekel van den MWM, Castelijns JA, Stel HV, Golding RP, Meijer CJLM, Snow GB. Modern imaging techniques and ultrasound guided aspiration cytology for the assessment of the neck node metastases; a prospective comparative study. *Eur Arch Otorhinolaryngol* 1993;250:11-7.
54. Baatenburg de Jong RJ, Rongen RJ, Lameris JS. Metastatic neck disease. Palpation vs ultrasound examination. *Arch Otolaryngol Head Neck Surg* 1989;115:689-90.
55. Baatenburg de Jong RJ, Rongen RJ, Verwoerd CDA, Overhagen van H, Lameris JS, Kneeg P. Ultrasound-guided fine needle aspiration biopsy of neck nodes. *Arch Otolaryngol Head Neck Surg* 1991;117:402-4.
56. Friedmann M, Roberts N, Kirschenbaum GL, Colombo J. Nodal size of metastatic squamous cell carcinoma of the neck. *Laryngoscope* 1993;103:854-6.
57. Stern WBR, Silver CE, Zeifer BA, Persky MS, Heller KS. Computed tomography of the clinical negative neck. *Head Neck* 1990;12:109-13.
58. Lenz M, Kersting-Sommerhoff B, Gross M. Diagnosis and treatment of the N0 neck in carcinomas of the upper aerodigestive tract: current status of diagnostic procedures. *Eur Arch Otorhinolaryngol* 1993;250:432-8.
59. Brekel van den MWM, Stel HV, Castelijns JA, Nauta JJP, Waal I van der, Valk J, Golding RP, Meijer CJLM, Snow GB. Cervical lymph node metastases: assessment of radiologic criteria. *Radiology* 1990;177:379-84.
60. Sorensen JA and Phelps ME. Physics in nuclear medicine, 2nd edition. Orlando: Grune and Stratton; 1987.
61. Hildmann H, Kosberg HD, Tiedjen KU. Lymphszintigraphische Untersuchungen der regionale Lymphwege bei Patienten mit Kopf-Hals-Tumoren. *HNO* 1987;35:31-3.
62. Watkinson JC, Todd CEC, Paskin L, Rankin S, Palmer T, Shaheen OH, Clark SEM. Metastatic carcinoma in the neck: a clinical, radiological, scintigraphic and pathological study. *Clin Otolaryngol* 1991;16:187-92.
63. Piepenburg R, Bockisch A, Hach A, Steinert H, Welkoborsky H-J, Kreuz S, Mann WJ, Hahn K. Bedeutung der Ganzkörper-Skelettszintigraphie im Rahmen des Staging von Malignomen in HNO-Bereich. *Laryngol Rhino Otol* 1992;71:605-10.
64. Heinritz H, Marienhagen J, Wolf F, Schuster B, Stenglein C, Iro H. Szintigraphische Darstellung von Kopf-Hals-Karzinomen mit <sup>99m</sup>Tc-Technetium (v) Dimercaptosuccinic acid. Ein prospective klinische Studie. *HNO* 1992;40:437-441.
65. Watkinson JC, Lazarus CR, Todd CEC, Maisey MN, Clarke SEM. Metastatic squamous carcinoma in the neck: an anatomical and physiological study using CT and SPECT <sup>99m</sup>Tc (V) DMSA. *Br J Radiol* 1991;64:909-14.
66. Oncel S, Duman Y, Arslanoglu S. Technetium 99m(v) dimercaptosuccinic acid SPECT scintigraphy in head and neck tumors. *Ann Otol Rhinol Laryngol* 1994;103:324-7.
67. Ercan MT, Aras T, Aktas A, Kaya S, Bekdik CF. Accumulation of <sup>99m</sup>Tc-gluthatione in head and neck tumors. *Nucl Med* 1994;33:224-8.
68. Cummings CW, Larson SM, Dobie RA, Weymuller EA, Rudd TG, Merello A. Assessment of cobalt 57 tagged bleomycin as a clinical aid in staging head and neck carcinoma. *Laryngoscope* 1981;91:529-37.
69. Goodwin DA, Meares CF, Riemer LH de, Diamanti CI, Goode RL, Baumert JE, Sartoris DJ, Landieri, Fawcett HD. Clinical studies with In-111 BLEDTA, a tumor-imaging conjugate of bleomycin with a bi-functional chelating agent. *J Nucl Med* 1981;22:787-92.
70. Teates CD, Preston DF, Boyd CM. Gallium-67 citrate imaging in head and neck tumors: report of cooperative group. *J Nucl Med* 1980;21:622-7.
71. Reiman EM, Mintum MA. Positron emission tomography. *Arch Intern Med* 1990;150:729-31.



72. Leskinen-Kallio S, Nägren K, Lehtikainen P, Ruotsalainen U, Teräs M, Joensuu H. Carbon-11-methionine and PET is an effective method to image head and neck cancer. *J Nucl Med* 1992;33:691-5.
73. Lindholm P, Leskinen-Kallio S, Minn H, Bergman J, Haaparanta M, Lehtikainen P, Nägren K, Ruotsalainen U, Teräs M, Joensuu H. Comparison of fluorine-18-fluorodeoxyglucose and carbon-11-methionine in head and neck cancer. *J Nucl Med* 1993;34:1711-6.
74. Reisser Ch, Haberkorn U, Strauss LG. The relevance of positron emission tomography for the diagnosis of head and neck tumors. *J Otolaryngol* 1993;22:231-8.
75. Zeitouni AG, Yamamoto L, Black M, Gjeddi A. Functional imaging of head and neck tumours using positron emission tomography. *J Otolaryngol* 1994;23:77-80.
76. Jabour BA, Choi Y, Hoh CK, Rege SD, Soong JC, Lufkin RB, Hanafey WN, Maddahi J, Chaiken L, Bailet J, Phelps ME, Hawkins RA, Abemeyor. Extracranial head and neck: PET imaging with 2-[F-18]fluoro-2-deoxy-d-glucose and MR imaging correlation. *Radiology* 1993;186:27-35.
77. Braams JW, Pruim J, Freling NJM, Nikkels PGJ, Roodenburg JLN, Boering G, Vaalburg W, Vermey A. Detection of lymph node metastases of squamous-cell cancer of the head and neck with FDG-PET and MRI. *J Nucl Med* 1995;36:211-6.
78. Vokes EE, Weichselbaum RR, Lippman SM, Hong WK. Head and neck cancer. *New Engl J Med* 1993;328:184-94.
79. Ervin TJ, Clark JR, Weichselbaum RR. Multidisciplinary treatment of advanced squamous carcinoma of the head and neck. *Semin Oncol* 1985;4(suppl 6):71-8.
80. Boysen M, Lovdal O, Navvig K, Tausjo J, Jacobsen A-B, Evensen JF. Combined radiotherapy and surgery in the treatment of neck node metastases from squamous cell carcinoma of the head and neck. *Acta Oncol* 1992;31:455-60.
81. Vokes EE. Head and neck cancer. In: Perry MC, ed. *The chemotherapy source book*. Williams and Wilkins, Baltimore 1992:918-31.
82. Vikram B. Changing patterns of failure in advanced head and neck cancer. *Arch Otolaryngol* 1984;110:564-5.
83. Goepfert H. Are we making any progress? *Arch Otolaryngol* 1984;110:562-3.
84. Stell PM, Rawson NSB. Adjuvant chemotherapy in head and neck cancer. *Br J Cancer* 1990;61:779-87.
85. Taylor SG, Applebaum E, Showel JL, Norusis M, Holinger LD, Hutchinson JC, Murthy AK, Caldarelli DD. A randomized trial of adjuvant chemotherapy in head and neck cancer. *J Clin Oncol* 1985;3:672-9.
86. Tannock IF, Browman G. Lack of evidence for a role of chemotherapy in the routine management of locally advanced head and neck cancer. *J Clin Oncol* 1986;4:1121-6.
87. Himmelweit B (Ed). *The collected papers of Paul Ehrlich*. Pergamon Press, Elmsford, New York, 1975.
88. Köhler G, Milstein C. Continuous cultures of fused cells secreting antibody of predefined specificity. *Nature* 1975;256:495-7.
89. Prehn RT. Tumor-specific antigens as altered growth factor receptors. *Cancer Res* 1989;49:2823-6.
90. Damjanov I, Knowles BB. Biology of disease: monoclonal antibodies and tumor-associated antigens. *Lab Invest* 1983;48:510-25.
91. Cobb LM. Intratumour factors influencing the access of antibody to tumour cells. *Cancer Immunol Immunother* 1989;28:235-40.
92. Jain RK. Physiological barriers to delivery of monoclonal antibodies and other macromolecules in tumors. *Cancer Res* 1990;50 (suppl):814-9s.
93. Sands H. Experimental studies of radioimmunodetection of cancer: an overview. *Cancer Res* 1990;50:809-13s.
94. Pak KY, Nedelman MA, Fogler WE, Tam SH, Wilson E, Haarlem LJM van, Colognola R, Warnaar SO, Daddona PE. Evaluation of the 323/A3 monoclonal antibody and the use of technetium-99m-labeled 323/A3 Fab' for the detection of pan adenocarcinoma. *Nucl Med Biol* 1991;18:483-97.
95. Hawkins RE, Llewellyn MB, Russell SJ. Adapting antibodies for clinical use. *BMJ* 1992;305:1348-52.
96. Stigland F, Ålström KR, Sundström B, Makiya R, Stendahl U. Alternative technologies to generate monoclonal antibodies. *Acta Oncol* 1993;32:841-4.
97. Wahl RL, Parker CW, Philpott GW. Improved radioimaging and tumor localization with monoclonal F(ab')<sub>2</sub>. *J Nucl Med* 1983;24:316-325.
98. Buraggi GL, Callegaro L, Mariani G, Turrin A, Cascinelli N, Attili A, Bombardieri E, Terno G, Plassio G, Dovis M, Mazzuca N, Natali PG, Scassellati GA, Rosa U, Ferrone S. Imaging with <sup>131</sup>I-labeled monoclonal antibodies to a high-molecular-weight melanoma-associated antigen in patients with melanoma: efficacy of whole immunoglobulin and its F(ab')<sub>2</sub> fragments. *Cancer Res* 1985;45:3378-87.
99. Buist MR, Kenemans P, Den Hollander W, Vermorken JB, Molthoff CJM, Burger CW, Helmerhorst TJM, Baak JPA, Roos JC. Kinetics and tissue distribution of the radiolabeled chimeric monoclonal antibody MOv18 IgG and F(ab')<sub>2</sub> fragments in ovarian cancer patients. *Cancer Res* 1993;53 5413-8.
100. Khazaeli MB, Conry RM, LoBuglio AF. Human immune response to monoclonal antibodies. *J Immunother* 1994;15:42-52.
101. Goldenberg DM. Imaging and therapy of gastrointestinal cancers with radiolabeled antibodies. *Am J Gastroenterol* 1991;86:1392-1403.
102. Stokkel MPM, Hoefnagel CA, Rutgers EMT. Unexpected brain uptake in radioimmunoscinigraphy using F(ab')<sub>2</sub> monoclonal antibodies. *Clin Nucl Med* 1993;18:78-9.
103. Mausner LF, Srivastava SC. Selection of radionuclides for radioimmunotherapy. *Med Phys* 1993;20:503-9.
104. Vaughan ATM, Keeling A, Yankuba SCS. The production and biological distribution of yttrium-90-labeled antibodies. *Int J Appl Radiat Isot* 1985;36:803-6.
105. Wessels BW, Rogus RD. Radionuclide selection and model absorbed dose calculations for radiolabeled tumor associated antibodies. *Med Phys* 1984;11:638-45.
106. Breitz HB, Weiden PL, Vanderheyden J-L, Appelbaum JW, Bjorn MJ, Fer MF, Wolf SB, Ratliff BA, Seiler CA, Foisie DC, Fisher DR, Schroff RW, Frizberg AR, Abrams PG. Clinical experience with rhenium-186-labeled monoclonal antibodies for radioimmunotherapy: results of phase I trials. *J Nucl Med* 1992;33:1099-112.
107. Weber DA, Eckerman KP, Dillman LT, Ryman JC, eds. *MIRD: radionuclide data and decay schemes*. The Society of Nuclear Medicine Inc, 1989.
108. Visser GWM, Gerretsen M, Herscheid JDM, Snow GB, Dongen GAMS van. Labelling of monoclonal antibodies with <sup>186</sup>Re using the MAG3 chelate for radioimmunotherapy of cancer: a technical protocol. *J Nucl Med* 1993;34:1953-63.
109. Schroff RW, Weiden PL, Appelbaum J, Fer MF, Breitz, Vanderheyden J-L, Ratliff B, Fisher D, Foisie D, Hanelin LG, Morgan AC, Fritzberg AR, Abrams PG. Rhenium-186 labeled antibody in patients with cancer: Report of a pilot phase I study. *Antibody Immunconj Radiophar* 1990;3:99-111.
110. Kemshead JT, Papanastassiou V, Coakman HB, Pizer BL. Monoclonal antibodies in the treatment of central nervous system malignancies. *Eur J Cancer* 1992;28:511-3.
111. Riva P, Arista A, Mariani G, Seccamani E, Lazzari S, Moscatelli G, Sturiale C, Sarti G, Franceschi G, Spinelli A, Vecchiotti G, Riva N, Natali P, Zardi L. Improved tumour targeting by direct intralesional injection of radiolabeled monoclonal antibody: A phase I study in brain glioma. *J Nucl Med* 1991;32:922.
112. Kalofonos HP, Pawlikowska TR, Hemingway A, Courtenay-Luck N, Dhokia B, Snook D, Sivolapenko GB, Hooker GR, McKenzie CG, Lavender PJ, Thomas DGT, Epenetos AA. Antibody guided diagnosis and therapy of brain gliomas using radiolabeled monoclonal antibodies against epidermal growth factor receptor and placental alkaline phosphatases. *J Nucl Med* 1989;30:1636-46.
113. Ward BG, Mather SJ, Hawkins LR, Crowther ME, Shephard JH, Granowska M, Britton KE, Slewin ML. Localization of radioiodine conjugated to the monoclonal antibody HMFG2 in human ovarian carcinoma: assessment of intravenous and intraperitoneal routes of administration. *Cancer Res* 1987;47:4719-23.
114. Haisma H, Mosely K, Bataille A, Griffiths TC, Knapp RC. Distribution and pharmacokinetics of radiolabeled monoclonal antibody OC 125 after intravenous and intraperitoneal administration in gynecologic tumors. *Am J Obstet Gynecol* 1987;159:4218-24.



115. Crippa F, Buraggi GL, DiRe E, Gasparini M, Seregni E, Canevari S, Gadina M, Presti M, Marini A, Seccamani E. Radioimmunoscintigraphy of ovarian cancer with MOv18 monoclonal antibody. *Eur J Cancer* 1991;27:724-9.
116. Larson SM, Carrasquillo JA, Colcher DC, Yokoyama K, Reynolds JC, Bacharach A, Raubitschek A, Pace L, Finn RD, Rotman M, Stabin M, Neumann RD, Sugarbaker P, Schlom J. Estimates of radiation absorbed dose intraperitoneally administered iodine-131 radiolabeled B72.3 monoclonal antibody in patients with peritoneal carcinomatosis. *J Nucl Med* 1991;32:1661-7.
117. Epenetos AA, Munro AJ, Stewart S, Rampling R, Lambert HB, McKenzie CG, Soutter P, Rahemtulla A, Hooker G, Sivolapenko GB, Snook D, Courtenay-Luck N, Dhokia B, Krausz T, Taylor-Papadimitriou J, Durbin H, Bodmer WF. Antibody-guided irradiation of advanced ovarian cancer with intraperitoneally administered radiolabeled monoclonal antibodies. *J Clin Oncol* 1987;5:1890-9.
118. Mach J-P, Pèlegri A, Buchegger F. Imaging and therapy with monoclonal antibodies in non-hematopoietic tumors. *Curr Opin Immunol* 1991;3:685-93.
119. Pectasides D, Stewart S, Courtenay-Luck N, Rampling R, Munro R, Krausz T, Dhokia B, Snook D, Hooker G, Durbin H, Taylor-Papadimitriou J, Bodmer WF, Epenetos AA. Antibody-guided irradiation of malignant pleural and pericardial effusions. *Br J Cancer* 1986;6:727-35.
120. Lashford LS, Davies AG, Richardson RB, Bourne SP, Bullimore JA, Eckert H, Kemshead JT, Coakham HB. A pilot study of <sup>131</sup>I monoclonal antibodies in the therapy of leptomeningeal tumors. *Cancer* 1988;61:857-68.
121. Bamias A, Keane P, Krausz T, Williams G, Epenetos AA. Intravesical administration of radiolabeled antitumor monoclonal antibody in bladder carcinoma. *Cancer Res* 1991;51:724-8.
122. Malamitsi J, Zorzos J, Varvarigou D, Archimandritis S, Dassios C, Skarlos DV, Dimitriou P, Likourinas M, Zizi A, Proukakis C. Immunolocalization of transitional cell carcinoma of the bladder with intravesically administered technetium-99m labelled HMFG1 monoclonal antibody. *Eur J Nucl Med* 1995;22:25-31.
123. Weinstein JN, Steller MA, Covell DG, Holton OD, Keenan AM, Sieber SM, Parker RJ. Monoclonal antitumor antibodies in the lymphatics. *Cancer Treat Rep* 1984;68:257-64.
124. Goldenberg DM. Future role of radiolabeled monoclonal antibodies in oncological diagnosis and therapy. *Sem Nucl Med* 1989;19:332-9.
125. Taylor JL, Taylor DN, Lowry C, Keeling AA, Bradwell AR, McIntosh A, Rhodes A. Radioimmunoscintigraphy of metastatic breast carcinoma. *Eur J Surg Oncol* 1992;18:57-63.
126. Goldenberg DM, Goldenberg H, Sharkey RM, Lee RE, Higgenbotham-Ford E, Horowitz JA, Hall TC, Pinsky CM, Hansen HJ. Imaging of colorectal carcinoma with radiolabeled antibodies. *Sem Nucl Med* 1989;19:262-281.
127. Abdel-Nabi H, Doerr RJ. Clinical applications of indium-111-labeled monoclonal antibody imaging in colorectal patients. *Sem Nucl Med* 1993;23:99-113.
128. Murray JL, Rosenblum MG, Sobol RE, Bartolomew RM, Plager CE, Haynie TP, Jahns MF, Glenn HJ, Lamki L, Benjamin RS, Papadopoulos N, Boddie AW, Frincke JM, David GS, Carlo DJ, Hersch EM. Radioimmunolabeling in malignant melanoma with <sup>111</sup>In-labeled monoclonal antibody 96.5. *Cancer Res* 1985;45:2367-81.
129. Salk D. Technetium-labeled monoclonal antibodies for imaging metastatic melanoma: results of a multicenter study. *Sem Oncol* 1988;15:608-18.
130. Rosen ST, Zimmer AM, Goldman-Leikin R, Gordon LI, Kazikiewicz JM, Kaplan EH, Variakojis D, Marder RJ, Dykewicz MS, Pergies A, Silverstein EA, Roenigk HH, Spies SM. Radioimmunodetection and radioimmunotherapy of cutaneous T cell lymphomas using an <sup>131</sup>I-labeled monoclonal antibody: an Illinois Cancer Council study. *J Clin Oncol* 1987;5:562-73.
131. Neal CE, Swenson LC, Fanning J, Texter JH. Monoclonal antibodies in ovarian and prostate cancer. *Sem Nucl Med* 1993;23:114-26.
132. Breitz HB, Sullivan K, Nelp WB. Imaging lung cancer with radiolabeled antibodies. *Sem Nucl Med* 1993;23:127-32.
133. Larson SM. Radioimmunology. Imaging and therapy. *Cancer* 1991;67:1253-60.
134. Goldenberg DM. Monoclonal antibodies in cancer detection and therapy. *Am J Med* 1993;94:297-312.
135. Ind TEJ, Granowska M, Britton KE, Morris G, Lowe DG, Hudson CN, Shepherd JH. Peroperative radioimmunodetection of ovarian carcinoma using a hand-held gamma detection probe. *Br J Cancer* 1994;70:1263-66.
136. Kairemo KJA. Positron emission tomography of monoclonal antibodies. *Acta Oncologica* 1993;32:825-30.
137. Fagerberg J, Frödin J-E, Wigzell H, Mellstedt H. Induction of an immune network cascade in cancer patients treated with monoclonal antibodies (ab<sub>1</sub>). I. May induction of ab<sub>1</sub>-reactive T cells and anti-anti-idiotypic antibodies (ab<sub>2</sub>) lead to regression after mAb therapy? *Cancer Immunol Immunother* 1993;37:264-70.
138. Bhattacharya Chatterjee M, Foon KA, Köhler H. Idiotype antibody immunotherapy of cancer. *Cancer Immunol Immunother* 1994;38:75-82.
139. Bier H. Monoklonale Antikörper. Ein ansatz zur diagnose und behandlung von mikrometastasen. *HNO* 1994;42:255-6.
140. Dongen GAMS van, Brakenhoff RH, Bree R de, Gerretsen M, Quak JJ, Snow GB. Progress in radioimmunotherapy of head and neck cancer. *Cancer Reports* 1994;1:259-64.
141. Falini B, Bolognesi A, Flenghi L, Tazzari PL, Broe MK, Stein H, Dürkop H, Aversa F, Corneli P, Pizzolo G, Barbabietola G, Sabatini E, Pileri S, Martelli MF, Strippa F. Response of refractory Hodgkin's disease to monoclonal anti-CD30 immunotoxin. *Lancet* 1992;339:1195-6.
142. Sung M-W, Yasumura S, Johnson JT, Van Dongen GAMS, Whiteside TL. Natural killer (NK) cells as effectors of antibody-dependent cytotoxicity with chimeric antibodies reactive with human squamous cell carcinomas of the head and neck. *Int J Cancer* 1995, in press.
143. Riethmüller G, Schneider-Gadicke E, Johnson JP. Monoclonal antibodies in cancer therapy. *Curr Opin Immun* 1993;5:732-39.
144. Janson CH, Tehrani M, Wigzell. Rational use of biological response modifiers in haematological malignancies - a review of treatment with interferon, cytotoxic cells and antibodies. *Leuk Res* 1989;13:1039-46.
145. Cheung NKV, Lazarus H, Miraldi FD, Abramowsky CR, Kallick S, Saarinen UM, Spitzer T, Strandjord SE, Coccia PF, Berger NA. Ganglioside G<sub>M2</sub> specific monoclonal antibody 3F8: a phase I study in patients with neuroblastoma and malignant melanoma. *J Clin Oncol* 1987;5:1430-40.
146. Ragnhammar P, Frödin J-E, Mellstedt H. Cytotoxicity of white cell activated by granulocyte-colony-stimulating factor and macrophage-colony-stimulating factor against tumor cells in the presence of various monoclonal antibodies. *Cancer Immunol Immunother* 1994;39:254-62.
147. Steplewski Z, Sun LK, Shearman CW, Ghayeb J, Daddona P, Koprowski H. Biological activity of human-mouse IgG1, IgG2, IgG3, and IgG4 chimeric monoclonal antibodies with antitumor specificity. *Proc Natl Acad Sci USA*, 1988;85:4852-6.
148. Sears HF, Herlyn D, Steplewski Z, Koprowski H. Phase II clinical trial of a murine monoclonal antibody cytotoxic for gastrointestinal adenocarcinoma. *Cancer Res* 1985;45:5910-3.
149. Tempero MA, Haga Y, Sivinski C, Steplewski Z, Kay HD, Pour P. Immunotherapy with monoclonal antibody (Mab) in pancreatic adenocarcinoma.
150. Saleh MN, Khazaeli MB, Grizzle WE, Wheeler RH, Lawson S, Liu T, Russel C, Meredith R, Schlom J, LoBuglio AF. Phase I clinical trial of murine monoclonal antibody D612 in patients with metastatic gastrointestinal cancer. *Cancer Res* 1993;53:4555-62.
151. Masucci G, Ragnhammar P, Frödin J-E, Hjelm A-L, Wersäll P, Fagerberg J, Osterborg A, Mellstedt H. Chemotherapy and immunotherapy of colorectal cancer. *Med Oncol Tumor Pharmacother* 1991;8:207-20.
152. Mujoo K, Cheresch DA, Yang HM, Reisfeld RA. Disialoganglioside-G<sub>M2</sub> on human neuroblastoma cells: target antigen for monoclonal antibody-mediated cellular cytotoxicity and suppression of tumor growth. *Cancer Res* 1987;47:1098-1104.
153. Riethmüller G, Schneider-Gadicke E, Schlimok G, Schmiegeler W, Raab R, Höffken K, Gruber R, Pichlmaier H, Hirche H, Pichlmaier R, Buggisch P, Witte J. Randomised trial of monoclonal antibody for adjuvant therapy of resected Dukes'C colorectal carcinoma. *Lancet* 1994;343:1177-883.
154. Bast RC. Progress in radioimmunotherapy. *New Engl J Med* 1993;329:1266-8.
155. Cortesina G, Sacchi M, Galeazzi E, De Stefani A. Immunology of head and neck cancer:



- perspectives. *Head Neck* 1993;15:74-7.
156. Ragnhammer P, Fagerberg J, Frodin J-E, Hjelm AL, Lindenmalm C, Magnusson I, Masucci G, Mellstedt H. Effect of monoclonal antibody 17-1A and GM-CSF in patients with advanced colorectal carcinoma: long lasting, complete remissions can be induced. *Int J Cancer* 1993;53:751-8.
  157. Langmuir VK, Fowler JF, Knox SJ, Wessels BW, Sutherland RM, Wong JYC. Radiobiology of radiolabeled antibody therapy as applied to tumor dosimetry. *Med Phys* 1993;20:601-10.
  158. Wessels BW, Harisiadis L, Carabell SC. Dosimetry and radiobiological efficacy of clinical radioimmunotherapy. *J Nucl Med* 1989;30:827.
  159. Order SE, Stillwagon GB, Klein JL, Leichner PK, Siegelman SS, Fishman EK, Ettinger DS, Haulk T, Kopher K, Finney K, et al. Iodine-131 antiferritin, a new treatment modality in hepatoma: a Radiation Therapy Oncology Group study. *J Clin Oncol* 1985;3:1573-82.
  160. Press OW, Eary JF, Appelbaum FR, Martin PJ, Badger CC, Nelp WB, Glenn S, Butchko G, Fischer D, Porter B, Matthews DC, Fischer LD, Bernstein ID. Radiolabeled-antibody therapy of B-cell lymphoma with autologous bone marrow support. *New Engl J Med* 1993;329:1219-24.
  161. Kaminski MS, Zasadny KR, Francis IR, Mulik AW, Ross CW, Moon S, Crawford SM, Burgess JM, Petry NA, Butchko GM, Glenn SD, Wahl RL. Radioimmunotherapy of B-cell lymphoma with [<sup>131</sup>I]anti-B1 (anti-CD20) antibody. *New Engl J Med* 1993;329:459-65.
  162. Larson SM, Carraquillo JA, McGruffin RW, Krohn KA, Ferrens JM, Hill LD, Beaumier PL, Reynolds JC, Hellström KE, Hellström I. Use of I-131 labeled, murine Fab against a high molecular weight antigen of human melanoma: preliminary experience. *Radiology* 1985;155:487-92.
  163. Hird V, Maraveyas A, Snook D, Dhokia B, Soutter WP, Meares C, Stewart JSW, Mason P, Lambert HE, Epenetos AA. Adjuvant therapy of ovarian cancer with radioactive monoclonal antibody. *Br J Cancer* 1993;68:403-6.
  164. Reilly RM. Radioimmunotherapy of malignancies. *Clin Pharm* 1991;10:359-75.
  165. Pizer BI, Papanastassiou V, Mosely R, Tzanis S, Hancock J, Kemshead JT, Coakham HB. Meningeal leukemia and medulloblastoma: preliminary experience with intrathecal radioimmunotherapy. *Antib Immunoonj Radiopharm* 1991;4:753-61.
  166. Siegel JA, Goldenberg DM, Badger CC. Radioimmunotherapy dose estimation in patients with B-cell lymphoma. *Med Phys* 1993;20:579-82.
  167. Ernst CS, Shen J-W, Litwin S, Herlyn M, Koprowski H, Sears HF. Multiparameter evaluation of the expression in situ of normal and tumor-associated antigens in human colorectal carcinoma. *J Natl Cancer Inst* 1986;77:387-95.
  168. Scheinberg DA, Strauss DJ, Yeh SD, Divgi C, Garin-Chesa P, Graham M, Pentlow K, Coit D, Oettgen HF, Old LJ. A phase I toxicity, pharmacology, and dosimetry trial of monoclonal antibody OKB7 in patients with Non-Hodgkin's lymphoma: effects of tumor burden and antigen expression. *J Clin Oncol* 1990;8:792-803.
  169. Beckett MJ, Lipford GB, Haley CL, Schellhammer PF, Wright GL. Monoclonal antibody PD41 recognizes an antigen restricted to prostate adenocarcinomas. *Cancer Res* 1991;51:1326-33.
  170. Oosterwijk E, Ruiter DJ, Hoedemaker PJ, Pauwels EKJ, Jonas U, Zwartendijk J, Warnaar SO. Monoclonal antibody G250 recognizes a determinant present in renal-cell carcinoma and absent from normal kidney. *Int J Cancer* 1986;38:489-94.
  171. Oosterwijk E, Bander NH, Divgi CR, Welt S, Wakka JC, Finn RD, Carswell EA, Larson SM, Warnaar SO, Fleuren GJ, Oettgen HF, Old LJ. Antibody localization in human renal cell carcinoma: a phase I study of monoclonal antibody G250. *J Clin Oncol* 1993;11:738-50.
  172. Molinolo A, Simpson JF, Thor A, Schlom J. Enhanced tumor binding using immunohistochemical analysis by second generation anti-tumor-associated glycoprotein 72 monoclonal antibodies versus monoclonal antibody B72.3 in human tissue. *Cancer Res* 1990;50:1291-98.
  173. Epenetos AA, Snook D, Durbin H, Johnson PM, Taylor-Papadimitriou J. Limitations of radiolabeled monoclonal antibodies for localization of human neoplasms. *Cancer Res* 1986;46:3183-91.
  174. Chatal J-F, Saccavini J-C, Gestin J-F, Thédrez P, Curtet C, Kremer M, Guerreau D, Nobile D, Fumoleau P, Guillard Y. Biodistribution of indium-111-labeled OC 125 monoclonal antibody intraperitoneally injected into patients operated on for ovarian carcinomas. *Cancer Res* 1989;49:3087-94.
  175. Zalutsky MR, Mosely RP, Coakham HB, Coleman RE, Bigner DD. Pharmacokinetics and tumor localization of [<sup>131</sup>I]-labeled anti-tenascin monoclonal antibody 81C6 in patients with gliomas and other intracranial malignancies. *Cancer Res* 1989;49:2807-13.
  176. Scheinberg DA, Straus DJ, Yeh SD, Divgi C, Garin-Chesa P, Graham M, Pentlow K, Coit D, Oettgen HF, Old LJ. A phase I toxicity, pharmacology, and dosimetry trial of monoclonal antibody OKB7 in patients with Non-Hodgkin's lymphoma: Effects of tumor burden and antigen expression. *J Clin Oncol* 1990;8:792-803.
  177. Larson SM, Carraquillo JA, Colcher DC, Yokoyama K, Reynolds JC, Bacharach A, Raubitschek A, Pace L, Finn RD, Rotman M, Stabin M, Neumann RD, Sugarbaker P, Schlom J. Estimates of radiation absorbed dose for intraperitoneally administered Iodine-131 radiolabeled B72.3 monoclonal antibody in patients with peritoneal carcinomatosis. *J Nucl Med* 1991;32:1661-7.
  178. Bares R, Fass J, Hauptmann S, Braun J, Grehl O, Reinartz R, Buell U, Schumpelick V, Mittmayer C. Quantitative analysis of anti-CEA antibody accumulation in human colorectal carcinomas. *J Nucl Med* 1993;32:65-72.
  179. Oosterwijk E, Bander NH, Divgi CR, Welt S, Wakka JC, Finn RD, Carswell EA, Larson SM, Warnaar SO, Fleuren GJ, Oettgen HF, Old LJ. Antibody localization in human renal cell carcinoma: a phase I study of monoclonal antibody G250. *J Clin Oncol* 1993;11:738-50.
  180. Rosenblum MG, Levin B, Roh M, Hohn D, McCabe R, Thompson L, Cheung L, Murray JL. Clinical pharmacology and tissue disposition studies of [<sup>131</sup>I]-labeled anticarcinoma human monoclonal antibody LiCo 16.88. *Cancer Immunol Immunother* 1994;39:397-400.
  181. Maraveyas A, Stafford N, Rowlinson-Busza G, Stewart JSW, Epenetos AA. Pharmacokinetics, biodistribution, and dosimetry of specific and control radiolabeled monoclonal antibodies in patients with primary head and neck squamous cell carcinoma. *Cancer Res* 1995;55:1060-9.
  182. Chatal J-F, Saccavini J-C, Gestin J-F, Thédrez P, Curtet C, Kremer M, Guerreau D, Nobile D, Fumoleau P, Guillard Y. Biodistribution of Indium-111-labeled OC 125 monoclonal antibody intraperitoneally injected into patients operated on for ovarian carcinomas. *Cancer Res* 1989;49:3087-94.
  183. Williams LE, Bares RB, Fass J, Hauptmann S, Schumpelick V, Buell U. Uptake of radiolabeled anti-CEA antibodies in human colorectal primary tumors as a function of tumor mass. *Eur J Nucl Med* 1993;20:345-7.
  184. Schmid U, Schirmacher V, Momburg F, Matzku S. Preferential antibody targeting to small lymphoma metastases in the absence of the primary tumour. *Eur J Cancer* 1993;29A:217-225.
  185. Schlom J, Horan Hand P, Greiner JW, Colcher D, Shrivastav S, Carraquillo JA, Reynolds JC, Larson SM, Raubitschek A. Innovations that influence the pharmacology of monoclonal antibody guided tumor targeting. *Cancer Res (suppl)* 1990;50:820-7s.
  186. Begent RHJ, Ledermann JA, Green AJ, Bagshawe KD, Riggs SJ, Searle F, Keep PA, Adam T, Dale RG, Glaser MG. Antibody distribution and dosimetry in patients receiving radiolabelled antibody therapy for colorectal cancer. *Br J Cancer* 1989;60:406-12.
  187. Marshall D, Pedley RB, Boden JA, Boden R, Begent RHJ. Clearance of circulating radio-antibodies using streptavidin or second antibodies in a xenograft model. *Br J Cancer* 1994;69:502-7.
  188. Doussal J-M le, Chetanneau A, Gruaz-Guyon A, Martin M, Gautherot E, Lehur P-A, Chatal J-F, Delaage M, Barbet J. Bispecific monoclonal antibody-mediated targeting of an Indium-111-labeled DTPA dimer to primary colorectal tumors: pharmacokinetics, biodistribution, scintigraphy and immune response. *J Nucl Med* 1993;34:1662-71.
  189. Blumenthal RD, Fand I, Sharkey RM, Boerman OC, Kashi R, Goldenberg DM. The effect of antibody protein dose on the uniformity of tumor distribution of radioantibodies: an autoradiographic study. *Cancer Immunol Immunother* 1991;33:351-8.
  190. Patt YZ, Lamki LM, Haynie TP, Unger MW, Rosenblum MG, Shirkoda A, Murray JL. Improved tumor localization with increased dose of Indium-111-labeled anti-carcinoembryonic antigen monoclonal antibody ZCE-025 in metastatic colorectal cancer. *J Clin Oncol* 1988;6:1220-30.
  191. Carraquillo JA, Abrams PG, Schroff RW, Reynolds JC, Woodhouse CS, Morgan AC, Keenan AM, Foon KA, Perentesis P, Marshall S, Horowitz M, Szymendra J, Englert J, Oldham RK, Larson SM. Effect of antibody dose on the imaging and biodistribution of Indium-111 9.2.27 anti-



- melanoma monoclonal antibody. *J Nucl Med* 1988;29:39-47.
192. Zenner HP. Monoklonale Antikörper zur Erkennung von Larynxkarzinomenzellen. *Arch Otorhinolaryngol* 1981;233:161-72.
  193. Carey TE, Kimmel KA, Schwartz DR, Richter DE, Baker SR, Krause CJ. Antibodies to human squamous cell carcinoma. *Otolaryngol Head Neck Surg* 1983;91:482-91.
  194. Kimmel KA, Carey TE. Altered expression in squamous carcinoma cells of an orientation restricted epithelial antigen detected by monoclonal antibody A9. *Cancer Res* 1986;46:3614-23.
  195. Boeheim K, Speak JA, Frei E, Bernal SD. SQM1 antibody defines a surface membrane antigen in squamous carcinoma of the head and neck. *Int J Cancer* 1985;36:137-42.
  196. Stahl RA, Speak JA, Bernal SD. Murine monoclonal antibody LAM2 defines cell membrane determinant with preferential expression on human lung small-cell carcinomas. *Int J Cancer* 1985;35:11-7.
  197. Kyoizumi S, Akiyama M, Kono N, Kobuke K, Hakoda M, Jones SL, Yamakido M. Monoclonal antibodies to human squamous cell carcinoma of the lung and their application to tumor diagnosis. *Cancer Res* 1985;45:3574-81.
  198. Prat M, Bussolita G, Spinnato MR, Comoglio PM. Monoclonal antibodies against the human epidermoid carcinoma A 431. *Cancer Detection and Prevention* 1985;8:169-79.
  199. Ranken R, White CF, Gottfried TG, Yonkovich SJ, Blazek BE, Moss MS, Fee WE, Liu Y-S V. Reactivity of monoclonal antibody 17.13. with human squamous cell carcinoma and its application to tumor diagnosis. *Cancer Res* 1987;47:5684-90.
  200. Myoken Y, Moroyama T, Michaiichi S, Takada K, Namba M. Monoclonal antibodies against human oral squamous cell carcinoma reacting with keratin proteins. *Cancer* 1987;60:2927-37.
  201. Giocanni J, Samsin J, Zanghellini E, Mazzeu C, Ettore F, Demard F, Chauvel P, Duplay H, Schneider M, Laurent J-C, Lalanne CM. Characterization of a new surface epitope specific for human epithelial cells defined by a monoclonal antibody and application to tumor diagnosis. *Cancer Res* 1987;47:4417-24.
  202. Samuel J, Noujaim AA, Williams DJ, Brezinska GS, Haines DM, Longenecker BM. A novel marker for basal (stem) cells of mammalian stratified squamous epithelia and squamous cell carcinomas. *Cancer Res* 1989;49:2465-70.
  203. Tatake RJ, Amin KM, Maniar HS, Jambhekar NA, Srikhande SS, Gangal SG. Monoclonal antibody against human squamous-cell-carcinoma-associated antigen. *Int J Cancer* 1989;44:840-5.
  204. Cobb LM. Intratumour factors influencing the access of antibody to tumour cells. *Cancer Immunol Immunother* 1989;28:235-40.
  205. Fantozzi RD. Development of monoclonal antibodies with specificity to oral squamous cell carcinoma. *Laryngoscope* 1991;101:1076-80.
  206. Parsons PG, Leonard JH, Kearsley JH, Takahashi H, Lin-Jian X, Moss DJ. Characterization of a novel monoclonal antibody, 3H-1, reactive with squamoproliferative lesions and squamous-cell cancers. *Int J Cancer* 1991;47:847-52.
  207. Yoshiura M, Murakami H, Tashiro H, Kurisu K. Production of a human monoclonal antibody to normal basal and squamous cell carcinoma-associated antigen. *J Oral Pathol Med* 1993;22:451-8.
  208. Harada H, Osaki Y, Kukita T, Kurisu K, Tashiro H, Yasumoto S. Monoclonal antibody G6K12 specific for membrane-associated differentiation marker of human stratified squamous epithelia and squamous cell carcinoma. *J Oral Pathol Med* 1993;22:145-52.
  209. Quak JJ, Balm AJM, Brakkee JGP, Scheper RJ, Meijer CJLM, Snow GB. Production of monoclonal antibodies to squamous cell carcinoma antigens. *Arch Otolaryngol Head Neck Surg* 1990;116:181-5.
  210. Quak JJ, Balm AJM, Van Dongen GAMS, Brakkee JGP, Scheper RJ, Snow GB, Meijer CJLM. A 22-kDa surface antigen detected by monoclonal antibody E48 is exclusively expressed in stratified and transitional epithelia. *Am J Pathol* 1990;136:191-7.
  211. Schrijvers AHGJ, Quak JJ, Uytendinck AM, Van Walsum M, Meijer CJLM, Snow GB, Van Dongen GAMS. MAb U36, a novel monoclonal antibody successful in immunotargeting of squamous cell carcinoma of the head and neck. *Cancer Res* 1993;53:4383-90.
  212. Quak JJ, Schrijvers AHGJ, Brakkee JGP, Davis HD, Scheper RJ, Balm AJM, Meijer CJLM, Snow GB, Van Dongen GAMS. Expression and characterization of two differentiation antigens in stratified squamous epithelia and carcinomas. *Int J Cancer* 1992;50:507-23.
  213. Quak JJ, Van Dongen GAMS, Gerretsen M, Hayashida D, Balm AJM, Brakkee JGP, Snow GB, Meijer CJLM. Production of monoclonal antibody (K931) to squamous cell carcinoma antigen identified as the 17-1A antigen. *Hybridoma* 1990;9:377-87.
  214. Koprowski H, Stepleski Z, Mitchell K, Herlyn M, Herlyn D, Fuhrer P. Colorectal carcinoma antigens detected by hybridoma antibodies. *Somat Cell Genet* 1979;5:957-72.
  215. Edwards DP, Grzyb KT, Dressler LG, Mansel RE, Zava DT, Sledge GW, McGuire WL. Monoclonal antibody identification and characterization of a M, 43,000 membrane glycoprotein associated with human breast cancer. *Cancer Res* 1986;46:1306-17.
  216. Takahashi H, Wilson B, Ozturk M, Mott P, Strauss W, Isselbacher KJ, Wands JR. In vivo localization of human colon adenocarcinoma by monoclonal antibody binding to a highly expressed cell surface antigen. *Cancer Res* 1988;48:6573-9.
  217. Tranter RMD, Fairweather DS, Bradwell AR, Dykes PW, Watson-James S, Chandler S. The detection of squamous cell tumours of the head and neck using radio-labelled antibodies. *J Laryngol Otol* 1984;98:71-4.
  218. Soo KC, Ward M, Roberts KR, Keeling F, Carter RL, McCready VR, Ott RJ, Powell E, Ozanne B, Westwood JH, Gusterson BA. Radioimmunoscintigraphy of squamous carcinomas of the head and neck. *Head Neck Surg* 1987;9:349-52.
  219. Kairemo KJA, Hopsu EVM. Immunoscintigraphy in laryngeal and pharyngeal carcinomas using indium-111 labelled monoclonal antibody. *Acta Oncol* 1990;29:533-8.
  220. Timon CI, McShane D, Hamilton D, Walsh MA. Head and neck cancer localization with indium labelled carcinoembryonic antigen: a pilot project. *J Otolaryngol* 1991;20:283-7.
  221. Baum RP, Adams S, Kiefer J, Niesen A, Knecht R, Howaldt H-P, Hertel A, Adamietz IR, Sykes T, Bomaface GR, Noujaim AA, Hör G. A novel technetium-99m labeled monoclonal antibody (174H.64) for staging head and neck cancer by immuno-SPECT. *Acta Oncol* 1993;32:747-51.
  222. Dvigi CR, Welt S, Kris M, Real FX, Yeh SDJ, Gralla R, Merchant B, Schweighart S, Unger M, Larson SM, Mendelson J. Phase I and imaging trial of Indium 111-labeled anti-epidermal growth factor receptor monoclonal antibody 225 in patients with squamous cell lung carcinoma. *J Natl Cancer Inst* 1991;83:97-104.
  223. Kairemo KJA, Hopsu EVM. Imaging of tumours in the parotid region with indium-111 labelled monoclonal antibody reacting with carcinoembryonic antigen. *Acta Oncol* 1990;29:539-43.
  224. Shikani AH, Richtsmeier WJ, Klein JL, Kopher KA. Radiolabeled antibody therapy for squamous cell carcinoma of the head and neck. *Arch Otolaryngol Head Neck Surg* 1992;118:521-5.
  225. Gerretsen M, Visser GWM, Walsum W van, Meijer CJLM, Snow GB, Dongen GAMS van. <sup>186</sup>Re-labeled monoclonal antibody E48 IgG mediated therapy of human head and neck squamous cell carcinoma xenografts. *Cancer Res* 1993;53:3524-9.
  226. Gerretsen M, Visser GWM, Brakenhoff RH, Snow GB, Dongen GAMS van. Complete ablation of small head and neck squamous cell carcinoma xenografts with <sup>186</sup>Re-labeled monoclonal antibody E48. *Cell Biophys* 1994;24:135-42.
  227. Ding L, Samuel J, MacLean GD, Noujaim AA, Diener E, Longenecker BM. Effective drug-antibody targeting using a novel monoclonal antibody against the proliferative compartment of mammalian squamous carcinomas. *Cancer Immunol Immunother* 1990;31:105-9.
  228. Donald PJ, Cardiff RD, Kendall K. Monoclonal antibody-porphyrin conjugate for head and neck cancer: The possible magic bullet. *Otolaryngol Head Neck Surg* 1991;105:781-7.
  229. Folli S, Westermann P, Braichotte D, Pelegri A, Wageniers G, Van de Bergh H, Mach J-P. Antibody-indocyanin conjugates for immunophotodetection of human squamous cell carcinomas in nude mice. *Cancer Res* 1994;54:2643-9.



## ADDENDUM. REMARKS ON ANALYSIS OF DATA.

For topographical evaluation on the detection of lymph node metastases, the findings were recorded per neck side (left or right) and per lymph node level (I to V) and compared to the histopathological outcome of the surgical specimen (gold standard). Per neck side or level (Fig. 2) diagnostic findings can be considered true positive (TP), false negative (FN), false positive (FP), or true negative (TN). To compare the diagnostic findings of the different techniques different statistical measures can be used. The sensitivity is defined as the chance of a positive test finding when a metastasis is present, while the specificity is the chance of a negative finding when no metastases is present in that side or level. The accuracy is the proportion of all test findings that are correct, whereas the overall error expresses the chance that the test findings are incorrect. The positive predictive value is defined as the probability of having metastasis, given a positive test finding, while the negative predictive value is the probability of not having metastasis if the test findings are negative.

To assess agreement between tests, the measure Kappa can be used. Kappa reflects agreement between tests beyond the agreement expected by chance alone. The size of Kappa, of course, depends both on the diagnostic tests and the group of patients. When Kappa is systematically smaller for one group of patients than for another, it is likely that this group is more difficult to assess than the other group of patients.

A few remarks on these statistical measures should be made. Because sensitivity and specificity express the relationship between test findings and the histopathological outcome (gold standard), these measures are generally accepted to be characteristics of a certain test. However, these statistical measures are dependent on the population studied. If the prevalence of lymph node metastases is low, the specificity will be relatively high. On the other hand if this prevalence is high, the sensitivity is relatively high. All other measures are also dependent on the patient population studied. Also the value of these parameters will not be very precise if the number of patients is low.

When data are available at the end of clinical trials, a statistical test (e.g., Student's t-test) is performed to compare the various outcomes. The statistical significant difference between data is reflected in its "p-value". If the p-value is less than the significance level which was chosen before the trial (in most cases  $p < 0.05$ ), the test is said to be statistically significant. If the standard deviation is high and/or the number of patients is low the p-value will be high. Therefore, statistics in small groups may be of limited value.

## REFERENCES

1. Fleiss JL. Statistical methods for rates and proportions. New York: John Wiley; 1981.
2. Altman DG. Practical statistics for medical research. London: Chapman & Hall; 1991.

## Chapter 2

## Clinical Imaging of Head and Neck Cancer with $^{99m}\text{Tc}$ -labeled Monoclonal Antibody E48 IgG or F(ab')<sub>2</sub>

Remco de Bree <sup>1</sup>, Jan C. Roos <sup>2</sup>, Jasper J. Quak <sup>1</sup>, Willem den Hollander <sup>2</sup>,  
Michiel W.M. van den Brekel <sup>1</sup>, Jacqueline E. van der Wal <sup>3</sup>, Hilde Tobi <sup>1</sup>,  
Gordon B. Snow <sup>1</sup>, and Guus A.M.S. van Dongen <sup>1</sup>

Departments of <sup>1</sup> Otolaryngology / Head and Neck Surgery,  
<sup>2</sup> Nuclear Medicine, and <sup>3</sup> Oral Pathology,  
Free University Hospital, Amsterdam, The Netherlands

Journal of Nuclear Medicine 1994; 35: 775-783

## ABSTRACT

In 32 patients, who were suspected of having neck lymph node metastasis from a histologically proven squamous cell carcinoma of the head and neck (HNSCC), the diagnostic value of  $^{99m}\text{Tc}$ -labeled (750 MBq) monoclonal antibody (1-2 mg) E48 IgG ( $n=17$ ) and its  $\text{F(ab')}_2$  fragment ( $n=15$ ) was evaluated and compared.

Preoperative findings on lymph node status obtained by radioimmunoscinigraphy (RIS), computerized tomography (CT), magnetic resonance imaging (MRI), and palpation were defined per side (left and/or right side of the neck) as well as per lymph node level (I through V) and compared to the histopathological outcome of the neck dissection specimen.

All 31 tumors at the primary site were visualized. RIS was correct in 201 of 221 levels (accuracy 91 %) and in 38 of 47 sides (accuracy 81 %). Fifteen levels and 7 sides with limited tumor load were scored falsely negative and 5 levels and 2 sides were scored falsely positive. Sensitivity and specificity of RIS were similar to those of palpation, CT, and MRI. The diagnostic value of RIS with E48  $\text{F(ab')}_2$  or E48 IgG appeared to be similar.

The present study shows that RIS with either E48  $\text{F(ab')}_2$  or E48 IgG is as valuable as the other imaging techniques. The selective accumulation of radioactivity in tumor tissues, in combination with the known intrinsic radiosensitivity of HNSCC, does justify the development of radioimmunoconjugates for radioimmunotherapy.

## INTRODUCTION

Squamous cell carcinoma (SCC) is the major histological type of neoplasms arising from the head and neck. Since the status of the cervical lymph nodes is the single most important tumor related prognostic factor, it is of great importance to know the exact involvement of the neck nodes <sup>1,2,3</sup>.

The assessment of the status of the neck nodes is mainly based on palpation, although this is generally accepted to be inaccurate. The overall error in the assessment of the presence or absence of cervical lymph node metastasis is 20 to 30 % <sup>4</sup>. The high false-positive and false-negative rates of palpation causes over- and undertreatment in many patients. Modern imaging techniques like computerized tomography (CT), magnetic resonance imaging (MRI), and ultrasound (US) appear to be superior to palpation. Since none of these techniques is fully accurate, the need for a more reliable technique remains. US-guided aspiration cytology has been proven to be superior to the current imaging techniques <sup>5</sup>. However, this technique strongly depends on the skill of the ultrasonographer and cytopathologist. Therefore, the assessment of the status of the neck in patients with SCC of the head and neck (HNSCC) needs further improvement.

Radioimmunoscinigraphy (RIS) with monoclonal antibodies (MAbs) is an innovative imaging technique <sup>6</sup>. In our institute we developed a murine monoclonal antibody, designated E48, with high specificity to HNSCC <sup>7</sup>. A strong reactivity of MAb E48 was seen towards primary as well as metastatic SCC <sup>8</sup>. The antibody has been demonstrated to localize SCC in the nude mice model with high specificity <sup>9</sup>. In this murine model, E48  $\text{F(ab')}_2$  fragment was shown to be superior for tumor detection as compared to the intact (IgG) antibody <sup>10</sup>. Therefore, we preferred to use  $^{99m}\text{Tc}$ -labeled E48  $\text{F(ab')}_2$  in a first clinical study to assess the safety and accuracy of RIS with this MAb in patients with histologically proven HNSCC and clinically suspected for having lymph node metastases. Recently, the promising preliminary results in the first 10 HNSCC patients were published <sup>11</sup>. RIS was found to detect all primary tumors and to be correct in 13 of 13 tumor involved neck sides and 17 of 20 tumor involved lymph node levels. Results with RIS were slightly better than with palpation, CT, or MRI. An unexpected finding in this study was the consistent uptake of activity in the normal oral mucosa and the adrenals. Uptake in the mouth may hamper the diagnosis of oral cancer and submandibular and subdiaphragmatic lymph nodes in RIS. Uptake in the adrenal may be a problem in radioimmunotherapy (RIT). Until now, no explanation has been found for the adrenal uptake. Immunohistochemical evaluation prior to this study showed no reactivity of MAb E48 with frozen adrenal tissues. The uptake in the mouth is probably due to specific antigen-antibody interaction, in which the immunoconjugate has overcome the natural barriers offered by the capillary endothelium and the basement membrane of the mucosal epithelium. We hypothesized that the uptake in normal mucosa of the oral cavity might be reduced when using  $^{99m}\text{Tc}$ -labeled E48 IgG.

Based on the first promising results <sup>11</sup>, we extended the RIS study with the option in mind to use either MAb E48  $\text{F(ab')}_2$  or IgG in future RIT studies. In the present report, imaging results with E48  $\text{F(ab')}_2$  in 15 HNSCC patients are compared to those of E48 IgG in 17 patients.



## PATIENTS AND METHODS

**Patient Study.** The protocol was approved by the Dutch Health Council and by the institutional review board of the Free University Hospital. Informed consent was obtained from all participants.

Thirty-two patients, who were at risk for having neck lymph node metastasis from a histological proven HNSCC and planned to undergo neck dissection(s), participated in this study. The primary tumor and the status of neck lymph nodes were classified according to the TNM system of the International Union Against Cancer, the UICC<sup>12</sup>. One patient had his primary tumor resected previously. Prior to enrollment, a biopsy of the primary tumor, if available, had to show a positive immunoperoxidase staining with MAb E48. Prior and up to 7 days after administration of <sup>99m</sup>Tc-labeled MAb E48, urine and blood were obtained for chemical analysis and assessment of MAb pharmacokinetics. Electrolytes, aspartate aminotransferase, alanine aminotransferase, alkaline phosphatase, gamma-glutamyl transferase, lactate dehydrogenase, urea nitrogen, creatinine, and uric acid were determined in serum. Hematological determinations included hemoglobin, hematocrit, platelet count, white blood cell count and differentiation, and sedimentation rate. Skin tests were not performed. Vital signs were recorded before and up to 3 h after injection.

Fifteen patients received 1-2 mg E48 F(ab')<sub>2</sub> radiolabeled with <sup>99m</sup>Tc (mean dose: 780 MBq, range 560-895 MBq) by i.v. injection in 5 minutes. Two of them received 10 mg unlabeled E48 F(ab')<sub>2</sub> one h prior to the administration of the labeled MAb with the option in mind to block the adrenal uptake. Seventeen patients received 1-2 mg E48 IgG radiolabeled with <sup>99m</sup>Tc (mean dose 760 MBq, range 510-865 MBq) by i.v. injection in 5 minutes. Patients receiving E48 F(ab')<sub>2</sub>, respectively E48 IgG, suffered from carcinoma of the larynx (n = 5, respectively n=5), tonsil (n=2, n=4), oral cavity except tongue (n=4, n=5), tongue (n=2, n=3), nose (n=1, n=0) and lower lip (n=1, n=0). The age of the patients receiving E48 F(ab')<sub>2</sub> was 61.7 ± 7.8 year (mean ± s.d.) and for those receiving E48 IgG 57.9 ± 9.1 year.

**Monoclonal Antibody E48.** Monoclonal antibody E48 was derived from mice immunized with cells from a metastasis of a moderately differentiated SCC of the larynx (T<sub>3</sub>N<sub>1</sub>M<sup>+</sup>). The antigen recognized by MAb E48 was found to be expressed by 94% of the primary head and neck tumors (N=128) and by the majority of cells within these tumors. A comparable reactivity pattern was observed in 26 tumor infiltrated lymph nodes from neck dissection specimens<sup>8</sup>. Antibody reactivity with normal tissue is restricted to normal stratified squamous epithelium and urothelium of the bladder.

**Antibody Preparation.** The E48 IgG and F(ab')<sub>2</sub> used in this study were supplied by Centocor Inc. (Leiden, the Netherlands). E48 IgG was purified from a concentrated tissue culture supernatant by affinity chromatography on a protein A-Sepharose column. For virus inactivation, IgG from the protein A eluate was treated for at least 6 h with Tween 80 and tri-*n*-butylphosphate. The protein A purified IgG was further purified on Q-Sepharose and subsequently digested to F(ab')<sub>2</sub> by pepsin at pH 3.9. The F(ab')<sub>2</sub> fragments were further purified by protein A chromatography to remove residual undigested IgG, followed by elution over a S-Sepharose column. The purity of F(ab')<sub>2</sub> preparations was evaluated by sodium dodecyl sulfate-polyacrylamide gel electrophoresis under non-reducing conditions and appeared to be more than 95%. This product was filtered through a 0.2-μm filter and dispensed aseptically in a closed environment under

anaerobic conditions. The preparation was found to be pyrogenic free.

**Preparation of <sup>99m</sup>Tc-labeled E48 IgG and F(ab')<sub>2</sub>.** All radiolabeling procedures were performed under aseptic conditions in a shielded laminar flow hood. All glassware, plastics, and solutions were sterile and pyrogen free. For labeling MAb E48 IgG or F(ab')<sub>2</sub> with <sup>99m</sup>Tc, a modification of the multistep procedure as described by Fritzberg et al.<sup>13</sup> was followed, using a S-benzoylmercaptopglycylglycylglycine chelator which was a gift from Mallinckrodt Medical B.V. (Petten, the Netherlands). The purified E48 IgG and F(ab')<sub>2</sub> were labeled with a specific activity of 566 ± 172 MBq/mg and 629 ± 166 MBq/mg protein, respectively. A mean of 98.2 ± 1.1 % and 98.1 ± 0.9 % of the <sup>99m</sup>Tc was bound to IgG and F(ab')<sub>2</sub>, respectively as determined by chromatography on ITLC-SG strips (Gelman Sciences, Ann Arbor, MI) with 0.1 M citrate buffer, pH 5.0. Every radiolabeled E48 IgG and E48 F(ab')<sub>2</sub> preparation was assayed for immunoreactivity by measuring the binding to glutaraldehyde fixed cells of the vulva SCC cell line A431<sup>10</sup>. As determined by a modified Lineweaver-Burk plot, the immunoreactive fractions of <sup>99m</sup>Tc-labeled E48 IgG and F(ab')<sub>2</sub> at infinite antigen excess were 80.6 ± 14.3 % and 77.0 ± 6.7 %, respectively. The affinity constants were 1.5 × 10<sup>10</sup> M<sup>-1</sup> for E48 IgG and 1.2 × 10<sup>10</sup> M<sup>-1</sup> for F(ab')<sub>2</sub> as determined by the Scatchard plot.

**Imaging studies.** All patients were examined by palpation, CT, MRI, and RIS of the neck prior to surgery. Preoperative palpation was performed by the same experienced head and neck surgeon. CT scans were obtained with a third generation Philips Tomoscan 350 (Philips Medical Systems, Best, The Netherlands) or with a fourth generation Siemens Somatom Plus (Siemens AG, Erlangen, Germany) after intravenous administration of contrast medium (Ultravist 300 mg Iodine/ml, Schering AG, Germany). Contiguous axial 5-6 mm scanning planes were used. MRI examinations were done on a 0.6 Tesla imaging system (Teslacon, Technicare - General Electric, Milwaukee) using a partial volume coil. Axial T1-weighted spin echo and Gadolinium-diethylenetriaminepentaacetic acid (Magnevist, Schering AG, Germany) enhanced T1-weighted gradient recalled echo images were made in all patients without claustrophobia. Slice thickness varied from 3 to 5 mm, with an interslice gap of 50% as described by Van den Brekel et al.<sup>14</sup>. Criteria for the optimal assessment of cervical lymph node metastases by CT or MRI, as defined in our institute, were used. At CT and MRI, neck levels were considered malignant if nodes with necrosis were depicted, or if the minimal diameter in the axial plane of a node was 11 mm or more for nodes located in level II (subdiaphragic) and 10 mm or more for all other nodes, or if groups of 3 or more borderline lymph nodes (1 or 2 mm smaller) were seen<sup>15</sup>.

The radioimmunoscinigrams were obtained with a large field of view gamma camera (Gemini; General Electric, Milwaukee, WI) equipped with a low energy parallel hole collimator, connected to a computer (Bartec, Farnborough, United Kingdom). Whole body images (anterior and posterior views) and planar images of the head and neck (anterior views) were obtained immediately, 16 h, and 21 h after injection. Single Photon Emission Computerized Tomography (SPECT) images of the head and neck were acquired 16 h after injection, while lateral scans of the head and neck were obtained 21 h after injection. Planar images included the following acquisition parameters: matrix size 128 x 128 (head and neck) or 256 x 256 (whole body) and at least 100 kilocounts were obtained per view during 5-20 min. Acquisition data for SPECT imaging: 64 angles were recorded, 30-second acquisition per angle, 360-degree circular orbit, and matrix size 64 x 64. Interpretation of increased uptake of activity was based on asymmetry and retention,



specially on late images.

CT, MRI, or RIS examinations were each scored by one experienced examiner. All examiners were blinded to the results of other examinations and the histopathological outcome. They only were informed about the site of the primary tumor. All patients had uni- or bilateral neck dissections performed between 2 and 7 days after administration of the radioimmunoconjugate. After fixation, all palpable and visible lymph nodes were dissected from the surgical specimen and cut into 2-4 mm-thick slices for microscopic examination. The size of lymph nodes does not change by fixation<sup>15</sup>. The different slices of one lymph node were examined by a pathologist and the percentage tumor involvement was estimated. The outcome of the histopathological examination of the neck dissection specimens was used as 'gold standard'.

For topographical evaluation the findings were recorded per side as well as per lymph node level (Fig. 1) according to the Memorial Sloan Kettering Cancer Center Classification<sup>16</sup>. Level I includes the contents of the submental and the submandibular triangles. Level II, III, and IV include the lymph nodes adjacent to the internal jugular vein and the lymph nodes contained within the fibroadipose tissue located medial to the sternocleidomastoid muscle. This area is arbitrarily divided into 3 equal parts, level II being the highest and level IV the lowest level. Level V includes the contents of the posterior cervical triangle. Lymph nodes located outside these levels are mentioned separately. These lymph nodes are included in the evaluation per side, but are not included in the evaluation per level.

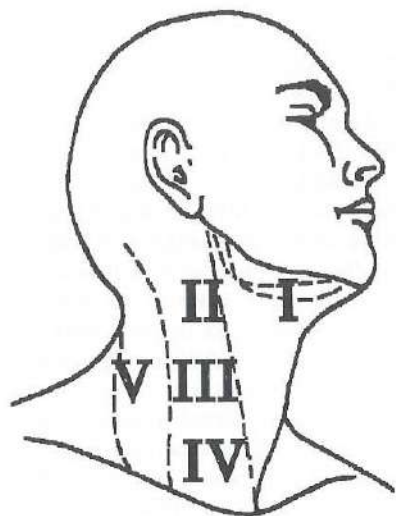


Figure 1. Lymph node levels in the neck according to the Memorial Sloan-Kettering Cancer Center Classification: I=submandibular; II=subdigastic; III=midjugular; IV=low jugular; V=posterior cervical triangle.

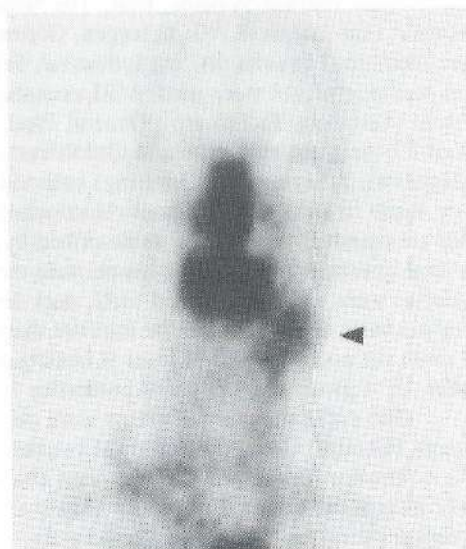


Figure 2. Patient 1. Planar anterior image of the head and neck 21 h after injection of <sup>99m</sup>Tc-labeled E48 F(ab')<sub>2</sub>. Note the intense activity in the nose and mouth. The primary tumor in the left tonsil is not visible on the planar anterior image, probably due to the high activity in the mouth. Uptake is seen in the left subdigastic and midjugular lymph node metastases (arrowhead).

**Statistical analysis.** The statistical analysis was focused on the comparison of the diagnostic tests. Comparison of the quality of diagnostic tests was as usual based on sensitivity, specificity and accuracy. Since these parameters were proportions, confidence intervals could be constructed in two ways. If the denominator was smaller than 100, exact 95% confidence intervals were determined. In larger samples, confidence intervals were calculated using the normal approximation.

To assess agreement between tests, the measured kappa ( $\kappa$ ) was used<sup>17</sup>.  $\kappa$  reflects agreement between tests beyond the agreement expected by chance alone. The size of  $\kappa$  depends both on the diagnostic tests and the group of patients. When  $\kappa$  is systematically smaller for one group of patients than for another, it is likely that this group is more difficult to diagnose than the other group of patients.

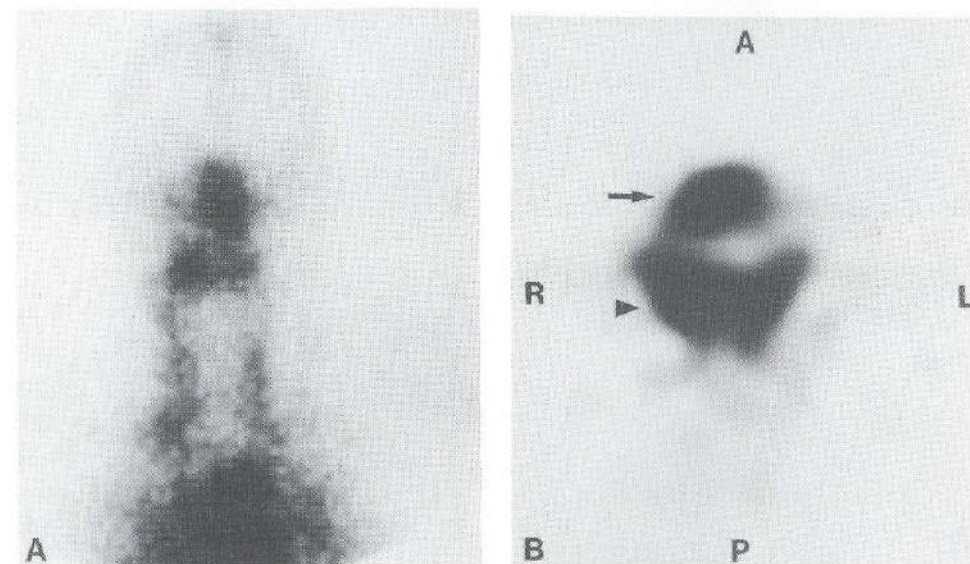


Figure 3. (A) Patient 32. Planar anterior image of the head and neck 21 h after injection of <sup>99m</sup>Tc-labeled E48 IgG. Increased activity is seen in the mouth region on the right. Only one spot can be distinguished. (B) Axial SPECT image of the same patient shows two separate spots representing the primary tumor in the anterior floor of mouth (arrow) and the subdigastic lymph node metastases (arrowhead) on the right. A=anterior; P=posterior; L=left; R=right.

## RESULTS

No adverse reactions were observed which could be related to the injection of the antibody and no significant changes were noted in blood and urine analysis. One patient developed exanthema which was probably related to a recently started diuretic treatment.

Besides all 30 histopathologically confirmed primary tumors one occult larynx carcinoma was visualized. Whole body images up to 21 h post injection showed blood pool activity with visualization of liver, lungs, heart, spleen, kidneys, and nose. Blood



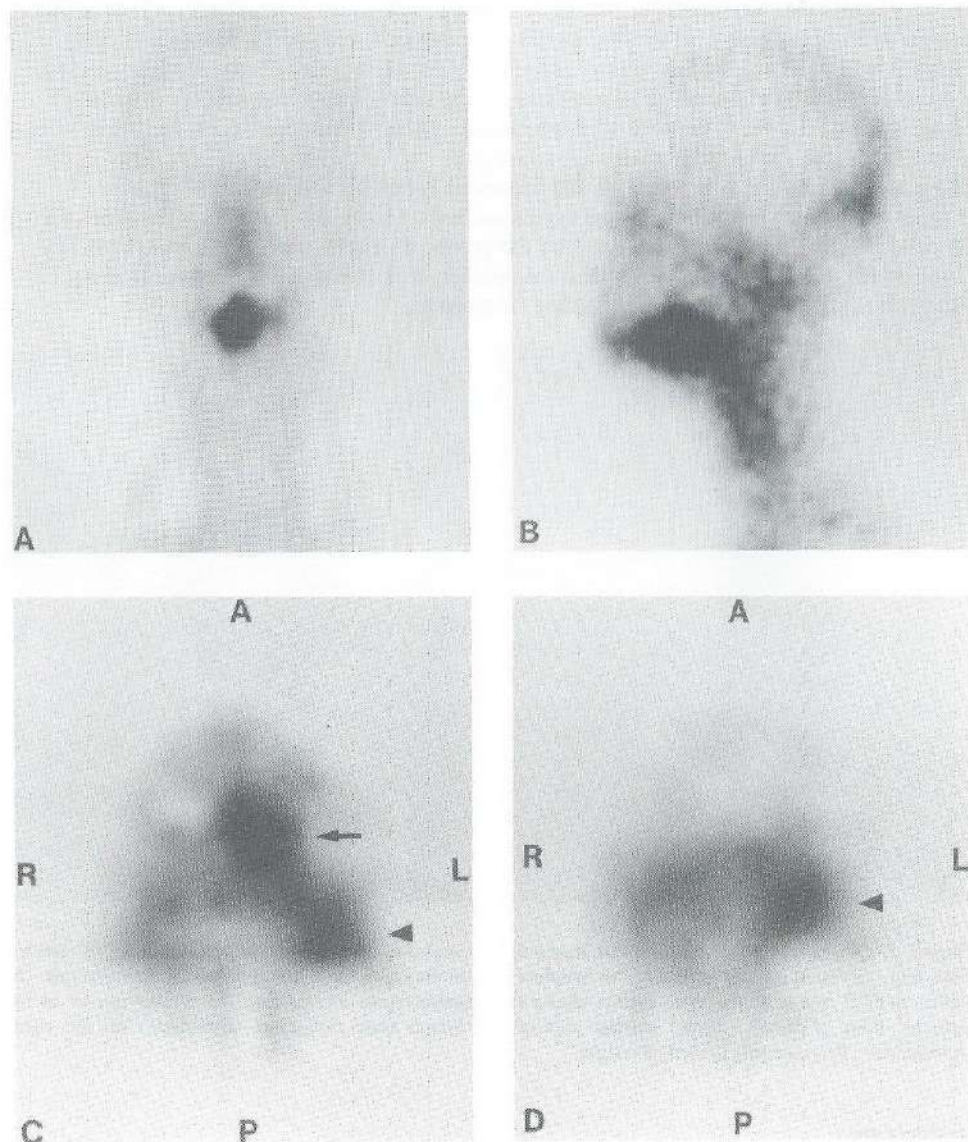


Figure 4. Patient 23. (A) Planar anterior image of the head and neck 21 h after injection of  $^{99m}\text{Tc}$ -labeled E48 IgG. Note the high activity in the primary tumor of the tongue. On this image the lymph node metastases in the left subdigastic and midjugular levels of the head and neck are not visualized. (B) The left lateral image shows the primary tumor in the tongue. The lymph node metastases are not visualized. (C) Axial SPECT images show the primary tumor (arrow) as well as the subdigastic lymph node metastasis (arrowhead) in one axial plane and separately (D), the midjugular lymph node metastasis (arrowhead) in a lower axial plane. A=anterior; P=posterior; R=right; L=left.

pool activity 16 and 21 h p.i. was probably less for E48 F(ab')<sub>2</sub> than for E48 IgG (Fig. 2, 3A, 4A, and 4B) as can be explained by the faster clearance of F(ab')<sub>2</sub> from the blood: F(ab')<sub>2</sub>  $t_{1/2\alpha}$ :  $2.23 \pm 0.41$  h,  $t_{1/2\beta}$ :  $19.6 \pm 4.46$  h and IgG  $t_{1/2\alpha}$ :  $6.61 \pm 0.59$  h and  $t_{1/2\beta}$ :  $78.10 \pm 15.01$  h. For average blood disappearance curves of E48 F(ab')<sub>2</sub> and E48 IgG see Figure 5. Uptake of activity was also seen in the adrenals, scrotal area, gallbladder, and sometimes intestine, at 16 and 21 h p.i., as described previously<sup>11</sup>, and appeared to be similar for F(ab')<sub>2</sub> and IgG. Besides this, uptake in the mouth was observed, which seemed to be lower for E48 IgG in comparison to E48 F(ab')<sub>2</sub> (see for representative anterior images Figure 2 and 3A). After injection of 10 mg of unlabeled E48 F(ab')<sub>2</sub> 1 h prior to administration of labeled E48 F(ab')<sub>2</sub>, visually the adrenals showed lower uptake. In one of these two patients no adrenals were visualized.

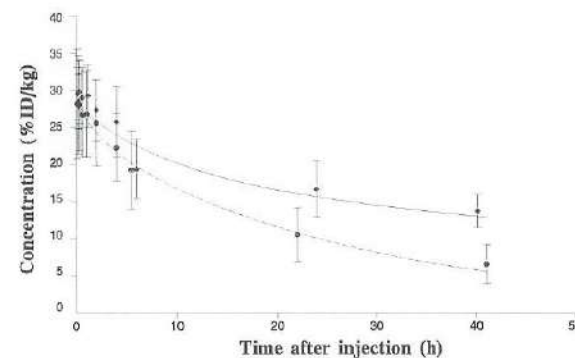


Figure 5. Average blood disappearance curves of  $^{99m}\text{Tc}$ -labeled E48 F(ab')<sub>2</sub> (---) and E48 IgG (—) from 15 and 17 patients, respectively.

Thirty-two patients underwent a neck dissection. In 15 of them a bilateral neck dissection was performed. A total number of 47 neck dissection specimens, containing 221 levels, were histopathologically examined. Forty-eight levels in 32 sides from 25 patients contained metastases of SCC. In one patient, because of movement artefacts, the quality of the MRI examination did not allow reliable interpretation. Four patients refused MRI examination because of claustrophobia. These patients were not included in the evaluation of MRI examination. Due to technical problems with the camera system, no SPECT images were acquired in four patients receiving E48 F(ab')<sub>2</sub>. In one patient, containing an undifferentiated small cell tumor with locally squamous cell differentiation, level III on the left side proved to contain a metastasis of an undifferentiated small cell carcinoma. Because no SCC metastasis was found, this lymph node was not included in the analysis.

The findings on palpation, CT, MRI, and RIS, were analyzed per level and per side and correlated with histopathological examinations (Table 1 and 2, respectively). Sensitivity of RIS, palpation, CT, and MRI for the whole group of patients was per level 68 %, 64 %, 68 %, and 62 % and per side 79 %, 88 %, 88 %, and 83 %, respectively. Only 7 of the 32 levels, which were scored true-positive by RIS, were clearly visualized on planar images. In all other cases SPECT images provided additional information (Fig. 3 and 4).



Table 1. Correlation of preoperative diagnostic findings with histopathological findings per level.

	TP	FN	FP	TN	sensitivity	specificity	accuracy	PPV	NPV
<b>F(ab')<sub>2</sub> (n=15)</b>									
palpation	15	8	4	90	65	96	90	79	92
CT	18	5	0	94	78	100	96	100	95
MRI	15	5	0	65	75	100	94	100	93
RIS	19	4	1	93	83	99	96	95	96
<b>IgG (n=17)</b>									
palpation	15	9	5	75	63	94	87	75	89
CT	14	10	9	71	58	89	82	61	88
MRI	11	11	4	73	50	95	85	73	87
RIS	13	11	4	76	54	95	86	76	87
<b>all (n=32)</b>									
palpation	30	17	9	165	64	95	88	79	91
CT	32	15	9	165	68	95	89	77	92
MRI	26	16	4	138	62	97	89	87	90
RIS	32	15	5	169	68	97	91	86	92

TP, true-positive; FN, false-negative; FP, false-positive; TN, true-negative;  
PPV, positive-predictive value; NPV, negative-predictive value.

Specificity of RIS, palpation, CT, and MRI was per level 97 %, 95 %, 95 %, and 97 % and per side 86 %, 79 %, 79 %, and 70 %, respectively. Interpretation of RIS for the whole group was correct in 201 of 221 levels (accuracy 91 %) and 38 of 47 sides (accuracy 81 %). RIS findings were false-positive in 5 levels and 2 sides. Fifteen levels and 7 sides were scored false-negative. Accuracy of palpation, CT, and MRI was per level, respectively, 88 %, 89 %, and 89 % and per side, respectively, 85 %, 85 %, and 79 %.

Sensitivity per level was 83 % for E48 F(ab')<sub>2</sub> and 54 % for E48 IgG. Sensitivity per side for these groups was, respectively, 94 % and 65 %. For E48 F(ab')<sub>2</sub> and E48 IgG the specificity of RIS per level was 99 % and 95 % and per side 100 % and 60 %; the accuracy of RIS per level was 96 % and 86 % and per side 96 % and 64 %, respectively.

The capacity of RIS in the detection of tumor involved neck levels/sides, which were missed (false-negative score) or detected (true-positive score) by palpation, CT, and/or MRI, is shown in Table 3.

Table 2. Correlation of preoperative diagnostic findings with histopathological findings per side.

	TP	FN	FP	TN	sensitivity	specificity	accuracy	PPV	NPV
<b>F(ab')<sub>2</sub> (n=15)</b>									
palpation	14	2	0	9	88	100	92	100	82
CT	15	1	0	9	94	100	96	100	90
MRI	12	1	0	5	92	100	94	100	83
RIS	15	1	0	9	94	100	96	100	90
<b>IgG (n=17)</b>									
palpation	15	2	3	2	88	40	77	83	50
CT	14	3	3	2	82	40	73	82	40
MRI	12	4	3	2	75	40	67	80	33
RIS	11	6	2	3	65	60	64	85	33
<b>all (n=32)</b>									
palpation	29	4	3	11	88	79	85	91	73
CT	29	4	3	11	88	79	85	91	73
MRI	24	5	3	7	83	70	79	89	58
RIS	26	7	2	12	79	86	81	93	63

TP, true-positive; FN, false-negative; FP, false-positive; TN, true-negative;  
PPV, positive-predictive value; NPV, negative-predictive value.

Using the 95 % confidence intervals of the diagnostic test no significant differences in sensitivity, specificity, and accuracy were found between RIS and the other diagnostic tests, except for RIS and palpation with respect to the sensitivity per side in the E48 IgG patient group. However, in a 99 % confidence interval no significant difference was found. The  $\kappa$  values per level for RIS with MAb E48 and palpation, CT, and MRI per level in the whole group of patients were 0.682, 0.689, and 0.698. The  $\kappa$  values of the different diagnostic methods per level ranged in the E48 F(ab')<sub>2</sub> group from 0.622 to 1, whereas in the E48 IgG group values between 0.444 and 0.877 were found.

Of the 23 tumor containing levels in the E48 F(ab')<sub>2</sub> group, 4 were missed, while 11 out of 24 in the E48 IgG group were missed. The paraffine slides of the missed metastatic lymph nodes were re-examined histopathologically. The false-negative findings proved to be all lymph nodes containing small tumor deposits (ranging from micrometastasis to tumors of 9x9 mm) or tumor deposits containing a large proportion of necrosis (n=2), keratin (n=3), or fibrin (n=5) deposits. In one patient, the missed node in level IV was close to level III. Besides this, the node also contained a small amount of



Table 3. Results of RIS in false-negative and true-positive findings by palpation, CT, and MRI.

	RIS (per level)		RIS (per side)	
false-negative				
palpation	6/17 (35%)	11/17 (65%)	2/4 (50%)	2/4 (50%)
CT	5/15 (33%)	10/15 (67%)	1/4 (25%)	3/4 (75%)
MRI	6/16 (38%)	10/16 (62%)	1/5 (20%)	4/5 (80%)
palpation, CT, and MRI	3/11 (27%)	8/11 (73%)	1/3 (33%)	2/3 (67%)
true-positive				
palpation	26/30 (87%)	4/30 (13%)	26/29 (90%)	3/29 (10%)
CT	28/32 (87%)	4/32 (13%)	26/29 (90%)	3/29 (10%)
MRI	23/26 (88%)	3/26 (12%)	23/24 (96%)	1/24 (4%)
palpation, CT, and MRI	27/32 (84%)	5/32 (16%)	24/26 (92%)	2/26 (8%)

tumor. In another patient, there was a high uptake of activity in the mouth, possibly obscuring activity uptake in a right submandibular lymph node metastasis. Two missed paralaryngeal lymph nodes were located too close to a larynx carcinoma. In one case, histopathological examination of a missed lymph node revealed metastases of an undifferentiated small cell tumor, while the primary tumor showed locally squamous cell differentiation only.

Of the 94 tumor-free levels in the E48 F(ab')<sub>2</sub> group, 1 was falsely scored positive, while 4 out of 80 in the E48 IgG group. For tumor-free sides these figures are 0 out of 9 in the F(ab')<sub>2</sub> group and 2 out of 5 in the IgG group.

## DISCUSSION.

A number of animal and patient studies have shown that F(ab')<sub>2</sub> fragments are better suited for radioimmunoscintigraphic detection of tumors than whole IgG, due to the higher tumor to non tumor ratios obtained with F(ab')<sub>2</sub> fragments<sup>18-20</sup>. Also for MAb E48 F(ab')<sub>2</sub>, when tested in HNSCC xenograft bearing nude mice, we observed such a superior quality for imaging<sup>10</sup>. For this reason initial RIS studies were performed with E48 F(ab')<sub>2</sub>. We recently reported on the first 10 head and neck cancer patients imaged with <sup>99m</sup>Tc-labeled E48 F(ab')<sub>2</sub> and mentioned the high uptake of activity in the mouth which may hamper the diagnosis of submandibular or subdiaphragic lymph nodes. We hypothesized that oral activity may be less when using whole IgG, one of the reasons to modify the initial study and to evaluate also MAb E48 IgG for its value in RIS<sup>11</sup>.

Considering the sensitivity and accuracy data as presented in this study for RIS with E48 IgG and F(ab')<sub>2</sub> it is tempting to state that F(ab')<sub>2</sub> fragments are better suited for

clinical RIS than whole IgG. The sensitivity and accuracy per level was found to be higher for E48 F(ab')<sub>2</sub> when compared to E48 IgG, 83 and 96% versus 54 and 86%. However, one should be careful with interpretation of these data since also CT and MRI scored better in the E48 F(ab')<sub>2</sub> group. Furthermore, the agreements ( $\kappa$ -values) between RIS and palpation, CT, and MRI in the F(ab')<sub>2</sub> patient group were generally better as compared to those in the IgG patient group. This was also the case for the agreements ( $\kappa$ -values) between palpation, CT, and MRI in these patient groups (data not shown). These data suggest differences in the composition of the groups. The fact that in the F(ab')<sub>2</sub> patient group as well as in the IgG patient group the sensitivity and accuracy for palpation, CT, MRI, and RIS were found to be similar, indicates that F(ab')<sub>2</sub> and IgG are equally well suited for RIS. To obtain additional information, we recently started a new protocol in which biodistribution data are obtained from surgical specimens of patients who receive <sup>131</sup>I-labeled E48 IgG and <sup>125</sup>I-labeled E48 F(ab')<sub>2</sub> simultaneously.

In the present study the pattern of oral accumulation of activity is different for IgG when compared to F(ab')<sub>2</sub>. In case of F(ab')<sub>2</sub>, activity is apparently distributed throughout the whole oral cavity, while in case of IgG accumulation seems to be restricted to a smaller area (Fig. 2 and 3A). Due to its reduced activity uptake in the oral cavity, the IgG may be favorable for the detection of submandibular or subdiaphragic lymph nodes. However, from the present study no conclusions can be drawn on this point due to the low numbers of submandibular and subdiaphragic lymph nodes. Definite proof requires sequential imaging procedures with IgG as well as with F(ab')<sub>2</sub> in patients with tumor involvement in these neck regions.

For the detection of lymph node metastases the diagnostic value of RIS with MAb E48, either E48 F(ab')<sub>2</sub> or E48 IgG, is comparable to that of palpation, CT, and MRI, as shown by sensitivity, specificity and accuracy (Table 1 and 2).

Until now, a limited number of clinical RIS studies in head and neck cancer patients have been described<sup>21-24</sup>. Results obtained in these studies are difficult to compare. Firstly, only a small proportion of the 5-15 patients included in these studies had lymph node involvement, thus limiting accurate calculation of sensitivity and specificity. Secondly, studies differ considerably with respect to (1) patient selection, (2) control of tumor deposits for antigen expression, (3) scintigraphic methods, (4) the way of topographical evaluation of the diagnostic findings, and (5) the way to confirm scintigraphic findings. With respect to this latter, from all mentioned studies it is not clear whether the examiner for RIS was blinded to the results of the other diagnostic examinations.

Most important in our study is the question: can RIS with MAb E48, either IgG or F(ab')<sub>2</sub> contribute to the preoperative staging of the neck in HNSCC patients, e.g. by complementing other methods used to assess nodal involvement? All patients who have nodal disease will need treatment of the regional lymphatics, while the neck needs no treatment if no metastasis is present. Recently the concept of selective neck dissection has been introduced<sup>25</sup>. Selective neck dissections are used in patients with only minimal nodal disease with the intention to reduce morbidity. Another tendency is a 'wait and see' policy for the clinically negative neck. Forementioned treatment and policy are, however, only acceptable if the assessment of the neck nodes is reliable. The assessment of the status of the neck in HNSCC patients, however, remains a problem. Not all enlarged nodes contain metastatic deposits. Nodes containing small deposits of carcinoma may not be enlarged.



All current imaging techniques except US-guided aspiration cytology use morphological criteria, whereas RIS uses specific binding of the MAb to target cells.

In the present study RIS, palpation, CT, and MRI were directly compared for their value in diagnosis of lymph node metastases. For each diagnostic modality, findings were recorded per side as well as per lymph node level and compared with histopathological findings. In our experience correlation of all image data per deposit, as performed in the other here mentioned studies, is inaccurate because precise localization of the deposits is impossible due to the lack of anatomical structures on the immunoscintigrams. It can be anticipated that the development of an accurate method to correlate all image modalities ("fused images") may resolve this problem. We think, however, that for the assessment of the potential of RIS for staging of the neck, analysis for tumor involvement per side as well as per level is satisfactory.

In one patient, RIS with MAb E48 was able to detect tumor involved lymph nodes, which were not detectable by other examinations, and thus contributed to the assessment of the status of the neck. In this patient receiving E48 F(ab')<sub>2</sub>, RIS resulted in upstaging of 3 levels and 1 side. In this study only 25% of the truly-positive RIS levels, were clearly visualized on planar images. Also in all other cases SPECT images provided most information. The smallest tumor involved lymph node detected, with SPECT, had diameters of 5 and 9 mm in the axial plane with a tumor load of more than 50 %. From the clinical point of view it is important to consider the consequences when decisions for surgery in the present study would have been based on RIS only. In that case 12 neck dissections (out of 14), which appeared to be free of tumor upon histopathological examination, would have been prevented by RIS. On the other hand 7 neck sides would have been undertreated while two sides would have been overtreated.

A major limitation of RIS with MAb E48 IgG or F(ab')<sub>2</sub> in its present form is the high percentage of false-negative scores. A total of 15 out of 47 levels and 7 out of 33 neck sides were falsely scored negative. All missed tumor involved lymph nodes were smaller than 2 cm in diameter. In these cases RIS was apparently unsuccessful due to the limited amount of antigen accessible for the MAb and maybe the limited sensitivity of a gamma camera. Consequently micrometastases, small tumor involved nodes, and tumor involved nodes with much keratin, necrosis, or fibrosis and with only a small proportion of viable tumor cells were not diagnosed. Fibrosis may also hamper the penetrance of the MAb to tumor cells. Close spatial relation of a metastatic node to an area of increased uptake may also hamper diagnosis: paralaryngeal nodes in larynx carcinoma and a submandibular node close to the mouth. While primary tumors were checked for antigen expression by immunohistochemistry on preoperative biopsies, we were not able to do so on the missed lymph node metastases. For proper histopathologic examination at our hospital surgical specimens are routinely fixed in formalin and embedded in paraffin, resulting in loss of E48 antigenicity.

Five levels and 2 sides were incorrectly scored positive. No clear explanation for these observations can be given. False-positive findings in RIS may be caused by blood pool activity and asymmetric anatomy of the neck. Three of these levels were also incorrectly scored positive by palpation, CT, or MRI. These findings indicate enlargement of lymph nodes in these levels.

In conclusion, imaging data presented in this study indicate that RIS is as reliable as the other imaging techniques. Despite this, we believe that RIS with MAb E48 in its present form will not sufficiently contribute to a more reliable selection of patients who

should be treated on behalf of their neck or of patients in whom a 'wait and see' policy is warranted. For this purpose the percentage of falsely scored negative neck levels / sides should be diminished. In this respect, the developing field of positron emission tomography (PET) might result in a diagnostic modality with a higher sensitivity. Other disadvantages of RIS at the moment, limiting the routine application, are the complexity and high costs in comparison to CT and MRI. The selective accumulation of radioactivity in tumor tissue in combination with the known intrinsic radiosensitivity of HNSCC, however, do justify the development of radioimmunoconjugates for radioimmunotherapy (RIT). From this point of view RIS can be regarded as a prelude to RIT. Among other possibilities, RIT may be especially attractive in an adjuvant setting or in support to external beam irradiation. In our department, preparations for a phase I adjuvant RIT trial with <sup>186</sup>Re-labeled chimeric MAb E48 IgG are in progress <sup>26,27</sup>.

## ACKNOWLEDGMENTS

The authors thank Drs. Hein Leverstein and Richard P. Wong Chung for clinical support, Henri Greuter for biochemical support, and Prof.dr. Chris J.L.M. Meyer for histopathological support. This work was supported by the Dutch Ministry of Economic Affairs and by Centocor Europe, Inc., Leiden, the Netherlands

## REFERENCES

1. Snow GB, Annayas AA, Slooten EA van, Bartelink H, Hart AAM. Prognostic factors of neck node metastases. *Clin Otolaryngol* 1982;7:182-92.
2. Leemans CR, Tiwari RM, Waal I van der, Karim ABMF, Nauta JJP, Snow GB. The efficacy of comprehensive neck dissection with or without postoperative radiotherapy in nodal metastases of squamous cell carcinoma of the upper respiratory and digestive tracts. *Laryngoscope* 1990;100:1194-8.
3. Leemans CR, Tiwari RM, Nauta JJP, Waal I van der, Snow GB. Regional lymph node involvement and its significance in the development of distant metastases in head and neck cancer. *Cancer* 1993;71:452-6.
4. Ali S, Tiwari RM, Snow GB. False positive and false negative neck nodes. *Head Neck Surg* 1985;8:78-82.
5. Brekel MWM van den, Castelijns JA, Stel HV, Golding RP, Meijer CLJM, Snow GB. Modern imaging techniques and ultrasound guided aspiration cytology for the assessment of the neck node metastases; a prospective comparative study. *Eur Arch Otorhinolaryngol* 1993;250:11-7.
6. Goldenberg DM. Future role of radiolabeled monoclonal antibodies in oncological diagnosis and therapy. *Semin Nucl Med* 1989;19:332-9.
7. Quak JJ, Balm AJM, Dongen GAMS van, Brakkee JPG, Scheper RJ, Snow GB, Meijer CJLM. A 22 kD surface antigen detected by a monoclonal antibody E48 is exclusively expressed in stratified squamous and transitional epithelia. *Am J Pathol* 1990;33:191-5.
8. Quak JJ, Gerretsen M, Schrijvers AHGJ, Meijer CJLM, Dongen GAMS van, Snow GB. Detection of squamous cell carcinoma xenografts in nude mice by radiolabeled monoclonal antibody E48. *Arch Otolaryngol/Head Neck Surg* 1991;117:1287-91.
9. Quak JJ, Balm AJM, Brakkee JPG, Davis HD, Scheper RJ, Meijer CJLM, Snow GB, Dongen GAMS van. Localization and imaging of radiolabeled monoclonal antibody E48 against squamous cell carcinoma of the head and neck in tumor bearing nude mice. *Int J Cancer* 1989;44:534-8.
10. Gerretsen M, Quak JJ, Suh JS, Walsum M van, Meijer CJLM, Snow GB, Dongen GAMS van.

**Biodistribution of Radiolabeled Monoclonal Antibody E48  
IgG and F(ab')<sub>2</sub> in Patients with Head and Neck Cancer**

Remco de Bree <sup>1</sup>, Jan C. Roos <sup>2</sup>, Jasper J. Quak <sup>1</sup>,  
Willem den Hollander <sup>2</sup>, Abraham J. Wilhelm <sup>3</sup>, Arthur van Lingen <sup>2</sup>,  
Gordon B. Snow <sup>1</sup>, and Guus A.M.S. van Dongen <sup>1</sup>

Departments of <sup>1</sup> Otolaryngology / Head and Neck Surgery,  
<sup>2</sup> Nuclear Medicine, and <sup>3</sup> Pharmacy,  
Free University Hospital, Amsterdam, The Netherlands

Clinical Cancer Research 1995; 1: 277-286



## ABSTRACT

Biodistribution and pharmacokinetics of radiolabeled monoclonal antibody (MAb) E48 IgG and E48 F(ab')<sub>2</sub> were analyzed and compared in 39 patients with histologically proven squamous cell carcinoma of the head and neck (HNSCC) who were included in a radioimmunoscinigraphy (RIS) study and underwent surgery 44 h after injection. Three groups of patients were distinguished: group I (n=19) received <sup>99m</sup>Tc-labeled E48 F(ab')<sub>2</sub>, group II (n=9) received <sup>99m</sup>Tc-labeled E48 IgG, and group III (n=11) received <sup>99m</sup>Tc- and <sup>131</sup>I-labeled E48 IgG as well as <sup>125</sup>I-labeled F(ab')<sub>2</sub>. Two patients of group I and four patients of group III received a high MAb dose (10-50 mg), while all other patients received a low MAb dose (1-4 mg).

From all patients of group II and III biopsies from the surgical specimen were obtained 44 h p.i.. Tumor uptake of <sup>99m</sup>Tc-labeled E48 IgG was high, ranging from 7.2 - 82.3 percent of the injected dose per kilogram (%ID/kg), with a mean of 30.6 ± 20.1 %ID/kg. The mean tumor to non-tumor ratio of this conjugate was 2.8 for mucosa, 4.6 for bone marrow aspirate, 4.1 for blood, 20.3 for fat, and 21.0 for muscle. Activity uptake in tumor positive lymph nodes was 4.7 times higher as compared to negative lymph nodes.

RIS 16 h p.i. revealed activity uptake in the primary tumor, lymph node metastases, the oral cavity, and adrenals. Using regions of interest (ROIs), the uptake in the adrenals was estimated to be 50 %ID/kg. If a high MAb dose was used no adrenals were visualized and the uptake in the oral cavity was clearly diminished, while the tumor uptake and tumor to non-tumor ratios were increased.

The mean elimination half lives  $t_{1/2\alpha}$  and  $t_{1/2\beta}$  in plasma were: for E48 IgG (n=20) 6.6 ± 2.6 and 54.1 ± 24.3 h and for E48 F(ab')<sub>2</sub> (n=19) 2.3 ± 0.4 and 19.9 ± 4.6 h, respectively. Tumor uptake of <sup>131</sup>I-labeled E48 IgG was 49% higher than of <sup>125</sup>I-labeled F(ab')<sub>2</sub>. For most tissues except normal oral mucosa, tumor to non-tumor ratios were slightly higher for F(ab')<sub>2</sub> than for IgG.

The present study shows that MAb E48 accumulates selectively and to a high level in HNSCC. Although no definite conclusions can be drawn which MAb form is more suitable, IgG or F(ab')<sub>2</sub>, MAb E48 seems to have potential for radioimmunotherapy in HNSCC patients.

## INTRODUCTION

Squamous cell carcinoma represents the vast majority of malignant tumors of the head and neck <sup>1</sup>. These tumors account for approximately 5% of all malignant neoplasms in northwestern Europe and the United States <sup>2</sup>. Head and neck squamous cell carcinomas (HNSCC) grow locally invasive and have a proclivity to metastasize to regional lymph nodes in the neck rather than to spread hematogenously. Therapeutic management of early stage disease (stage I and II), consists of surgery or radiotherapy alone, whereas advanced stages (stage III and IV) are treated with a combination of these modalities. Such treatment results in a good locoregional control in the early stages. However, in patients with stage III and IV, the failure rate is high. Despite surgery and postoperative radiotherapy locoregional recurrence occurs in 50-60% of these patients. Moreover, 15-25% of these patients develop clinically manifest distant metastases <sup>3</sup>. The actual incidence of distant metastases in HNSCC patients may even be much higher as autopsy studies reported on an incidence of 40-57% <sup>4</sup>.

The high failure rate in advanced disease warrants the development of adjuvant systemic therapeutic modalities after surgery and radiotherapy. However, the high expectations as to chemotherapy have not become true, and its application is limited to the palliation of recurrent and metastatic disease <sup>5-7</sup>. Therefore, development of a more effective adjuvant systemic therapy remains a major challenge in head and neck oncology.

Among other therapeutic approaches the use of monoclonal antibodies for selective delivery of radionuclides to residual disease seems to be promising <sup>8,9</sup>. This may be particularly true for tumors with a high intrinsic sensitivity for radiation like hematological neoplasms and HNSCC <sup>10</sup>. For this application we developed MAb E48 which shows selective reactivity with squamous epithelia and their malignant counterparts <sup>11</sup>. The E48 antigen is a surface membrane bound antigen of 22 kDa located on desmosomes and along the cell membrane. MAb E48 was shown to be highly capable for selective tumor targeting in animal models as well as in patients <sup>12-14</sup>. Recently, we reported on the scintigraphical detection of metastatic disease with MAb E48 IgG or F(ab')<sub>2</sub> in patients with histologically proven HNSCC and with clinical evidence of cervical lymph node involvement <sup>13,14</sup>. In this study, preoperative findings on lymph node status obtained by radioimmunoscinigraphy (RIS) were compared to computerized tomography (CT), magnetic resonance imaging (MRI), palpation, and finally with the histopathological outcome of the neck dissection specimen. Data revealed that RIS with MAb E48 is as good as the conventional diagnostic methods for the detection of lymph node metastases. Furthermore, these studies showed that E48 IgG and F(ab')<sub>2</sub> are equally well suited for tumor detection. We observed an unwanted consistent accumulation of MAb E48 in the oral cavity and adrenals.

These data justified further evaluation of MAb E48 for its therapeutic applicability. Armed with <sup>131</sup>Iodine (<sup>131</sup>I) or <sup>186</sup>Rhenium (<sup>186</sup>Re), E48 IgG was shown to be highly capable of eradicating established human HNSCC xenografts in nude mice <sup>15,16</sup>. Complete ablation of small HNSCC was observed in this animal model by a single bolus injection of <sup>186</sup>Re-labeled E48 IgG <sup>17</sup>. Results obtained in this animal model, however, have to be interpreted with caution due to e.g. the absence of normal tissue expressing the particular antigen and the high tumor uptake of the MAb in these animals when compared to patients. Of paramount importance for ranking the suitability of a MAb for clinical



radioimmunotherapy (RIT) is its biodistribution in patients comprising the relative uptake in tumor tissue and normal tissues.

The purpose of the present study was to analyze and compare the biodistribution and pharmacokinetics of E48 IgG and F(ab')<sub>2</sub> in 39 patients with HNSCC. The RIS results in 28 of these patients were published previously<sup>14</sup>. Some patients (n=11) received IgG and F(ab')<sub>2</sub> simultaneously, using different radionuclides. As a bridging study to RIT some patients (n=6) received a higher dose of MAb E48. We measured the absolute uptake in the primary tumor, lymph node metastasis, mucosa, and several other tissues by taking biopsies from the surgical specimen as well as bone marrow 44 h after injection of the radioimmunoconjugate. Moreover, the accumulation of activity in the oral cavity, tongue, and adrenal glands was estimated with regions of interest on planar images.

## PATIENTS AND METHODS

**Patient Study.** The protocol was approved by the Dutch Health Council and by the institutional review board of the Free University Hospital. Informed consent was obtained from all participants.

Thirty-nine patients with HNSCC participated in this study. Nineteen patients (1-19, group I) were injected with E48 F(ab')<sub>2</sub>, 9 patients (20-28, group II) with E48 IgG, and 11 patients (29-39, group III) with E48 IgG and F(ab')<sub>2</sub> simultaneously (E48 IgG/F(ab')<sub>2</sub>). Prior to enrollment a biopsy of the primary tumor had to show positive immunoperoxidase staining with E48 IgG. Patients of group I, II, and III suffered from carcinoma of the larynx (n=9, n=3, n=3, respectively), tonsil (n=2, n=4, n=1), oral cavity except tongue (n=4, n=1, n=4), tongue (n=2, n=1, n=3), nose (n=1, n=0, n=0), and lower lip (n=1, n=0, n=0).

All patients received 1-2 mg E48 IgG or F(ab')<sub>2</sub> radiolabeled with <sup>99m</sup>Tc (mean dose 722 ± 74 MBq and 722 ± 81 MBq, respectively) by intravenous injection in 5 min for imaging and biodistribution purposes. Two patients of group I (patient 18 and 19) were additionally injected intravenously with 10 mg unlabeled E48 F(ab')<sub>2</sub> 1 h before administration of the radiolabeled dose E48 F(ab')<sub>2</sub>. Four patients of group III received additionally 10 mg (patient 36) or 50 mg (patient 37-39) unlabeled E48 IgG at the time of injection of the radiolabeled dose E48 IgG. Patients of group III received <sup>99m</sup>Tc-labeled E48 IgG and additionally a low dose of <sup>131</sup>I-labeled E48 IgG (2.5 ± 0.9 MBq) and <sup>125</sup>I-labeled E48 F(ab')<sub>2</sub> (2.5 ± 0.8 MBq) to compare the biodistribution of whole IgG and its F(ab')<sub>2</sub> fragment in biopsies in the same patient. These patients received sodiumperchlorate to prevent uptake of radioactive iodine in the thyroid gland. Patients of group I were operated 2-5 days p.i.. All patients of group II and III, injected with E48 IgG or E48 IgG/F(ab')<sub>2</sub>, were operated 44 h after injection, except for patient 39, who was operated 9 days p.i.. Trying to diminish the activity uptake in the adrenals by suppression of its endocrine function, 4 patients (32-35) of group III received 4-8 mg dexamethasone orally 5 h prior to injection. In one patient this administration was repeated after 12 h.

Prior and up to 7 days after administration of <sup>99m</sup>Tc-labeled MAb E48, urine and blood samples were obtained for analysis. Electrolytes, aspartate aminotransferase, alanine aminotransferase, alkaline phosphatase, gamma-glutamyl transferase, lactate dehydrogenase, urea nitrogen, creatinine, and uric acid were determined in serum. Hematological

determinations included hemoglobin, hematocrit, platelet count, white blood cell count and differentiation, and sedimentation rate. Skin tests were not performed. Vital signs were recorded before and up to 3 h after injection.

**Monoclonal Antibody E48.** Monoclonal antibody E48 was derived from mice immunized with cells from a metastasis of a moderately differentiated squamous cell carcinoma of the larynx (T<sub>3</sub>N<sub>1</sub>M<sup>+</sup>, classification according to the International Union Against Cancer<sup>18</sup>). The antigen recognized by MAb E48 was found to be expressed by 94 % of the primary head and neck tumors (n=196). In 70 % of these tumors the antigen was expressed by the majority of cells within these tumors. A comparable reactivity pattern was observed in 32 tumor infiltrated lymph nodes from neck dissection specimens<sup>19</sup>. Antibody reactivity with normal tissue is restricted to normal stratified squamous epithelium and urothelium of the bladder.

**Antibody Preparation.** The E48 IgG and F(ab')<sub>2</sub> used in this study were supplied by Centocor, Inc., Leiden, the Netherlands. E48 IgG was purified from a concentrated tissue culture supernatant by affinity chromatography on a protein A-Sepharose column. For virus inactivation, IgG from the protein A eluate was treated for at least 6 h with Tween 80 and tri-*n*-butylphosphate. The protein A purified IgG was further purified on Q-Sepharose and subsequently digested to F(ab')<sub>2</sub> by pepsin at pH 3.9. The F(ab')<sub>2</sub> fragments were further purified by protein A chromatography to remove residual undigested IgG, followed by elution over a S-Sepharose column. The purity of F(ab')<sub>2</sub> preparations was evaluated by sodium dodecyl sulfate-polyacrylamide gel electrophoresis under nonreducing conditions and appeared to be more than 95 %. This product was filtered through a 0.2-μm filter and dispensed aseptically in a closed environment under anaerobic conditions. The preparation was found to be pyrogenic free.

**Preparation of radiolabeled E48 IgG and F(ab')<sub>2</sub>.** All radiolabeling procedures were performed under aseptic conditions in a shielded laminar flow hood. All glassware, plastics, and solutions were sterile and pyrogen free.

For labeling MAb E48 IgG or E48 F(ab')<sub>2</sub> with <sup>99m</sup>Tc, a modification of the multistep procedure as described by Fritzberg et al.<sup>20</sup> was followed, using a S-benzoylmercaptoglycylglycylglycine chelator which was a gift from Mallinckrodt, Petten, the Netherlands. The purified E48 IgG and E48 F(ab')<sub>2</sub> were labeled with a specific activity of 556 ± 168 MBq/mg and 641 ± 178 MBq/mg protein, respectively. A mean of 98.7 ± 0.7 % and 98.2 ± 1.1 % of the <sup>99m</sup>Tc was bound to E48 IgG and E48 F(ab')<sub>2</sub>, respectively, as determined by chromatography on ITLC-SG strips (Gelman Sciences, Ann Arbor, MI) with 0.1 M citrate buffer, pH 5.0. Every radiolabeled E48 IgG and E48 F(ab')<sub>2</sub> preparation was assayed for immunoreactivity by measuring the binding to glutaraldehyde fixed cells of the vulva SCC cell line A431<sup>21</sup>. As determined by modified Lineweaver-Burk plot, the immunoreactive fractions of <sup>99m</sup>Tc-labeled E48 IgG and E48 F(ab')<sub>2</sub> at infinite antigen excess were 79 ± 13 % and 79 ± 10 %, respectively. Labeling of E48 IgG and E48 F(ab')<sub>2</sub> with <sup>131</sup>I and <sup>125</sup>I for biodistribution measurements was carried out using a one vial method as described by Haisma et al.<sup>22</sup>. The purified E48 IgG and E48 F(ab')<sub>2</sub> were <sup>131</sup>I- and <sup>125</sup>I-labeled with a specific activity of 3.6 ± 0.9 MBq/mg and 2.9 ± 1.0 MBq/mg protein, respectively. Using the same methods as described above, the mean <sup>131</sup>I- and <sup>125</sup>I-incorporation percentages were 97.2 ± 1.6 % and 95.8 ± 2.0 %, respectively. The immunoreactive fractions of <sup>131</sup>I-labeled E48 IgG and <sup>125</sup>I-labeled E48 F(ab')<sub>2</sub> at infinite antigen excess always exceeded 70 %. The affinity



constants were  $1.5 \times 10^{10} \text{ M}^{-1}$  for E48 IgG and  $1.2 \times 10^{10} \text{ M}^{-1}$  for E48  $\text{F(ab')}_2$  as determined by the Scatchard plot.

**Radioimmunoscintigraphy.** The radioimmunoscintigrams were obtained with a large field of view gamma camera (Gemini; General Electric, Milwaukee, WI) equipped with a low energy parallel hole collimator and connected to a computer (Bartec, Farnborough, United Kingdom). Whole body images (anterior and posterior views) and planar images of the head and neck (anterior views) were obtained immediately, 16 h, and 21 h after injection. Planar images included the following acquisition parameters: matrix size  $128 \times 128$  (head and neck) or  $256 \times 256$  (whole body) and at least 100 kilocounts per view during 5–20 min. Single photon emission computerized tomography (SPECT) images of the head and neck were acquired 16 h p.i., while lateral views of the head and neck were obtained 21 h p.i..

For topographical evaluation the findings on RIS and the pathological outcome (the gold standard) were recorded and compared per side as well as per level according to the Memorial Sloan Kettering Classification<sup>23</sup> as previously illustrated in Chapter 1 and 2.

**Biodistribution.** In all patients injected with E48 IgG (group II) or E48 IgG/ $\text{F(ab')}_2$  (group III) biopsies of the primary tumor and several other tissues were taken from the surgical specimen. In these patients blood and bone marrow aspiration and biopsy were taken under general anesthesia just before surgery. All biopsies were weighed and the amounts of  $^{99\text{m}}\text{Tc}$ ,  $^{125}\text{I}$ , and  $^{131}\text{I}$  were measured by differential counting methods in a well-counter (1282 Compugamma, LBK Wallac, Turku, Finland) to compare biodistribution of E48 IgG and E48  $\text{F(ab')}_2$ . The effect of self-absorption by volume effects was corrected by comparison of the sample with a set of reference samples, prepared by diluting an equal amount of the standard in different volumes of saline. All data were corrected for decay and converted to percentages injected dose per kilogram (%ID/kg) tissue. Tumor to non-tumor ratios were calculated, using matched uptake values of one patient. If in a patient several biopsies of one kind of tissue were taken, the mean uptake in this tissue was calculated and used for further analysis. After counting, all biopsies were assessed histopathologically to determine the presence or absence of HNSCC.

**Regions of interest.** To get information on the activity uptake at sites, which were not included in the surgical specimen, regions of interest (ROIs) were drawn on the planar views for all 19 E48  $\text{F(ab')}_2$  and for 9 E48 IgG patients in order to obtain the  $^{99\text{m}}\text{Tc}$  counts within these ROIs. In the patients of group III (E48 IgG/ $\text{F(ab')}_2$ ) these measurements could not be performed because of the substantial contribution to the late images of the additionally injected  $^{131}\text{I}$ . ROIs were drawn around the primary tumor, mouth, and tongue on the anterior view of the head and neck at 16 h p.i.. Correction for background was done by measuring counts in a region as much as comparable to the chosen ROI (Fig. 1A). These corrected counts were compared to the counts of a standard obtained directly after the imaging of the head and neck.

From the posterior whole body views 0, 16, and 21 h p.i. counts in the whole body were corrected for background. ROIs were drawn around the visible adrenals on these views at 16 h p.i.. The region for background activity was chosen below the left kidney. The counts in the whole body and adrenals were compared to a standard located between the legs (Fig. 1B).

The counts were not corrected for attenuation and scatter. To allow for comparison of IgG and  $\text{F(ab')}_2$  uptake in the mouth, tongue, and adrenals, the activity values were

expressed as percentage of injected dose (%ID) after correction for decay and camera efficiency. For comparison of tumor uptake in different patients the %ID was divided by the surface area of the ROI.

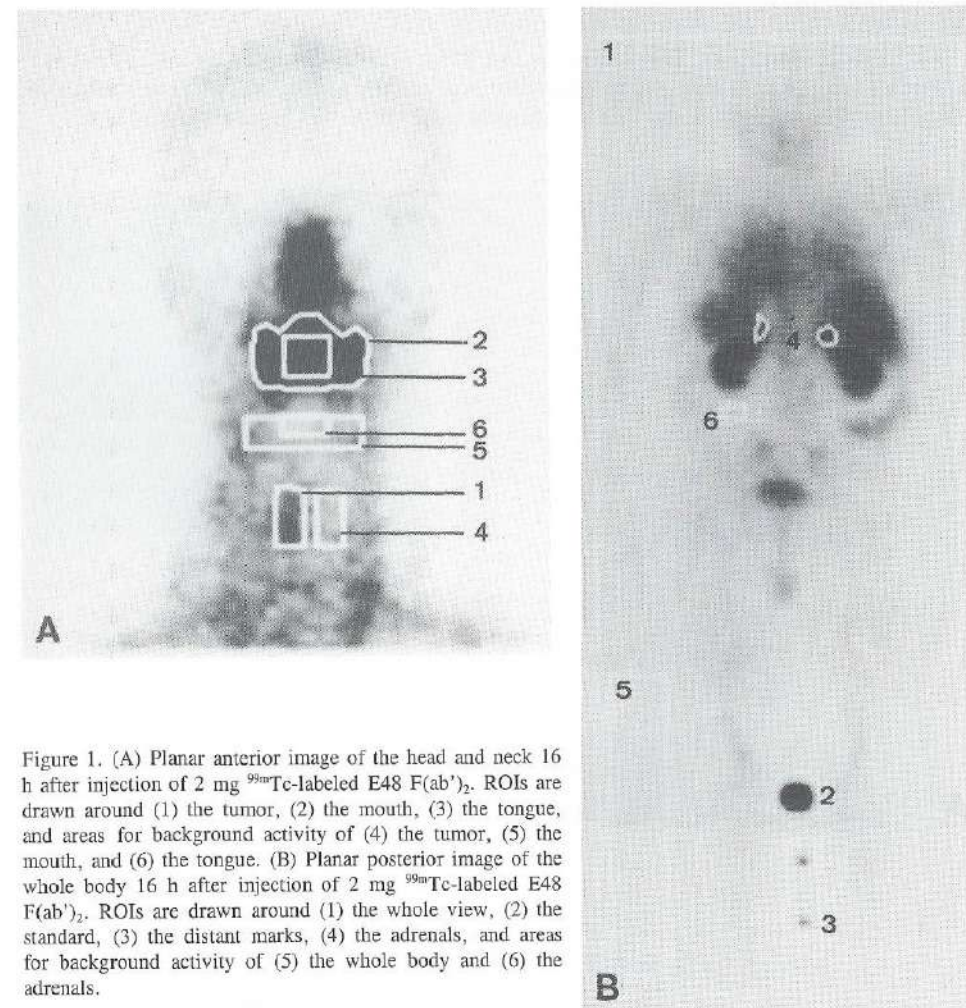


Figure 1. (A) Planar anterior image of the head and neck 16 h after injection of 2 mg  $^{99\text{m}}\text{Tc}$ -labeled E48  $\text{F(ab')}_2$ . ROIs are drawn around (1) the tumor, (2) the mouth, (3) the tongue, and areas for background activity of (4) the tumor, (5) the mouth, and (6) the tongue. (B) Planar posterior image of the whole body 16 h after injection of 2 mg  $^{99\text{m}}\text{Tc}$ -labeled E48  $\text{F(ab')}_2$ . ROIs are drawn around (1) the whole view, (2) the standard, (3) the distant marks, (4) the adrenals, and areas for background activity of (5) the whole body and (6) the adrenals.

**Pharmacokinetics.** Blood samples were obtained from the arm opposite to the injection site for the determination of the activity up to 40 h p.i.. Aliquots of blood samples were measured for  $^{99\text{m}}\text{Tc}$ ,  $^{131}\text{I}$ , and  $^{125}\text{I}$  activity in a well-counter, compared to an aliquot retained from the conjugate preparation, and corrected for decay. Blood activity was expressed as the percentage of the injected dose per kilogram (%ID/kg). HPLC analysis of the serum samples up to 21 p.i. revealed that more than 95 % of the radioactivity was bound to the MAb. The pharmacokinetics were analyzed modeling a



time versus radioactivity curve for each infusion. A MW/Pharm program (MediWare, Groningen, The Netherlands) was used for non-linear Bayesian estimation of pharmacokinetic parameters. One-, two-, and three-compartment models were fit to the data. The peeling algorithm was used to estimate initial parameters. A Bayesian least-square method was used to estimate the final parameters: the initial ( $t_{1/2\alpha}$ ) and final half-lives ( $t_{1/2\beta}$ ).

**Statistical analysis.** The Student's *t* test for paired and unpaired data was used to test the statistical significance of the difference between the uptake of E48 F(ab')<sub>2</sub> and E48 IgG as assessed by biopsies and ROIs. Statistical differences was reached at  $p < 0.05$ .

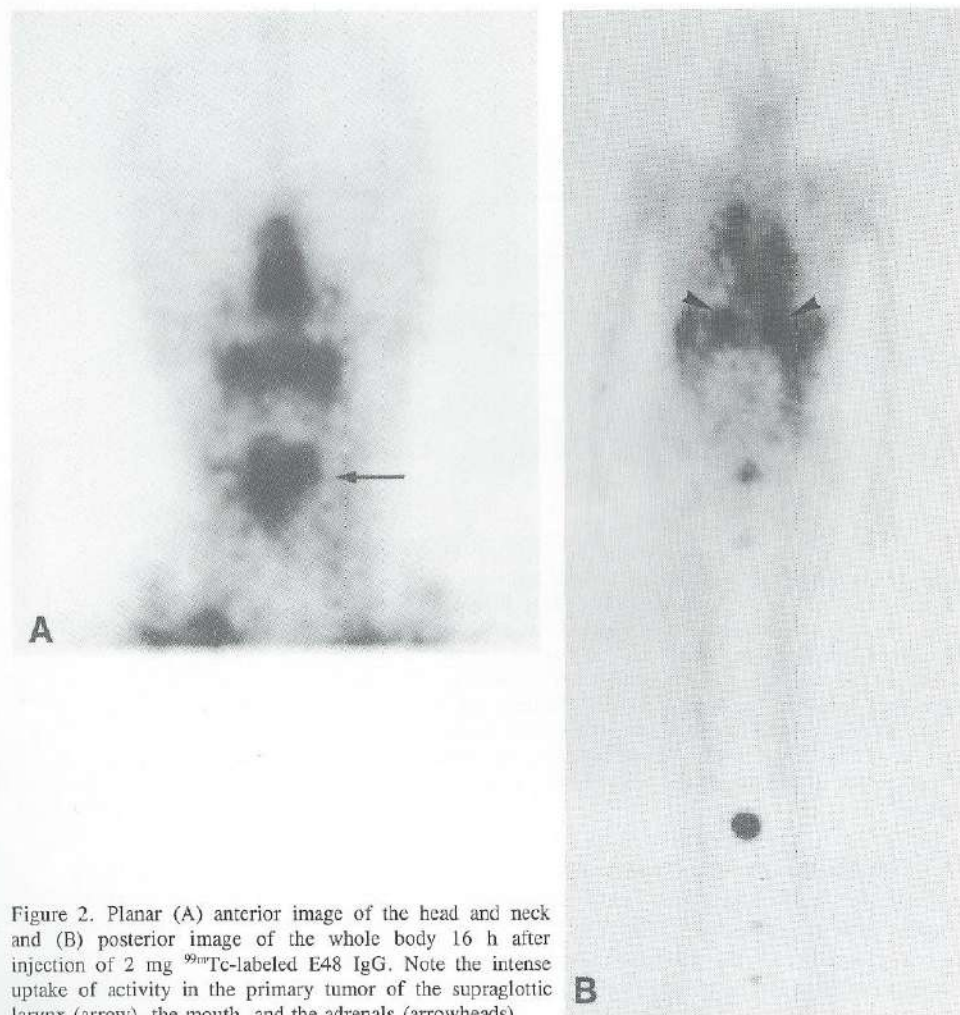


Figure 2. Planar (A) anterior image of the head and neck and (B) posterior image of the whole body 16 h after injection of 2 mg <sup>99m</sup>Tc-labeled E48 IgG. Note the intense uptake of activity in the primary tumor of the supraglottic larynx (arrow), the mouth, and the adrenals (arrowheads).

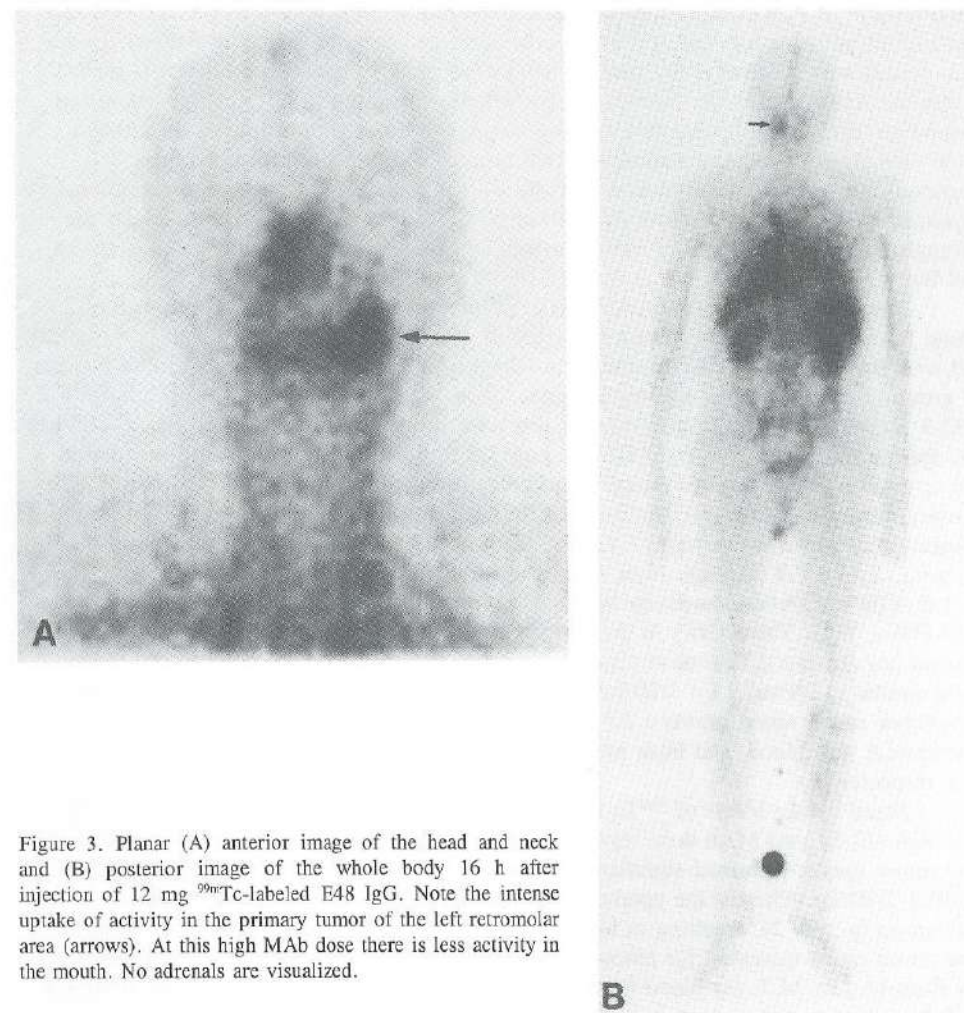


Figure 3. Planar (A) anterior image of the head and neck and (B) posterior image of the whole body 16 h after injection of 12 mg <sup>99m</sup>Tc-labeled E48 IgG. Note the intense uptake of activity in the primary tumor of the left retromolar area (arrows). At this high MAb dose there is less activity in the mouth. No adrenals are visualized.

## RESULTS

No adverse reactions were observed which could be related to the injection of the antibody and no significant changes were noted in blood and urine.

**Radioimmunoscinigraphy.** In 39 patients all 34 primary tumors were visualized. RIS was correct in 215 of 243 levels and 38 of 51 sides of the neck. The RIS results for the first 28 patients have been described previously<sup>14</sup>. Whole body images up to 21 h p.i. showed decreasing blood pool activity with visualization of liver, lungs, heart, spleen, kidneys, and nose. Blood pool activity was less pronounced for E48 F(ab')<sub>2</sub> as compared to E48 IgG. Uptake of activity was also seen in the adrenals, mouth, scrotal area, and



sometimes intestine and gallbladder, at 16 and 21 h p.i. (Fig. 2A and B), as described previously<sup>14</sup>. In one patient injected with 1.2 mg E48 F(ab')<sub>2</sub>, one with 1.1 mg E48 IgG, and in four with 2-4 mg E48 IgG/F(ab')<sub>2</sub> the adrenals were not clearly visualized. In the first patient who received 4 mg dexamethasone 5 h prior to injection no adrenals were visualized. However, in the following three patients the adrenals were clearly visualized, despite an increase of dexamethasone dose and repetition of administration. In three of these patients dexamethasone administration resulted in almost complete adrenal depression of its endocrine function (cortisol < 30 nmol/l). In contrast, upon additional administration of unlabeled MAb E48 (10 or 50 mg) in six patients, in five patients the adrenals were not visualized, while the mouth uptake also was less pronounced (Fig. 3A and B).

**Biodistribution.** The activity uptake in biopsies from the surgical specimen of group II and III patients are shown in Figure 4. The counts in biopsies 9 days p.i. (patient 39) were too low for a reliable evaluation. Uptake of <sup>99m</sup>Tc-labeled E48 IgG in all patients of group II and III was the highest in tumor tissue: 30.6 ± 20.1 (mean ± SD); range 7.2 - 82.3 %ID/kg. High <sup>99m</sup>Tc activity was also seen in normal mucosa (13.6 ± 6.5 %ID/kg) and tongue tissue (10.7 ± 1.8 %ID/kg), but was significantly ( $p < 0.01$ ) lower than in tumor tissue. Tumor positive lymph nodes contained significantly ( $p < 0.02$ ) more <sup>99m</sup>Tc activity than tumor negative lymph nodes: 7.2 ± 5.6 %ID/kg and 2.0 ± 0.6 %ID/kg, respectively, with a mean ratio of 4.7 ± 4.3. Low activity was seen in bone marrow biopsies: 2.4 ± 0.9 %ID/kg. Bone marrow aspiration showed a mean <sup>99m</sup>Tc activity of 7.4 ± 1.8 %ID/kg, while the activity in blood was slightly higher (8.1 ± 1.3 %ID/kg, mean ratio 0.9 ± 0.1). The activity in the bone marrow aspirate was mainly located in the plasma (supernatant). The mean plasma activity of the bone marrow aspirate and blood were similar (12.9 and 13.4 %ID/kg, respectively, mean ratio 1.0 ± 0.1). Mean tumor to non-tumor ratios varied between 2.8 for mucosa and 99.9 for parotid gland tissue (Fig. 5). For muscle, fat, blood, and bone marrow aspirate these ratios were 21.0, 20.3, 4.1, and 4.6, respectively.

Mean uptake levels of <sup>99m</sup>Tc-labeled E48 IgG was also calculated at low (1-4 mg) and high (12-51 mg) MAb dose separately. With the addition of 10-50 mg unlabeled E48 IgG tumor uptake increased significantly ( $p < 0.05$ ) from 25.8 ± 17.9 %ID/kg to 54.1 ± 16.1 %ID/kg, whereas the uptake in normal mucosa and other tissues was not influenced ( $p > 0.2$ ), resulting in higher tumor to non-tumor ratios. The mean tumor to non-tumor ratios increased for mucosa from 2.5 to 3.7, for muscle from 15.9 to 46.7, for fat from 17.2 to 34.7, for blood from 3.2 to 7.6, and for bone marrow aspirate from 4.2 to 8.4.

Simultaneous measurements of <sup>131</sup>I-labeled E48 IgG and <sup>125</sup>I-labeled E48 F(ab')<sub>2</sub> 44 h p.i. resulted in a mean tumor uptake of 27.8 ± 18.5 %ID/kg and 18.7 ± 11.2 %ID/kg ( $p < 0.2$ ), respectively. The mean tumor to non-tumor ratio of <sup>131</sup>I-labeled E48 IgG was lower, however not significant, as compared to <sup>125</sup>I-labeled E48 F(ab')<sub>2</sub>: for muscle 18.1 and 22.9, for fat 18.0 and 27.0, for blood 4.3 and 7.0, and for bone marrow aspirate 3.3 and 5.2, respectively. An exception formed the normal mucosa in which the mean ratio of <sup>131</sup>I-labeled E48 IgG was similar to <sup>125</sup>I-labeled E48 F(ab')<sub>2</sub>: 2.1 and 1.9, respectively. When additionally 10-50 mg unlabeled E48 IgG was administered also the tumor uptake of <sup>125</sup>I-labeled E48 F(ab')<sub>2</sub> increased significantly ( $p < 0.05$ ) from 14.1 ± 8.7 %ID/kg ( $n=7$ ) to 29.5 ± 8.5 %ID/kg ( $n=3$ ).

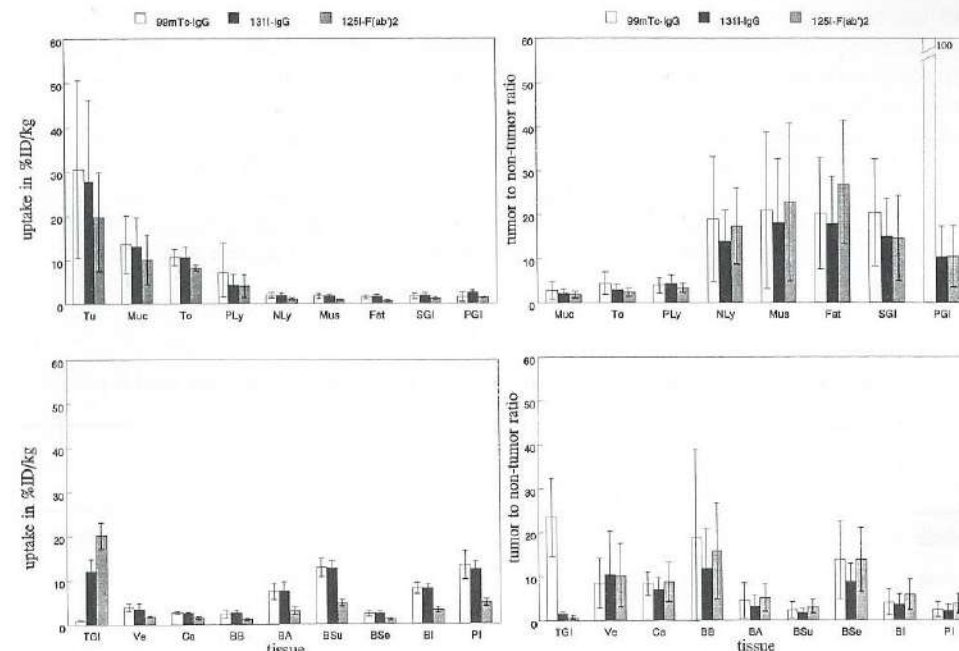


Figure 4. Uptake of <sup>99m</sup>Tc-labeled E48 IgG, <sup>131</sup>I-labeled E48 IgG, and <sup>125</sup>I-labeled E48 F(ab')<sub>2</sub> in tumor (Tu;  $n=18,10$ , and 10, respectively), mucosa (Muc;  $n=16,10,10$ ), tongue (To;  $n=4,3,3$ ), positive lymph node (PLy;  $n=11,6,6$ ), negative lymph node (NLy;  $n=10,8,8$ ), muscle (Mus;  $n=19,10,10$ ), fat (Fat;  $n=18,10,10$ ), submandibular gland (SGI;  $n=8,8,8$ ), parotid gland (PGI;  $n=3,2,2$ ), thyroid gland (TGI;  $n=2,2,2$ ), vein (Ve;  $n=9,9,9$ ), cartilage (Ca;  $n=2,2,2$ ), bone marrow biopsy (BB;  $n=13,10,10$ ), total bone marrow aspiration (BA;  $n=12,8,8$ ), supernatant of bone marrow aspiration (BSu;  $n=8,6,6$ ), sediment of bone marrow aspiration (BSe;  $n=8,6,6$ ), blood (BI;  $n=15,10,10$ ), and plasma (PI;  $n=15,10,10$ ).

Figure 5. Tumor to non-tumor ratios of <sup>99m</sup>Tc-labeled E48 IgG, <sup>131</sup>I-labeled E48 IgG, and <sup>125</sup>I-labeled E48 F(ab')<sub>2</sub> in mucosa (Muc;  $n=16,10$ , and 10, respectively), tongue (To;  $n=4,3,3$ ), positive lymph node (PLy;  $n=10,6,6$ ), negative lymph node (NLy;  $n=10,8,8$ ), muscle (Mus;  $n=18,10,10$ ), fat (Fat;  $n=17,10,10$ ), submandibular gland (SGI;  $n=8,8,8$ ), parotid gland (PGI;  $n=3,2,2$ ), thyroid gland (TGI;  $n=2,2,2$ ), vein (Ve;  $n=9,9,9$ ), cartilage (Ca;  $n=2,2,2$ ), bone marrow biopsy (BB;  $n=13,10,10$ ), total bone marrow aspiration (BA;  $n=11,8,8$ ), supernatant of bone marrow aspiration (BSu;  $n=8,6,6$ ), sediment of bone marrow aspiration (BSe;  $n=8,6,6$ ), blood (BI;  $n=15,10,10$ ), and plasma (PI;  $n=15,10,10$ ).

**Regions of interest.** Planar images obtained in 28 patients injected with E48 F(ab')<sub>2</sub> or IgG (group I and II), were used for biodistribution estimations of sites, which were not included in the surgical specimens. In some patients the activity uptake in the tumor could not be assessed due to the lack of a suitable background region. Particularly, in patients with a tumor of the oral cavity no reliable ROIs for the tumor, mouth, and tongue could be drawn. Although the adrenals in almost all patients injected with 1-2 mg MAb E48 were visualized, in some patients a reliable ROI could not be drawn, due to overprojection of other abdominal structures.



Retention of activity in the whole body was significantly higher for  $^{99m}\text{Tc}$ -labeled E48 IgG as compared to  $^{99m}\text{Tc}$ -labeled E48 F(ab')<sub>2</sub>; after 16 h the percentage of the whole body activity directly after injection was  $97.9 \pm 12.5\%$  and  $89.1 \pm 6.0\%$  ( $p < 0.05$ ), respectively (Table 1). With the ROI technique there was no significant difference in tumor uptake per area between E48 IgG and E48 F(ab')<sub>2</sub> at 16 h p.i.. The uptake of E48 IgG in the mouth was almost half of the E48 F(ab')<sub>2</sub> uptake ( $p < 0.1$ ). The uptake in the central area of the mouth, the tongue region, was also less for E48 IgG as compared to E48 F(ab')<sub>2</sub>, but did not reach statistical significance. In the adrenals the uptake of E48 IgG was similar to E48 F(ab')<sub>2</sub>. The uptake of E48 F(ab')<sub>2</sub> in the adrenals was lower if unlabeled E48 F(ab')<sub>2</sub> was given before, while the tumor uptake per area was similar (Table 1).

Table 1. Measured activity in ROIs of whole body, tumor, mouth, and adrenals in group I and II patients 16 h p.i..

		1-2 mg E48 IgG			1-2 mg E48 F(ab') <sub>2</sub>			p
		mean	SD	n	mean	SD	n	
whole body	% <sup>a</sup>	97,9	12,5	8 <sup>c</sup>	89,1	6,0	13 <sup>c</sup>	< 0.05
tumor	%ID/A <sup>b</sup>	0,013	0,003	6 <sup>c</sup>	0,013	0,006	9 <sup>c</sup>	> 0.2
mouth	%ID	0,131	0,023	3 <sup>c</sup>	0,201	0,054	9 <sup>c</sup>	< 0.1
tongue	%ID	0,048	0,007	3 <sup>c</sup>	0,067	0,023	9 <sup>c</sup>	> 0.2
adrenals	%ID	0,312	0,091	14 <sup>d</sup>	0,301	0,195	23 <sup>d</sup>	> 0.2
		1-2 mg E48 F(ab') <sub>2</sub>			11-12 mg E48 F(ab') <sub>2</sub>			p
		mean	SD	n	mean	SD	n	
tumor	%ID/A <sup>b</sup>	0,013	0,006	9 <sup>c</sup>	0,013	0,013	2 <sup>c</sup>	> 0.2
adrenals	%ID	0,301	0,194	23 <sup>d</sup>	0,037	0,013	2 <sup>d</sup>	< 0.1

<sup>a</sup>%, percentage of whole body activity at 0 h p.i.; <sup>b</sup>%ID/A, percentage of the injected dose per pixel;

<sup>c</sup>, number of patients; <sup>d</sup>, number of visible adrenals.

**Pharmacokinetics.** The time versus radioactivity curves of E48 IgG and F(ab')<sub>2</sub> best fitted a two-compartment model. Significant ( $p < 0.001$ ) faster elimination from the blood was observed for  $^{99m}\text{Tc}$ -labeled E48 F(ab')<sub>2</sub> as compared to E48 IgG: at 1-2 mg,  $t_{1/2} \alpha$  and  $t_{1/2} \beta$  were for E48 F(ab')<sub>2</sub>  $2.3 \pm 0.4$  and  $19.9 \pm 4.6$  h and for E48 IgG  $6.6 \pm 2.6$  and  $54.1 \pm 24.3$  h, respectively. An increase in MAb dose did not influence the clearance from the blood:  $t_{1/2} \alpha$  and  $t_{1/2} \beta$  were for  $^{99m}\text{Tc}$ -labeled E48 IgG at 10 mg  $8.6$  and  $48.2$  h and at 50 mg  $7.3 \pm 0.1$  and  $56.4 \pm 5.9$  h, respectively.

## DISCUSSION

In earlier reports <sup>13,14</sup> we demonstrated that  $^{99m}\text{Tc}$ -labeled MAb E48 IgG or F(ab')<sub>2</sub> can be used for tumor detection with radioimmunoscintigraphy. In these studies MAb E48 was able to visualize all primary tumors ( $n=31$ ) as well as 68% of the tumor involved lymph nodes. The missed nodes contained only a small amount of tumor cells. These findings indicate that MAb E48 may also be suitable for radioimmunotherapy (RIT), especially because HNSCC is known to be a radiosensitive tumor type. For RIT it is necessary that a MAb, after administration to the patient, accumulates selectively and to a high level in the tumor.

In the present study we compared the uptake of radiolabeled MAb E48 IgG and F(ab')<sub>2</sub> in HNSCC and some normal tissues, 44 h after injection. The uptake of  $^{99m}\text{Tc}$ -labeled E48 IgG in HNSCC was high ( $30.6 \pm 20.1\%$  ID/kg), as compared to the uptake of other MAbs in other types of tumors <sup>24,31</sup>.

Biodistribution data on  $^{99m}\text{Tc}$ -labeled MAb E48 IgG revealed that tumor positive lymph nodes contained 4.7 times more activity than tumor negative lymph nodes. The uptake in tumor positive lymph nodes was much less than in primary tumors. However, this difference should be interpreted with caution, because the proportion of tumor cells present in the lymph nodes is difficult to assess and shows great variation: some positive lymph nodes contain only a few tumor cells, whereas other nodes are totally occupied by tumor tissue.

As known from extensive immunohistochemical screening, the MAb E48 defined antigen is also expressed in normal squamous epithelium like oral mucosa and skin <sup>11</sup>. Despite the fact that the level of E48 antigen expression is apparently the same in these normal tissues as in HNSCC,  $^{99m}\text{Tc}$ -labeled MAb E48 IgG uptake 44 h p.i. was significantly higher in HNSCC than in oral mucosa and tongue mucosa. Since biopsies show variance in amount of normal and malignant squamous cells and other cells, the exact extent of the difference in uptake levels is difficult to assess. Moreover, RIS studies did not reveal marked uptake of the MAb in the skin. The higher uptake of MAb E48 IgG in HNSCC may be due to the better accessibility of the E48 antigen in malignant tissue than in normal tissue. Penetration of MAbs into the tumor is facilitated by the presence of fenestrated endothelium and the absence of a basement membrane. On the other hand, antigens present in normal squamous epithelium are particularly poorly accessible for MAbs. In this tissue, MAbs must pass across the endothelial cells by intracytoplasmic vesicles and transendothelial cell channels <sup>32</sup>.

An unexpected finding was the high uptake of activity in the adrenals. Using ROIs in patients injected with 1-2 mg  $^{99m}\text{Tc}$ -labeled MAb E48 IgG, it is estimated that 0.3 %ID was present in an adrenal 16 h p.i. Assuming that one adrenal weighs 6 g, the uptake in adrenal tissue is 50 %ID/kg, about 2 times higher than in tumor tissue 44 h p.i.. Immunohistochemical evaluation showed no reactivity of MAb E48 with 5 frozen adrenal tissues. Four other MAbs (323/A3 F(ab')<sub>2</sub>, chimeric SF-25 IgG, K928 IgG <sup>19</sup>, and U36 IgG) labeled in the same way as MAb E48 showed no uptake of activity in the adrenals. Therefore, the adrenal uptake does not seem to be related to the labeling technique used. The fact that no adrenals were visualized after administration of a higher MAb dose (10-50 mg) indicates that a limited number of good accessible binding sites may be present in the adrenals which become saturated after a higher dose. In contrast, administration of



dexamethasone did not decrease the activity uptake. We recently cloned the E48 encoding cDNA which may open new avenues for analyzing E48 antigen expression in adrenal tissue by Northern blotting and PCR-techniques (manuscript in preparation). Since MAb doses of 10-50 mg are recommended for clinical RIT, uptake in the adrenal glands probably will not hamper RIT. A high MAb dose administration may provide even additional advantages in comparison to low dose administration as indicated by the significant higher tumor uptake of the radioimmunoconjugate and the probably higher tumor to non-tumor ratios in patients receiving a high E48 IgG dose.

No selective accumulation of radioactivity was observed in any other normal tissue. For example, the activity in the bone marrow aspirate 44 h after administration of  $^{99m}\text{Tc}$ -labeled MAb E48 was almost the same as in blood and 4.6 times less than in the tumor. Radioactivity in the bone marrow aspirate was not confined to the cellular compartment as became apparent on centrifugation. This is important since, in general, bone marrow is the dose limiting organ in RIT.

One of the aims of this study was to analyze whether MAb E48 IgG or  $\text{F(ab')}_2$  is better suited for RIT. For this purpose we administered E48 IgG and  $\text{F(ab')}_2$ , simultaneously, both in an radioiodinated form. This is important for a proper comparison since tissue uptake values may depend on the kind of radioconjugate used. In this study, tissue uptake levels of  $^{131}\text{I}$ -labeled E48 IgG were lower than those of coadministered  $^{99m}\text{Tc}$ -labeled E48 IgG, probably due to the process of dehalogenation.

Unfortunately, no definite answer has been obtained as to which antibody form is better for RIT, IgG or  $\text{F(ab')}_2$ . On one hand, tumor uptake levels were on average 49% higher for IgG than for  $\text{F(ab')}_2$ . On the other hand, tumor to non-tumor ratios were in general lower for IgG. However, the opposite was true for oral mucosa including the tongue, sites with relatively high activity uptake. The analysis of biodistribution on images obtained 16 h p.i., as well as measurement of biopsies from the surgical specimens obtained 44 h p.i. revealed relatively lower uptake in the mouth region for IgG in comparison to  $\text{F(ab')}_2$ . Also other considerations might indicate the advantage of whole IgG. The use of IgG in RIT may provide additional advantage because of its ability to mediate antibody-dependent cell cytotoxicity (ADCC). As stated previously we intend to use  $^{186}\text{Re}$ -labeled chimeric MAb E48 for radioimmunotherapy of minimal residual disease. For this purpose we recently developed a technical protocol for labeling of MAbs with  $^{186}\text{Re}$  using the  $\text{MAG}_3$  chelate <sup>33</sup>. For the same purpose, we constructed a chimeric (mouse/human) MAb E48 containing the human  $\gamma_1$  heavy chain (manuscript in preparation). This cMAb appeared to be highly effective in mediating ADCC even when loaded with 16  $\text{MAG}_3$  groups (manuscript in preparation). When using this cMAb for RIT of minimal residual disease it can be anticipated that ADCC activity may be supportive to irradiation, especially in eradicating single disseminated cells or small cell aggregates.

When combining the biodistribution data obtained herein with data obtained from previous animal studies we might be able to speculate about the potential of  $^{186}\text{Re}$ -labeled E48 IgG for eradicating HNSCC in patients. As shown before <sup>16</sup>, it is possible to eradicate 50% of large HNSCC xenograft bearing nude mice by treatment with 18.5 MBq  $^{186}\text{Re}$ -labeled MAb E48 IgG. Because the mean maximum uptake in these tumors was assessed to be 10,000 %ID/kg, it can be calculated that the amount of  $^{186}\text{Re}$  in the xenografts was 1,850 MBq/kg. As shown in the present study in patients the average uptake of MAb E48 IgG, 44 h p.i. in tumors of 0.5 - 6 cm was  $30.6 \pm 20.1$  %ID/kg. Assuming that the maximum tolerated radiation dose of  $^{186}\text{Re}$ -labeled E48 IgG is about 7,400 MBq, the same

as found for other  $^{186}\text{Re}$ -labeled MAbs <sup>34</sup>, we expect that in clinical RIT studies with  $^{186}\text{Re}$ -labeled MAb E48 it will be possible to reach an average uptake level in the tumor of 2,260 MBq/kg (30.6 % of 7,400 MBq per kg). This is higher than the level obtained in xenografts responding to RIT. Taking into account the higher uptake by small tumors in comparison to large tumors <sup>25</sup> we think that sufficient high radiation doses can be achieved to eliminate minimal residual disease.

A main limitation of the forementioned calculation is that no data are available on MAb E48 IgG tumor retention in HNSCC patients. Before starting clinical RIT studies we will obtain imaging and biodistribution data up to 7 days p.i., using  $^{131}\text{I}$  as imaging radionuclide instead of  $^{99m}\text{Tc}$ . The efficacy of adjuvant RIT with MAb E48 will be first evaluated in HNSCC patients who are at high risk for developing distant metastases and locoregional recurrences.

## ACKNOWLEDGEMENTS

The authors thank Drs. Hein Leverstein and Richard P. Wong Chung for clinical support, Henri Greuter for laboratory support, and Dr. Jacqueline E. van der Wal for pathological support. This work was supported by the Dutch Ministry of Economic Affairs and by Centocor Europe, Inc., Leiden, the Netherlands

## REFERENCES

1. Zarbo RJ, Crissman JD. The surgical pathology of head and neck cancer. *Semin Oncol* 1988;15:10-9.
2. Blitzer PH. Epidemiology of head and neck cancer. *Semin Oncol* 1988;15:2-9.
3. Choski AJ, Dimery IW, Hong WK. Adjuvant chemotherapy of head and neck cancer: the past, the present and the future. *Semin Oncol* 1988;15 suppl 3:45-59.
4. Zbaren P, Lehmann W. Frequency and sites of distant metastases in head and neck squamous cell carcinoma. *Arch Otolaryngol Head Neck Surg* 1987;113:762-4.
5. Head and neck contracts program. Adjuvant chemotherapy for advanced head and neck squamous carcinoma: Final report of the head and neck contracts program. *Cancer* 1987;60:301-11.
6. Stell PM, Rawson NSB. Adjuvant chemotherapy in head and neck cancer. *Br J Cancer* 1990;61:779-87.
7. Vokes EE, Weiselbaum RR, Lippman SM, Hong WK. Head and neck cancer. *N Engl J Med* 1993;328:184-94.
8. Dongen GAMS van, Brakenhoff RH, Bree R de, Gerretsen M, Quak JJ, Snow GB. Progress in radioimmunotherapy of head and neck cancer. *Oncology Reports* 1994;1:259-64.
9. Gerretsen M, Quak JJ, Brakenhoff RH, Snow GB, Dongen GAMS van. The feasibility of radioimmunotherapy in head and neck cancer. *Eur J Cancer Oral Oncol* 1994;30B:82-7.
10. Wessels BW, Harisiadis L, Carabell SC. Dosimetry and radiobiological efficacy of clinical radioimmunotherapy. *J Nucl Med* 1989;30:827.
11. Quak JJ, Dongen GAMS van, Balm AJM, Brakkee JPG, Scheper RJ, Snow GB, Meijer CJLM. A 22-kd surface antigen detected by monoclonal antibody E48 is exclusively expressed in stratified squamous and transitional epithelia. *Am J Pathol* 1990;36:191-7.
12. Quak JJ, Balm AJM, Brakkee JGP, Scheper RJ, Haisma HJ, Braakhuis BJM, Meijer CJLM, Snow GB. Localization and imaging of radiolabelled monoclonal antibody against squamous-cell carcinoma of the head and neck in tumor-bearing nude mice. *Int J Cancer* 1989;44:534-8.
13. Dongen GAMS van, Leverstein H, Roos JC, Quak JJ, Brekel MWM van den, Lingen A van, Martens HJM, Castelijns JA, Visser GWM, Meijer CJLM, Teule JJ, Snow GB. Radioimmunoscintigraphy of head and neck cancer. *Int J Cancer* 1994;55:100-10.



- igraphy of head and neck tumors using  $^{99m}\text{Tc}$ -labeled monoclonal antibody E48 F(ab')<sub>2</sub>. *Cancer Res* 1992;52:2569-74.
14. Bree R de, Roos JC, Quak JJ, Hollander W den, Brekel MWM van den, Wal JE van der, Tobi H, Snow GB, Dongen GAMS van. Clinical imaging of head and neck cancer with  $^{99m}\text{Tc}$ -labeled monoclonal antibody E48 IgG or F(ab')<sub>2</sub>. *J Nucl Med* 1994;34:775-83.
15. Gerretsen M, Schrijvers AHGJ, Walsum M van, Braakhuis BJM, Snow GB, Dongen GAMS van. Radioimmunotherapy of head and neck squamous cell carcinoma with  $^{131}\text{I}$ -labelled monoclonal antibody E48. *Br J Cancer* 1992;66:496-502.
16. Gerretsen M, Visser GWM, Walsum M van, Meijer CJLM, Snow GB, Dongen GAMS van.  $^{186}\text{Re}$ -labeled monoclonal antibody E48 immunoglobulin G-mediated therapy of human head and neck squamous cell carcinoma xenografts. *Cancer Res* 1993;53:3524-9.
17. Gerretsen M, Visser GWM, Brakenhoff RH, Walsum M van, Snow GB, Dongen GAMS van. Complete ablation of small squamous cell carcinoma xenografts with  $^{186}\text{Re}$ -labeled monoclonal antibody E48. *Cell Biophysics* 1994;24:1-6.
18. Hermanek P, Sobin LH, eds. TNM classification of malignant tumors, 4th edition. Berlin: Springer Verlag; 1987: 13-26.
19. Bree R de, Roos JC, Quak JJ, Hollander W den, Snow GB, Dongen GAMS van. Clinical screening of monoclonal antibodies 323/A3, cSF-25, and K928 for suitability of targeting tumors in the upper-aerodigestive and respiratory tract. *Nucl Med Commun* 1994;15:613-27.
20. Fritzberg AR, Abrams PG, Beaumier PL, Kasina S, Morgan AC, Rao TN, Reno JM, Sanderson JA, Srinivasan A, Willber DS, Vanderheyden J-L. Specific and stable labeling of antibodies with technetium-99m with a diamide dithiolate chelating agent. *Proc Natl Acad Sci USA* 1988;85:4025-29.
21. Gerretsen M, Quak JJ, Suh JS, Walsum M van, Meijer CJLM, Snow GB, Dongen GAMS van. Superior localisation and imaging of radiolabelled monoclonal antibody E48 F(ab')<sub>2</sub> fragment in xenografts of human squamous cell carcinoma of the head and neck and of the vulva as compared to monoclonal antibody E48 IgG. *Br J Cancer* 1991;63:37-44.
22. Haisma HJ, Hilgers J, Zurawski VR. Iodination of monoclonal antibodies for diagnosis and radiotherapy using a convenient one vial method. *J Nucl Med* 1986;27:1890-5.
23. Shah JP, Strong E, Vikram B. Neck dissection: Current status and future possibilities. *Clin Bull* 1981;11:25-33.
24. Epenetos AA, Snook D, Durbin H, Johnson PM, Taylor-Padimitriou J. Limitations of radiolabeled monoclonal antibodies for localization of human neoplasms. *Cancer Res* 1986;46:3183-91.
25. Chatal J-F, Saccavini J-C, Geste J-F, Thedrez P, Curtet C, Kremer M, Guerreau D, Nobile D, Fumoleau P, Guillard Y. Biodistribution of indium-111-labeled OC 125 monoclonal antibody intraperitoneally injected into patients operated on for ovarian carcinomas. *Cancer Res* 1989;49:3087-94.
26. Zalutsky MR, Mosely RP, Coakham HB, Coleman RE, Bigner DD. Pharmacokinetics and tumor localization of  $^{131}\text{I}$ -labeled anti-tenascin monoclonal antibody 81C6 in patients with gliomas and other intracranial malignancies. *Cancer Res* 1989;49:2807-13.
27. Scheinberg DA, Straus DJ, Yeh SD, Divgi C, Garin-Chesa P, Graham M, Pentlow K, Coit D, Oettgen HF, Old LJ. A phase I toxicity, pharmacology, and dosimetry trial of monoclonal antibody OKB7 in patients with Non-Hodgkin's lymphoma: Effects of tumor burden and antigen expression. *J Clin Oncol* 1990;8:792-803.
28. Larson SM, Carrasquillo JA, Colcher DC, Yokoyama K, Reynolds JC, Bacharach A, Raubitschek A, Pace L, Finn RD, Rotman M, Stabin M, Neumann RD, Sugarbaker P, Schlom J. Estimates of radiation absorbed dose for intraperitoneally administered Iodine-131 radiolabeled B72.3 monoclonal antibody in patients with peritoneal carcinomatosis. *J Nucl Med* 1991;32:1661-7.
29. Bares R, Fass J, Hauptmann S, Braun J, Grehl O, Reinartz R, Buell U, Schumpelick V, Mittmayer C. Quantitative analysis of anti-CEA antibody accumulation in human colorectal carcinomas. *J Nucl Med* 1993;32:65-72.
30. Oosterwijk E, Bander NH, Divgi CR, Welt S, Wakka JC, Finn RD, Carswell EA, Larson SM, Warnaar SO, Fleuren GJ, Oettgen HF, Old LJ. Antibody localization in human renal cell carcinoma: a phase I study of monoclonal antibody G250. *J Clin Oncol* 1993;11:738-50.
31. Buist MR, Kenemans P, Hollander W den, Vermorken JB, Molthoff CJM, Burger CW, Helmerhorst TJM, Baak JPA, Roos JC. Kinetics and tissue distribution of the radiolabeled chimeric monoclonal antibody MOv18 IgG and F(ab')<sub>2</sub> fragments in ovarian cancer patients. *Cancer Res* 1993;53:5413-8.
32. Cobb LM. Intratumour factors influencing the access of antibody to tumour cells. *Cancer Immunol Immunother* 1989;28:235-40.
33. Visser GWM, Gerretsen M, Herscheid JDM, Snow GB, Dongen GAMS van. Labeling of monoclonal antibodies with  $^{186}\text{Re}$  using the MAG<sub>3</sub> chelate for radioimmunotherapy of cancer: a technical protocol. *J Nucl Med* 1993;34:1953-63.
34. Breitz HB, Weiden PL, Vanderheyden J-L, Appelbaum JW, Bjorn MJ, Fer MF, Wolf SB, Ratliff BA, Seiler CA, Foisie DC, Fisher DR, Schroff RW, Fritzberg AR, Abrams PA. Clinical experience with rhenium-186-labeled monoclonal antibodies for radioimmunotherapy: results of phase I trials. *J Nucl Med* 1992;33:1099-112.



**Clinical Screening of Monoclonal Antibodies 323/A3, cSF-25,  
and K928 for Suitability of Targeting Tumors  
in the Upper Aerodigestive and Respiratory Tract**

Remco de Bree <sup>1</sup>, Jan C. Roos <sup>2</sup>, Jasper J. Quak <sup>1</sup>, Willem den Hollander <sup>2</sup>,  
Gordon B. Snow <sup>1</sup>, and Guus A.M.S. van Dongen <sup>1</sup>

Departments of <sup>1</sup>Otolaryngology / Head and Neck Surgery  
and <sup>2</sup>Nuclear Medicine,  
Free University Hospital, Amsterdam, The Netherlands

Nuclear Medicine Communications 1994; 15: 613-627



## ABSTRACT

Immunohistochemical characterization of three monoclonal antibodies (MAbs), designated 323/A3, SF-25, and K928, on a panel of 330 head and neck and lung tumors indicated their potential for targeting tumors in the upper-aerodigestive and respiratory tract. Subsequently, MAbs were screened in a clinical phase I/II radioimmunoscinigraphy (RIS) trial for the detection of primary tumors and lymph node metastases in patients with histologically proven squamous cell carcinoma of the head and neck (HNSCC). In 10 HNSCC patients MAbs 323/A3 F(ab')<sub>2</sub> (n=3), chimeric (mouse-human) SF-25 IgG (n=1), and K928 IgG (n=6) were evaluated for their suitability of tumor targeting.

MAb 323/A3 and K928 were shown to be capable for detection of HNSCC. However, there was uptake at non-tumor sites, for MAb 323/A3 in thyroid gland, liver, and skeleton probably bone marrow and for MAb K928 in liver, spleen, and the skeleton probably bone marrow. At higher K928 dose, uptake in the liver was diminished but still substantial. MAb cSF-25 was not capable to detect HNSCC, due to the rapid and extensive uptake at non-tumor sites like liver, spleen, brain, and the skeleton probably bone marrow. Radioactivity uptake at non-tumor sites could be mainly explained by the presence of good accessible antigenic sites and will definitely limit the application of these pan-carcinoma MAbs for therapeutic purposes.

## INTRODUCTION

Among the potential applications of tumor-preferential MAbs is the selective delivery of radionuclides to primary tumors and particularly to lymph node and distant metastases for diagnostic and therapeutic purposes. At present, there is only a small number of MAbs available directed against squamous cell carcinoma (SCC). Recently we described the production of a panel of high affinity MAbs reactive with membrane antigens expressed by SCC of distinct sites of origin: head and neck, lung, esophagus, cervix, and skin <sup>1-4</sup>.

Two of these MAbs designated MAb E48 and MAb U36 are selectively reactive with squamous and transitional epithelia and their malignant counterparts, indicating that the corresponding antigens are related to squamous differentiation <sup>1,4</sup>. Initial preclinical and clinical studies indicated that MAb E48 and MAb U36 may be well suited for targeting of head and neck squamous cell carcinoma (HNSCC) <sup>4-11</sup>.

Because MAbs E48 and U36 seem to be excellent candidate MAbs for targeting SCC of the head and neck, we hypothesized that MAb E48 and U36 might be of value for targeting SCC in the whole upper-aerodigestive and respiratory tract, including the lung. Unfortunately, as became apparent from immunohistochemical screening of SCC of the lung, expression patterns of the E48 and U36 antigens in these tumors are very heterogeneous. This may be related to the mixed differentiation features (squamous and adeno) as often observed in these tumors. Therefore, MAbs E48 and U36 can not be used as single agent for targeting SCC of the lung. MAbs recognizing several types of carcinoma, squamous cell carcinoma as well as adenocarcinoma, may be better suited for this application.

In our laboratory, we have developed 3 MAbs reactive with so-called pan-carcinoma markers <sup>2,3</sup>. These MAbs designated K931, K984, and K928 are reactive with e.g. SCC of the head and neck and lung, small cell lung cancer, and adenocarcinoma of lung, breast, colon, and ovary. The MAbs were selected after extensive immunohistochemical characterization on tumor and normal tissues. In these studies, it was proven that the antigen recognized by MAb K984 is similar to the one recognized by MAb SF-25, an antibody produced by the group of Wands <sup>2,12,13</sup>. Furthermore, MAb K931 was found to recognize a similar antigen as MAb 17-1A and MAb 323/A3, MAbs produced by the groups of Koprowski and McGuire, respectively <sup>3,14,15</sup>.

In this study the potential of pan-carcinoma MAbs 323/A3, chimeric (human-mouse) SF-25, and K928 for selective targeting of tumors in the upper-aerodigestive and respiratory tract is evaluated. Since practice has learned that many MAbs with favorable characteristics on the basis of their immunohistochemical reactivity profile show uptake at unexpected and unwanted non-target sites in patients, this study was designed as an initial screening test with a limited number of patients. To allow for direct comparison with SCC-preferential MAbs E48 and U36, the present RIS study was also performed in patients suffering from a SCC in the head and neck and at risk for having lymph node metastases.



## METHODS

**Patient Study.** The protocols were approved by the Dutch Health Council and by the institutional review board of the Free University Hospital. Informed consent was obtained from all participants.

Ten patients (Table 1), who were at risk for having neck lymph node metastasis from a histologically proven head and neck squamous cell carcinoma and planned to undergo neck dissection(s), participated in this study. The primary tumor and the status of neck lymph nodes were classified according to the TNM system of the International Union Against Cancer, UICC<sup>16</sup>. Prior to enrollment, a biopsy of the primary tumor had to show a positive immunoperoxidase staining with the MAb used for radioimmunosintigraphy in that particular patient. Prior and up to 7 days after administration of <sup>99m</sup>Tc-labeled MAb, blood was obtained for analysis. Electrolytes, aspartate aminotransferase, alanine aminotransferase, alkaline phosphatase, gamma-glutamyl transferase, lactate dehydrogenase, urea nitrogen, creatinine, and uric acid were determined in serum. Hematological determinations included hemoglobin, hematocrit, platelet count, white blood cell count and differentiation, and sedimentation rate. Skin tests were not performed. Vital signs were recorded before and up to 3 h after injection.

Patients received 1–2 mg 323/A3 F(ab')<sub>2</sub> (patient 1–3), 0.9 mg cSF-25 IgG (patient 4), or 2–4 mg K928 IgG (patient 5–10) labeled with <sup>99m</sup>Tc (773 ± 21 MBq, 791 MBq, and 669 ± 113 MBq, respectively; mean ± s.d.), by intravenous injection in 5 minutes. Patients 8, 9, and 10 received, just before injection of the radiolabeled MAb K928, unlabeled K928 IgG in a dose of 10, 20, and 30 mg, respectively.

Table 1. Patient and tumor characteristics and injected MAb dose.

patient	age	sex	stage <sup>a</sup>	primary tumor site <sup>a</sup>	MAb dose (mg)
323/A3 F(ab') <sub>2</sub>					
1	67	M	pT3N0	oral cavity, floor of mouth	1.4
2	56	M	pT4N0	larynx, glottic larynx	1.4
3	63	M	pT1N0	larynx, supraglottic larynx	1.0
cSF-25 IgG					
4	38	M	pT2N2c	oropharynx, tonsillar fossa	0.9
K928 IgG					
5	73	M	pT2N2b	oral cavity, floor of mouth	2.7
6	78	M	pT2N2b	oral cavity, lateral tongue	4.0
7	57	M	pT3N3	hypopharynx	3.7
8	66	M	pT3N2b	hypopharynx, pyriform sinus	13.1
9	73	M	pT3N2c	oropharynx, tonsillar fossa	23.6
10	53	M	pT3N2b	oropharynx, soft palate	33.5

<sup>a</sup>: according to the TNM system of the UICC and all tumors are squamous cell carcinomas.

**Monoclonal Antibodies.** MAb 323/A3 was developed and characterized for binding on formalin-fixed sections of normal human tissues and tumors using immunoperoxidase staining by Edwards et al.<sup>15</sup>. MAb 323/A3 was derived by immunization of mice with MCF-7 human breast cancer cells. The antigen recognized by MAb 323/A3 is a 43 kDa protein located on the outer cell surface and is evidently similar to the one recognized by MAb K931 and MAb 17-1A<sup>2,17</sup>. This antigen was also found to be expressed in endometrial, colon, thyroid, and prostate carcinoma. Among the normal tissues, reactivity of MAb 323/A3 was observed with kidney and colon. In a note added to the original manuscript<sup>15</sup>, authors stated that immuno-fluorescent staining of frozen sections of human tissues showed a somewhat wider range of MAb 323/A3 distribution on normal tissues than was observed in the studies using immunoperoxidase staining of formalin-fixed paraffin-embedded sections. Unfortunately, authors did not provide the results with frozen sections. In the present study we extended the immunohistochemical analysis of MAb 323/A3 on HNSCC and lung tumors (Table 2).

cMAb SF-25 is the chimeric (mouse-human) IgG<sub>1</sub> form of MAb SF-25, a MAb developed and characterized by Takahashi et al.<sup>12,13</sup>. MAb SF-25 was derived after immunization of mice with viable cells of the human hepatoma cell line FOCUS. The antigen recognized by MAb SF-25 is a 125 kDa protein expressed by adenocarcinomas of the colon and among normal tissues in the distal tubule of the kidney. We found that the antigen recognized by MAb SF-25 is similar to the one recognized by MAb K984<sup>3</sup>. In the present study, we extended the immunohistochemical analysis of cMAb SF-25 on HNSCC and lung tumors (Table 2).

MAb K928 was derived after immunization of mice with viable cells of the HNSCC cell line UM-SCC-22A. The antigen recognized by MAb K928 is a 50–55 kDa protein located on the outer cell surface<sup>3</sup>. The K928 defined antigen is expressed by lung, breast, and ovary carcinomas and HNSCC. Among the normal tissues the MAb was found to be reactive with suprabasal layers of normal stratified squamous epithelium, pneumocytes in lung, duct and acinar cells of salivary glands, bile ducts and canaliculi in liver, oviduct epithelium, all epithelial cells in mammae and urinary bladder, and in cells of renal tubuli. Antibodies with similar features to MAb K928 have not been described before. In the present study we extended the immunohistochemical analysis of MAb K928 on HNSCC and lung tumors (Table 2).

**Immunoperoxidase staining.** Because solid data were not available, we analysed the reactivity of MAbs 323/A3, cSF-25, and K928 with tumors of the upper-aerodigestive and respiratory tract more extensively using a semi-quantitative scoring method. The SCC-preferential MAbs E48 and U36 were included for comparison. Reactivity of these MAbs was analysed on a panel of primary (n=196) and metastatic (n=31) squamous cell carcinoma of the head and neck, as well as of squamous cell carcinoma (n=34), adenocarcinoma (n=42), and small cell carcinoma (n=27) of the lung. MAb reactivity was determined by an indirect immunoperoxidase technique. In short, 5 µm thick sections of frozen tissue biopsies were cut on a cryostat microtome and mounted on poly-L-lysine coated glass slides, dried, fixed in 2% paraformaldehyde in PBS for 10 min and dried again. After washing in PBS, the specimens were incubated with undiluted hybridoma culture supernatant (MAbs K928, E48, and U36), or purified MAb at a concentration of 5 µg/ml (MAbs 323/A3 and cSF-25) for 60 minutes at room temperature. After washing in PBS, the specimen were incubated with peroxidase labeled rabbit anti-mouse IgG



(Dakopatts, P260) diluted 1:100 for 60 minutes. Finally, the formed complex was visualised by 3 min development with diaminobenzidine (DAB, Sigma, St. Louis, MO, USA) and 0.03%  $H_2O_2$  in Tris-HCl (pH 7.6). Sections were washed for 1 min with running tap-water and counterstained with hematoxylin for 45 sec, dehydrated and covered in malinol. Isotype-matched control antibodies and PBS served as negative controls.

Immunohistochemical stainings were scored semi-quantitatively (see Table 2 for score-ranges) by two independent observers in a double-blind fashion.

**Antibody Preparations.** The 323/A3 F(ab')<sub>2</sub>, cSF-25 IgG, and K928 IgG used in the RIS studies were supplied by Centocor Inc. (Leiden, the Netherlands). The intact MABs were purified from a concentrated tissue culture supernatant by affinity chromatography on a protein A-Sepharose column. For virus inactivation, IgG from the protein A eluate was treated for at least 6 h with Tween 80 and tri-n-butylphosphate. The protein A purified IgG was further purified on Q-Sepharose and in case of MAb 323/A3 subsequently digested to F(ab')<sub>2</sub> by pepsin at pH=3.9. The F(ab')<sub>2</sub> fragments were further purified by protein A chromatography to remove residual undigested IgG, followed by elution over a S-Sepharose column. The purity of IgG and F(ab')<sub>2</sub> preparations was evaluated by sodium dodecyl sulfate-polyacrylamide gel electrophoresis under non-reducing conditions and appeared to be more than 95%. These products were filtered through a 0.2- $\mu$ m filter and dispensed aseptically in a closed environment under anaerobic conditions. The preparations were found to be pyrogenic free.

**Preparation of the immunoconjugates.** All radiolabeling procedures were performed under aseptic conditions in a shielded laminar flow hood. All glassware, plastics, and solutions were sterile and pyrogen free. For labeling MAb IgG or F(ab')<sub>2</sub> with <sup>99m</sup>Tc, a modification of the multistep procedure as described by Fritzberg et al.<sup>18,19</sup> was followed, using a S-benzoylmercaptoglycylglycylglycine chelator which was a gift from Mallinckrodt Medical B.V. (Petten, the Netherlands). A mean of 98.3  $\pm$  0.8%, 99.7%, and 97.3  $\pm$  2.6% of the <sup>99m</sup>Tc was bound to 323/A3 F(ab')<sub>2</sub>, cSF-25 IgG, and K928 IgG, respectively, as determined by chromatography on ITLC-SG strips (Gelman Sciences, Ann Arbor, MI) with 0.1 M citrate buffer, pH 5.0. Every radiolabeled IgG and F(ab')<sub>2</sub> preparation was assayed for immunoreactivity by measuring the binding to 0.1% glutaraldehyde fixed cells. The colon carcinoma cell line LS174T<sup>20</sup> was used for assaying the immunoreactivity of MAb 323/A3, the breast carcinoma cell line ZR-75<sup>21</sup> for MAb cSF-25, and the HNSCC line UM-SCC-22B<sup>22</sup> for MAb K928. As determined by a modified Lineweaver-Burk plot, the immunoreactive fractions of <sup>99m</sup>Tc-labeled 323/A3 F(ab')<sub>2</sub>, cSF-25 IgG, and K928 IgG at infinite antigen excess were 80.3  $\pm$  1.2%, 98%, and 72.9  $\pm$  8.9%, respectively.

**Imaging studies.** All patients were examined by palpation, CT, MRI, and RIS of the neck prior to surgery, except for patient 10 who did not undergo MRI examination because of claustrophobia. Preoperative palpation was performed by the same experienced head and neck surgeon. CT scans were obtained for the 323/A3 and cSF-25 studies with a third generation Philips Tomoscan 350 (Philips Medical Systems, Best, the Netherlands) and for the K928 study with a fourth generation Siemens Somatom Plus (Siemens AG, Erlangen, Germany) after intravenous administration of contrast medium (Ultravist 300 mg Iodine/ml, Schering AG, Germany). Contiguous axial 5-6 mm scanning planes were used. MRI examinations were done on a 0.6 Tesla imaging system (Teslacon, Technicare - General Electric, Milwaukee) using a partial volume coil. Axial T1-weighted spin echo and Gadolinium-diethylenetriaminepentaacetic acid (Magnevist, Schering AG, Germany)

enhanced T1-weighted gradient recalled echo images were made in all patients without claustrophobia. Slice thickness varied from 3 to 5 mm, with an interslice gap of 50% as described by Van den Brekel et al.<sup>23</sup>. Criteria for the optimal assessment of cervical lymph node metastases by CT or MRI, as defined in our institute, were used<sup>10,11,23</sup>.

Planar radioimmunoscinograms of the whole body (anterior and posterior views) and the head and neck (anterior views) were obtained immediately, 16 h, and 21 h after injection, on a large field of view gamma camera (Gemini; General Electric, Milwaukee, WI) equipped with a low energy collimator, connected to a computer (Bartec, Farborough, United Kingdom). Single Photon Emission Computerized Tomography (SPECT) images of the head and neck were acquired 16 h after injection, while lateral planar images of the head and neck were obtained 21 h after injection, as described previously<sup>10,11</sup>.

CT, MRI, and RIS examinations were each scored by one experienced examiner. All examiners were blinded to the results of other examinations and the pathological outcome. They only were informed about the site of the primary tumor. All patients had uni- or bilateral neck dissections performed between 2 and 7 days after administration of the radioimmunoconjugate. After fixation, all palpable and visible lymph nodes were dissected from the surgical specimen and cut into 4 mm-thick slices for microscopic examination. The size of lymph nodes does not change by fixation<sup>24</sup>. The outcome of the histopathological examination of the neck dissection specimens was used as 'gold standard'.

For topographical evaluation, the findings were recorded per side as well as per lymph node level<sup>10,11</sup> according to the Memorial Sloan Kettering Cancer Center Classification<sup>25</sup>.

**Biodistribution studies.** Patient blood samples were obtained up to the time of operation. Using the aliquots retained from the conjugate preparation, a weighed dilution of the injected dose was prepared. Aliquots of the samples and the standard were counted in one run. All patients injected with MAb K928 were operated 2 days after injection. Only in these patients bone marrow biopsies and aspirations were taken under general anesthesia just before operation. Biopsies of tumor and several normal tissues were taken from the surgical specimens. In one patient, undergoing a jejunum interposition after laryngectomy and pharyngectomy, also biopsies of liver and skin were taken. All blood samples and biopsies were weighed and the amount of <sup>99m</sup>Tc was measured in a well-counter (LBK Wallac, 1282 Compugamma). All data were corrected for decay and converted to percentage of the injected doses per kilogram of tissue (%ID/kg).

Accumulation of MAb cSF-25 in non-target organs was assessed from computer regions of interest. Activity uptake levels were estimated from whole body views at 0, 16, and 21 h p.i.. Uptake levels were calculated from geometrical means after decay and machine drift correction and were not corrected for background. Values are given as percentage from whole body content at t=0.

## RESULTS

**Reactivity of MABs with tumors of the upper-aerodigestive and respiratory tract.** Strong reactivity of MAb 323/A3 (> 50% of the tumor cells stained positive) was observed with 58% of the primary HNSCC (n=195), 64% of HNSCC lymph node



metastases (n=28), 88% of SCC of the lung (n=34), 100% of adenocarcinomas of the lung (n=42), and 85% of small cell lung carcinomas (n=27). MAb cSF-25 showed such marked reactivity in 77% of the primary HNSCC (n=196), 77% HNSCC lymph node metastases (n=31), 50% of SCC of the lung (n=34), and 66% of adenocarcinomas of the lung (n=42). Reactivity with small cell lung carcinomas was negligible. For MAb K928 strong reactivity was observed with 81% of the primary HNSCC (n=195), 84% of HNSCC lymph node metastases (n=31), 53% of SCC of the lung (n=34), and 85% of adenocarcinomas of the lung (n=42). Reactivity with small cell lung carcinomas was negligible. For comparison, the reactivity profiles of the SCC-specific MAbs E48 and U36 on the same panel of tumors are also given in Table 2. Data indicate that HNSCC, primary tumor as well as metastases, stained most extensively with MAb U36, equally well with MAbs cSF-25, K928, and E48, and worst with MAb 323/A3. In contrast, MAb 323/A3 showed the best immunohistochemical reactivity on lung carcinoma, including SCC, adenocarcinomas, and small cell carcinomas. MAb E48 showed the worst reactivity with all histological types of lung carcinoma, while MAb U36 showed a substantial reactivity with SCC of the lung but not with adenocarcinomas and small cell carcinomas.

Table 2. Semi-quantitative scorings of immunoperoxidase stainings with MAbs 323/A3, SF-25, K928, E48, and U36 on frozen sections of tumors of the upper-aerodigestive and respiratory tract per score-range (percentage positive cells) as number of positive tumors/number of tumors tested (percentage).

		323/A3	SF-25	K928	E48	U36
HNSCC primary tumor	(0 - 10%)	7/195 (24%)	8/196 (5%)	12/195 (7%)	20/196 (11%)	2/196 (1%)
	(10 - 50%)	35/195 (18%)	36/196 (18%)	23/195 (12%)	37/196 (19%)	6/196 (3%)
	(50 - 95%)	105/195 (54%)	132/196 (67%)	139/195 (71%)	99/196 (50%)	124/196 (64%)
	(> 95%)	8/195 (4%)	20/196 (10%)	21/195 (10%)	40/196 (20%)	64/196 (32%)
HNSCC lymph node	(0 - 10%)	4/28 (14%)	4/31 (13%)	0/31 (0%)	5/31 (16%)	1/31 (3%)
	(10 - 50%)	6/28 (22%)	3/31 (10%)	5/31 (16%)	9/31 (29%)	2/31 (6%)
	(50 - 95%)	16/28 (57%)	22/31 (71%)	20/31 (65%)	12/31 (39%)	20/31 (65%)
	(> 95%)	2/28 (7%)	2/31 (6%)	6/31 (19%)	5/31 (16%)	8/31 (26%)
SCC lung	(0 - 10%)	0/34 (0%)	4/34 (12%)	4/34 (12%)	17/34 (50%)	6/34 (18%)
	(10 - 50%)	4/34 (12%)	13/34 (38%)	12/34 (35%)	8/34 (23%)	10/34 (29%)
	(50 - 95%)	21/34 (62%)	17/34 (50%)	12/34 (35%)	7/34 (21%)	16/34 (47%)
	(> 95%)	9/34 (26%)	0/34 (0%)	6/34 (18%)	2/34 (6%)	2/34 (6%)
Adeno- carcinoma lung	(0 - 10%)	0/42 (0%)	7/42 (17%)	2/42 (5%)	34/42 (81%)	23/42 (55%)
	(10 - 50%)	0/42 (0%)	7/42 (17%)	4/42 (10%)	6/42 (14%)	7/42 (17%)
	(50 - 95%)	8/42 (19%)	8/42 (19%)	24/42 (57%)	2/42 (5%)	9/42 (21%)
	(> 95%)	34/42 (81%)	20/42 (47%)	12/42 (28%)	0/42 (0%)	3/42 (7%)
Small cell carcinoma lung	(0 - 10%)	1/27 (4%)	24/27 (89%)	27/27 (100%)	27/27 (100%)	27/27 (100%)
	(10 - 50%)	3/27 (11%)	3/27 (11%)	0/27 (0%)	0/27 (0%)	0/27 (0%)
	(50 - 95%)	4/27 (15%)	0/27 (0%)	0/27 (0%)	0/27 (0%)	0/27 (0%)
	(> 95%)	19/27 (70%)	0/27 (0%)	0/27 (0%)	0/27 (0%)	0/27 (0%)

**Clinical studies.** The patients included in these studies are described in Table 1. No adverse reactions were observed and no significant changes were noted in blood and urine analyses.

**323/A3 F(ab')<sub>2</sub> study.** All 3 primary tumors were visualized. A representative image is shown by Fig. 1. Unfortunately for determining the diagnostic value of RIS, none of these patients had lymph node metastasis as revealed by histopathological examination of the neck dissection specimen. While palpation, CT, and MRI scored false-positive in these patients, no false-positive findings were obtained by RIS. Head and neck and whole body images at 16 and 21 h p.i. showed hardly any blood pool activity and clear visualization of the thyroid gland, liver, and the skeleton probably bone marrow (Fig. 1 and 2). With respect to the latter it can not be distinguished whether accumulation occurs in bone or bone marrow. Also kidneys, urine bladder, scrotal area, and gut were visualized. The spleen was hardly visible. Activity uptake in the thyroid gland hampers tumor detection with radiolabeled 323/A3 in the head and neck region as illustrated for patient 2 with a laryngeal carcinoma in Figure 1A. In this particular patient SPECT images were required to distinguish activity uptake in the primary tumor (Fig. 1B) and the thyroid gland (Fig. 1C). The mean pharmacokinetic curve is shown in Figure 3A.

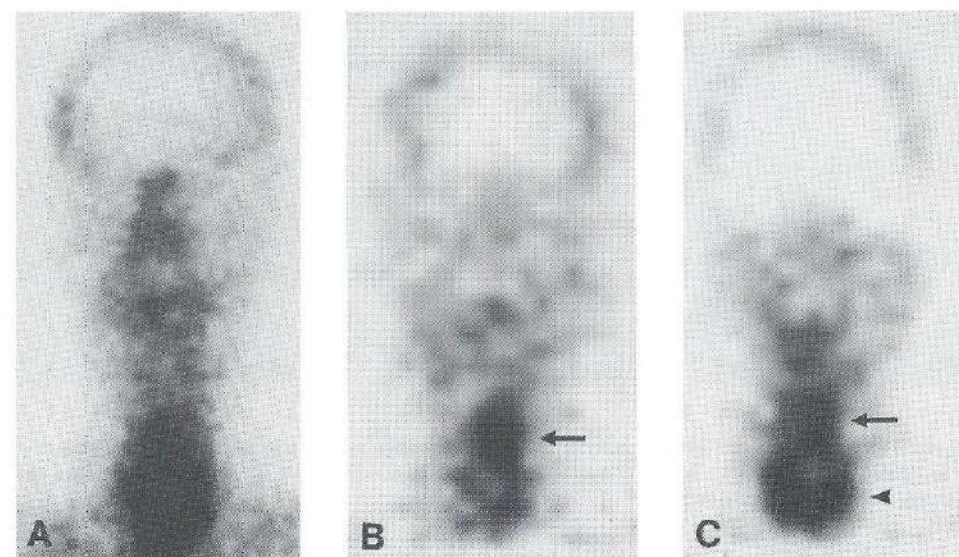


Figure 1. (A) Planar anterior image of the head and neck of patient 2, 16 h after injection of <sup>99m</sup>Tc-labeled 323/A3 F(ab')<sub>2</sub>. Increased uptake is seen in the laryngeal area. (B) Coronal SPECT images of the same patient show the primary laryngeal tumor (arrow) and (C) more anteriorly the thyroid gland (arrowhead).



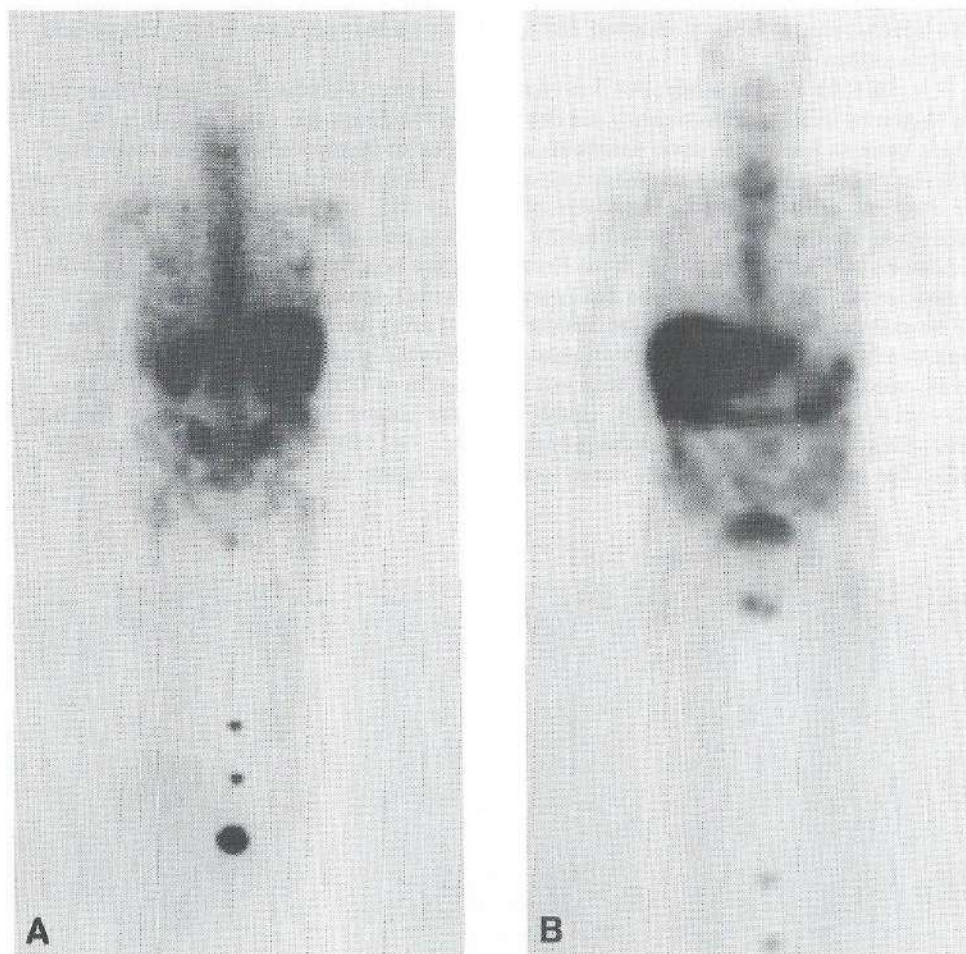


Figure 2. (A) Planar anterior and (B) posterior images of the whole body of patient 2, 16 h after injection of  $^{99m}\text{Tc}$ -labeled 323/A3  $\text{F}(\text{ab}')_2$ . Note the uptake in the liver, transverse colon, kidneys, urine bladder, and skeleton, probably bone marrow.

**cSF-25 study.** After injection a rapid, extensive, and selective uptake of activity was seen in the liver, spleen, and brain (Fig. 4A and B). No side effects occurred. There was also high uptake of activity in the skeleton probably bone marrow (Fig 4A). Neither the primary tumor nor the lymph node metastases were visualized. The pharmacokinetic curve showed a rapid decrease in plasma activity, with a 80% decrease within 30 min. after injection (Fig 3B). Biodistribution data derived from computer regions of interest showed activity of liver, spleen, and brain of 45%, 10%, and 1% of the injected dose, respectively, within 15 min after injection. These values were 27, 7, and 1%, respectively, 21 h after injection.

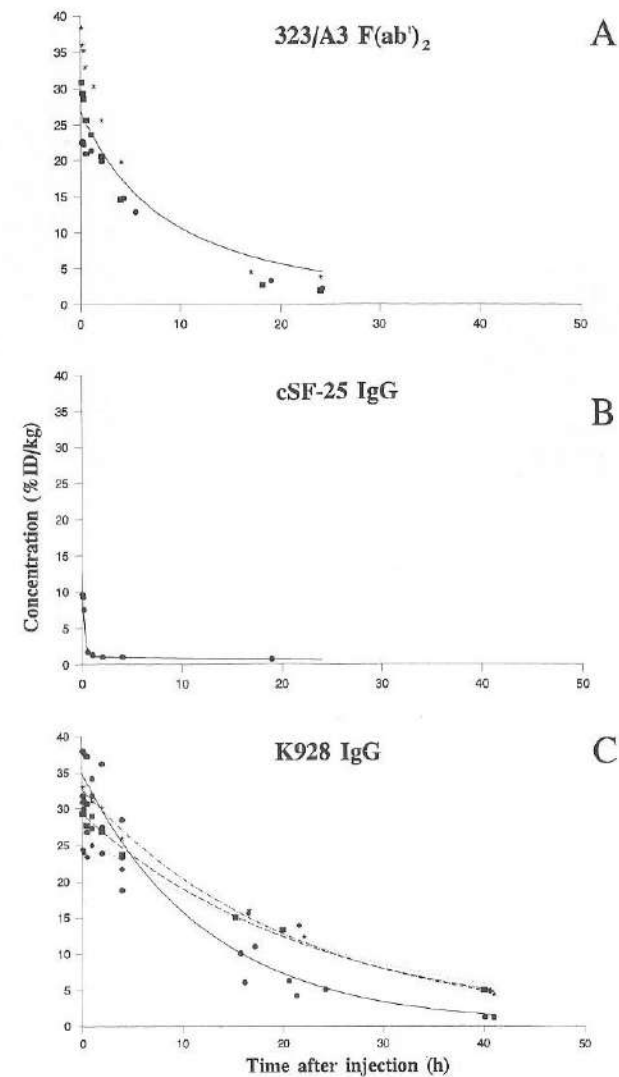


Figure 3. (A) Mean blood disappearance curve of  $^{99m}\text{Tc}$ -labeled 323/A3  $\text{F}(\text{ab}')_2$  in patient 1, 2, and 3: ●, ■, and ★, respectively. (B) Blood disappearance curve of  $^{99m}\text{Tc}$ -labeled cSF-25 IgG in patient 4. (C) Mean blood disappearance curve of 3-4 mg (—)  $^{99m}\text{Tc}$ -labeled K928 IgG in patients 5-7: ●. Blood disappearance curves of 13 mg (---), 24 mg (- · - · -), and 34 mg (· · · · ·)  $^{99m}\text{Tc}$ -labeled K928 IgG in respectively, patient 8, 9, and 10: ■, ★, and ♦.



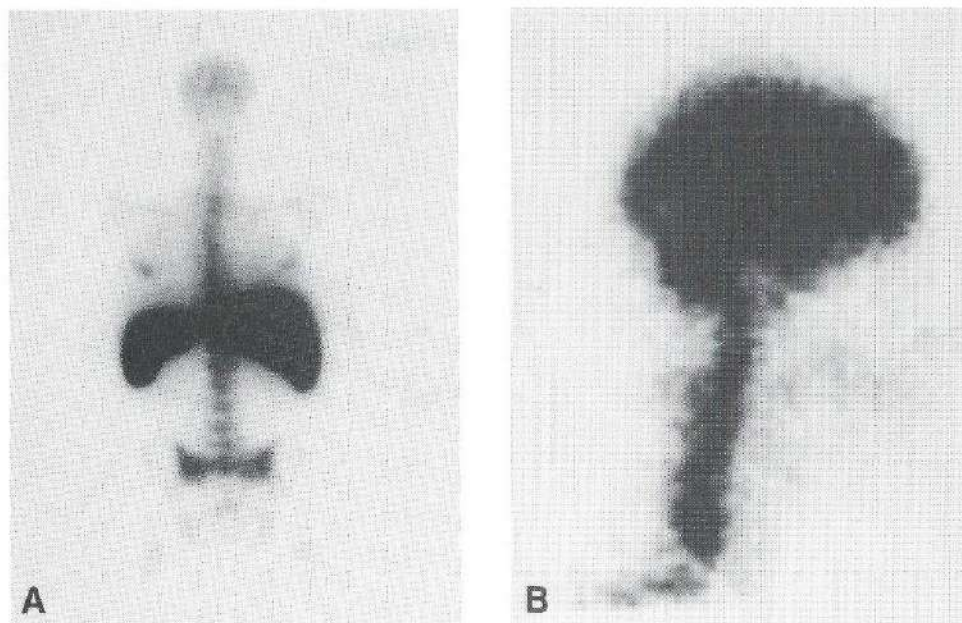


Figure 4. Planar posterior image of the whole body of patient 4, immediately after injection of  $^{99m}\text{Tc}$ -labeled cSF-25. Note the extensive uptake in liver, spleen, and skeleton, probably bone marrow. No blood pool activity is seen. (B) Planar right lateral image of the head and neck of the same patient 21 h after injection, showing activity in the whole brain area. The primary tumor in the right tonsillar fossa is not visualized.

Table 3. Correlation of preoperative diagnostic findings with histopathological findings in K928-patients.

	true-positive	false-negative	false-positive	true-negative
Per side				
palpation	7	0	0	1
CT	5	2	0	1
MRI	5	1	0	1
RIS	6	1	1	0
Per level				
palpation	8	7	1	23
CT	9	6	1	23
MRI	8	4	1	21
RIS	8	7	1	23

Table 4. Biodistribution of  $^{99m}\text{Tc}$ -labeled K928 IgG 44 h p.i. in %ID/kg.

	patient	5	6	7	8	9	10
	dose unlabeled	0 mg	0 mg	0 mg	10 mg	20 mg	30 mg
tissue							
tumor		4.6	7.0	5.0	10.6	8.0	12.6
mucosa		1.6	0.6	0.8	5.0	2.5	3.2
muscle			0.4	0.2	0.3	0.5	1.2
fat			0.6	0.1	0.6	0.1	0.9
submandibular gland			2.4		3.2	2.0	3.7
bone marrow biopsy			3.8	6.1	2.7	1.6	2.1
total bone marrow aspirate		0.8	0.8	1.1	3.0	2.2	3.9
supernatant bone marrow aspirate		1.1	1.1	1.2	4.5		1.3
sediment bone marrow aspirate		1.0		1.4	1.4	1.1	1.7
blood		1.0	0.8	0.7	2.8	2.4	4.7
plasma		1.2		1.1	4.4	4.1	6.5
skin				0.6			
liver				8.1			

**K928 study.** All 6 primary tumors were visualized. From the 6 patients, lymph nodes present in 8 neck sides and in 39 levels were examined histopathologically for tumor involvement. Metastases of SCC were found in 7 sides and 15 levels. Preoperative diagnostic findings obtained with RIS, palpation, CT, and MRI are summarized in Table 3. RIS was correct in 6 of 7 tumor involved neck sides and in 8 of 15 involved lymph node levels. By palpation, CT, and MRI, respectively, 8 out of 15, 9 out of 15, and 8 out of 12 tumor involved lymph node levels were detected. False-positive findings were obtained with RIS, palpation, CT, and MRI in one level each. No explanation was found for the false-positive RIS observation. RIS visualized a tumor deposit in one lymph node level, which was not detected by other diagnostic techniques. Tumor deposits in 4 of the 7 levels missed by RIS, were detected by the other diagnostic techniques. Histopathological examination revealed that the smallest tumor involved lymph node detected by RIS had diameters of 4 and 5 mm in the axial plain with a tumor load of 50 %. Paraffin sections of metastatic lymph nodes missed by RIS were evaluated histopathologically. In patient 7, the extension of a large tumor from levels I,II, and III of the neck into level IV was not determined correctly, probably due to the lack of anatomical structures in RIS images. In patient 8 and 9, the missed tumor involved lymph nodes were located close to a large primary tumor. The missed lymph nodes in patient 10 contained only a small proportion of tumor.



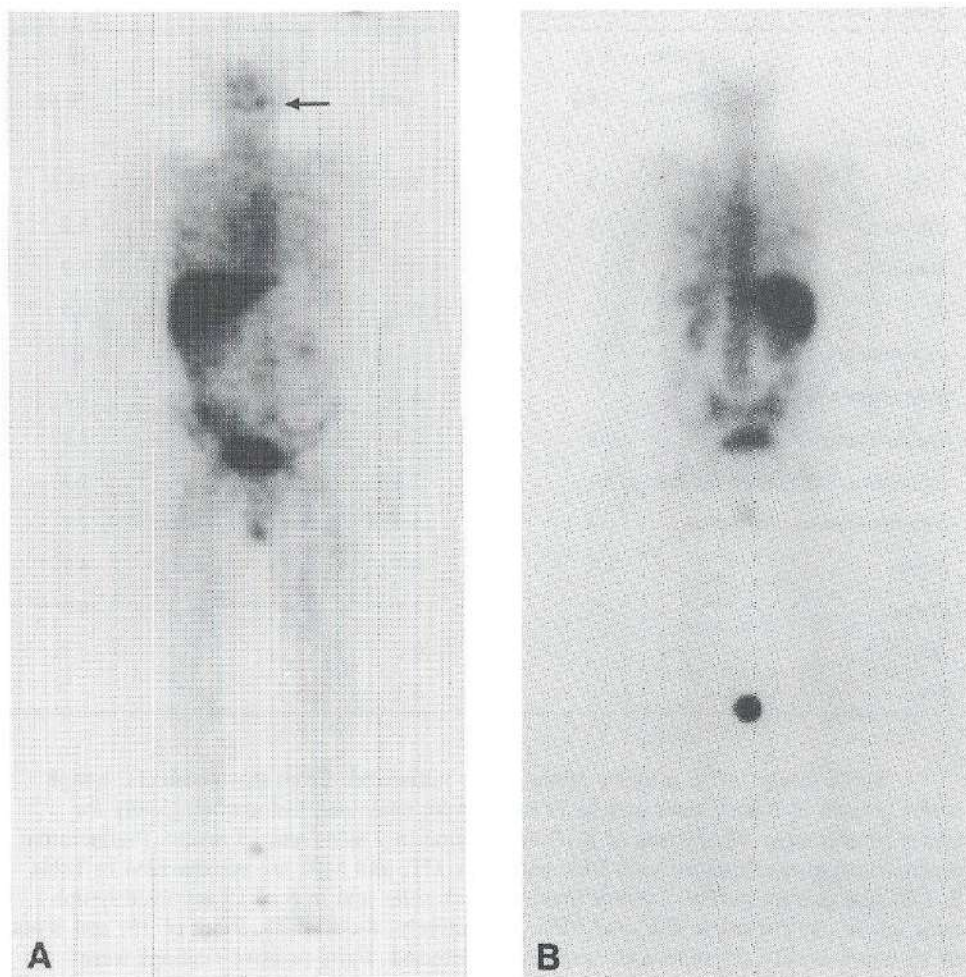


Figure 5. (A) Planar anterior and (B) posterior images of the whole body of patient 6, 16 h after injection of 4 mg  $^{99m}\text{Tc}$ -labeled K928 IgG. The primary tumor of the left lateral tongue (arrow) is visualized on the anterior whole body image. Note the intense uptake in the liver and skeleton, probably bone marrow. Activity in the blood pool is low when compared to the liver activity.

Whole body images at 16 and 21 h p.i. showed hardly blood pool activity and clear visualization of liver, spleen, and the skeleton probably bone marrow (Fig. 5). Kidneys, urine bladder, and gut were also visualized. When the MAb K928 dose was increased, the blood pool activity 16 h p.i. increased in comparison to liver activity. Moreover, visualization of the spleen was more pronounced and visualization of the skeleton was less pronounced (Fig. 6).

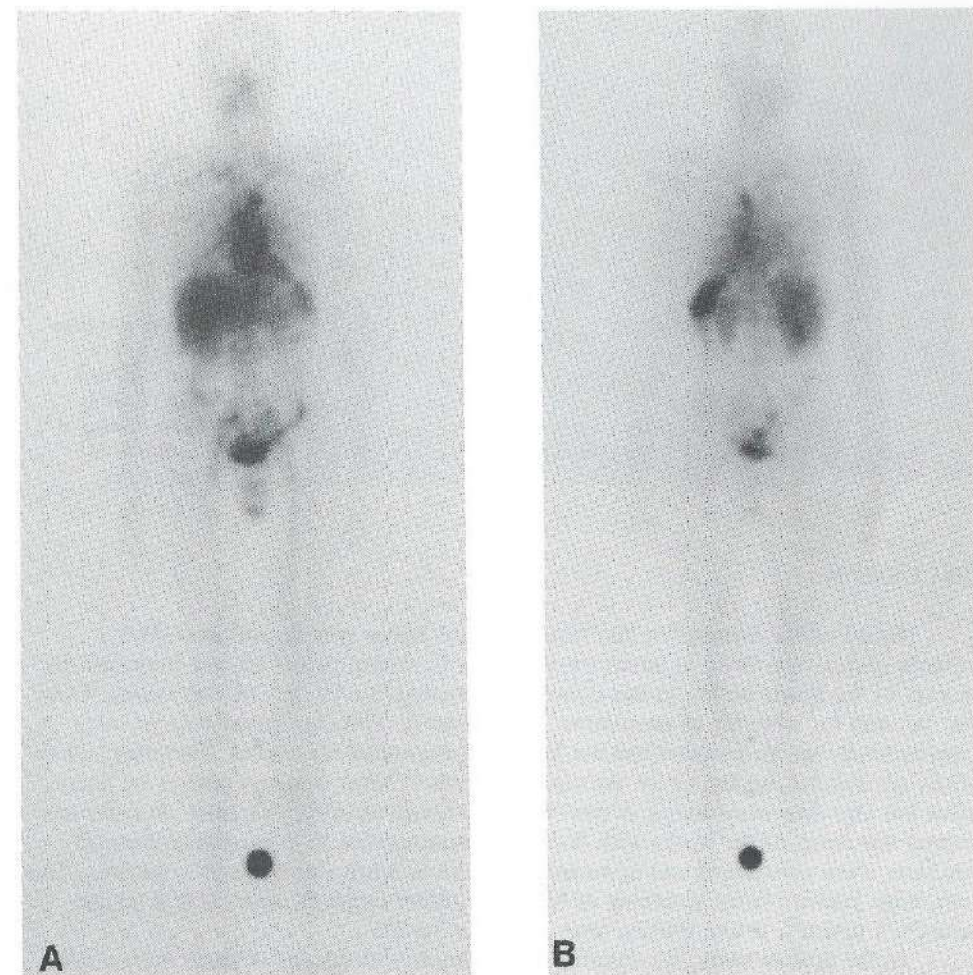


Figure 6. (A) Planar anterior and (B) posterior images of the whole body of patient 10, 16 h after injection of 34 mg  $^{99m}\text{Tc}$ -labeled K928 IgG. The liver and skeleton (probably bone marrow) are visualized, but are less intense compared to patients receiving a lower dose of K928 IgG, as illustrated by Figure 5. Note also the higher blood pool activity and more intense uptake in the spleen when compared to Figure 5.

Biodistribution data showed 44 h p.i. a relatively low uptake in the tumor ranging from 4.6 to 7.0 %ID/kg, when no additional unlabeled MAb dose was administered (Table 4). In one patient, undergoing a jejunum interposition after laryngectomy and pharyngectomy, biopsies revealed a higher activity uptake in the liver than in the tumor. Also activity levels in submandibular glands and in bone marrow biopsies were found to be relatively high. Increase of MAb dose clearly resulted in a prolonged residence time of activity in the blood (Fig. 3C) and in an increased uptake in the tumor (Table 4).



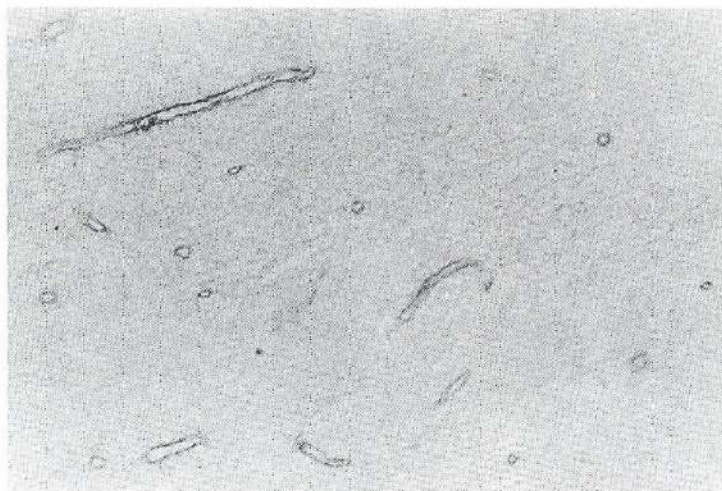


Figure 7.  
Immunoperoxidase  
staining of brain  
tissue with MAb  
SF-25. There is  
distinct staining of  
endothelium of  
blood vessels.

## DISCUSSION

Based on the assumption that tumors possess tumor specific antigens (TSAs), antigens exclusively found in tumor tissue but not in normal tissue, Ehrlich proposed the concept of the magic bullet. In this concept, monoclonal antibodies (MAbs) against TSAs may be used for targeting of neoplasms. Unfortunately, TSAs are found only in experimentally induced tumors and not in so-called spontaneous tumors. Therefore, most MAbs are directed against tumor associated antigens (TAAs), antigens present on tumor tissue but also detectable among normal tissues although in lower quantities. Practice has learned that many of the MAbs with favorable characteristics in immunohistochemical selection, show unexpected and unwanted localizations when administered to patients. This knowledge justifies initial screening of MAbs for tumor-targeting capacity in a limited number of patients, before starting more extensive studies.

In the present study, we describe the preliminary evaluation of three immunohistochemically well characterized MAbs, 323/A3, cSF-25, and K928, for selective tumor-targeting in HNSCC patients. Immunohistochemical data provided by the original manuscripts<sup>3,12,15</sup> and by Table 2 of this paper indicate that these pan-carcinoma MAbs may have potential for targeting several types of carcinoma in the upper-aerodigestive and respiratory tract: squamous cell carcinoma, adenocarcinoma, as well as small cell carcinoma. It is of note that for the scintigraphical evaluation MAbs were labeled with <sup>99m</sup>Tc using the MAG<sub>3</sub> chelate, as described before<sup>10,11,19</sup>. Of the conjugates prepared for these studies, HPLC analysis of serum samples taken up to 24 h after injection revealed that > 95% of the <sup>99m</sup>Tc was bound to the MAb. Reanalysis after storage at 4°C for 24 h gave the same result, indicating that radioimmunoconjugates were very stable. As determined by the modified Lineweaver-Burk plot, the immunoreactive fraction before injection was consistently > 61%, while the radioimmunoconjugates retained full binding capacity up to 24 h after injection (data not shown).

Immunohistochemical data provided in this paper indicate that MAb 323/A3 shows an extensive reactivity with all histological types of lung tumors. Remarkably, MAb 323/A3 is also reactive with HNSCC but not with the normal counterpart, oral squamous epithelium. It should be noticed, however, that for HNSCC 323/A3 reactivity is rather heterogeneous, limiting its applicability for targeting HNSCC. In our clinical RIS study 323/A3 F(ab')<sub>2</sub> was able to target antigen positive primary HNSCC. Because all three patients turned out to be free of tumor in the neck, no data on targeting of lymph node metastases could be obtained. A drawback of MAb 323/A3 is its accumulation in the thyroid gland which hampers tumor detection in the neck. The possibility that activity uptake is a result of detached <sup>99m</sup>Tc can be ruled out since RIS with 4 other identically labeled MAbs did not show uptake in the thyroid gland. Immunohistochemical analysis performed at our laboratory revealed that MAb 323/A3 is reactive with thyroid tissue (data not shown). Such reactivity was not observed by Edwards et al.<sup>15</sup> in their initial immunohistochemical characterization of MAb 323/A3, but this may be due to the use of formalin fixed sections, which in our hands resulted in loss of antigenicity. Reactivity with thyroid tissue was also demonstrated before with other MAbs recognizing an antigen similar to 17-1A, including our own produced MAb K931<sup>2,26</sup>. Besides this, RIS studies revealed accumulation of radioactivity in the liver and the skeleton (probably bone marrow), which may also be related to the presence of antigen: with 3 MAbs recognizing the 17-1A antigen, MAb 323/A3, 17-1A, and K931, reactivity with bile canaliculi and bile ducts has been described<sup>2,26,27</sup>. However, no explanation was found for the relatively high uptake of MAb 323/A3 in the skeleton. Immunohistochemical analyses did not reveal reactivity of MAb 323/A3 with cellular components in the sediment of bone marrow aspirates. Especially when MAb 323/A3 is considered for therapeutic application, reactivity with forementioned normal tissues may be a limiting factor.

Reactivity with normal tissues will definitely hamper the clinical utility of MAb cSF-25. Within 30 min after administration of <sup>99m</sup>Tc-labeled cSF-25 IgG, 80% of the activity disappeared from the blood, while preferential accumulation was observed in the liver, spleen, brain, and bone marrow. The massive accumulation in the liver, spleen, and bone marrow can be explained by the reactivity of MAb cSF-25 with Kupffer cells in the liver, the red pulpa and follicle centra in the spleen, and cellular components in the sediment of bone marrow aspirates, as we observed in immunohistochemical evaluation of MAb cSF-25 (data not shown). Such reactivity was not described by Takahashi et al.<sup>12</sup> in their original paper on immunohistochemical characterization of SF-25. Reactivity with Kupffer cells has also been observed previously with our MAb K984, recognizing a similar antigen as SF-25. Accumulation in the brain was an unexpected finding, especially because it is anticipated that monoclonal antibodies normally can not pass the blood-brain barrier. Most recently, Stokkel et al.<sup>28</sup> reported on a case study in which <sup>123</sup>I-labeled SF-25 F(ab')<sub>2</sub> was administered to a patient with an adenocarcinoma of the breast. They also observed activity uptake in the brains, but did not report on uptake in liver, spleen, and bone marrow. They explained the brain uptake by the degradation of the antibody into smaller labeled fragments, making them able to pass the blood-brain barrier. In our study, in which the integrity of the radiolabeled MAb was monitored before as well as after administration by HPLC analysis, we did not find any evidence for fragment formation. Neither for 4 other MAbs evaluated in clinical RIS studies and labeled in the same way as cSF-25, we ever observed fragment formation or brain accumulation. Immunohistoche-



mical analysis of MAb SF-25 for reactivity with brain tissue obtained from cerebellum, hypothalamus, and motoric cortex revealed distinct staining with endothelium of blood vessels in the brain (Fig. 7). Based on these results we decided to stop any further evaluation of this MAb.

MAb K928 was shown to detect HNSCC, although also for this MAb unwanted localization was observed. RIS with K928 IgG showed all primary tumors. For the detection of neck lymph node metastases RIS with K928 IgG was as valuable as CT and MRI. The uptake of  $^{99m}\text{Tc}$ -labeled K928 IgG in tumors (4.6-12.6 %ID/kg, 44 h p.i.) was found to be comparable to the uptake of other MAbs in solid tumors (1-10 %ID/kg)<sup>29,30</sup>. A major limitation of RIS with K928 IgG is the high percentage of false-negative scores. A total of 7 out of 15 levels and 1 out of 7 neck sides were falsely scored negative. All missed tumor involved lymph nodes were smaller than 22 mm in diameter. In these cases RIS was apparently unsuccessful due to the limited amount of antigen accessible for the MAb and maybe the limited sensitivity of a gamma camera. Consequently, micrometastasis, small tumor involved nodes, and tumor involved nodes with much keratin or necrosis and with only a small proportion of viable cells were not diagnosed. Close spatial relation of a metastatic node to an area of increased uptake may also hamper diagnosis. Unwanted uptake of radioactivity was observed in the liver and the spleen, which can be explained by the reactivity of MAb K928 with bile ducts and canaliculi in liver and the red pulpa in the spleen. Biodistribution data obtained from biopsies revealed also a relatively high radioactivity uptake in salivary glands and bone marrow. The high uptake in bone marrow can be explained by reactivity of MAb K928 with cellular components in the sedimentation fraction of the bone marrow aspirate as became apparent from immunohistochemical stainings. The high uptake in salivary gland can be explained by the presence of the antigen in this tissue<sup>3</sup>.

In our study, by increasing the MAb dose activity, uptake of MAb K928 in the liver was diminished, activity clearance from the blood decreased, and a higher percentage of uptake in the tumor was observed (Fig. 3C, 5, and 6 and Table 4). Based on these results one can state that MAb K928 can be made 'operationally' tumor selective by dose escalation. Nevertheless, the observed reactivity with bone marrow cells will definitely limit the therapeutic applicability of MAb K928.

A limitation shared by all three pan-carcinoma MAbs evaluated in this study, is the accumulation in normal tissues which seems to be the result of MAb-antigen interaction. Selectivity of MAb accumulation depends on antigen distribution and accessibility. For instance, MAbs can hardly penetrate into skin<sup>31</sup>. In contrast, MAbs can easily penetrate into tumor tissue, since tumor endothelium is often fenestrated and the basement membrane is mostly defective. But MAbs can also easily penetrate in liver, spleen, and bone marrow since in these tissues barriers are missing. In intestines, endocrine and exocrine glands, and kidneys the basement membrane is usually intact, but the endothelium is fenestrated. Therefore, it can be expected that even with low expression of antigen in the thyroid (MAb 323/A3), liver (MAbs 323/A3, cSF-25, K928), spleen (cSF-25, K928), salivary gland (K928), endothelium (cSF-25), or bone marrow (323/A3, K928) extensive MAb accumulation in these tissues may occur shortly after administration to the patient.

Remains the question whether one of these MAbs may have a clinical value for diagnosis or therapy of tumors in the upper-aerodigestive and respiratory tract. It seems to us that for targeting HNSCC the previously described MAb E48<sup>10,11,32</sup> and MAb U36 are

superior when compared to the herein described MAbs.

For targeting of lung carcinomas, MAb E48 does not seem to be suitable, while MAb U36 possibly can only be used for targeting SCC. From the three MAbs evaluated in this study, especially MAb 323/A3 needs in our view further attention. The reactivity of this MAb with various histological types of lung tumor is, in comparison to other MAbs, superior. Unfortunately, in the primary RIS evaluation of MAb 323/A3 shown in this paper, no biopsies were taken. To assess the value of MAb 323/A3 for targeting of lung carcinoma more properly, RIS studies guided by biodistribution and dosimetric estimates, have to be performed at increasing MAb dose in lung cancer patients.

## ACKNOWLEDGEMENTS

The authors thank Drs. Hein Leverstein and Richard P. Wong Chung for clinical support, Marijke van Walsum for immunohistochemical stainings, Henri Greuter for biopsy measurements, Abraham J. Wilhelm for pharmacokinetics, and Jacqueline E. van der Wal and Paul van der Valk for histopathological support.

## REFERENCES

1. Quak JJ, Balm AJM, Dongen GAMS van, Brakkee JPG, Scheper RJ, Snow GB, Meijer CJLM. A 22 kD surface antigen detected by monoclonal antibody E48 is exclusively expressed in stratified squamous and transitional epithelia. *Am J Pathol* 1990;33:191-5.
2. Quak JJ, Dongen GAMS van, Gerretsen M, Hayashidi D, Balm AJM, Brakkee JGP, Snow GB, Meijer CJLM. Production of monoclonal antibody (K931) to a squamous cell carcinoma antigen identified as the 17-1A antigen. *Hybridoma* 1990;9:377-87.
3. Quak JJ, Schrijvers AHGJ, Brakkee JGP, Davis HD, Scheper RJ, Balm AJM, Meijer CJLM, Snow GB, Dongen GAMS van. Expression and characterization of two differentiation antigens in stratified squamous epithelia and carcinomas. *Int J Cancer* 1992;50:507-13.
4. Schrijvers AHGJ, Quak JJ, Uytendinck AM, Walsum M van, Meijer CJLM, Snow GB, Dongen GAMS van. MAb U36, a novel monoclonal antibody successful in immunotargeting of squamous cell carcinoma of the head and neck. *Cancer Res* 1993;53:4383-90.
5. Quak JJ, Balm AJM, Brakkee JPG, Davis HD, Scheper RJ, Meijer CJLM, Snow GB, Dongen GAMS van. Localization and imaging of radiolabeled monoclonal antibody E48 against squamous cell carcinoma of the head and neck in tumor bearing nude mice. *Int J Cancer* 1989;44:534-8.
6. Gerretsen M, Quak JJ, Suh JS, Walsum M van, Meijer CJLM, Snow GB, Dongen GAMS van. Superior localization and imaging of radiolabeled monoclonal antibody E48 F(ab')<sub>2</sub> fragments in xenografts of human squamous cell carcinoma of the head and neck and the vulva as compared to monoclonal antibody E48 IgG. *Br J Cancer* 1991;63:37-44.
7. Gerretsen M, Schrijvers AHGJ, Walsum M van, Braakhuis BJM, Snow GB, Dongen GAMS van. Radioimmunotherapy of head and neck squamous cell carcinoma with  $^{131}\text{I}$ -labeled monoclonal antibody E48. *Br J Cancer* 1992;66:496-502.
8. Gerretsen M, Visser GWM, Walsum M van, Meijer CJLM, Snow GB, Dongen GAMS van.  $^{186}\text{Re}$ -labeled monoclonal antibody E48 IgG mediated therapy of human head and neck squamous cell carcinoma xenografts. *Cancer Res* 1993;53:3524-29.
9. Gerretsen M, Visser GWM, Brakenhoff RH, Snow GB, Dongen GAMS van. Complete ablation of small head and neck cancer xenografts with  $^{186}\text{Re}$ -labeled MAb E48 IgG. *Cell Biophys* 1994;24:135-42.
10. Dongen GAMS van, Leverstein H, Roos JC, Quak JJ, Brekel M van den, Lingen A van, Martens HJM, Castelijns J, Visser GWM, Meijer CJLM, Teule JJ, Snow GB. Radioimmunoscintigraphy of head and neck cancer using  $^{99m}\text{Tc}$ -labeled monoclonal antibody E48 F(ab')<sub>2</sub>. *Cancer Res* 1992;52:2569-74.
11. Bree R de, Roos JC, Quak JJ, Hollander W den, Brekel MWM van den, Wal JE van der, Tobi H, Snow GB, Dongen GAMS van. Clinical imaging of head and neck cancer with  $^{99m}\text{Tc}$ -labeled mono-



- clonal antibody E48 IgG or F(ab')<sub>2</sub>. J Nucl Med 1994;35:775-83.
12. Takahashi H, Wilson B, Ozturk M, Motte P, Straus W, Isselbacher KJ, Wands JR. In vivo localization of human colon adenocarcinoma by monoclonal antibody binding to a highly expressed cell surface antigen. Cancer Res 1988;48:6573-9.
13. Takahashi H, Nakada T, Puisieux I. Inhibition of human colon cancer growth by antibody-directed human LAK cells in SCID mice. Science 1993;259:1460-3.
14. Koprowski H, Steplewski Z, Mitchell K, Herlyn M, Herlyn D, Fuhrer P. Colorectal carcinoma antigens detected by hybridoma antibodies. Somat Cell Genet 1979;5:957-72.
15. Edwards DP, Grzyb KT, Dressler LG, Mansel RE, Zava DT, Sledge GW, McGuire WL. Monoclonal antibody identification and characterization of a M, 43,000 membrane glycoprotein associated with human breast cancer. Cancer Res 1986;46:1306-17.
16. Hermanek P, Sobin LH, eds. TNM classification of malignant tumors, 4th edition. Berlin: Springer Verlag; 1987.
17. Pak KY, Nedelman MA, Fogler WE, Tam SH, Wilson E, Haarlem LJM van, Clognola R, Warnaar SO, Daddona PE. Evaluation of the 323/A3 monoclonal antibody and the use of technetium-99m-labeled 323/A3 Fab' for the detection of pan adenocarcinoma. Nucl Med Biol 1991;18:483-97.
18. Fritzberg AR, Abrams PG, Beaumier PL, Kasina S, Morgan AC, Rao TN, Sanderson JA, Srinivasan A, Wilbur DS, Vanderheyden J-L. Specific and stable labeling of antibodies with technetium-99m with a diamide dithiolate chelating agent. Proc Natl Acad Sci USA 1988;85:4025-9.
19. Visser GWM, Gerretsen M, Herscheid J, Snow GB, Dongen GAMS van. Labeling of monoclonal antibodies with <sup>186</sup>Re using the MAG<sub>3</sub> chelate for radioimmunotherapy of cancer: a technical protocol. J Nucl Med 1993;34:1953-63.
20. Tom BH, Rutzy LP, Jakstys MM, Oyasa R, Kaye CI, Kahan BD. Human colonic adenocarcinoma cells. I. Establishment and description of a new line. In vitro 1976;12:180-91.
21. Engel LW, Young NA. Human breast carcinoma cells in continuous culture: a review. Cancer Res 1978;38:4327-39.
22. Grenman RG, Carey TE, McClatchey KD. In vitro radiation resistance among cell lines established from patients with squamous cell carcinoma of the head and neck. Cancer 1991;67:2741-7.
23. Brekel MWM van den, Castelijns JA, Stel HV, Valk J, Croll GA, Golding RP, Luth WJ, Meijer CJLM, Snow GB. Detection and characterization of metastatic cervical adenopathy by MR imaging: comparison of different MR techniques. J Comp Assist Tomogr 1990;14:581-9.
24. Brekel MWM van den, Stel HV, Castelijns JA, Nauta JJP, Waal I van der, Valk J, Golding RP, Meijer CJLM, Snow GB. Cervical lymph node metastases: assessment of radiologic criteria. Radiology 1990;177:379-84.
25. Shah JP, Strong E, Vikram B. Neck dissection: Current status and future possibilities. Clin Bulletin 1981;11:25-33.
26. Shen J-W, Atkinson B, Koprowski H, Sears HF. Binding of murine immunoglobulin to human tissues after immunotherapy with anticolorectal carcinoma monoclonal antibody. Int J Cancer 1984;33:465-68.
27. Göttinger HG, Funke I, Johnson JP, Gokel JM, Riethmüller G. The epithelial cell surface antigen 17-1A, a target for antibody-mediated tumor therapy: its biochemical nature, tissue distribution and recognition by different monoclonal antibodies. Int J Cancer 1986;38:47-53.
28. Stokkel MPM, Hoefnagel CA, Rutgers EMT. Unexpected brain uptake in radioimmuno-scintigraphy using F(ab')<sub>2</sub> monoclonal antibodies. Clin Nucl Med 1993;18:709-10.
29. Goldenberg DM. Challenges to therapy of cancer with monoclonal antibodies. J Natl Cancer Inst 1991;83:78-9.
30. Epenetos AA, Snook D, Durbin H, Johnson PM, Taylor-Papadimitriou J. Limitations of radiolabeled monoclonal antibodies for localization of human neoplasms. Cancer Res 1986;46:3183-91.
31. Cobb LM. Intratumor factors influencing the access of antibody to tumour cells. Cancer Immunol Immunother 1989;28:235-40.
32. Dongen GAMS van, Brakenhof RH, Bree R de, Gerretsen M, Quak JJ, Snow GB. Progress in radioimmunotherapy of head and neck cancer: review. Oncology Reports 1994;1:259-64.

## Chapter 5

## Radioimmunoscinigraphy and Biodistribution of <sup>99m</sup>Tc-labeled Monoclonal Antibody U36 in Patients with Head and Neck Cancer

Remco de Bree <sup>1</sup>, Jan C. Roos <sup>2</sup>, Jasper J. Quak <sup>1</sup>, Willem den Hollander <sup>2</sup>,  
Gordon B. Snow <sup>1</sup>, and Guus A.M.S. van Dongen <sup>1</sup>

Departments of <sup>1</sup> Otolaryngology / Head and Neck Surgery  
and <sup>2</sup> Nuclear Medicine,  
Free University Hospital, Amsterdam, the Netherlands

Clinical Cancer Research 1995; 1: June



## ABSTRACT

Sofar, monoclonal antibody (MAb) E48 is the most promising antibody described for specific targeting of squamous cell carcinoma of the head and neck (HNSCC) in patients. Based on its more homogeneous reactivity pattern on HNSCC, the novel MAb U36 may be even better suited for targeting. In this study the biodistribution of MAb U36 was evaluated by radioimmunoscinigraphy (RIS) and by biopsy measurements in 10 patients, who were suspected of having neck lymph node metastases from a histologically proven HNSCC and who were planned to undergo resection of the primary tumor and neck dissection. Patients received 1.8-53.0 mg MAb U36 IgG labeled with  $756 \pm 95$  MBq  $^{99m}\text{Tc}$  intravenously.

Preoperatively, palpation, Computerized Tomography (CT), Magnetic Resonance Imaging (MRI), and RIS were performed. Images included planar and Single Photon Emission Computerized Tomography (SPECT) images of the head and neck and planar images of the whole body. The diagnostic findings were recorded per side as well as per lymph node level of the neck and compared to the histopathological outcome. Radioactivity in blood samples and biopsies from the surgical specimens were measured.

All 10 primary tumors were visualized by RIS. All diagnostic modalities were correct in 7 out of 14 tumor involved lymph node levels. The missed lymph node metastases comprised micrometastases, small tumor involved nodes ( $< 9$  mm), and tumor involved nodes with much necrosis, keratin, or fibrin. There were no false-positive observations with MAb U36. Besides activity uptake in tumor tissue, only slight accumulation of activity was observed in the mouth, lungs, liver, spleen, kidneys, and scrotal area. Biopsies from the surgical specimen showed a high tumor uptake of  $20.4 \pm 12.4$  %ID/kg (range 8.0 - 43.0 %ID/kg), 44 h p.i.. Increase of MAb dose did not influence uptake of activity in tumor tissue. The mean tumor to non-tumor ratio at this time point was 2.3 for mucosa, 2.8 for blood, 3.0 for bone marrow aspirate, 12.9 for fat, and 13.0 for muscle tissue.

The present clinical study shows that  $^{99m}\text{Tc}$ -labeled U36 IgG accumulates selectively and to a high level in HNSCC. The tumor targeting results for U36 IgG are comparable to those previously described for E48 IgG. Based on the results of ongoing biodistribution studies, in which both MAbs E48 and U36, labeled with different iodine isotopes are simultaneously evaluated for tumor uptake and retention in HNSCC patients, one of these MAbs will be selected for future adjuvant radioimmunotherapy trials.

## INTRODUCTION

Squamous cell carcinoma represents about 90% of all head and neck cancers. Worldwide, the incidence of head and neck squamous cell carcinoma (HNSCC) is about 500,000. Despite intensive efforts in prevention, screening, and therapy, in the last decades the 5-year survival rates have not improved substantially. This is mainly due to the development of locoregional recurrences and distant metastases, caused by the persistence of minimal residual disease after surgery<sup>1,2</sup>. Patients with advanced stage HNSCC and particularly those with multiple lymph node involvement are at risk for failure at primary and distant sites<sup>3,4</sup>. It is obvious that these patients need adjuvant therapy. Unfortunately, chemotherapy is only of value for palliation of HNSCC<sup>2</sup>. Since HNSCC has a high intrinsic sensitivity for irradiation<sup>5</sup>, we focus on the use of monoclonal antibodies (MAbs) labeled with radionuclides for radioimmunotherapy (RIT).

For this purpose we produced a panel of MAbs directed against HNSCC<sup>6-9</sup>. Two of these MAbs, designated E48 and U36, are exclusively reactive with normal and malignant squamous and transitional epithelia. MAb E48 recognizes a Mr 16,000 outer cell surface antigen probably involved in cell-cell adhesion<sup>10</sup>. MAb E48 was shown to be highly capable for selective tumor targeting in HNSCC patients<sup>11-13</sup>. The high and selective tumor uptake of radiolabeled MAb E48 is promising for the application of MAb E48 in RIT<sup>13,14</sup>. However, a limitation of MAb E48 is the heterogeneity of the E48 antigen expression in 30% of HNSCC<sup>15</sup>. As a consequence not all HNSCC patients will be eligible for RIT with MAb E48. For this reason we recently developed a new MAb designated U36. MAb U36 recognizes a Mr 200,000 antigen which is homogeneously expressed in 96% of HNSCC<sup>15</sup>. In HNSCC xenograft bearing nude mice, radiolabeled MAb U36 showed high uptake and good retention in tumor tissue<sup>9</sup>.

In this study the potential of MAb U36 for targeting HNSCC in patients is evaluated. To allow for comparison with MAb E48 we investigated  $^{99m}\text{Tc}$ -labeled MAb U36, using radioimmunoscinigraphy (RIS) and measurements of activity in blood samples and biopsies obtained from surgical specimens, in the same way as we previously described for MAb E48<sup>11-13</sup>.

## PATIENTS AND METHODS

**Patient Study.** The protocol was approved by the Dutch Health Council and by the institutional review board of the Free University Hospital. Informed consent was obtained from all participants.

Ten patients, who were suspected of having neck lymph node metastasis from a histologically proven HNSCC and planned to undergo a resection of the primary tumor and a neck dissection, participated in this study. The primary tumor and the status of neck lymph nodes were classified according to the TNM system of the International Union Against Cancer, the UICC<sup>16</sup>. See for patient and tumor characteristics and injected MAb dose Table 1. Prior to enrollment, a biopsy of the primary tumor had to show a positive immunoperoxidase staining with MAb U36. Semiquantitative evaluation of these stainings revealed reactivity of MAb U36 with 75-100% of the cells within these tumors. Prior and up to 7 days after administration of  $^{99m}\text{Tc}$ -labeled MAb U36, urine and blood were obtained for chemical analysis and assessment of MAb pharmacokinetics. Electrolytes,



Table 1. Patient and tumor characteristics and injected MAb dose.

patient	age	sex	stage <sup>a</sup>	primary tumor site <sup>a</sup>	MAb dose (mg)
1	51	F	pT2N2b	oropharynx, posterior third of tongue	2.8
2	58	M	pT4N2b	hypopharynx, pyriform sinus	2.2
3	75	M	pT4N1	larynx, supraglottic larynx	1.8
4	52	M	pT4N2b	oral cavity, retromolar area	2.2
5	58	M	pT4N2b	hypopharynx, pyriform sinus	2.1
6	77	M	pT4N1	hypopharynx, pyriform sinus	13.0
7	62	M	pT4N1	oral cavity, inferior alveolar process	13.0
8	69	M	pT4N2b	oral cavity, retromolar area	51.8
9	53	M	pT3N2b	hypopharynx, pyriform sinus	53.0
10	53	M	pT3N2b	oropharynx, tonsillolinguual sulcus	52.1

<sup>a</sup>: according to the TNM system of the UICC and all tumors are squamous cell carcinomas.

aspartate aminotransferase, alanine aminotransferase, alkaline phosphatase, gamma-glutamyl transferase, lactate dehydrogenase, urea nitrogen, creatinine, and uric acid were determined in serum. Hematological determinations included hemoglobin, hematocrit, platelet count, white blood cell count and differentiation, and sedimentation rate. Skin tests were not performed. Vital signs were recorded before and up to 3 h after injection. Prior and six weeks after injection serum samples were obtained from the patients for the assessment of human anti-mouse antibody (HAMA) development with a MAb U36 related HAMA assay (see chapter 6) essentially according to a method described by Massuger et al.<sup>17</sup>.

Patients received  $2.4 \pm 0.5$  mg U36 IgG radiolabeled with <sup>99m</sup>Tc (mean  $756 \pm 95$  MBq) by intravenous (i.v.) injection in 5 minutes. As a bridging study between RIS and RIT two patients (6 and 7) received simultaneously 10 mg unlabeled U36 IgG and three patients (8-10) received additionally 50 mg unlabeled U36 IgG.

**Monoclonal Antibody U36.** Monoclonal antibody U36 was derived after immunization of mice with viable cells of the HNSCC cell line UM-SCC-22B. The antigen recognized by MAb U36 is a Mr 200,000 protein located at the outer cell surface<sup>9</sup>. The MAb U36 defined antigen is expressed by 99% of the primary HNSCCs (n=196). A comparable reactivity pattern was observed in 28 lymph nodes metastases<sup>15</sup>.

**Antibody Preparation.** The U36 IgG used in this study was supplied by Centocor Inc. (Leiden, the Netherlands). U36 IgG was purified from a concentrated tissue culture supernatant by affinity chromatography on a protein A-Sepharose column. For virus inactivation, IgG from the protein A eluate was treated for at least 6 h with Tween 80 and tri-*n*-butylphosphate. The protein A purified IgG was further purified on Q-Sepharose. The preparation was found to be pyrogen free.

**Preparation of <sup>99m</sup>Tc-labeled U36 IgG.** All radiolabeling procedures were performed under aseptic conditions in a shielded laminar flow hood. All glassware, plastics, and solutions were sterile and pyrogen free. For labeling MAb U36 IgG with <sup>99m</sup>Tc, a modification of the multistep procedure as described by Fritzberg et al.<sup>18</sup> was

followed, using a S-benzoylmercaptoglycylglycylglycine chelator<sup>19</sup> which was a gift from Mallinckrodt Medical B.V. (Petten, The Netherlands). A mean of  $98.2 \pm 1.2\%$  of the <sup>99m</sup>Tc was bound to IgG as determined by chromatography on ITLC-SG strips (Gelman Sciences, Ann Arbor, MI) with 0.1 M citrate buffer, pH 5.0. Every radiolabeled U36 IgG preparation was assayed for immunoreactivity by measuring the binding to glutaraldehyde fixed cells of the HNSCC cell line UM-SCC-14C<sup>9</sup>. As determined by a modified Lineweaver-Burk plot, the immunoreactive fraction of <sup>99m</sup>Tc-labeled U36 IgG at infinite antigen excess was  $74.7 \pm 9.0\%$ . The affinity constant for U36 IgG was  $3.5 \times 10^{10} \text{ M}^{-1}$  as determined by the Scatchard plot.

**Imaging studies.** All patients were examined by palpation, CT, MRI, and RIS of the neck prior to surgery. Preoperative palpation was performed by the same experienced head and neck surgeon. CT scans were obtained with a fourth generation Siemens Somatom Plus (Siemens AG, Erlangen, Germany) after intravenous administration of contrast medium (Ultravist 300 mg iodine/ml, Schering AG, Germany). Contiguous axial 5-6 mm scanning planes were used. MRI examinations were done on a 0.6 Tesla imaging system (Teslacon, Technicare - General Electric, Milwaukee) using a partial volume coil. Axial T1-weighted spin echo and Gadolinium-diethylenetriaminepentaacetic acid (Magnevist, Schering AG, Germany) enhanced T1-weighted gradient recalled echo images were made in all patients without claustrophobia. Slice thickness varied from 3 to 5 mm, with an interslice gap of 50% as described by Van den Brekel et al.<sup>20</sup>. Criteria for the optimal assessment of cervical lymph node metastases by CT or MRI, as defined in our institute, were used. At CT and MRI, neck levels were considered malignant if nodes with central necrosis were depicted, or if the minimal diameter in the axial plane of a node was 11 mm or more for nodes located in level II (subdigastric) and 10 mm or more for all other nodes, or if groups of 3 or more borderline lymph nodes (1 or 2 mm smaller) were seen<sup>21</sup>.

RIS was performed with a large field of view gamma camera (Dual Head Genesys Imaging System, ADAC laboratories, Milpitas) equipped with low energy parallel hole collimators and connected to a computer (Pegasys, ADAC laboratories, Milpitas). Planar anterior and posterior images of the head and neck and the whole body were acquired immediately, at 16 h, and at 21 h after injection. Single Photon Emission Computerized Tomography (SPECT) images of the head and neck were acquired 16 h after injection, while lateral scans of the head and neck were obtained 21 h after injection. Planar images included the following acquisition parameters: matrix size 128 x 128 (head and neck) or 256 x 256 (whole body) and at least 100 kilocounts were obtained per view during 5-20 min. Acquisition data for SPECT imaging: 64 angles were recorded, 30-second acquisition per angle, 360-degree circular orbit, and matrix size 64 x 64. Interpretation of the images was based on asymmetry and retention of activity, especially on late images.

CT, MRI, or RIS examinations were each scored by one experienced examiner. All examiners were blinded to the results of other examinations and the pathological outcome. They only were informed about the site of the primary tumor. All patients had neck dissections performed 2 days after administration of the radioimmunoconjugate. After fixation, all palpable and visible lymph nodes were dissected from the surgical specimen and cut into 2-4 mm-thick slices for microscopic examination. The size of lymph nodes does not change by fixation<sup>21</sup>. The different slices of one lymph node were examined by a pathologist and the percentage tumor involvement was estimated. The



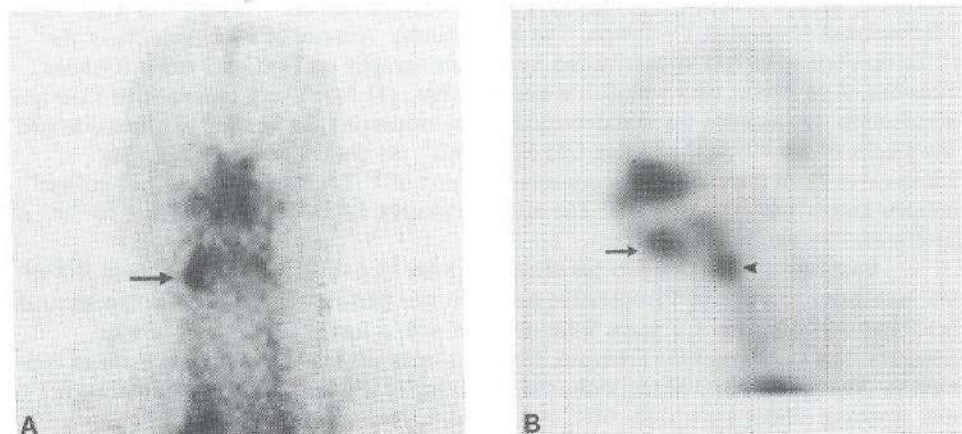
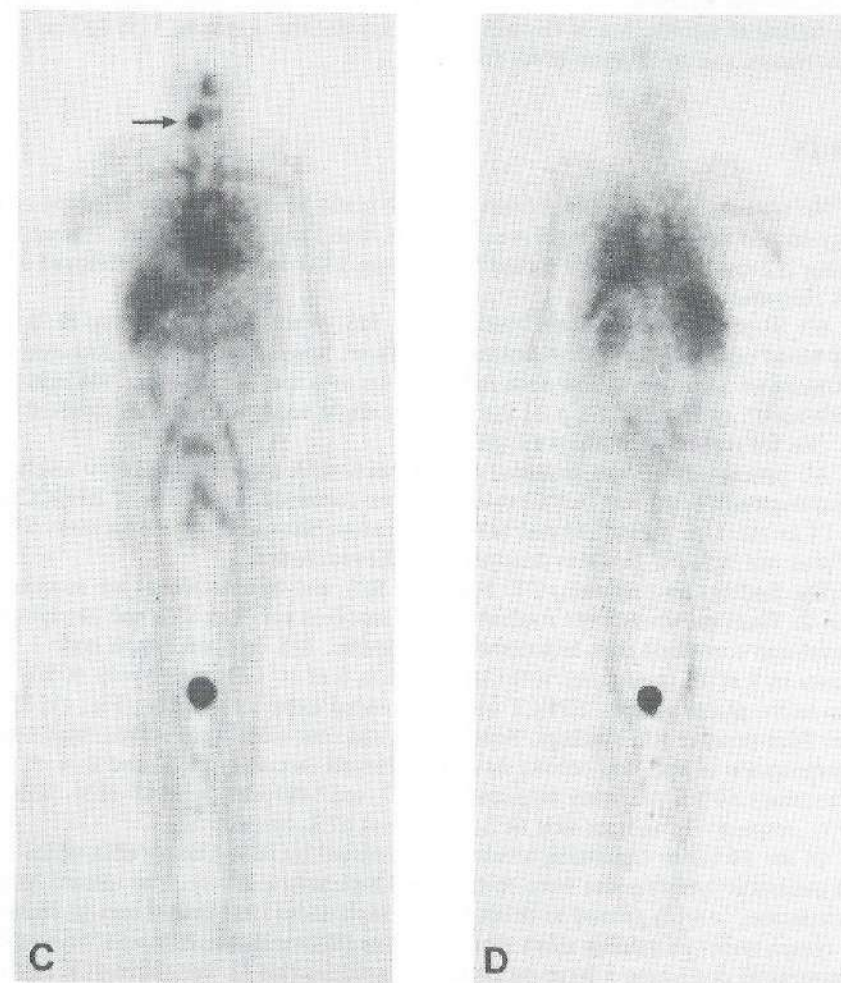


Figure 1. (A) Planar anterior image of the head and neck of patient 7 with a carcinoma of the right inferior alveolar process 16 h after injection of  $^{99m}\text{Tc}$ -labeled U36 IgG. Increased uptake is seen in the mouth on the right side. Only one spot can be distinguished (arrow). (B) A sagittal SPECT slice of the same patient shows the two separate spots, representing the primary tumor in the lower jaw (arrow) and the subdiaphragic lymph node metastasis (arrowhead). (C) Anterior and (D) posterior whole body images 16 h p.i.. Note the clear visualization of the primary tumor (arrow).

outcome of the histopathological examination of the neck dissection specimens was used as 'gold standard'.

For topographical evaluation the findings were recorded per side as well as per lymph node level according to the Memorial Sloan Kettering Cancer Center Classification<sup>22</sup>. Level I includes the contents of the submental and the submandibular triangles. Level II, III, and IV include the lymph nodes adjacent to the internal jugular vein and the lymph nodes contained within the fibroadipose tissue located medial to the sternocleidomastoid muscle. This area is arbitrarily divided into three equal parts, level II being the highest and level IV the lowest level. Level V includes the contents of the posterior cervical triangle.

**Pharmacokinetics.** Blood samples were obtained from the arm opposite the injection site for determination of activity up to 44 h p.i.. Aliquots of blood samples were measured for  $^{99m}\text{Tc}$  activity in a well-counter (1282 Compugamma, LKB Wallac, Turku, Finland), compared to an aliquot retained from the conjugate preparation, and corrected for decay. Blood activity was expressed as the percentage of the injected dose per kg. HPLC analysis of the serum samples up to 21 h p.i. revealed that more than 95% of the radioactivity was bound to the MAb. The pharmacokinetics were analyzed modeling a time versus radioactivity curve for each infusion. A MW/Pharm program (MediWare, Groningen, The Netherlands) was used for nonlinear Bayesian estimation of pharmacokinetic parameters. One-, two-, and three-compartment models were fit to the data. The peeling algorithm was used to estimate initial parameters. A Bayesian least-square method was used to estimate the final parameters: the initial ( $t_{1/2} \alpha$ ) and final half-lives ( $t_{1/2} \beta$ ).



**Biodistribution.** In all patients biopsies of the primary tumor and several other tissues were taken from the surgical specimen. In these patients blood and bone marrow aspiration and biopsy were taken under general anesthesia just before surgery. All biopsies were weighed and the amount of  $^{99m}\text{Tc}$  was measured in a well-counter. The effect of self-absorption by volume effects was corrected by comparison of the sample with a set of reference samples, prepared by diluting an equal amount of the standard in different volumes of saline. All data were corrected for decay, scattered radiation, and converted to percentages injected dose per kilogram (%ID/kg) tissue. Tumor to non-tumor ratios were calculated, using matched uptake values of one patient. If in a patient several biopsies of one kind of tissue were taken, the mean uptake in this tissue was calculated and used for further analysis. After counting, all biopsies were assessed histopathologically to determine the presence or absence of HNSCC.



**Statistical analysis.** The Student's *t* test for paired and unpaired data was used to test the statistical significance of the differences between the uptake of U36 IgG in different tissues and at different MAb doses.

## RESULTS

No adverse reactions were observed which could be related to the injection of the antibody and no significant changes were noted in blood and urine analysis. Patient 3 (receiving 2.2 mg U36 IgG) and patient 6 (receiving 13.0 mg U36 IgG) developed a HAMA response.

All 10 primary tumors were visualized by RIS. Whole body images up to 21 h p.i. showed blood pool activity with visualization of liver, lungs, heart, spleen, kidneys, and nose. Uptake of activity was also seen in the scrotal area and sometimes in the intestine and gallbladder, at 16 and 21 h p.i.. Besides this, slight accumulation was observed in the mouth. See for representative images Figure 1.

All patients underwent unilateral neck dissection. A total number of 50 levels were histopathologically examined. All 10 operated sides contained metastases of HNSCC in totally 14 levels. One patient refused MRI examination because of claustrophobia. This patient was not included in the evaluation of MRI examination.

The findings on palpation, CT, MRI, and RIS, and histopathology are summarized in Table 2. Findings which were evaluable were analyzed per neck side and per lymph node level and correlated with histopathological results. RIS detected lymph node metastases in 7 of 14 (sensitivity 50%) levels and in 6 of 10 sides (sensitivity 60%). In addition to the planar images, SPECT images provided extra information (Fig. 1). There were no false-positive RIS findings. Seven levels and four sides were scored false-negative. Interpretation of RIS was correct in 43 of 50 levels (accuracy 86%) and in 6 of 10 sides (accuracy 60%). Accuracy of palpation, CT, and MRI was per level 86%, 83%, and 87%, respectively and per side 60%, 80%, and 67%, respectively.

Of the 14 tumor containing levels 7 were missed by RIS. The paraffin slides of the missed metastatic lymph nodes were re-examined histopathologically. The missed lymph node metastases (*n*=14) proved to be all small lymph nodes (less than 9 mm in diameter, *n*=5), lymph nodes containing small tumor deposits (micrometastasis, *n*=5), or lymph node metastases containing a large proportion of necrosis (*n*=3), keratin (*n*=1), or fibrin (*n*=1) deposits.

**Pharmacokinetics.** The time versus radioactivity curve of U36 IgG best fit a two-compartment model. The mean initial ( $t_{1/2\alpha}$ ) and final half-lives ( $t_{1/2\beta}$ ) for U36 IgG at 2 mg dose were  $6.7 \pm 2.6$  h and  $50.9 \pm 22.7$  h, respectively. Increase in MAb dose did not influence the clearance from the blood:  $t_{1/2\alpha}$  and  $t_{1/2\beta}$  were for  $^{99m}\text{Tc}$ -labeled U36 IgG at 10 mg  $5.1 \pm 1.1$  h and  $50.3 \pm 9.4$  h and at 50 mg  $4.5 \pm 2.3$  h and  $50.8 \pm 24.2$  h, respectively.

Table 2. Correlation of preoperative diagnostic findings with histopathological findings.

	true-positive	false-negative	false-positive	true-negative
<b>Per side</b>				
palpation	6	4	0	0
CT	8	2	0	0
MRI <sup>a</sup>	6	3	0	0
RIS	6	4	0	0
<b>Per level</b>				
palpation	7	7	0	36
CT	7	7	2	36
MRI <sup>a</sup>	7	6	0	32
RIS	7	7	0	36

<sup>a</sup> MRI in only 9 patients.

**Biodistribution.** The uptake values and tumor to non-tumor ratios of  $^{99m}\text{Tc}$ -labeled U36 IgG in biopsies from the surgical specimen as well as in blood and bone marrow are shown in Table 3. Activity uptake was the highest in tumor tissue:  $20.4 \pm 12.4$  (mean  $\pm$  SD), range 8.0 - 43.0 %ID/kg. High  $^{99m}\text{Tc}$  activity was also seen in normal mucosa ( $10.1 \pm 6.4$  %ID/kg), but was significantly ( $p < 0.05$ ) lower than in tumor tissue. Tumor positive lymph nodes contained significantly ( $p < 0.01$ ) more  $^{99m}\text{Tc}$  activity than tumor negative lymph nodes:  $4.2 \pm 1.7$  and  $1.7 \pm 0.4$  %ID/kg, respectively, with a mean ratio of 3.2. Low activity was seen in bone marrow biopsies:  $3.0 \pm 1.1$  %ID/kg. Bone marrow aspiration showed a mean  $^{99m}\text{Tc}$  activity of  $7.2 \pm 1.4$  %ID/kg, while the activity in blood was slightly higher ( $7.8 \pm 1.7$  %ID/kg, mean bone marrow to blood ratio:  $0.9 \pm 0.0$ ). The activity in the bone marrow aspirate was mainly located in the plasma (supernatant). The mean plasma activity of the bone marrow aspirate and blood plasma were similar ( $12.3 \pm 3.0$  and  $12.5 \pm 2.6$  %ID/kg, respectively; mean bone marrow plasma to blood plasma ratio  $1.0 \pm 0.1$ ). Mean tumor to non-tumor ratios varied between  $2.3 \pm 1.5$  for mucosa and  $14.3 \pm 9.9$  for tumor negative lymph nodes (Table 3). For muscle, fat, blood, and bone marrow aspirate these ratios were  $13.0 \pm 8.7$ ,  $12.9 \pm 5.0$ ,  $2.8 \pm 1.9$ , and  $3.0 \pm 2.0$ , respectively.

Mean uptake of  $^{99m}\text{Tc}$ -labeled U36 was also calculated at low (2 mg) and high (12-52 mg) MAb dose separately. Higher MAb dose did not influence the tumor uptake of  $^{99m}\text{Tc}$ -labeled U36 IgG: at 2 mg  $24.8 \pm 15.4$  %ID/kg and at 12-52 mg  $16.1 \pm 5.6$  %ID/kg ( $p > 0.2$ ). Also the uptake in other tissues and the tumor to non-tumor ratios were not influenced by an increase of the MAb dose.



Table 3. Uptake and tumor to non-tumor ratios of  $^{99m}\text{Tc}$ -labeled U36 IgG in biopsies obtained from the surgical specimens 44 h p.i..

	uptake (% ID/kg)		tumor to non-tumor ratio		n <sup>a</sup>
	mean $\pm$ SD	range	mean $\pm$ SD	range	
tumor	20.4 $\pm$ 12.4	8.0 - 43.0			10
mucosa	10.1 $\pm$ 6.4	4.6 - 28.0	2.3 $\pm$ 1.5	0.8 - 5.7	10
positive lymph node	4.2 $\pm$ 1.7	1.7 - 6.4	5.7 $\pm$ 4.6 <sup>b</sup>	1.8 - 17.3 <sup>b</sup>	8
negative lymph node	1.7 $\pm$ 0.4	1.0 - 2.2	14.3 $\pm$ 9.9	4.9 - 33.9	7
muscle	1.6 $\pm$ 0.3	1.2 - 2.2	13.0 $\pm$ 8.7	4.0 - 32.8	10
fat	1.4 $\pm$ 0.6	0.6 - 2.3	12.9 $\pm$ 5.0	5.6 - 23.3	9
submandibular gland	3.9 $\pm$ 2.7	1.2 - 9.7	8.8 $\pm$ 5.8	2.2 - 16.4	7
thyroid gland	7.1 $\pm$ 4.0	2.1 - 11.7	9.0 $\pm$ 8.6	0.7 - 20.8	3
vein	3.7 $\pm$ 1.5	1.8 - 7.4	6.0 $\pm$ 4.0	2.2 - 14.7	10
cartilage	2.5 $\pm$ 1.7	0.9 - 5.6	14.2 $\pm$ 17.6	3.6 - 49.3	5
bone marrow biopsy	3.0 $\pm$ 1.1	1.6 - 5.0	6.4 $\pm$ 3.5	2.8 - 13.8	9
total bone marrow aspiration	7.2 $\pm$ 1.4	5.4 - 10.5	3.0 $\pm$ 2.0	1.1 - 7.5	10
supernatant bone marrow aspiration	12.3 $\pm$ 3.0	9.7 - 20.1	1.7 $\pm$ 1.1	0.6 - 4.1	10
sediment bone marrow aspiration	2.5 $\pm$ 0.5	2.0 - 3.8	8.8 $\pm$ 5.8	2.4 - 20.1	10
blood	7.8 $\pm$ 1.7	5.9 - 11.9	2.8 $\pm$ 1.9	1.0 - 7.0	10
plasma	12.5 $\pm$ 2.6	9.9 - 19.1	1.7 $\pm$ 1.1	0.6 - 4.0	10

<sup>a</sup> Number of patients from whom biopsies were obtained.<sup>b</sup> Primary tumor to lymph node metastases ratio.

## DISCUSSION

Radioimmunotherapy is a challenging option for adjuvant therapy of HNSCC especially because of the intrinsic sensitivity of HNSCC for irradiation<sup>5</sup>. For effective adjuvant radioimmunotherapy it can be anticipated that all tumor deposits, including malignant cell clusters and small tumor nodules should be efficiently targeted. Thus, a MAb is required which accumulates selectively and to a high level in tumor tissue. Based on this assumption, criteria can be set for the selection of MABs to be used for this purpose. Ideally, the MAB should recognize an antigen located at the outer surface of tumor cells. The MAB should be preferentially of the IgG class rather than of the IgM class since these latter is restricted in the penetration into tumor nodules due to its large size. The antigen should be expressed by all tumors and by all tumor cells within these tumors, but not by normal tissues, especially not those which are easily accessible for MABs. Besides favorable immunohistochemical characteristics, the MAB has to show tumor selectivity in tumor targeting studies in patients. Data presented in this paper and in a previous paper<sup>9</sup> indicate that MAB U36 may be better suited for targeting head and neck cancer than any other MAB described up till now.

Most MABs directed against HNSCC do not fulfil forementioned criteria<sup>23-38</sup>. Some of these MABs are very poorly characterized<sup>23,29,35</sup>, some are directed against antigens which are predominantly localized intracellularly<sup>31,33,36</sup>, some show a very heterogeneous reactivity pattern on tumors<sup>34,36,38</sup>, while others are of the IgM class<sup>25,26,27,30,36-38</sup>. Besides this, some MABs meet limitations for tumor targeting due to their reactivity with normal tissues<sup>24-26,28,31</sup>. Cross-reactivity with normal tissues also limits the use of so-called pan-carcinoma MABs, MABs reactive with several types of tumor including HNSCC<sup>7,8,15</sup>.

Because of these drawbacks only a few MABs have been administered to HNSCC patients<sup>11,12,15,39-43</sup>. Among these are pan-carcinoma MABs which in clinical RIS studies showed extensive accumulation at non-tumor sites, thus hampering their applicability for therapy<sup>15,44</sup>. Better results have been obtained with MABs selectively reactive with HNSCC. Baum et al.<sup>43</sup> recently reported on a RIS study in which  $^{99m}\text{Tc}$ -labeled MAB 174H.64 showed good tumor targeting. Unfortunately, tissue uptake levels were not determined for this MAB. Especially the internal localization of the 174H.64 antigen may be a serious problem for RIT. The most extensively studied MAB for targeting of head and neck cancer is MAB E48. Our group already showed the good tumor targeting capacity of MAB E48 using RIS and biopsy measurements<sup>13</sup>. A limitation of this MAB is its heterogeneous reactivity with about 30% of the head and neck tumors, a reason to develop new MABs more homogeneously reactive with HNSCC<sup>9</sup>. Another reason to search for improved MABs at that time was the high uptake of MAB E48 in the adrenals as observed in RIS studies using low doses (1-2 mg) of MAB. Later studies indicated, however, that adrenal uptake was strongly diminished when a higher MAB E48 dose of 12-52 mg was used<sup>13</sup>. These data indicate that MAB E48 may be suitable for RIT although not for all HNSCC patients.

As a result of our renewed effort to develop MABs suitable for in vivo tumor targeting MAB U36 was developed. As stated above MAB U36 may have superior qualities for tumor targeting. MAB U36 is of the IgG<sub>1</sub> subclass and shows high affinity binding with a 200,000 kDa surface antigen expressed by normal squamous epithelia and squamous cell carcinoma. Up to 96% of the 196 stained HNSCC tumors showed strong reactivity (>50% of the tumor cells stained). MAB U36 shows a more extensive reactivity with HNSCC than other MABs for which such quantitative figures are available<sup>25,45,46</sup>. For example MAB E48, evaluated on the same panel of tumors as MAB U36, showed a similar strong reactivity in 70% of the tumors. Most other MABs used for clinical targeting of other tumor types show a more heterogeneous reactivity pattern<sup>47-49</sup>.

The present study demonstrates that MAB U36 indeed harbors potential for selective tumor targeting in HNSCC patients. All primary tumors were visualized with  $^{99m}\text{Tc}$ -labeled U36 IgG on planar anterior views of the head and neck. For the detection of lymph node metastases RIS with  $^{99m}\text{Tc}$ -labeled U36 IgG was as reliable as the other diagnostic modalities, palpation, CT, and MRI. However, in this small group of patients RIS could only detect lymph node metastases which were also detected by the other diagnostic modalities. Thus, RIS did not improve the diagnosis of the neck. Analysis of the missed lymph nodes revealed the presence of only a small amount of viable tumor cells. Furthermore, MAB U36 was bound to these cells as was demonstrated immunohistochemically by using peroxidase labeled rabbit anti-mouse IgG (data not shown). Therefore, tumor containing lymph nodes were missed by RIS probably due to



the limited amount of antigen accessible for the MAb and maybe due to the limited sensitivity of a gamma camera. Other disadvantages of RIS limiting routine application are the complexity, the high costs, and the lack of anatomical structures for orientation as compared to CT and MRI. Therefore, the use of radiolabeled MAb U36 for diagnostic purposes seems to be limited, as was previously also found for MAb E48<sup>11,12</sup>.

Another, more challenging application of radiolabeled MABs is radioimmunotherapy. In RIS, <sup>99m</sup>Tc-labeled U36 IgG showed selective tumor targeting. Tumor uptake of <sup>99m</sup>Tc-labeled U36 IgG as assessed in biopsies from the surgical specimens was high as compared to the uptake of other MABs in other tumors<sup>13</sup>. Uptake in tumor tissue and tumor positive lymph nodes was significantly higher than in normal mucosa and tumor negative lymph nodes, respectively. Activity uptake in tumors was also higher than in other normal tissues, as is reflected in the mean tumor to non-tumor ratios ranging from 6.4 for bone marrow biopsy to 13.0 for muscle. The activity in bone marrow aspirate was almost the same as in blood and was mainly based on plasma activity as became apparent upon centrifugation. This is particularly important since in general bone marrow is the dose limiting organ in RIT. MAB U36 did not show uptake in the adrenal glands as MAB E48 did at a low MAB dose of 1-2 mg.

Whether MAB U36 is better suited for RIT than MAB E48 with respect to tumor uptake levels and tumor to non-tumor ratios is not clear as yet. Tumor uptake levels and tumor to non-tumor ratios of radiolabeled U36 IgG, 44 h p.i., are similar to those previously found for 1-2 mg radiolabeled E48 IgG (e.g. mean tumor uptake MAB U36:  $24.8 \pm 15.4$  %ID/kg (n=5), mean tumor uptake MAB E48:  $25.8 \pm 17.9$  %ID/kg (n=15)). However, tumor uptake levels of MAB E48 IgG increased twofold when the MAB dose was increased to 10-50 mg, a phenomenon not observed with MAB U36 IgG. This discrepancy can not be explained by alterations in MAB pharmacokinetics since these pharmacokinetics remained the same for both upon MAB dose escalation<sup>13</sup>. Because MAB U36 and MAB E48 uptake levels were measured in different and small groups of patients, these differences should be interpreted with caution. Moreover, the variance of tumor load in biopsies may influence this comparison as well. To make direct comparisons possible, we recently started a study in which U36 IgG and E48 IgG labeled with different radionuclides are co-injected in HNSCC patients. Based on the results from this study one of these MABs will be selected for adjuvant clinical RIT trials.

Besides this, we will also focus on the use of unconjugated MABs for adjuvant therapy of head and neck cancer. The feasibility of this approach was recently demonstrated in a randomized trial in which murine MAB 17-1A (IgG<sub>2a</sub>) was used in adjuvant therapy of resected Dukes' C colorectal carcinoma<sup>50</sup>. After a mean follow-up of 5 years antibody treatment reduced the overall death rate by 30%. Treatment with MAB 17-1A prolonged distant relapse while no effect was seen on local relapse. Anti-tumor effects with MAB 17-1A were also observed in tumor bearing nude mice and in these studies evidence was found for a mechanism of antibody dependent cellular cytotoxicity (ADCC)<sup>51</sup>.

Recently, we finished the chimerization of the murine MAB E48 (IgG<sub>1</sub>) to a mouse/human IgG<sub>1</sub>. This chimeric MAB (cMAB) E48 was shown to be highly capable for mediation of ADCC in vitro. We also constructed a cMAB U36 IgG<sub>1</sub> which is currently evaluated for its ADCC capacity. Unconjugated cMAB U36 and cMAB E48, either alone or in combination, will be evaluated in an adjuvant therapy trial in a group of patients at high risk for developing local recurrences and distant metastases.

## ACKNOWLEDGMENTS

The authors thank Corlinda ten Brink for labeling support, Dr. Bram J. Wilhelm for pharmacokinetic determinations, Henri Greuter for biopsy measurements, Dr. Michiel W.M. van den Brekel for CT and MRI examinations, and Dr. Jacqueline E. van der Wal for histopathological support. This work was supported by the Dutch Ministry of Economic Affairs and by Centocor Europe, Inc., Leiden, The Netherlands.

## REFERENCES

1. Hong WK, Lippman SM, Wolf GT. Recent advances in head and neck cancer - larynx preservation and cancer chemoprevention: the seventeenth annual Richard and Hinda Rosenthal Foundation Award Lecture. *Cancer Res* 1993;53:5113-20.
2. Stell PM, Rawson NSB. Adjuvant chemotherapy in head and neck cancer. *Br J Cancer* 1990;61:779-87.
3. Leemans CR, Tiwari RM, Nauta JJP, Waal I van der, Snow GB. Recurrence at the primary site in head and neck cancer and the significance of neck lymph node metastases as a prognostic factor. *Cancer* 1993;73:187-90.
4. Leemans CR, Tiwari RM, Nauta JJP, Waal I van der, Snow GB. Regional lymph node involvement and its significance in the development of distant metastases in head and neck cancer. *Cancer* 1992;71:452-6.
5. Wessels BW, Harisiadis L, Carabell SC. Dosimetry and radiobiological efficacy of clinical radioimmunotherapy. *J Nucl Med* 1989;30:827.
6. Quak JJ, Balm AJM, Dongen GAMS van, Brakkee JPG, Scheper RJ, Snow GB, Meijer CJLM. A 22-kDa surface antigen detected by monoclonal antibody E48 is exclusively expressed in stratified squamous and transitional epithelia. *Am J Pathol* 1990;136:191-7.
7. Quak JJ, Dongen GAMS van, Hayashida D, Balm AJM, Brakkee RJ, Snow GB, Meijer CJLM. Production of monoclonal antibody (K931) to a squamous cell carcinoma antigen identified as the 17-1A antigen. *Hybridoma* 1990;9:377-87.
8. Quak JJ, Schrijvers AHGJ, Brakkee JPG, Davis HD, Scheper RJ, Meijer CJLM, Snow GB, Dongen GAMS van. Expression and characterization of two differentiation antigens in stratified squamous epithelia and carcinomas. *Int J Cancer* 1992;50:507-13.
9. Schrijvers AHGJ, Quak JJ, Uytendinck AM, Walsum M van, Meijer CJLM, Snow GB, Dongen GAMS van. MAB U36, a novel monoclonal antibody successful in immunotargeting of squamous cell carcinoma of the head and neck. *Cancer Res* 1993;53:4383-90.
10. Schrijvers AHGJ, Gerretsen M, Fritz J, Walsum M van, Quak JJ, Snow GB, Dongen GAMS van. Evidence for a role of the monoclonal antibody E48 defined antigen in cell-cell adhesion in squamous epithelia and head and neck squamous cell carcinomas. *Exp Cell Res* 1991;196:264-9.
11. Dongen GAMS van, Leverstein H, Roos JC, Quak JJ, Brekel M van den, Lingen A van, Martens HJM, Castelijns J, Visser GWM, Meijer CJLM, Teule JJ, Snow GB. Radioimmunoscinigraphy of head and neck tumors using <sup>99m</sup>Tc-labeled monoclonal antibody E48 F(ab')<sub>2</sub>. *Cancer Res* 1992;52:2569-74.
12. Bree R de, Roos JC, Quak JJ, Hollander W den, Brekel MWM van den, Wal JE van der, Tobi H, Snow GB, Dongen GAMS van. Clinical imaging of head and neck cancer with <sup>99m</sup>Tc-labeled monoclonal antibody E48 IgG or F(ab')<sub>2</sub>. *J Nucl Med* 1994;35:775-83.
13. Bree R de, Roos JC, Quak JJ, Hollander W den, Wilhelm AJ, Lingen A, Snow GB, Dongen GAMS van. Biodistribution of radiolabeled monoclonal antibody E48 IgG and F(ab')<sub>2</sub> in patients with head and neck cancer. *Clin Cancer Res* 1995;1:277-86.
14. Dongen GAMS van, Brakenhoff RH, Bree R de, Gerretsen M, Quak JJ, Snow GB. Progress in radioimmunotherapy of head and neck cancer. *Oncology Reports* 1994;1:259-64.
15. Bree R de, Roos JC, Quak JJ, Hollander W den, Snow GB, Dongen GAMS van. Clinical screening



- of monoclonal antibodies 323/A3, cSF-25, and K928 for suitability of targeting tumors in the upper-aerodigestive and respiratory tract. *Nucl Med Commun* 1994;15:613-27.
16. Hermanek P, Sobin LH, eds. TNM classification of malignant tumors, 4th edition. Berlin: Springer Verlag; 1987:13-26.
  17. Massuger LFAG, Thomas CMG, Segers MFG, Corstens FHM, Verheijen RHM, Kenemans P, Poels LG. Specific and nonspecific immunoassays to detect HAMA after administration of indium-111-labeled OV-TL-3 F(ab')<sub>2</sub> monoclonal antibody to patients with ovarian cancer. *J Nucl Med* 1992;33:1958-63.
  18. Fritzberg AR, Abrams PG, Beaumier PL, Kasina S, Morgan AC, Rao TN, Sanderson JA, Srinivasan A, Wilbur DS, Vanderheyden J-L. Specific and stable labeling of antibodies with technetium-99m with a diamide dithiolate chelating agent. *Proc Natl Acad Sci USA* 1988;85:4025-9.
  19. Visser GWM, Gerretsen M, Herscheid J, Snow GB, Dongen GAMS van. Labeling of monoclonal antibodies using the MAG<sub>3</sub> chelate for radioimmunotherapy of cancer: a technical protocol. *J Nucl Med* 1993;34:1953-63.
  20. Brekel MWM van den, Castelijns JA, Stel HV, Valk J, Croll GA, Golding RP, Luth WJ, Meijer CJLM, Snow GB. Detection and characterization of metastatic cervical adenopathy by MR imaging: comparison of different MR techniques. *J Comp Assist Tomogr* 1990;14:581-9.
  21. Brekel MWM van den, Stel HV, Castelijns JA, Nauta JJP, Waal I van der, Valk J, Meijer CJLM, Snow GB. Cervical lymph node metastases: assessment of radiologic criteria. *Radiology* 1990;177:379-84.
  22. Shah JP, Strong E, Vikram B. Neck dissection: Current status and future possibilities. *Clin Bulletin* 1981;11:25-33.
  23. Zenner HP. Monoklonale Antikörper zur Erkennung von Larynxkarzinomenzellen. *Arch Otorhinolaryngol* 1981;233:161-72.
  24. Carey TE, Kimmel KA, Schwartz DR, Richter DE, Baker SR, Krause CJ. Antibodies to human squamous cell carcinoma. *Otolaryngol Head Neck Surg* 1983;91:482-91.
  25. Kimmel KA, Carey TE. Altered expression in squamous carcinoma cells of an orientation restricted epithelial antigen detected by monoclonal antibody A9. *Cancer Res* 1986;46:3614-23.
  26. Boeheim K, Speak JA, Frei E, Bernal SD. SQM1 antibody defines a surface membrane antigen in squamous carcinoma of the head and neck. *Int J Cancer* 1985;36:137-42.
  27. Stahel RA, Speak JA, Bernal SD. Murine monoclonal antibody LAM2 defines cell membrane determinant with preferential expression on human lung small-cell carcinomas. *Int J Cancer* 1985;35:11-7.
  28. Kyoizumi S, Akiyama M, Kono N, Kobuke K, Hakoda M, Jones SL, Yamakido M. Monoclonal antibodies to human squamous cell carcinoma of the lung and their application to tumor diagnosis. *Cancer Res* 1985;45:3274-81.
  29. Prat M, Bussolita G, Spinnato MR, Comoglio PM. Monoclonal antibodies against the human epidermoid carcinoma A 431. *Cancer Detection and Prevention* 1985;8:169-79.
  30. Ranken R, White CF, Gottfried TG, Yonkovich SJ, Blazek BE, Moss MS, Fee WE, Liu Y-S V. Reactivity of monoclonal antibody 17.13. with human squamous cell carcinoma and its application to tumor diagnosis. *Cancer Res* 1987;47:5684-90.
  31. Myoken Y, Moroyama T, Michaiichi S, Takada K, Namba M. Monoclonal antibodies against human oral squamous cell carcinoma reacting with keratin proteins. *Cancer* 1987;60:2927-37.
  32. Gioanni J, Samsin M, Zanghellini E, Mazeau C, Ettore F, Demard F, Chauvel P, Duplay H, Schneider M, Laurent J-C, Lalanne CM. Characterization of a new surface epitope specific for human epithelial cells defined by a monoclonal antibody and application to tumor diagnosis. *Cancer Res* 1987;47:4417-24.
  33. Samuel J, Noujaim AA, Williams DJ, Brezinska GS, Haines DM, Longenecker BM. A novel marker for basal (stem) cells of mammalian stratified squamous epithelia and squamous cell carcinomas. *Cancer Res* 1989;49:2465-70.
  34. Tatake RJ, Amin KM, Maniar HS, Jambhekar NA, Srikhande SS, Gangal SG. Monoclonal antibody against human squamous-cell-carcinoma-associated antigen. *Int J Cancer* 1989;44:840-5.
  35. Fantozzi RD. Development of monoclonal antibodies with specificity to oral squamous cell carcinoma. *Laryngoscope* 1991;101:1076-80.
  36. Parsons PG, Leonard JH, Kearsley JH, Takahashi H, Lin-Jian X, Moss DJ. Characterization of a novel monoclonal antibody, 3H-1, reactive with squamoproliferative lesions and squamous-cell cancers. *Int J Cancer* 1991;47:847-52.
  37. Yoshiura M, Murakami H, Tashiro H, Kurisu K. Production of a human monoclonal antibody to normal basal and squamous cell carcinoma-associated antigen. *J Oral Pathol Med* 1993;22:451-8.
  38. Harada H, Osaki Y, Kukita T, Kurisu K, Tashiro H, Yasumoto S. Monoclonal antibody G6K12 specific for membrane-associated differentiation marker of human stratified squamous epithelia and squamous cell carcinoma. *J Oral Pathol Med* 1993;22:145-52.
  39. Tranter RMD, Fairweather DS, Bradwell AR, Dykes PW, Watson-James S, Chandler S. The detection of squamous cell tumours of the head and neck using radio-labelled antibodies. *J Laryngol Otol* 1984;98:71-4.
  40. Soo KC, Ward M, Roberts KR, Keeling F, Carter RL, McCready VR, Ott RJ, Powell E, Ozanne B, Westwood JH, Gusterson BA. Radioimmunoscinigraphy of squamous carcinomas of the head and neck. *Head Neck Surg* 1987;9:349-52.
  41. Kairemo KJA, Hopsu EVM. Immunoscintigraphy in laryngeal and pharyngeal carcinomas using indium-111 labelled monoclonal antibody. *Acta Oncol* 1990;29:533-8.
  42. Timon CI, McShane D, Hamilton D, Walsh MA. Head and neck cancer localization with indium labelled carcinoembryogenic antigen: a pilot project. *J Otolaryngol* 1991;20:283-7.
  43. Baum RP, Adams S, Kiefer J, Niesen A, Knecht R, Howaldt H-P, Hertel A, Adamietz IR, Sykes T, Boniface GR, Noujaim AA, Hör G. A novel technetium-99m labeled monoclonal antibody (174H.64) for staging head and neck cancer by immuno-SPECT. *Acta Oncol* 1993;32:747-51.
  44. Dvigi CR, Welt S, Kris M, Real FX, Yeh SDJ, Gralla R, Merchant B, Schweighart S, Unger M, Larson SM, Mendelsohn J. Phase I and imaging trial of Indium 111-labeled anti-epidermal growth factor receptor monoclonal antibody 425 in patients with squamous cell lung carcinoma. *J Natl Cancer Inst* 1991;83:97-104.
  45. Böheim K, Schwarzfürter H, Böheim C, Frei E, Bernal SD. Immunohistochemical identification of squamous carcinoma of the head and neck with monoclonal antibody SQM1. *Acta Otolaryngol* 1986;102:333-40.
  46. Kearsley JH, Leonard JH, Takahashi H, Battistutti D, Parsons PG, Moss DJ. Prognostic significance of monoclonal antibody 3H-1 reactivity with squamous-cell head-and-neck cancers. *Int J Cancer* 1991;47:853-7.
  47. Ernst CS, Shen J-W, Litwin S, Herlyn M, Koprowski H, Sears HF. Multiparameter evaluation of the expression in situ of normal and tumor-associated antigens in human colorectal carcinoma. *J Natl Cancer Inst* 1986;77:387-95.
  48. Scheinberg DA, Strauss DJ, Yeh SD, Dvigi C, Garin-Chesa P, Graham M, Pentlow K, Coit D, Oettgen HF, Old LJ. A phase I toxicity, pharmacology, and dosimetry trial of monoclonal antibody OKB7 in patients with Non-Hodgkin's lymphoma: effects of tumor burden and antigen expression. *J Clin Oncol* 1990;8:792-803.
  49. Molinolo A, Simpson JF, Thor A, Schlom J. Enhanced tumor binding using immunohistochemical analysis by second generation anti-tumor-associated glycoprotein 72 monoclonal antibodies versus monoclonal antibody B72.3 in human tissue. *Cancer Res* 1990;50:1291-8.
  50. Riethmüller G, Schneider-Gädick E, Schlimok G, Schmiegel W, Raab R, Höfken K, Gruber R, Pichlmaier H, Hirsche H, Pichlmayr R, Witte J. Randomised trial of monoclonal antibody for adjuvant therapy of resected Dukes' C colorectal carcinoma. *Lancet* 1994;343:1177-83.
  51. Herlyn D, Koprowski H. IgG2a monoclonal antibodies inhibit human tumor growth through interaction with effector cells. *Proc Natl Acad Sci USA* 1982;79:4761-5.



---

## Chapter 6

### **Selection of Monoclonal Antibody E48 IgG or U36 IgG for Adjuvant Therapy in Head and Neck Cancer Patients**

Remco de Bree <sup>1</sup>, Jan C. Roos <sup>2</sup>, Jasper J. Quak <sup>1</sup>,  
Gerard J. van Kamp <sup>3</sup>, Willem den Hollander <sup>2</sup>,  
Gordon B. Snow <sup>1</sup>, and Guus A.M.S. van Dongen <sup>1</sup>

Departments of <sup>1</sup> Otolaryngology / Head and Neck Surgery,  
<sup>2</sup> Nuclear Medicine, and <sup>3</sup> Clinical Chemistry,  
Free University Hospital, Amsterdam, The Netherlands

International Journal of Cancer 1995, submitted



## ABSTRACT

Data from recent clinical radioimmunoscintigraphy studies indicate that  $^{99m}\text{Tc}$ -labeled monoclonal antibodies (MAbs) E48 and U36 are equally well capable of selective targeting squamous cell carcinoma of the head and neck (HNSCC). Also the percentage injected dose per kilogram 2 days after injection was found to be similarly high for both MAbs, a mean of  $30.6 \pm 20.1$  %ID/kg for E48 IgG and  $20.4 \pm 12.4$  %ID/kg for U36 IgG. MAb E48 showed a homogeneous reactivity with 70% of the HNSCCs while for MAb U36 this was 96%. In the present study we describe additional aspects of murine and chimeric MAb (mMAb and cMAb) E48 and U36 out of consideration for selection of one MAb for adjuvant MAb-based therapy. To make direct comparison possible ten patients received 11 (n=5) or 51 mg (n=5) of both E48 IgG and U36 IgG labeled with  $^{131}\text{I}$  and  $^{125}\text{I}$  simultaneously and underwent surgery 7-8 days after injection. The mean uptake of iodine-labeled E48 IgG and U36 IgG was the highest in tumor tissue,  $8.9 \pm 8.9$  and  $8.2 \pm 4.4$  %ID/kg, respectively. Tumor to non-tumor ratios for oral mucosa, skin, muscle, blood, and bone marrow aspirate were in case of E48 IgG 2.5, 5.5, 25.2, 4.7, and 4.0, respectively, and in case of U36 IgG 2.3, 4.1, 21.0, 5.8, and 5.8, respectively. The distribution of MAbs E48 and U36 throughout tumors which have been collected in previous studies was heterogeneous when administered at a dose of 1 or 12 mg, and homogeneous when administered at a dose of 52 mg. Administration of E48 IgG resulted in a human anti-mouse antibody response in 13 out of 28 patients, while for U36 IgG this figure was 3 out of 18. cMAb E48 was shown to be highly effective in mediating antibody dependent cellular cytotoxicity *in vitro* while cMAb U36 and mMAbs E48 and U36 were not effective at all. Rationals are provided which give priority to the start of adjuvant radioimmunotherapy trials with  $^{186}\text{Re}$ -labeled cMAb U36 IgG in head and neck cancer patients who are at a high risk for development of locoregional recurrences and distant metastases.

## INTRODUCTION

During 1994 approximately 42,100 Americans developed head and neck cancer and 11,725 died from it. Worldwide more than 500,000 new cases are projected annually, and the incidence is rising. In head and neck cancer, squamous cell carcinoma accounts for approximately 90% of all tumors <sup>1</sup>. About one-third of these patients presents with early stage (I and II) head and neck squamous cell carcinoma (HNSCC), while two-thirds presents with advanced disease (stage III and IV) <sup>2</sup>. Although early stage HNSCC can be cured with surgery or radiotherapy alone in the great majority of cases, the local failure rate after surgery and/or radiotherapy in advanced stages is more than 50%. Moreover, about 25% of these patients develops distant metastases <sup>3</sup>.

Despite an increase in the locoregional control of HNSCC, due to improved surgery and radiotherapy, current therapy regimens have failed as yet to increase the 5-year survival rate in HNSCC patients <sup>1</sup>. Whereas fewer patients tend to die from uncontrolled locoregional disease, more patients are exposed to the risk of developing distant metastases. Therefore, an effective systemic adjuvant therapy is needed. To date there is no evidence that adjuvant chemotherapy has any survival benefit <sup>4</sup>. Among the innovative approaches for improving therapy of cancer is the use of monoclonal antibodies (MAbs). MAbs labeled with radionuclides offer the potential of highly localized radiation treatment of cancer <sup>5</sup>. Radioimmunotherapy (RIT) may be particularly suitable for treatment of HNSCC due to the intrinsic radiosensitivity of this tumor type <sup>6</sup>. In other therapeutic approaches unconjugated MAbs are used to obtain cytotoxicity, e.g. by mediation of immunological effector mechanisms such as antibody dependent cellular cytotoxicity (ADCC) <sup>7</sup>.

For effective adjuvant therapy it is needed that all tumor deposits, including tumor nodules, malignant cell clusters, and single tumor cells are adequately targeted. Several MAb characteristics are considered to be of importance for effective therapy with radiolabeled or unconjugated MAbs. For both approaches a high and selective uptake as well as a good retention of the MAb in the tumor is needed.

When  $\beta$ -emitters are used for RIT, it is not necessary that radiolabeled MAbs bind to each single cell within a tumor. Therefore, RIT may be effective in the treatment of larger tumors, even when the distribution of the radiolabeled MAb throughout the tumor is heterogeneous. In contrast, for unconjugated MAbs, assumed to be effective by mediating ADCC, it is probably necessary that each single tumor cell becomes adequately targeted. For larger tumor nodules this will be much more of a problem than for single tumor cells and small cell aggregates due to the fact that the MAbs have to penetrate into central cell layers. For being effective in ADCC, murine MAbs should be preferably of the IgG<sub>2a</sub> isotype. Even better, chimerized, humanized or human MAbs are used and for the most efficient mediation of ADCC these MAbs should preferably contain a human  $\gamma 1$  constant region <sup>8</sup>. Such MAbs may also be less immunogenic than murine MAbs which is of importance when repeated administrations are needed for effective therapy <sup>9</sup>.

For the use in adjuvant therapy of HNSCC we produced a panel of MAbs. Two of these MAbs, designated E48 and U36, are selectively reactive with normal and malignant squamous and transitional epithelia <sup>10,11</sup>. While MAb E48 shows a homogeneous reactivity with 70% of HNSCC, for MAb U36 this is even 96% <sup>12</sup>. The biodistribution of  $^{99m}\text{Tc}$ -labeled E48 IgG and U36 IgG has been evaluated by radioimmunoscintigraphy <sup>13-15</sup> and by biopsy measurement in 24 and 10 HNSCC patients <sup>15,16</sup>, respectively. All patients were



suspected of having neck lymph node metastases from a histologically proven HNSCC and were planned to undergo resection of the primary tumor and neck dissection. Both MABs were shown to be highly capable for selective tumor targeting in HNSCC patients and the tumor uptake 2 days after injection was similarly high,  $30.6 \pm 20.1$  %ID/kg for MAB E48 and  $20.4 \pm 12.4$  %ID/kg for MAB U36<sup>15,16</sup>. Most recently, chimeric (mouse/human) E48 IgG<sub>1</sub> and U36 IgG<sub>1</sub> have been constructed<sup>17</sup>.

Data obtained from these studies justify the further development of one of these MABs for adjuvant therapy. In this paper we further evaluate the potential of these MABs for adjuvant therapy in a comparative way. To eliminate interindividual variations MAB E48 and U36 were now administered simultaneously. We report on (1) the biodistribution of simultaneously injected iodine-labeled E48 IgG and U36 IgG, 7-8 days after injection, (2) the distribution of the MABs throughout the tumor in relation to the administered MAB dose, (3) the immunogenicity of the MABs, and (4) the potential of the murine and chimeric versions of the MABs to mediate ADCC. Based on our present and previous data, and on data from the literature we come to a design for a first MAB-based adjuvant therapy trial in head and neck cancer patients.

## PATIENTS AND METHODS

**Patient Study.** The protocol on simultaneous injection of iodine-labeled E48 IgG and U36 IgG was approved by the Dutch Health Council and by the institutional review board of the Free University Hospital. Informed consent was obtained from all patients. As far as data presented in this paper were obtained from previous studies on administration of radiolabeled E48 IgG or U36 IgG alone, the patient populations have been described before<sup>14-16</sup>. In these studies, 19 patients received E48 F(ab')<sub>2</sub>, 9 patients E48 IgG, 15 patients E48 F(ab')<sub>2</sub> as well as E48 IgG, and 10 patients U36 IgG.

In the present study, ten patients with HNSCC were injected with iodine-labeled E48 IgG and U36 IgG simultaneously. Prior to enrollment a biopsy of the primary tumor had to show E48 IgG and U36 IgG-positive immunoperoxidase staining with more than 75% of the tumor cells. Patients suffered from carcinoma of the tonsil (n=1), posterior pharyngeal wall (n=1), retromolar area (n=1), floor of the mouth (n=2), and tongue (n=5). The primary tumor and the status of the neck lymph nodes were classified according to the TNM system of the International Union Against Cancer, the IJCC<sup>18</sup>.

All patients received  $1.0 \pm 0.2$  mg E48 IgG and  $1.1 \pm 0.2$  mg U36 IgG radiolabeled with either <sup>131</sup>I (mean dose  $75.8 \pm 3.8$  MBq) or <sup>125</sup>I (mean dose  $3.2 \pm 0.5$  MBq) by intravenous injection in 5 min. Imaging and biodistribution assessment were performed 7-8 days after injection. Unfortunately, due to the low administered radioactivity dose, scatter and sometimes iodine uptake in the thyroid gland, the quality of the images was too poor for proper analysis of the neck, and therefore, images are not included in this paper. Patient and tumor characteristics and injected MAB dose are listed in Table 1. In 5 cases E48 IgG was labeled with <sup>125</sup>I and U36 IgG with <sup>131</sup>I. In the other 5 cases E48 IgG and U36 IgG were labeled with <sup>131</sup>I and <sup>125</sup>I, respectively. Five patients received additionally 10 mg, and 5 patients received additionally 50 mg both unlabeled E48 IgG as well as unlabeled U36 IgG at the time of injection of the radiolabeled MABs. To prevent uptake of radioactive iodine in the thyroid gland, all patients received Lugol's solution 3 times 0.3 ml a day for 7 days starting one day pre-injection.

Table 1. Patient and tumour characteristics and injected MAB doses.

patient	age	sex	stage <sup>a</sup>	primary tumour site <sup>a</sup>	E48 IgG dose (mg)	U36 IgG dose (mg)
1	59	M	pT3N1	oral cavity, lateral tongue	11.0	11.0
2	52	F	pT3N0	oral cavity, floor of mouth	10.6	11.0
3	54	M	pT3N2b	oral cavity, lateral tongue	11.5	11.0
4	41	M	pT3N1	oral cavity, lateral tongue	11.0	11.4
5	45	M	pT3N2b	oropharynx, tonsil	11.0	11.3
6	50	M	pT3N2b	oropharynx, posterior pharyngeal wall	51.0	51.3
7	65	M	pT2N2b	oral cavity, lateral tongue	51.2	50.7
8	68	M	pT3N1	oral cavity, lateral tongue	51.0	51.5
9	50	M	pT4N2b	oral cavity, retromolar area	51.3	51.0
10	65	M	pT3N2c	oral cavity, floor of mouth	51.0	50.7

<sup>a</sup>: All tumours are squamous cell carcinomas and are staged according to the TNM system of the IJCC.

Prior and up to 7 days after administration of the radioimmunoconjugates, urine and blood were obtained for analysis. Glucose, protein, and the content of the sediment were determined in urine. Electrolytes, aspartate aminotransferase, alanine aminotransferase, alkaline phosphatase, gamma-glutamyl transferase, lactate dehydrogenase, urea nitrogen, creatinine, and uric acid were determined in serum. Hematologic determinations included hemoglobin, hematocrit, platelet count, white blood cell count and differentiation, and sedimentation rate. Skin tests were not performed. Vital signs were recorded before and up to 3 hr after injection.

**Monoclonal antibodies E48 and U36.** MAB E48 was derived from a mouse immunized with cells from a metastasis of a moderately differentiated squamous cell carcinoma of the larynx. The antigen recognized by MAB E48 is a 16-22 kDa glycosyl-phosphatidylinositol-anchored membrane protein located on the outer cell surface<sup>19</sup>. The MAB E48 defined antigen was expressed in 94% of the primary HNSCCs (n=196). In 70% of these tumors the antigen was expressed by the majority of the cells within these tumors. A comparable reactivity pattern was observed in 31 tumor infiltrated lymph nodes from neck dissection specimens<sup>12</sup>. MAB reactivity with normal tissues is restricted to normal stratified squamous epithelium and urothelium of the bladder.

MAB U36 was derived after immunization of mice with viable cells of the HNSCC cell line UM-SCC-22B. The antigen recognized by MAB U36 is a 200 kDa protein located at the outer cell surface<sup>11</sup>. The MAB U36 defined antigen is expressed by 99% of the primary HNSCCs (n=196). In 96% of these tumors the antigen was expressed by the majority of cells within these tumors. A comparable reactivity pattern was observed in 31 lymph node metastases<sup>12</sup>. MAB reactivity with normal tissues is restricted to normal stratified squamous epithelium and urothelium of the bladder.

Chimeric (mouse/human) MABs E48 and U36 containing the human  $\gamma 1$  constant region were constructed by recombinant DNA technology as described before. Upon



chimerization MAbs retained their affinity and specificity as evaluated by Scatchard's analyses, immunohistochemical staining, Western blotting, and biodistribution experiments in nude mice bearing human HNSCC xenografts<sup>17</sup> (manuscript in preparation).

**Antibody preparations for clinical use.** The E48 and U36 IgG preparations used in this study were supplied by Centocor Inc. (Leiden, The Netherlands). E48 IgG and U36 IgG were purified from concentrated tissue culture supernatant by affinity chromatography on protein A-Sepharose columns. For virus inactivation, IgG from the protein A eluate was treated for at least 6 hr with Tween 80 and tri-*n*-butylphosphate. The protein A purified IgG was further purified on Q-Sepharose. The final preparation was found to be pyrogenic free.

**Radiolabeling of E48 IgG and U36 IgG.** All radiolabeling procedures were performed under aseptic conditions in a shielded laminar flow hood. All glassware, plastics, and solutions were sterile and pyrogen free. Labeling of E48 IgG and U36 IgG with iodine was carried out using a one vial method as described by Haisma et al<sup>20</sup>. MAb IgG in phosphate buffered saline, pH = 7.4, and <sup>131</sup>I or <sup>125</sup>I were mixed in a vial coated with Iodogen (Sigma Aldrich, Bornem, Belgium). After 10 min, 1 ml AG1-X-8 resin (BioRad, Veenendaal, The Netherlands) in PBS, 1% BSA was added to the reaction mixture to absorb free iodine. To remove the resin and to sterilize the product, the reaction mixture was filtered through a 0.22 µm filter (Millipore, Etten-Leur, The Netherlands). The purified E48 IgG was <sup>131</sup>I or <sup>125</sup>I-labeled with a specific activity of  $79.2 \pm 25.7$  MBq/mg or  $3.1 \pm 0.4$  MBq/mg protein, respectively. For U36 IgG these values were  $64.8 \pm 19.6$  MBq/mg and  $3.5 \pm 0.4$  MBq/mg protein, respectively. The mean <sup>131</sup>I and <sup>125</sup>I-incorporation percentages were  $98.5 \pm 1.3\%$  and  $97.1 \pm 2.2\%$ , respectively, as determined by chromatography on ITLC-SG strips (Gelman Sciences, Ann Arbor, MI) with 0.1 M citrate buffer, pH 5.0. Every radiolabeled E48 IgG and U36 IgG preparation was assayed for immunoreactivity by measuring the binding to 2% paraformaldehyde fixed cells of the HNSCC cell line UM-SCC-22A and the HNSCC cell line UM-SCC-14C, respectively<sup>21</sup>. As determined by a modified Lineweaver-Burk plot, the immunoreactive fractions of <sup>131</sup>I- or <sup>125</sup>I-labeled E48 IgG and U36 IgG at infinite antigen excess always exceeded 68%. The affinity constants were  $1.2 \times 10^{10}$  M<sup>-1</sup> for E48 IgG and  $3.5 \times 10^{10}$  M<sup>-1</sup> for U36 IgG as determined by Scatchard's analysis.

**Biodistribution of MAbs 7-8 days after injection.** Biopsies of the primary tumor and several other tissues were taken from the surgical specimen of all patients. Blood and bone marrow biopsy and aspiration were taken under general anesthesia just before surgery. All biopsies were weighed and the amounts of <sup>125</sup>I and <sup>131</sup>I were measured by differential counting methods in a well-counter (1282 Compugamma, LKB Wallac, Turku, Finland) to compare biodistribution of E48 IgG and U36 IgG. The effect of self-absorption by volume effects was corrected by comparison of the sample with a set of reference samples, prepared by diluting an equal amount of the standard in different volumes of saline. All data were corrected for decay and converted to percentage injected dose per kilogram (%ID/kg) tissue. If in a patient several biopsies of one kind of tissue were taken, the mean uptake in this tissue was calculated and used for further analysis. Tumor to non-tumor ratios were calculated using matched uptake values of each patient. After counting, all biopsies were analysed histopathologically to determine the presence or absence of HNSCC.

**Pharmacokinetics.** Blood samples were obtained from the arm opposite to the injection site for the determination of the activity up to 7-8 days p.i.. Aliquots of blood

samples were measured for <sup>131</sup>I- and <sup>125</sup>I-activity in a well-counter, compared to an aliquot retained from the conjugate preparation, and corrected for decay. Blood activity was expressed as the percentage of the injected dose per kg. HPLC analysis of the serum samples revealed that more than 95% of the radioactivity was bound to the MAb. The pharmacokinetics were analysed modeling a time versus radioactivity curve for each infusion. A MW/Pharm program (MediWare, Groningen, the Netherlands) was used for non-linear Bayesian estimation of pharmacokinetic parameters. One-, two-, and three-compartment models were fit to the data. The peeling algorithm was used to estimate initial parameters. A Bayesian least-square method was used to estimate the final parameters: the initial ( $t_{1/2\alpha}$ ) and final half-lives ( $t_{1/2\beta}$ ). Urine was collected over the first 48 h. Aliquots of urine samples were measured for <sup>131</sup>I- and <sup>125</sup>I-activity in a well-counter, compared to an aliquot retained from the conjugate preparation, and corrected for decay. Excretion in the urine was expressed as the percentage of the injected dose in this period. Blood activity was expressed as the percentage of the injected dose per kg.

**Statistical analysis.** The Student's *t* test for paired and unpaired data was used to determine the statistical significance of the difference between the uptake of E48 IgG and U36 IgG. Statistical difference was reached at  $p < 0.05$ .

**Distribution of the MAbs throughout tumor.** Cryosections were made from tumor biopsies obtained from patients included in previous studies<sup>15,16</sup>. These biopsies had been taken two days after injection of either E48 IgG or U36 IgG. The level of in vivo accumulation in the tumor and the distribution of the injected MAb throughout the tumor was compared with the maximal MAb binding on serial sections. In short, 5 µm thick sections of frozen tissue biopsies were cut on a cryostat microtome and mounted on poly-L-lysine coated glass slides, dried, fixed in 2% paraformaldehyde in PBS for 10 min, and dried again.

To assess the distribution of the injected MAb throughout the tumor the specimens were incubated for 30 min with rabbit anti-mouse IgG (DAKO, Glostrup, Denmark) diluted 1:25 in PBS/1% normal rabbit serum/1% BSA. The dishes were washed 3 times with PBS and incubated for 1 hr with alkaline phosphatase monoclonal anti-alkaline phosphatase (APAAP, DAKO) diluted in PBS/1% BSA. The dishes were washed again with PBS/1%BSA, rinsed with 0.1 M Tris, pH 8.2, and incubated in the dark for 20 min with Naphthol AS-TR-phosphate/Fast Red Violet LB substrate (both from Sigma). The substrate was prepared as follows: 6 mg naphthol AS-TR-phosphate dissolved in 250 µl dimethylformamide was added to 10 ml 0.1 M Tris-HCl, pH 8.2, containing 10 µl 1 M levamisole. Immediately before this preparation was used 10 mg Fast Red Violet LB was added and the solution was filtered. Sections were washed 1 min with running tap-water and counterstained with hematoxylin for 45 sec, dehydrated, and covered with Kaiser's glycerol gelatin (Merck, Amsterdam, The Netherlands).

Maximal MAb binding was assessed in the same way except that the specimen was incubated with undiluted hybridoma culture supernatant containing the MAb corresponding to the MAb used for injection. Isotype-matched control MAbs and PBS served as negative controls.

#### Human anti-mouse antibody (HAMA) responses.

**Patients:** In the present study all data on HAMA responses of patients included in the present or previous RIS studies<sup>14-16</sup>, and injected with E48 F(ab')<sub>2</sub>, E48 IgG, U36 IgG or combinations thereof, are presented. The presence of human anti-mouse antibodies was tested in patients' sera before and 4-8 weeks after injection of radiolabeled E48 F(ab')<sub>2</sub>



(group 1:  $n=16$ ); E48 IgG (group 2:  $n=5$ ); E48 F(ab')<sub>2</sub> plus E48 IgG (group 3:  $n=13$ ); U36 IgG (group 4:  $n=8$ ); or E48 IgG plus U36 IgG (group 5:  $n=10$ ).

Fourteen patients in group 1 received 1 mg and two patients 11 mg E48 F(ab')<sub>2</sub>. The five patients of group 2 received 1 mg E48 IgG. Ten patients in group 3 received 2 mg, one patient 12 mg, and two patients 52 mg E48 IgG simultaneously with 1 mg E48 F(ab')<sub>2</sub>. Four patients in group 4 received 2 mg, two patients 12 mg, and two patients 52 mg U36 IgG. Five patients in group 5 received simultaneously 11 mg E48 IgG and 11 mg U36 IgG, while five patients received simultaneously 51 mg E48 IgG and 51 mg U36 IgG.

**Assay:** Microtiter plates were coated with a 200  $\mu$ l/well coating solution, over-night at room temperature. The coating solution contained 100  $\mu$ l goat polyclonal anti-mouse IgG antibodies (DAKO Z0420) in 100 ml carbonate buffer (0.01 M NaHCO<sub>3</sub>, H<sub>2</sub>O adjusted to pH 9.6 with 0.025 M Na<sub>2</sub>CO<sub>3</sub>·10H<sub>2</sub>O). After washing three times with 200  $\mu$ l/well washing buffer (PBS with 0.02% Tween 20) 200  $\mu$ l/well mouse MAb solution was added consisting of 25  $\mu$ l MAb solution (1 mg/ml E48 F(ab')<sub>2</sub>, E48 IgG, or U36 IgG) in 25 ml assay buffer (PBS with 5% goat serum). After another washing step with 3 x 220  $\mu$ l/well washing buffer, 100  $\mu$ l pre-diluted patient serum samples and controls were added in duplicate. Samples were prediluted stepwise: 1:50, 1:200, 1:800, and 1:3200; as controls a negative serum was diluted 1:50 and a positive serum was diluted 1:1500. The assay buffer was used as a blank. After incubation for 60 min at 37°C and washing with 3 x 220  $\mu$ l/well washing buffer, 150  $\mu$ l anti-human IgG conjugate solution was added (5  $\mu$ g rabbit polyclonal anti-human IgG conjugated with horse raddish peroxidase (DAKO P0212) in 25 ml assay buffer). After incubation for 60 min at 37 °C, the plate was washed again with 220  $\mu$ l washing buffer and 200  $\mu$ l substrate solution containing 30 mg OPD (o-phenylenediamine·2HCl; 2 tablets Sigma P4664) in 20 ml citric acid/phosphate buffer (0.02 M Na<sub>2</sub>HPO<sub>4</sub>·2H<sub>2</sub>O adjusted to pH 5.5 with 0.01 M citric acid) plus 45  $\mu$ l 10% H<sub>2</sub>O<sub>2</sub> solution, was added per well and allowed to react at room temperature for approximately 30 min, till the absorbance of the control serum wells reached a value of approximately 1.0. The reaction was stopped by adding 50  $\mu$ l 4N H<sub>2</sub>SO<sub>4</sub>, and the extinction was measured at 490 nm in a plate reader. The reciprocal serum dilution yielding an absorbance reading of 1.0 is called the HAMA titer and is calculated from the formula: HAMA titer = (A-1)x(Z-Y)/(A-B) + Y, where Y = serum dilution corresponding to the nearest optical density (= A) above 1.0 and Z = serum dilution corresponding to the nearest optical density (= B) below 1.0. A HAMA titer of  $\geq 500$  was arbitrarily considered to be positive. HAMA titers provided are the mean of duplicate or triplicate analyses. Standard errors of the mean have been omitted as they were less than 8%. Sera obtained from patients injected with a combination of E48 F(ab')<sub>2</sub> and IgG were analysed with an E48 F(ab')<sub>2</sub> and an E48 IgG related HAMA assay which means that E48 F(ab')<sub>2</sub>, respectively, E48 IgG was used as catcher. Analogically, E48 IgG and U36 IgG related HAMA assays were used for the analysis of sera obtained from patients who had received E48 IgG and U36 IgG simultaneously.

**Antibody dependent cellular cytotoxicity.** UM-SCC-22A cells served as target cells, and peripheral blood mononuclear cells (PBMC) obtained from healthy volunteers as effector cells in ADCC assays. PBMC were isolated from whole blood by separation on Ficoll-Paque gradients (Pharmacia Biotech, Roosendaal, The Netherlands). Cells collected from the interface were washed twice in Hanks' balanced salt solution (Gibco

Life Technologies, Breda, The Netherlands) by centrifugation, and incubated overnight in DMEM/5% FCS in 5% CO<sub>2</sub> at 37°C.

Target cells were trypsinized by 0.05% trypsin, 0.02% EDTA in PBS (Gibco Life Technologies), washed with tissue culture medium, and resuspended in tissue culture medium at a concentration of 10<sup>5</sup> cells/ml. For ADCC assays with mAb E48 or cAb E48, 2.5  $\mu$ Ci sodium [<sup>51</sup>Cr]chromate was immediately added together with 5x10<sup>3</sup> cells (50  $\mu$ l) in the wells of 96-wells U-bottomed plates (Greiner N.V./S.A., Westmalle, Belgium). Since the reactivity of MAb U36 with UM-SCC-22A cells is lost upon trypsinization of these cells, the ADCC assay was slightly modified for testing the ADCC mediating activity of mAb U36 and cAb U36. In this case UM-SCC-22A cells were incubated for 48 hr in 96-wells U-bottomed plates before 2.5  $\mu$ Ci <sup>51</sup>Cr was added, thus allowing total recovery of U36 antigen expression and MAb U36 binding (as assessed by ELISA methods). At the moment of <sup>51</sup>Cr addition, each well contained 5x10<sup>3</sup> target cells.

After incubation of the cells for 16 hr with <sup>51</sup>Cr in 5% CO<sub>2</sub> at 37°C, the cells were washed 3 times with DMEM/5% FCS, effector cells were added at different effector:target (E:T) ratios ranging from 6.25 to 100:1, and MAbs were added to a final concentration of 10  $\mu$ g/ml. Plates were centrifuged at 65xg for 30 seconds and incubated in 5% CO<sub>2</sub> at 37°C for 5 hr after which medium was harvested from each well. All assays were performed in triplicate. Radioactivity was counted in a gamma counter (1282 CompuGamma). Maximal radionuclide release was determined by incubation of target cells in the presence of 5% Triton X-100. Natural killer (NK) cell release (antibody independent lysis) was measured by incubation of target/effector cells in the presence of the murine IgG<sub>1</sub> control anti-myosin MAb Myoscent (Centocor Inc.) which does not bind to the target cells. The percentage of specific lysis was calculated as the [(experimental release-background release)/(Triton release-background release)]x100. Background release is defined as the release in the absence of specific antibody (=spontaneous release + NK release). Standard deviations were typically 0-8%.

## RESULTS

No adverse reactions were observed which could be related to the simultaneous injection of iodine-labeled MAb E48 and MAb U36 and no significant changes were noted in blood and urine parameters.

**Biodistribution of MAbs E48 and U36, 7-8 days after injection.** The activity uptake in biopsies from the surgical specimen are shown in Table 2. The mean uptake of iodine was the highest in tumor tissue: 8.9  $\pm$  8.9 %ID/kg (range 1.8 - 31.2) for iodine-labeled E48 IgG and 8.2  $\pm$  4.4 %ID/kg (range 2.9 - 15.2) for iodine-labeled U36 IgG. High iodine uptake was also seen in normal squamous epithelium of oral mucosa (4.1  $\pm$  1.4 %ID/kg in case of E48 IgG and 4.0  $\pm$  1.4 %ID/kg in case of U36 IgG), tongue tissue (5.8  $\pm$  2.7 and 4.4  $\pm$  2.3 %ID/kg, respectively), and skin (2.5  $\pm$  1.0 and 2.5  $\pm$  1.0 %ID/kg, respectively). These uptake levels were lower than in tumor tissue, but only significantly for U36 IgG uptake in mucosa and tongue ( $p < 0.01$  and  $p < 0.02$ , respectively). Tumor positive lymph nodes contained more iodine than tumor negative nodes: in case of E48 IgG this was 1.3  $\pm$  1.2 and 0.6  $\pm$  0.3 %ID/kg, respectively ( $p < 0.2$ , mean ratio 2.0  $\pm$  1.1), while in case of U36 IgG this was 2.0  $\pm$  1.1 and 0.7  $\pm$  0.4 %ID/kg, respectively ( $p < 0.01$ , mean ratio 3.0  $\pm$  1.2). Iodine uptake in other normal



tissues was low, except for iodine-labeled U36 IgG in glandular tissue ( $3.9 \pm 1.2$  %ID/kg). Low levels of activity were seen in bone marrow biopsies: for iodine-labeled E48 IgG and U36 IgG this was  $0.4 \pm 0.2$  and  $0.5 \pm 0.2$  %ID/kg, respectively. Bone marrow aspirations showed a mean iodine level of  $1.2 \pm 0.4$  for E48 IgG and of  $1.5 \pm 0.5$  %ID/kg for U36 IgG, while the activity levels in blood were almost similar ( $1.4 \pm 0.4$  and  $1.5 \pm 0.6$  %ID/kg, mean ratios  $0.9 \pm 0.0$  and  $1.0 \pm 0.1$ , respectively). The activity in the bone marrow aspirate was mainly located in the plasma (supernatant). The mean plasma activity in the bone marrow aspirate was slightly lower than in blood plasma: for E48 IgG this was  $1.7 \pm 0.7$  and  $2.1 \pm 0.5$  %ID/kg and for U36 IgG this was  $2.1 \pm 0.9$  and  $2.3 \pm 0.8$  %ID/kg, respectively; mean ratios were  $0.9 \pm 0.3$  and  $1.0 \pm 0.1$ , respectively.

Table 2. Uptake of simultaneously injected iodine-labeled E48 IgG and U36 IgG in biopsies obtained from the surgical specimens 7-8 days after injection in %ID/kg.

	<sup>125</sup> I/ <sup>131</sup> I-labeled E48 IgG		<sup>131</sup> I/ <sup>125</sup> I-labeled U36 IgG		n <sup>a</sup>
	mean $\pm$ SD	range	mean $\pm$ SD	range	
tumor	$8.9 \pm 8.9$	1.8 - 31.2	$8.2 \pm 4.4$	2.9 - 15.2	10
mucosa	$4.1 \pm 1.4$	2.0 - 6.8	$4.0 \pm 1.4$	1.6 - 5.8	10
tongue	$5.8 \pm 2.7$	1.8 - 8.8	$4.4 \pm 2.3$	1.3 - 7.9	5
skin	$2.5 \pm 1.0$	1.3 - 4.2	$2.5 \pm 1.0$	1.5 - 4.2	5
positive lymph node	$1.3 \pm 1.2$	0.4 - 4.6	$2.0 \pm 1.1$	0.5 - 4.6	9
negative lymph node	$0.6 \pm 0.3$	0.3 - 1.3	$0.7 \pm 0.4$	0.3 - 1.4	10
muscle	$0.4 \pm 0.2$	0.2 - 0.7	$0.4 \pm 0.2$	0.2 - 1.0	10
fat	$0.3 \pm 0.2$	0.2 - 0.7	$0.4 \pm 0.2$	0.1 - 1.0	10
submandibular gland	$1.1 \pm 0.6$	0.6 - 2.5	$3.9 \pm 1.2$	2.0 - 5.8	10
sublingual gland	0.2		1.4		1
vein	$0.7 \pm 0.3$	0.4 - 1.1	$0.8 \pm 0.3$	0.3 - 1.4	7
bone marrow biopsy	$0.4 \pm 0.2$	0.2 - 0.7	$0.5 \pm 0.2$	0.2 - 0.7	6
total bone marrow aspiration	$1.2 \pm 0.4$	0.7 - 1.7	$1.5 \pm 0.5$	0.4 - 1.8	6
supernatant bone marrow aspiration	$1.7 \pm 0.7$	0.7 - 2.9	$2.1 \pm 0.9$	0.5 - 3.0	6
sediment bone marrow aspiration	$0.8 \pm 0.9$	0.3 - 2.9	$0.5 \pm 0.2$	0.2 - 0.7	6
blood	$1.4 \pm 0.4$	0.8 - 1.9	$1.5 \pm 0.6$	0.3 - 2.7	9
plasma	$2.1 \pm 0.5$	1.3 - 2.9	$2.3 \pm 0.8$	0.6 - 3.8	9

<sup>a</sup> Number of patients from whom biopsies were obtained.

For iodine-labeled E48 IgG the mean tumor to non-tumor ratios varied between 1.8 for tongue and 34.2 for fat tissue, while for iodine-labeled U36 IgG these values varied between 2.1 for sublingual gland and 28.7 for fat tissue (Fig. 1). For mucosa, tongue, skin, submandibular gland, muscle, blood, and bone marrow aspirate these ratios were in case of E48 IgG 2.5, 1.8, 5.5, 9.8, 25.2, 4.7, and 4.0, respectively, and in case of U36 IgG 2.3, 2.3, 4.1, 2.4, 21.0, 5.8, and 5.8, respectively. Increase of MAb doses from 11 to 51 mg did not alter the activity levels in tissues and the tumor to non-tumor ratios. There were no significant differences in uptake values and tumor to non-tumor ratios between E48 IgG and U36 IgG, except for the uptake in glandular tissue ( $p < 0.001$ ).

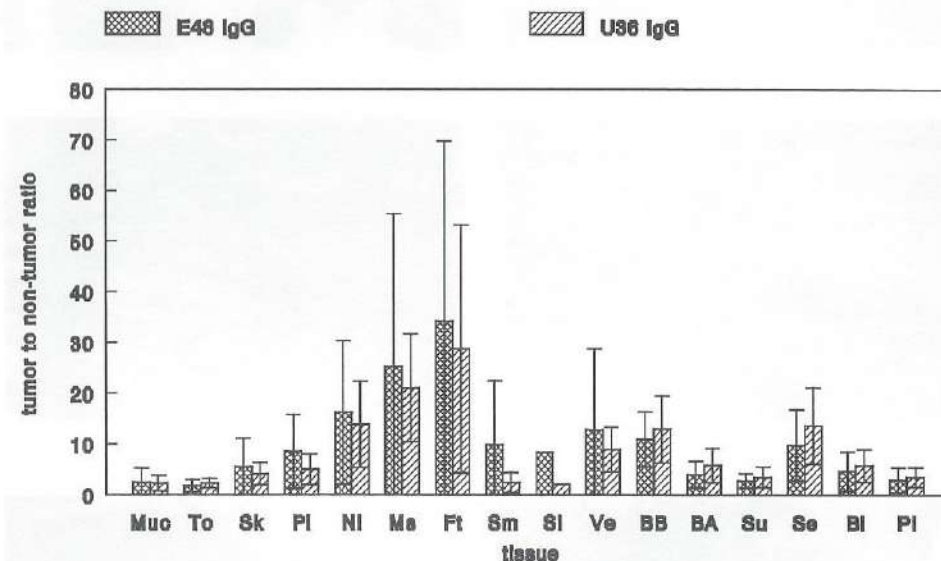


Figure 1. Tumor to non-tumor ratios of simultaneously injected iodine-labeled E48 IgG and U36 IgG in mucosa (Mc; n= 10), tongue (To; n=5), skin (Sk; n=5), positive lymph node (PL; n=9), negative lymph node (NL; n=10), muscle (Ms; n=10), fat (Ft; n=10), submandibular gland (Sm; n=10), sublingual gland (SI; n=1), vein (Ve; n=7), bone marrow biopsy (BB; n=6), total bone marrow aspiration (BA; n=6), supernatant of bone marrow aspiration (Su; n=6), sediment of bone marrow aspiration (Se; n=6), blood (Bl; n=9), and plasma (Pl; n=9).

**Pharmacokinetics.** The time versus radioactivity curves of iodine-labeled E48 IgG and U36 IgG best fit a two-compartment model. There was no significant difference in elimination from the blood for iodine-labeled E48 IgG and U36 IgG:  $t_{1/2\alpha}$  and  $t_{1/2\beta}$  were for E48 IgG  $5.1 \pm 5.3$  and  $81.3 \pm 81.6$  hr and for U36 IgG  $6.1 \pm 3.0$  and  $66.1 \pm 29.5$  hr, respectively.

There was also no significant difference in the excretion of iodine-labeled E48 IgG and U36 IgG in urine during the first 48 hr:  $23.0 \pm 6.0$  and  $21.4 \pm 5.1$  % of the injected dose, respectively.



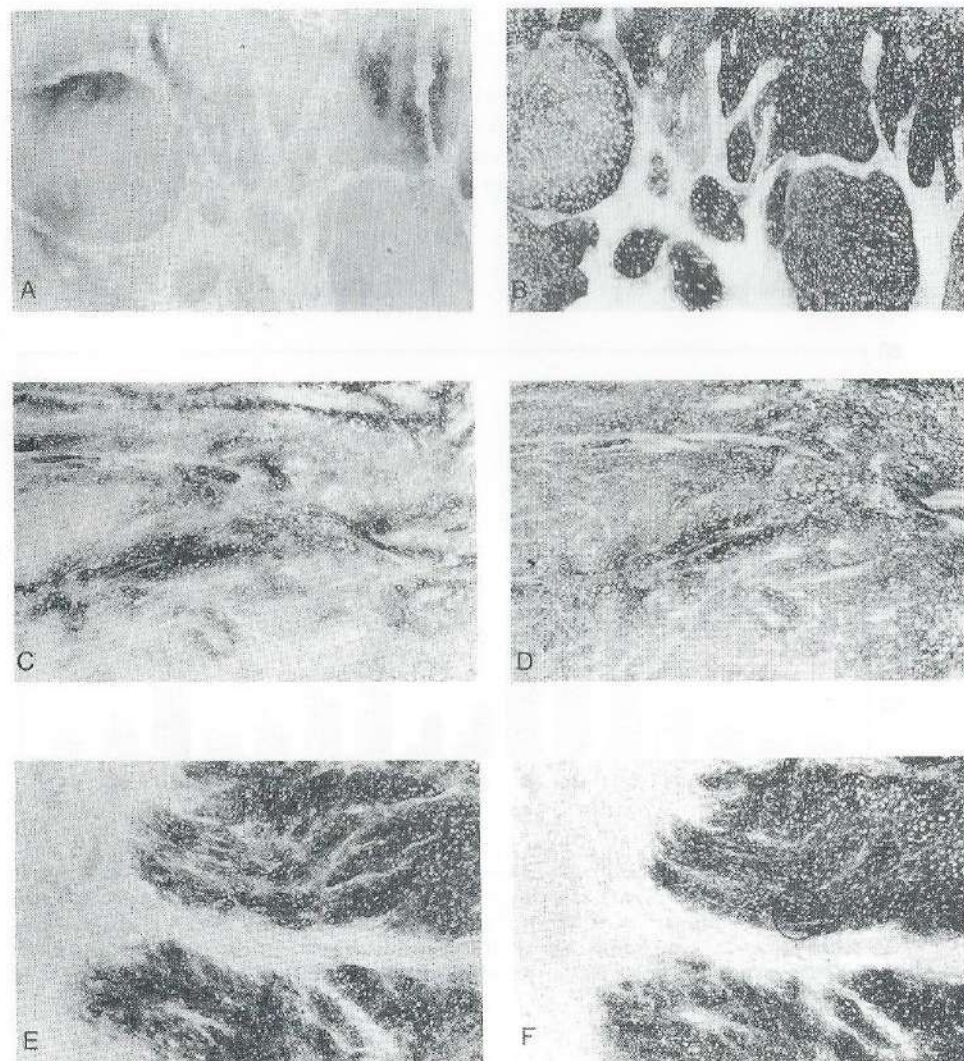


Figure 2. Distribution of E48 IgG throughout tumor biopsies obtained from HNSCC patients 2 days after injection of 2 (A,B), 12 (C,D), and 52 mg (E,F). A, C, and E represent MAb distribution as assessed by immunohistochemical staining with rabbit anti-mouse IgG. B,D, and F represent antigen expression (maximal MAb binding) as assessed by immunohistochemistry with E48 IgG followed by rabbit anti-mouse IgG. Note the more homogeneous distribution at higher dose, reaching occupation of almost all antigen-binding sites at 52 mg MAb E48.

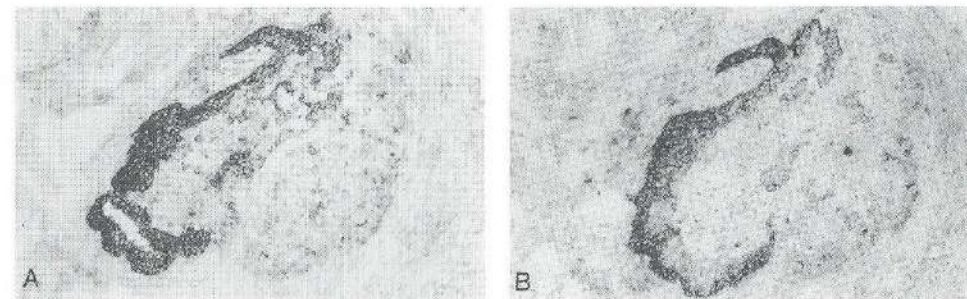


Figure 3. Distribution of U36 IgG throughout a tumor infiltrated lymph node 2 days after injection of 52 mg U36 IgG. (A) represents MAb distribution as assessed by immunohistochemical staining with rabbit anti-mouse IgG. (B) represents antigen expression (maximal MAb binding) as assessed by immunohistochemistry with U36 IgG followed by rabbit anti-mouse IgG. Note the occupation of almost all antigen-binding sites in this lymph node metastasis.

**Distribution of the MAbs E48 and U36 throughout the tumor.** Distribution of MAbs throughout the tumor was analysed immunohistochemically in tumor biopsies obtained from patients who had been injected with either E48 IgG or U36 IgG alone. Fig. 2 shows typical E48 IgG uptake in tumor biopsy specimens of three patients who received 2, 12, and 52 mg E48 IgG. Serial sections of each biopsy were incubated with rabbit anti-mouse IgG to demonstrate *in vivo* tumor uptake of E48 IgG (sections A,C,E), or with MAb E48 followed by rabbit anti-mouse IgG to demonstrate total E48 antigen expression, the maximal E48 IgG binding (sections B,D,F). After injection of 2 mg, a very heterogeneous distribution of E48 IgG was observed. After injection of 12 mg MAb the distribution was much more homogeneous, while after injection of 52 mg the majority of antigenic sites became evidently occupied by E48 IgG. A comparable distribution pattern was observed for U36 IgG as illustrated for a tumor infiltrated lymph node obtained from a patient who had received 52 mg U36 IgG (Fig. 3). E48 IgG or U36 IgG could be detected in all tumor biopsies of patients who received 12 or 52 mg MAb, also in biopsies from tumor deposits not detected by RIS.

**Immunogenicity of MAbs E48 and U36.** To assess the immunogenicity of MAb E48 and U36, serum samples obtained from patients before and 4-8 weeks after injection of E48 F(ab')<sub>2</sub> (group 1), E48 IgG (group 2), E48 F(ab')<sub>2</sub> plus E48 IgG (group 3), U36 IgG (group 4), and E48 IgG plus U36 IgG (group 5) were analysed for the presence of human anti-mouse antibodies (HAMA) with an in house E48 F(ab')<sub>2</sub>, E48 IgG and/or U36 IgG related HAMA assay. Considering a HAMA titer of  $\geq 500$  to be positive, pre-MAb infusion samples were negative (HAMA titers  $< 50$ ) for all patients (Fig. 4). Three out of 16 patients (19%) who had received 1 mg (n=14) or 11 mg (n=2) E48 F(ab')<sub>2</sub> alone showed a HAMA response as measured in the F(ab')<sub>2</sub> related HAMA assay. The highest titer found was 811. Three out of 5 patients (40%) who had received 1 mg E48 IgG alone showed an anti-E48 IgG response with titers of 1558 and 4154, respectively.



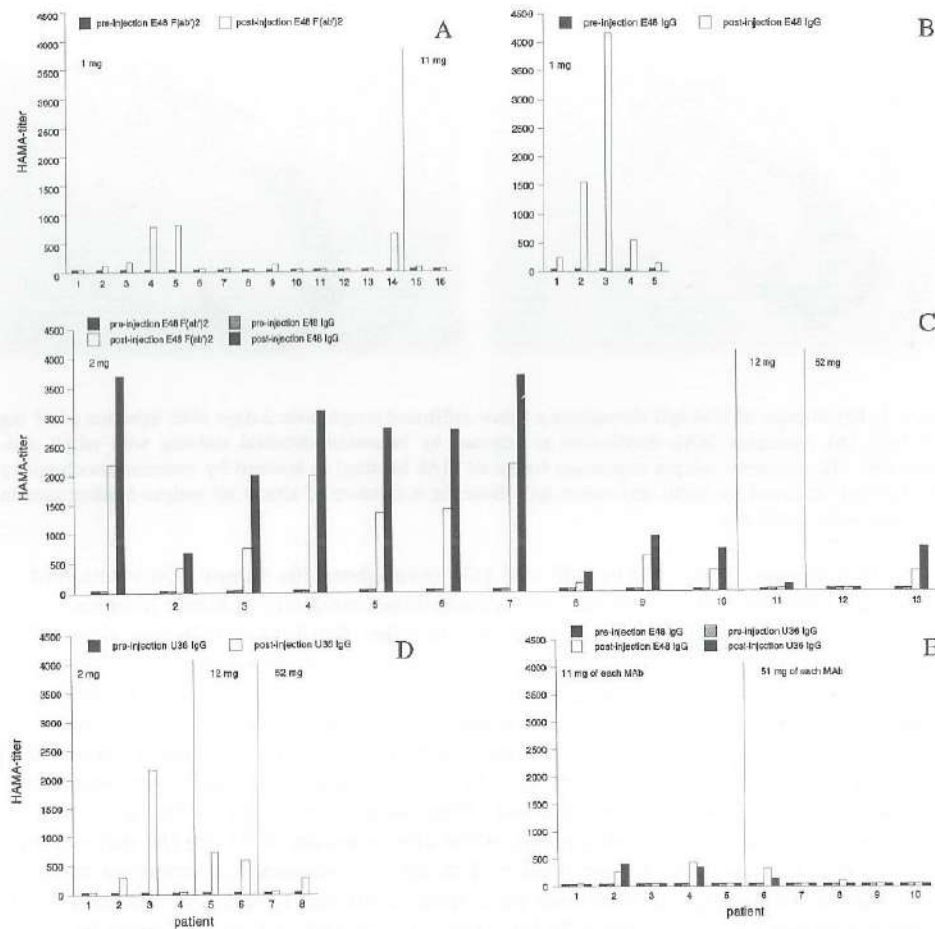


Figure 4. Individual human anti-mouse antibodies (HAMA) titers before and 4-8 weeks after injection of (A) E48 F(ab')<sub>2</sub>, (B) E48 IgG, (C) E48 F(ab')<sub>2</sub> plus E48 IgG, (D) U36 IgG, and (E) E48 IgG plus U36 IgG at different MAb doses.

Ten out of 13 patients (77%) who received a cocktail of 1 mg E48 F(ab')<sub>2</sub> and 1-51 mg E48 IgG showed a HAMA response with titers up to 3709, when measured in the E48 IgG related HAMA assay. When the same sera were analysed with the F(ab')<sub>2</sub> related HAMA assay, 7 out of 13 appeared to be positive.

HAMA responses were also observed in 3 out of 8 patients (37%) who had received 2-52 mg U36 IgG. None of the 10 patients who received 11 or 51 mg E48 IgG together with 11 or 51 mg U36 IgG showed a HAMA response when measured in the E48 IgG or U36 IgG related HAMA assay.

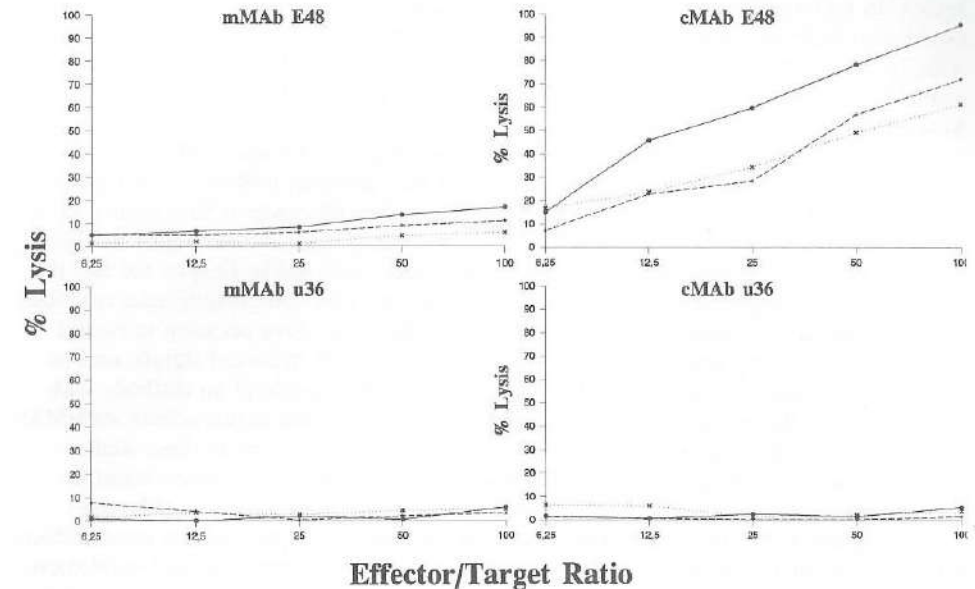


Figure 5. Specific lysis of UM-SCC-22A cells as target cells after addition of peripheral blood mononuclear cells as effector cells at different effector:target ratios and murine MAb E48 IgG or U36 IgG or chimeric MAb E48 IgG or U36 IgG.

#### ADCC-mediating potential of mMABs and cMABs E48 and U36.

ADCC assays with MABs E48 and U36 revealed that spontaneous chromium release never exceeded 20%, while antibody independent killing was less than 10%. When cMAB E48 was included in this assay at an effector:target ratio of 100:1, specific lysis percentages of 62, 72, and 96% were found, respectively (Fig. 5). For cMAB U36 these values were 1.2, 5.2, and 3.5%, for mMAB E48 6, 11, and 17%, and for mMAB U36 5.4, 3.0, and 4.7%. cMAB SF-25 served as a positive control in each ADCC assay and gave specific lysis percentages between 63 and 78% (data not shown).

#### DISCUSSION

While in previous clinical studies we demonstrated a selective and a similarly high uptake level of E48 IgG and U36 IgG in antigen positive HNSCC 2 days after injection<sup>15,16</sup>, in the present study we show that the level of both MABs in HNSCC remains high 7-8 days after injection. Distribution of the MABs throughout the tumor was heterogeneous when 2 mg of MAB had been injected. At a MAB dose of 12 mg the distribution was much more homogeneous and at 52 mg the majority of antigenic sites became occupied



by the MABs. While chimeric E48 IgG appeared to have a high ADCC-mediating potency, this was not the case for murine E48 IgG, murine U36 IgG, and chimeric U36 IgG. U36 IgG appeared to be less immunogenic than E48 IgG. Since it has been established from previous studies that MAb E48 shows a homogeneous reactivity pattern with 70 % of the HNSCC and MAb U36 with 96% of these tumors<sup>12</sup>, all data are now available for a rational design of adjuvant therapy trials with unconjugated or conjugated MABs in head and neck cancer patients.

Recently, a wave of optimism has been engendered in the use of MABs for adjuvant therapy of solid tumors. In a randomised trial in which mMAb 17-1A (IgG<sub>2a</sub>) was used in adjuvant therapy of resected Dukes' C colorectal cancer a 30% reduction of the 5 year death rate was observed<sup>7</sup>. In this study patients received 500 mg of the MAb 2 weeks after surgery followed by four 100 mg infusions each month. Despite the fact that 80% of the treated patients developed HAMA responses, only four anaphylactic reactions were encountered. Forementioned study by Riethmüller et al. gave occasion to Nossal<sup>22</sup> to write the following phrase in a commentary: "The real and historical significance of Riethmüller's study lies in the fact that it records the first example of an antibody with proven life-saving benefit in a common solid-organ cancer". Anti-tumor effects with MAB 17-1A had been observed previously in tumor bearing nude mice and in these studies evidence was found for an effector cell dependent mechanism<sup>23</sup>. Also when tested in vitro murine MAB 17-1A appeared to be effective in mediating ADCC<sup>24</sup>. Although ADCC appears to be the most probable reaction mechanism causing the anti-tumor effects exerted by MAB 17-1A in vivo, other mechanisms like complement mediated cytotoxicity, idiotype-anti-idiotype cascade, or T cells reacting to murine immunoglobulins can not be excluded.

In line with these promising data on unconjugated MAB 17-1A one could decide to start adjuvant therapy trials with unconjugated cMAb E48 in head and neck cancer patients. In contrast to cMAb U36, cMAb E48 is highly capable of mediating ADCC. However, more detailed analysis of Riethmüller's data elicits some limitations in the use of unconjugated MABs. Treatment with 17-1A caused prevention or delay of distant metastases but had no effect on local relapses<sup>7</sup>. The ineffectiveness of MAB 17-1A to eradicate local and regional recurrences may be explained by the larger volume of such metastatic tumor deposits. Since effector cells for ADCC are mainly located on the borders of tumor loci<sup>25,26</sup>, tumor cells located in central layers of tumor nodules will not be affected. Another explanation might be related to deficiencies in cellular immune functions in cancer patients. For HNSCC patients immunosuppression has frequently been described<sup>27</sup>. In these patients the degree of immunodeficiency is variable, and immune function depression has been demonstrated to be hierarchical, more at the local level than at the regional level, and lowest at the systemic level<sup>28</sup>.

Compared to therapy with unconjugated MABs, radioimmunotherapy may be a better option. As stated before, this may be particularly true because of the radiosensitivity of HNSCC<sup>9</sup>. For this approach, we developed analogous <sup>99m</sup>Tc- and <sup>186</sup>Re-labeling chemistry for MABs directed to HNSCC, with the clinical option in mind to use <sup>99m</sup>Tc and <sup>186</sup>Re as a "matched pair" for imaging, dosimetry calculations, and therapy<sup>29</sup>. <sup>186</sup>Re-MAB conjugates produced according to this method showed exactly the same pharmacokinetic behaviour in vivo as <sup>99m</sup>Tc-MAB conjugates<sup>30</sup>.

A prerequisite for successful RIT is that MABs are able to deliver enough radioactivity to each tumor deposit. In this and previous papers we have shown

biodistribution data indicating that E48 IgG and U36 IgG are equally well suited for targeting antigen positive tumor deposits. Because of its more homogeneous reactivity pattern on sections of HNSCC, however, we think that MAB U36 is better qualified for RIT than MAB E48. For <sup>99m</sup>Tc-labeled MAB U36 we found a mean tumor uptake of 20.4 %ID/kg 2 days after injection<sup>15</sup>, while 7 days after injection the mean activity level of iodine labeled MAB U36 in the tumor was still 8.2 %ID/kg. However, due to dehalogenation of the immunoconjugate this latter value may be an underestimation of the real retention of the MAB in the tumor. Also the tumor to non-tumor ratios may not be fully reliable due to the different rates of dehalogenation in normal and malignant tissues. In a previous study we found 2 days after injection 10% lower uptake levels in the tumor for <sup>131</sup>I-labeled E48 IgG than for co-administered <sup>99m</sup>Tc-labeled E48 IgG, while uptake levels of these conjugates were the same in normal tissues<sup>16</sup>. Nevertheless, when using forementioned biodistribution values of U36 IgG an approximate dosimetry calculation can be made for tumors with a diameter of at least one centimetre. Assuming that patients tolerate a dose of 200 mCi <sup>186</sup>Re, as was the case in a first phase I clinical trial with <sup>186</sup>Re-labeled NR-LU-10 IgG described by Breitz et al.<sup>31</sup>, and assuming an energy per transition of 0.73 g.cGy/( $\mu$ Ci.h) for <sup>186</sup>Re<sup>32</sup>, one may expect an absorbed tumor dose of approximately 20 Gy. To estimate whether this will be sufficient for obtaining cures in adjuvant therapy trials with HNSCC patients, we recently performed RIT studies with <sup>186</sup>Re-labeled E48 IgG in nude mice bearing HNSCC of variable size. A single treatment of mice bearing xenografts with a mean volume of 140 mm<sup>3</sup> with 200-600  $\mu$ Ci <sup>186</sup>Re-labeled E48 IgG resulted in 18-50% complete remissions while the absorbed tumor dose was 11-34 Gy<sup>33</sup>. However, when mice with xenografts of 75 mm<sup>3</sup> were treated with 600  $\mu$ Ci <sup>186</sup>Re-labeled E48 IgG, 100% complete remissions were observed<sup>34</sup>. In these latter tumors the mean absorbed dose was 85 Gy. These studies indicate that the decreased energy absorption in smaller tumors is compensated by the higher tumor uptake of MABs. Also recent results from clinical RIT studies using intraperitoneally administered <sup>186</sup>Re-labeled NR-LU-10 IgG in adjuvant therapy of ovarian cancer patients showed that RIT may be particularly effective in eradicating minimal residual disease<sup>35</sup>. While none of the tumors with a diameter > 1 cm responded, 4 out of 7 tumors with a diameter < 1 cm showed size reduction. Unfortunately, in this study no tumor uptake levels were assessed for NR-LU-10 IgG. The preferential effectiveness of radiolabeled NR-LU-10 IgG in the treatment of small tumors can be explained by the observations of Chatal et al. who demonstrated in a similar group of patients a higher accumulation of MABs in smaller tumor loads<sup>36</sup>. Assessment of the biodistribution of <sup>111</sup>In-labeled MAB OC125 intraperitoneally injected into patients with ovarian carcinoma revealed low accumulation in large tumors (1.4 - 3.2 %ID/kg) but significant higher accumulation in small tumor nodules (130  $\pm$  18 %ID/kg) and malignant cell clusters (median 330 with a maximum of 4160 %ID/kg).

These dosimetrical estimations indicate the feasibility of adjuvant RIT with radiolabeled U36 IgG in head and neck cancer patients. However these considerations assume a uniform distribution of radioactivity throughout the tumor. Heterogeneous distribution of a radioimmunoconjugate throughout the tumor is unwanted in RIT because this can result in overkill in certain tumor areas while leaving other areas relatively unaffected. In the present study we show that the distribution of MAB U36 becomes more homogeneous when a higher MAB dose is administered, a phenomenon also observed in other preclinical and clinical studies<sup>37,38</sup>. With respect to this, a MAB U36 dose of about



50 mg is recommended for future RIT studies because this dose resulted in homogeneous distribution throughout the tumor with occupation of the majority of antigenic sites. A much higher MAb dose will result in saturation of antigenic sites, while other disadvantages are related to costs and possibly to the immunogenicity of the MAb.

Although uptake of U36 IgG was the highest in tumor tissue, 2 as well as 7 days after injection, there was also high uptake in normal squamous epithelia like oral mucosa, tongue, and skin which can be explained by the presence of U36 antigen in these tissues. However, it can be calculated from the biodistribution data that the absorbed dose for large tumors will on average be two times more than for normal squamous epithelia. In adjuvant therapy this difference may be larger due to the higher MAb uptake in small tumors than in large tumors. In that case anti-tumor effects can be expected with less toxic side effects caused by concomitant irradiation of normal squamous epithelium. At the point of uptake at non-tumor sites, the use of E48 IgG does not provide advantages in comparison to U36 IgG.

In our view, it may be beneficial when a MAb used for RIT also harbors ADCC mediating potential. It can be anticipated that ADCC activity may be supportive to irradiation, especially in eradicating single disseminated cells or cell aggregates. We showed that E48 IgG became highly effective in mediating ADCC upon replacement of the murine  $\gamma 1$  constant region for the human  $\gamma 1$  region. Also upon coupling of 8 MAG3 chelate groups, which in our method is necessary for labeling of MAbs with  $^{186}\text{Re}$ , the ADCC-mediating capacity of cMAb E48 did not become impaired (data not shown). Unfortunately, until now we were not able to demonstrate any ADCC-mediating capacity of cMAb U36. Cloning strategies and expression vectors used for the construction of cMAb U36 and cMAb E48 were the same. In contrast, host cells used for transfection were different for both cMAbs, while the ADCC assay initially developed for evaluating cMAb E48 had to be adapted for testing cMAb U36 due to the sensitivity of the U36 antigen for trypsin treatment. It is unlikely, however, that these factors are responsible for the ineffectiveness of cMAb U36 in ADCC assays. A more likely explanation is that the epitope recognized by MAb U36 is not a favorable target epitope for ADCC. Mediation of ADCC via the MAb Fc regions is dependent on the distance between Fc tails, and this distance may be related to the epitopes recognized. To test whether the ineffectiveness of cMAb U36 is related to the topological orientation of the U36 epitope we will generate stable transfectants expressing length variants of the U36 antigen and use them as target cells in ADCC assays with cMAb U36.

In the present study U36 IgG appeared to be less immunogenic than E48 IgG. Until now just 3 out of 18 patients receiving 1-52 mg U36 IgG showed a HAMA response when measured in the U36 IgG related HAMA assay, and this frequency may become even lower when cMAb U36 is used in RIT studies. However, data on HAMA responses presented in this paper have to be interpreted with caution. Firstly, patients received different MAb doses and the MAb dose may influence the incidence of HAMA responses. Seybold et al.<sup>39</sup> evaluated a long-term HAMA-follow up after radioimmunoscintigraphy using anti-granulocyte and anti-tumor MAbs in 230 patients. After a first injection of 0.15-1 mg the HAMA incidence was typically about 9%. The incidence increased when more MAb protein was applied, especially after repeated injections. Secondly, a part of the patients included in our studies may have been immunosuppressed, thus influencing the HAMA incidence. Thirdly, a part of the patients received more than one MAb-conjugate and it is unknown whether co-administration of MAbs affects the

HAMA responses to the individual MAbs. With respect to this, our data show a remarkable phenomenon which can not be explained at this moment. While E48 IgG, injected either alone or in combination with E48 F(ab')<sub>2</sub>, showed high HAMA incidences of 60 and 77%, respectively, no HAMA responses were found when E48 IgG had been administered in combination with U36 IgG. In this latter study neither anti-U36 IgG responses were observed. More studies are needed to demonstrate that reduction of HAMA incidences is a general phenomenon when cocktails of MAbs are used.

In general, immunogenicity of a MAb is considered to be a problem especially when the MAb is administered repeatedly. Although uncommon, adverse reactions like anaphylactic reactions can occur<sup>7</sup>. Furthermore, rapid clearance of infused MAb will occur upon subsequent administrations resulting in a diminished targeting efficiency of the MAb to the tumor<sup>9</sup>. When a MAb is used for single course therapy in a cancer patient not previously treated with MAb, forementioned unwanted phenomena will not occur, and in this case immunogenicity may even be beneficial. The anti-idiotypic network may be activated resulting in internal image antibodies resembling the nominal antigen. This development of anti-anti-idiotypic MAbs may contribute to improved survival<sup>40</sup>. An anti-idiotypic response can of course still occur when using cMAbs<sup>9</sup>.

Based on forementioned considerations, especially the more homogeneous reactivity pattern on HNSCC, we will give priority to an adjuvant RIT study with  $^{186}\text{Re}$ -labeled cMAb U36 IgG in head and neck cancer patients. Patients will receive a single injection with this radioimmunoconjugate at a protein dose of 50 mg. In this study, a group of patients treated for locoregional stage III and IV disease according to standard therapy (surgery and/or radiotherapy), but at high risk for developing locoregional recurrences and distant metastases, will be randomized for none adjuvant therapy or for adjuvant therapy with  $^{186}\text{Re}$ -labeled cMAb U36. Since most of the patients show locoregional or distant relapse within 2 years, the first indications on the effectiveness of RIT can be expected in a short period of time. Before starting adjuvant therapy trials, a phase I trial has first to demonstrate that  $^{186}\text{Re}$ -labeled cMAb U36 is well tolerated by patients with advanced disease.

## ACKNOWLEDGMENTS

The authors thank Ing. Corlinda B.M. ten Brink for immunohistochemistry, Dr. Abraham J. Wilhelm for pharmacokinetic determinations, Henri Greuter for biopsy measurements, Harry Twaalfhoven for HAMA determinations, Ronald Schoots and Dr. Frank B. van Gog for ADCC testing, and Dr. Arthur van Lingen for dosimetric calculations.

This work was supported by the Dutch Ministry of Economic Affairs and by Centocor Europe, Inc., Leiden, The Netherlands.



## REFERENCES

- Boring CC, Squires TS, Tong T, Montgomery S. Cancer statistics 1994. *CA Cancer J Clin* 1994;44:7-26.
- Vernham GA, Crowther JA. Head and neck carcinoma - stage at presentation. *Clin Otolaryngol* 1994;19:120-4.
- Stupp R, Weichselbaum RR, Vokes EE. Combined modality therapy of head and neck cancer. *Semin Oncol* 1994;21:349-58.
- Stell PM, Rawson NSB. Adjuvant chemotherapy in head and neck cancer. *Br J Cancer* 1990;61:779-87.
- Goldenberg DM. Future role of radiolabeled monoclonal antibodies in oncological diagnosis and therapy. *Semin Nucl Med* 1989;19:332-9.
- Wessels BW, Harisiadis L, Carabell SC. Dosimetry and radiobiological efficacy of clinical radioimmunotherapy. *J Nucl Med* 1989;30:827.
- Riethmüller G, Schneider-Gädick E, Schlimok G, Schmiegler W, Höffken K, Gruber R, Pichlmaier H, Hirche H, Pichlmayr R, Buggisch P, Witte J, the German Cancer Aid 17-1A Study Group. Randomised trial of monoclonal antibody for adjuvant therapy of resected Dukes'C colorectal carcinoma. *Lancet* 1994;343:1177-83.
- Steplewski Z, Sun LK, Shearman CW, Ghayeb J, Daddona P, Koprowski H. Biological activity of human-mouse IgG1, IgG2, IgG3, and IgG4 chimeric monoclonal antibodies with antitumor specificity. *Proc Natl Acad Sci USA* 1988;85:4852-6.
- Khazaeli MB, Conry R, LoBuglio AF. Human immune response to monoclonal antibodies. *J Immunother* 1994;15:42-52.
- Quak JJ, Dongen GAMS van, Balm AJM, Brakkee JPG, Scheper RJ, Snow GB, Meijer CJLM. A 22-kd surface antigen detected by monoclonal antibody E48 is exclusively expressed in stratified squamous and transitional epithelia. *Am J Pathol* 1990;136:191-7.
- Schrijvers AHGJ, Quak JJ, Uytendinck AM, Walsum M van, Meijer CJLM, Snow GB, Dongen GAMS van. MAb U36, a novel monoclonal antibody successful in immunotargeting of squamous cell carcinoma of the head and neck. *Cancer Res* 1993;53:4383-90.
- Bree R de, Roos JC, Quak JJ, Hollander W den, Snow GB, Dongen GAMS van. Clinical screening of monoclonal antibodies 323/A3, cSF-25, and K928 for suitability of targeting tumors in the upper-aerodigestive and respiratory tract. *Nucl Med Commun* 1994;15:613-27.
- Dongen GAMS van, Leverstein H, Roos JC, Quak JJ, Brekel MWM van den, Lingen A van, Martens HJM, Castelijns JA, Visser GWM, Meijer CJLM, Teule GJJ, Snow, GB. Radioimmunoscinigraphy of head and neck cancer using <sup>99m</sup>Tc-labeled monoclonal antibody E48 F(ab')<sub>2</sub>. *Cancer Res* 1992;52:2569-74.
- Bree R de, Roos JC, Quak JJ, Hollander W den, Brekel MWM van den, Wal JE van der, Tobi H, Snow GB, Dongen GAMS van. Clinical imaging of head and neck cancer with technetium-99m-labeled monoclonal antibody E48 IgG or F(ab')<sub>2</sub>. *J Nucl Med* 1994;35:775-83.
- Bree R, Roos JC, Quak JJ, Hollander W den, Snow GB, Dongen GAMS van. Radioimmunoscinigraphy and biodistribution of monoclonal antibody U36 in patients with head and neck cancer. *Clin Cancer Res* 1995;1:June.
- Bree R de, Roos JC, Quak JJ, Hollander W den, Wilhelm AJ, Lingen A van, Snow GB, Dongen GAMS van. Biodistribution of radiolabeled monoclonal antibody E48 IgG and F(ab')<sub>2</sub> in patients with head and neck cancer. *Clin Cancer Res* 1995;1:277-286.
- Brakenhoff RH, Gog FB van, Looney JE, Walsum M van, Snow GB, Dongen GAMS van. Construction and characterization of the chimeric monoclonal antibody E48 for therapy of head and neck cancer. *Cancer Immunol Immunother* 1995, in press.
- Hermanek P, Sobin, LH, eds. TNM classification of malignant tumors, 4th edition. Berlin: Springer Verlag;1987:13-26.
- Brakenhoff RH, Gerretsen M, Knippels PMC, Dijk M van, Essen H van, Olde-Weghuis D, Sinke R, Snow GB, Dongen GAMS van. The human E48 antigen, highly homologous to the murine Ly-6 antigen ThB, is a GPI-anchored molecule apparently involved in keratinocyte cell-cell adhesion. *J Cell Biol* 1995, in press.
- Haisma HJ, Hilgers J, Zurawski VR. Iodination of monoclonal antibodies for diagnosis and therapy using a convenient one vial method. *J Nucl Med* 1986;27:1890-5.
- Gerretsen M, Quak JJ, Suh JS, Walsum M van, Meijer CJLM, Snow GB, Dongen GAMS van. Superior localisation and imaging of radiolabelled monoclonal antibody E48 F(ab')<sub>2</sub> fragment in xenografts of human squamous cell carcinoma of the head and neck and of the vulva as compared to monoclonal antibody E48 IgG. *Br J Cancer* 1991;63:37-44.
- Nossal GJV. Minimal residual disease as the target for immunotherapy of cancer. *Lancet* 1994;343:1171-4.
- Herlyn D, Koprowski H. IgG2a monoclonal antibodies inhibit human tumour growth through interaction with effector cells. *Proc Natl Acad Sci USA* 1982;79:4761-5.
- Velders MP, Litvinov SV, Warnaar SO, Gorter A, Fleuren GJ, Zurawski VR, Coney LR. New chimeric anti-pancarcinoma monoclonal antibody with superior cytotoxicity-mediating potency. *Cancer Res* 1994;54:1753-9.
- Ravenswaay-Claassen HH van, Kluin PM, Fleuren GJ. On the possible role of CD16+ macrophages in antitumor cytotoxicity. *Lab Invest* 1992;67:166-74.
- Shetty J, Frödin JE, Christensson B, Grant C, Jacobsson B, Sundelius S, Sylven M, Mellstedt H. Immunohistochemical monitoring of metastatic colorectal carcinoma in patients treated with monoclonal antibodies (MAb 17-1A). *Cancer Immunol Immunother* 1988;27:154-62.
- Wanebo HJ, Blackinton D, Kouttab Mehta S. Contribution of serum inhibitory factors and immune cellular defects to the suppressed cell-mediated immunity in patients with head and neck cancer. *Am J Surg* 1993;166:389-96.
- Wang MB, Lichtenstein A, Mickel RA. Hierarchical immunosuppression of regional lymph nodes in patients with head and neck squamous cell carcinoma. *Arch Otolaryngol/Head Neck Surg* 1991;105:517-27.
- Visser GWM, Gerretsen M, Herscheid JDM, Snow GB, Van Dongen GAMS van. Labeling of monoclonal antibodies with <sup>186</sup>Re using the MAG3 chelate for radioimmunotherapy of cancer: a technical protocol. *J Nucl Med* 1993;34:1953-63.
- Gog F van, Visser GWM, Klok R, Schors R van der, Snow GB, Dongen GAMS van. Monoclonal antibodies labeled with rhenium-186 using the MAG3 chelate for clinical application: relationship between the number of chelated groups and biodistribution characteristics. *J Nucl Med* 1995, submitted.
- Breitz HB, Weiden PL, Vanderheyden J-L, Appelbaum JW, Bjorn MJ, Fer MF, Wolf SB, Ratliff BA, Seiler CA, Poesie DC, Fisher DR, Schroff RW, Fritzberg AR, Abrams PG. Clinical experience with rhenium-186-labeled monoclonal antibodies for radioimmunotherapy: Results of phase I trials. *J Nucl Med* 1992;33:1099-112.
- Weber DA, Eckerman KF, Dillman LT, Ryman JC, eds. MIRD: radionuclide data and decay schemes. The Society of Nuclear Medicine Inc. 1989.
- Gerretsen M, Visser GWM, Walsum M van, Meijer CJLM, Snow GB, Dongen GAMS van. <sup>186</sup>Re-labeled monoclonal antibody E48 immunoglobulin G-mediated therapy of human head and neck squamous cell carcinoma xenografts. *Cancer Res* 1993;53:3524-9.
- Gerretsen M, Visser GWM, Brakenhoff RH, Walsum M van, Snow GB, Dongen GAMS van. Complete ablation of small squamous cell carcinoma xenografts with <sup>186</sup>Re-labeled monoclonal antibody E48. *Cell Biophys* 1994;24:135-42.
- Jacobs AL, Fer M, Su FM, Breitz H, Thompson J, Goodgold H, Cain J, Heaps J, Weiden P. A phase-I trial of a rhenium 186-labeled monoclonal antibody administered intraperitoneally in ovarian carcinoma: Toxicity and clinical response. *Obstet Gynecol* 1993;82:586-93.
- Chatal J-F, Saccavini J-C, Gustin J-F, Thédrez P, Curter C, Kremer M, Guerreau D, Nolibé D, Fumoleau P, Guillard Y. Biodistribution of indium-111-labeled OC 125 monoclonal antibody intraperitoneally injected into patients operated on for ovarian carcinomas. *Cancer Res* 1989;49:3087-94.
- Blumenthal RD, Fand I, Sharkey RM, Boerman OC, Kashi R, Goldenberg D. The effect of antibody protein dose on the uniformity of tumor distribution of radioantibodies: an autoradiographic study. *Cancer Immunol Immunother* 1991;33:351-8.
- Oosterwijk E, Bander NH, Divgi CR, Welt S, Wakka JC, Finn RD, Carswell EA, Larson SM,



- Warnaar SO, Fleuren GJ, Oettgen HF, Old LJ. Antibody localization in human renal cell carcinoma: a phase I study of monoclonal antibody G250. *J Clin Oncol* 1993;11:738-50.
39. Seybold K, Trinkler M, Frey LD, Lochner JT. Long-term HAMA follow-up after immunoscintigraphy using anti-granulocyte and anti-tumour MAb: Advanced experiences in 210 patients. Proceedings of the 9th annual meeting of the International research Group on Immunoscintigraphy and Immunotherapy p28.
40. Fagenberg J, Frödin J-E, Wigzell H, Mellstedt H. Induction of an immune cascade in cancer patients treated with monoclonal antibodies (ab1). I. May induction of ab1-reactive T cells and anti-anti-idiotypic antibodies (ab3) lead to tumor regression after mAb therapy? *Cancer Immunol Immunother* 1993;37:264-70.

## Chapter 7

## Summary



In this thesis five monoclonal antibodies (MAbs), E48, 323/A3, SF-25, K928, and U36 were evaluated for clinical targeting of squamous cell carcinoma in the head and neck (HNSCC). In **chapter 1** it is concluded that pre-treatment assessment of the status of the lymph nodes in the neck is essential for optimal treatment planning. Despite an increase in the locoregional control of HNSCC, due to improved surgery and radiotherapy, current therapy regimens have failed as yet to increase the 5-year survival rate in HNSCC patients. Whereas fewer patients tend to die from uncontrolled locoregional disease, more patients are exposed to the risk of developing distant metastases. Therefore, an effective systemic adjuvant therapy is needed. To date there is no evidence that adjuvant chemotherapy has any survival benefit.

In **chapter 2** it is shown that for the detection of lymph node metastases radioimmunoscintigraphy (RIS) with  $^{99m}\text{Tc}$ -labeled MAb E48 is as reliable as conventional imaging techniques like CT and MRI. The intact MAb E48 IgG and its  $\text{F(ab')}_2$  fragment are equally well suited for RIS. However, from this study it was concluded that RIS will not sufficiently contribute to a more reliable staging of the neck. A limitation of RIS is that anatomical structures are lacking which hampers the assessment of the exact localization and extension of tumor deposits. Whereas micrometastases were missed by CT and MRI, small tumor deposits were neither detected by RIS. Other disadvantages are the complexity and high costs of RIS. For these reasons we believe that there is no justification for the routine application of RIS in head and neck cancer patients. This RIS study, however, showed selective tumor uptake of MAb E48 in primary tumors and lymph node metastases. Knowing that HNSCC are intrinsically radiosensitive, these data justified further development of radioimmunoconjugates for radioimmunotherapy (RIT). A point of concern with respect to the application of MAb E48 in RIT was the high uptake of activity in the adrenals and the mouth. A suitable MAb for RIT should accumulate selectively and to a high level in tumor deposits.

In **chapter 3** the uptake of E48 IgG and  $\text{F(ab')}_2$  in tumor and normal tissues is described. Biodistribution was assessed by biopsies from the surgical specimen 2 days after injection and by regions of interest on planar radioimmunoscintigrams until 21 hrs after injection. The mean uptake of  $^{99m}\text{Tc}$ -labeled E48 IgG in tumor tissue appeared to be  $30.6 \pm 20.1\%$  of the injected dose/kg, which is 5 times higher than found for most other MAbs in other solid tumor types. In this study it appeared that the uptake of activity in the adrenals and the mouth was diminished by increasing the MAb dose. No advantage was found for the use of E48  $\text{F(ab')}_2$  in comparison to E48 IgG. Although tumor to non-tumor ratios were generally higher for E48  $\text{F(ab')}_2$  than for E48 IgG, the opposite was true for the oral mucosa including the tongue, sites with relatively high activity uptake. Moreover, the uptake of  $^{131}\text{I}$ -labeled E48 IgG in the tumor was higher than of  $^{125}\text{I}$ -labeled E48  $\text{F(ab')}_2$  after simultaneous injection. Also other considerations might indicate the advantage of whole IgG. The use of IgG in RIT may provide an additional advantage because of its ability to mediate antibody dependent cellular cytotoxicity (ADCC). Moreover, in general, an intact MAb retains longer in tumor tissue than its fragments. Therefore, E48 IgG seems to be more suitable for RIT as compared to E48  $\text{F(ab')}_2$ . A limitation in the use of MAb E48 for RIT in general is the relatively heterogeneous E48 antigen expression in about 30% of HNSCCs.

For that reason also three other MAbs, designated 323/A3, SF-25, and K928, were evaluated for their capacity to target HNSCC. In comparison to MAb E48, these pan-carcinoma MAbs have the advantage that they not only show reactivity with HNSCC

but also with other tumor types such as non-small cell and small cell carcinoma of the lung, as demonstrated in **chapter 4**. These MAbs were screened in a clinical RIS study for the detection of head and neck cancer in the same way as we did for MAb E48. MAbs 323/A3 and K928 were shown to be capable for the detection of head and neck cancer, whereas SF-25 was not capable due to the rapid and extensive uptake at non-tumor sites such as liver, spleen, brain, and skeleton, probably bone marrow. There was also uptake of MAb 323/A3 in the thyroid gland, liver, and skeleton, probably bone marrow, and uptake of MAb K928 in liver, spleen, and skeleton, probably bone marrow. Radioactivity at non-tumor sites could be mainly explained by the presence of good accessible antigenic sites and will definitively limit the application of these pan-carcinoma MAbs for therapeutic purposes.

From forementioned studies it became clear that a squamous cell specific MAb like MAb E48 is better suited for targeting HNSCC than pan-carcinoma MAbs. A drawback of MAb E48 is its limited reactivity with a proportion of HNSCCs. For that reason in **chapter 5** a second HNSCC specific MAb designated U36 was evaluated in a clinical RIS study. A clear advantage of MAb U36 in comparison to MAb E48 is its more homogeneous reactivity with HNSCCs. Comparable to MAb E48, MAb U36 accumulates selectively and to a high level in HNSCC. Only slight accumulation was observed in the mouth.

To compare the selective HNSCC targeting of E48 IgG and U36 IgG, in **chapter 6** both MAbs labeled with  $^{125}\text{I}$  or  $^{131}\text{I}$  were injected simultaneously. To obtain data on tumor retention of these MAbs for dosimetric estimations patients were operated 7-8 days after injection. Biopsies from the surgical specimen showed a similarly high uptake of both MAbs in tumor tissue. Also tumor to non-tumor ratios were comparable. In this chapter it was also shown by immunohistochemistry that the distribution of these MAbs throughout tumors is heterogeneous when administered at doses of 1 to 12 mg, and homogeneous when administered at a dose of 52 mg, resulting in occupation of the majority of antigenic sites. Analysis of human anti-mouse antibody (HAMA) responses showed that murine MAb E48 IgG is more immunogenic than murine MAb U36 IgG. Chimeric (mouse-human) MAb E48 was shown to be highly effective in mediating ADCC in vitro, while chimeric MAb U36 and murine MAb E48 and U36 were not effective at all.

In previous animal studies in our laboratory complete remissions were obtained in HNSCC xenograft bearing nude mice by RIT with  $^{186}\text{Re}$ -labeled E48 IgG. When combining the biodistribution data as reported in chapter 3, 5, and 6 with data obtained from these animal studies, we can anticipate that sufficient high radiation dose can be achieved in patients to eliminate minimal residual disease by RIT with  $^{186}\text{Re}$ -labeled E48 IgG or U36 IgG.

As outlined in the discussion of chapter 6 priority will be given to an adjuvant RIT study with  $^{186}\text{Re}$ -labeled chimeric MAb U36 IgG in HNSCC patients at high risk for developing locoregional recurrences and distant metastases after standard locoregional treatment.



## Chapter 8

### Samenvatting



In dit proefschrift "klinische 'targeting' van hoofd/hals-kanker met radioactief-gelabelde monoclonale antilichamen" werd van vijf monoclonale antilichamen (MAbs), E48, 323/A3, SF-25, K928 en U36, de geschiktheid voor detectie en behandeling van plaveiselcelcarcinomen in het hoofd/hals-gebied (HHPCCs) geëvalueerd. In **hoofdstuk 1** werd geconcludeerd dat het pre-operatieve onderzoek naar de aanwezigheid van tumorweefsel in de lymfeklieren in de hals essentieel is voor de planning van de optimale behandeling. Hoewel door recente ontwikkelingen in de chirurgie en de radiotherapie de locoregionale controle van HHPCC vergroot is, hebben de huidige therapeutische behandelwijzen geen verbetering in de 5-jaars overleving gebracht. Terwijl minder patiënten overlijden aan ongecontroleerde locoregionale ziekte, worden meer patiënten blootgesteld aan het risico om metastasen op afstand te ontwikkelen. Daarom is er behoefte aan een effectieve systemische adjuvante therapie. Momenteel zijn er geen aanwijzingen dat adjuvante chemotherapie enig effect heeft op de overleving.

In **hoofdstuk 2** werd aangetoond dat voor de detectie van lymfekliermetastasen radioimmunosintigrafie (RIS) met  $^{99m}\text{Tc}$ -gelabeld MAb E48 even betrouwbaar is als conventionele diagnostische technieken zoals CT en MRI. Het intacte MAb E48 IgG en zijn  $\text{F(ab')}_2$ -fragment bleken even geschikt te zijn voor RIS. Uit deze studie werd echter geconcludeerd dat RIS niet wezenlijk bijdraagt aan een betrouwbaardere staging van de hals. Een beperking van RIS is de afwezigheid van anatomische structuren, wat de bepaling van de exacte localisatie en uitgebreidheid van de tumoren niet goed mogelijk maakt. Kleine hoeveelheden tumorweefsel, zoals micrometastasen, konden niet opgespoord worden met RIS, een probleem dat zich ook voordoet met CT en MRI. Andere nadelen van RIS zijn de complexiteit en de hoge kosten. Vanwege deze redenen denken wij dat er geen plaats is voor de routinematige toepassing van RIS bij patiënten met hoofd/hals-kanker. Deze RIS-studie toonde echter wel dat MAb E48 selectief ophoopt in primaire tumoren en lymfekliermetastasen. Wetende dat HHPCC intrinsiek gevoelig is voor radiotherapie, rechtvaardigen deze gegevens de verdere ontwikkeling van radioimmunoconjugaten voor radioimmunotherapie (RIT). Een punt van aandacht met betrekking tot de toepassing van MAb E48 in RIT was de relatief hoge opname van activiteit in de bijnieren en de mond.

Een geschikt MAb voor RIT zou selectief en in hoge mate moeten ophopen in tumorweefsel. In **hoofdstuk 3** werd de opname van E48 IgG en  $\text{F(ab')}_2$  in tumorweefsel en normale weefsels beschreven. De biodistributie werd bepaald met behulp van bipten uit het operatiepreparaat 2 dagen na injectie en met behulp van 'regions of interest' in planaire radioimmunosintigrammen tot 21 uur na injectie. De gemiddelde opname van  $^{99m}\text{Tc}$ -gelabeld E48 IgG in tumorweefsel bleek  $30,6 \pm 20,1\%$  van de geïnjecteerde dosis/kg te zijn. Dit is vijf maal hoger dan gevonden wordt voor de meeste andere MAbs in andere solide tumoren. In deze studie bleek dat de opname van activiteit in de bijnieren en mond verminderd werd door een verhoging van de MAb dosis van 2 naar 12 tot 52 mg, terwijl de MAb opname in tumorweefsel juist hoger werd. E48  $\text{F(ab')}_2$  had geen voordeel boven E48 IgG. Terwijl de tumor:non-tumor ratios in het algemeen hoger waren voor E48  $\text{F(ab')}_2$  dan voor E48 IgG, was het tegenovergestelde waar voor de orale mucosa inclusief de tong, plaatsen met een relatief hoge opname van activiteit. Bovendien was bij gelijktijdige toediening de opname van  $^{131}\text{I}$ -gelabeld E48 IgG in de tumor hoger dan die van  $^{125}\text{I}$ -gelabeld E48  $\text{F(ab')}_2$ . Ook andere overwegingen zouden kunnen wijzen op een voordeel van het intacte IgG. Het gebruik van IgG in RIT kan een aanvullend voordeel verschaffen, omdat dit molecuul antilichaam-afhankelijke cellulaire cytotoxiciteit

(ADCC) kan mediëren. Bovendien is in het algemeen de retentie van intacte MAbs langer dan die van fragmenten. Daarom lijkt E48 IgG beter geschikt voor RIT dan E48  $\text{F(ab')}_2$ . Een beperking van het gebruik van MAb E48 voor RIT echter is de relatief heterogene E48 antigeen-expressie in ongeveer 30% van de HHPCCs.

Vanwege deze laatste redenen werden ook drie andere MAbs, genaamd 323/A3, SF-25 en K928, geëvalueerd voor 'targeting' van HHPCC. In vergelijking met MAb E48 hebben deze pan-carcinoma MAbs het theoretisch voordeel dat ze niet alleen reactief zijn met HHPCC maar ook met andere tumor-types zoals kleincellige en niet-kleincellige carcinomen van de long (**hoofdstuk 4**). Deze MAbs werden gescreend in een klinische RIS-studie voor hun waarde bij de detectie van lymfekliermetastasen van hoofd/hals-kanker op dezelfde wijze als MAb E48. MAbs 323/A3 en K928 bleken in staat te zijn om hoofd/hals-kanker te detecteren, terwijl SF-25 daartoe echter niet in staat was als gevolg van de snelle verdwijning uit het bloed en de uitgebreide opname in normale weefsels als de lever, de milt, de hersenen en het skelet (waarschijnlijk het beenmerg). Voor MAb 323/A3 werd opname in de schildklier, de lever en het skelet (waarschijnlijk het beenmerg) gevonden en voor MAb K928 in de lever, de milt en het skelet (waarschijnlijk ook het beenmerg). De opname van radioactiviteit in 'normaal' weefsel kon voornamelijk verklaard worden door de aanwezigheid van goed toegankelijke antigeen-moleculen. Deze beperkte tumor-selectiviteit zal zeker de toepassing van deze pan-carcinoma MAbs voor therapeutische doeleinden beperken.

Uit de bovengenoemde studies bleek duidelijk dat een plaveiselcel-specifiek MAb zoals MAb E48 beter geschikt is voor 'targeting' van HHPCC dan pan-carcinoma MAbs. Een beperking van MAb E48 is zijn beperkte reactiviteit met een deel van de HHPCCs. Daarom werd in **hoofdstuk 5** een tweede HHPCC-specifiek MAb, genaamd U36, geëvalueerd in een klinische RIS-studie. Een duidelijk voordeel van MAb U36 in vergelijking met MAb E48 is de homogenere reactiviteit met HHPCCs. MAb U36 accumuleert, vergelijkbaar met MAb E48, selectief en in hoge mate in HHPCC. Er werd slechts een geringe opname in de mond waargenomen.

Om de selectieve HHPCC 'targeting' van E48 IgG en U36 IgG direct te kunnen vergelijken, werden in studies zoals beschreven in **hoofdstuk 6** beide MAbs gelabeld met  $^{125}\text{I}$  en  $^{131}\text{I}$  en vervolgens gelijktijdig geïnjecteerd. Om gegevens over retentie van beide MAbs in tumorweefsel te verkrijgen werden de patiënten 7 dagen na injectie geopereerd. In bipten uit het operatiepreparaat werd een gelijke hoge opname van beide MAbs in tumorweefsel aangetoond. Ook de tumor:non-tumor ratios waren vergelijkbaar. In dit hoofdstuk werd met behulp van immunohistochemie aangetoond dat de distributie van deze MAbs over de tumor heterogeen was wanneer een dosis van 1 tot 12 mg toegediend werd, en dat de distributie homogeen was wanneer een dosis van 52 mg toegediend werd, resulterend in een bezetting van het grootste deel van de antigeen-plaatsen. Analyse van humane anti-muize antilichaam (HAMA) reacties toonde dat muize MAb E48 IgG sterker immunogeen was dan muize MAb U36 IgG. Chimeer (muis/humaan) MAb E48 was effectief in mediëring van ADCC in vitro, terwijl muize MAbs E48 en U36 en chimeer MAb U36 in het geheel niet effectief waren.

In eerdere dierexperimentele studies in ons laboratorium werden complete remissies verkregen bij HHPCC-xenograft-dragende naakte muizen door RIT met  $^{186}\text{Re}$ -gelabeld E48 IgG. Wanneer we de biodistributiegegevens zoals vermeld in hoofdstuk 3, 5 en 6 combineren met gegevens uit deze dierexperimentele studies, kunnen we verwachten



dat MAbs E48 en U36 in staat moeten zijn voldoende straling naar tumorweefsel te kunnen brengen voor het elimineren van 'minimal residual disease' in patiënten.

Zoals geschetst in de discussie van hoofdstuk 6 zal prioriteit worden gegeven aan een adjuvante RIT-studie met  $^{186}\text{Re}$ -gelabeld chimeer MAb U36 IgG in HHPCC-patiënten met een hoog risico op het krijgen van een locoregionaal recidief en metastasen op afstand na standaard locoregionale therapie.

## DANKWOORD

Hierbij wil ik een ieder danken die een bijdrage heeft geleverd aan het tot stand komen van dit proefschrift. Met name de goede samenwerking tussen de afdelingen Keel-, Neus- en Oorheelkunde en de Nucleaire Geneeskunde van het Academisch Ziekenhuis van de Vrije Universiteit was essentieel. Ook vele andere afdelingen zijn bij dit onderzoek betrokken zijn geweest. Zonder te pretenderen volledig te zijn wil ik enkele personen met name bedanken.

Mijn promotor, prof.dr. G.B. Snow, wil ik bedanken voor zijn belangstelling, zijn waardevolle kritiek en begeleiding en met name de discussies over de manuscripten. Bedankt voor de ruimte die u mij geboden heeft om wetenschappelijk onderzoek te verrichten.

Het enthousiasme van mijn copromotoren dr. G.A.M.S. van Dongen en dr. Jan C. Roos is altijd een grote stimulans voor mij geweest. Beste Guus, je was een geweldige begeleider. Je stond altijd klaar om te helpen, ongeacht tijdstip, dag en plaats. Bedankt voor de hieruit ontstane vriendschap. Beste Jan, allereerst bedankt voor de gastvrijheid op je afdeling. Ik heb onze vele discussies als zeer waardevol ervaren. Ook bedankt voor het zetten van de punten (niet alleen op de 'i') en komma's.

Mijn referent prof.dr. E.K.J. Pauwels en de andere leden van de beoordelingscommissie, prof.dr. H.M. Pinedo, prof.dr. P. Kenemans, prof.dr. R.J. Scheper, prof.dr. S.O. Warnaar en dr. R.P. Baum, wil ik bedanken voor het kritisch beoordelen van het manuscript.

Verder wil ik dr. J.J. Quak bedanken voor het begeleiden van het klinische deel van de studies. Jasper, jammer dat er niet meer copromotoren toegestaan waren. Ook bedankt voor de kritiek op de manuscripten.

Drs. H. Leverstein en drs. R.P. Wong Chung wil ik bedanken voor de hulp bij het verrichten van deze klinische onderzoeken. Hein en Dick, bedankt voor het aangeleverde patiëntenmateriaal.

Iedereen van de sectie tumorbiologie van de KNO-heelkunde, bedankt voor de plezierige samenwerking. Corlinda ten Brink, Miriam van Dijk en Marijke van Walsum wil ik bedanken voor de immunohistochemische kleuringen van bipten en het labelingswerk. Dr. R.H. Brakenhoff, Ruud onze discussies waren leerzaam voor mij.

Willem den Hollander en Henri Greuter, bedankt voor het labelen van de antilichamen en de metingen van de activiteitsopname in de bipten.

Dr. J.E. van der Wal, Jacqueline, bedankt voor de histopathologische (her)beoordeling van de bipten en het leren 'uitsnijden' van het neckdissectie-preparaat. Dr. Willem B.F. de Jong en Willem W. de Jong, bedankt voor de hulp hierbij.

Dr. M.W.M. van den Brekel en dr. J.A. Castelijns, Michiel en Jonas, bedankt voor het (her)beoordelen van de CT- en MRI-scans. Ik heb er zelf veel van geleerd.

Dr. Arthur van Lingen, drs. Bram J. Wilhelm, drs. Hilde Töbi en dr. Gerard J. van Kamp, bedankt voor het bewerken en verzamelen van de gegevens uit deze studies.

De medewerkers van de operatiekamers en de operateurs, dank voor de hulp bij het verzamelen van bipten. Verder wil ik alle collegae en medewerkers van de afdelingen Keel-, Neus- en Oorheelkunde, Nucleaire Geneeskunde, Operatiekamers AVB, Radiodiagnostiek bedanken voor de prettige samenwerking en steun. In het bijzonder wil ik nog een ieder bedanken die heeft bijgedragen aan het volgens de tijdschema's van de protocollen laten verlopen van de onderzoeken: Trudi voor het plannen van de operaties,



Ton en Suzette voor het plannen van de onderzoeken op de nucleaire geneeskunde en de administratie van de CT en MRI voor het plannen van deze onderzoeken.

Ook wil ik nog bedanken diegene die hebben bijgedragen aan de vormgeving van de artikelen en dit proefschrift. Bart Dijkstra, bedankt voor het geduld als ik niet wist hoe ik die foto's nou precies wilde hebben. Ook de andere medewerkers van de audiovisuele dienst, bedankt voor het flitsende fotowerk. Mart van Loon, bedankt voor het gereedmaken van de afbeeldingen voor fotografie. Jaap en Hans, bedankt voor het fotografische vakwerk.

En natuurlijk Fred Snel, bedankt voor je enorme hulp tot op het allerlaatste moment. Gelukkig had jij voor elk probleem met de computer wel een oplossing.

## CURRICULUM VITAE

De auteur van dit proefschrift werd geboren op 5 december 1966 te Utrecht. Na het behalen van het eindexamen gymnasium aan het Christelijk Gymnasium Utrecht in 1984, werd begonnen met de studie geneeskunde aan de Rijksuniversiteit Utrecht. Het artsexamen werd behaald op 29 november 1991.

Hierna was hij tot september 1992 werkzaam als arts-assistent algemene heelkunde in het Eemland Ziekenhuis, locatie St. Elisabeth Ziekenhuis te Amersfoort. Vanaf die datum was hij tot juli 1994 als assistent-in-opleiding (AIO) werkzaam op de afdeling Keel-, Neus- en Oorheelkunde van de Vrije Universiteit. In deze periode werd de basis gelegd voor dit proefschrift. Vervolgens was hij enkele maanden werkzaam als assistent-geneeskundige-niet-in-opleiding (AGNIO), waarna hij in november 1994 startte met zijn opleiding tot Keel-, Neus- en Oorarts in het Academisch Ziekenhuis van de Vrije Universiteit (opleider: prof.dr. G.B. Snow).



## PUBLICATIONS

### Publications concerning this thesis

Quak JJ, Bree R de, Brakenhoff R, Gerretsen M, Dongen GAMS van, Roos J, Snow GB. Monoklonale antilichamen in hoofd-hals carcinomen: fundamentele, diagnostische en therapeutische aspecten. (abstract) Ned Tijdschr Geneesk 1993; 137: 1371.

Quak JJ, Gerretsen M, Bree R de, Brakenhoff R, Dongen GAMS van, Snow GB. Perspectives of monoclonal antibodies for detection and treatment of head and neck tumours. Anticancer Res 1993; 13: 2533-40.

Bree R de, Quak JJ, Roos JC, Hollander W den, Dongen GAMS van, Snow GB. Perspectieven voor radioimmunotherapie bij patienten met hoofd/hals kanker. (abstract) Presented on the 6th SEOHS, Nijmegen 1993. Ned Tijdschr Geneesk 1994; 138: 1983-4.

Dongen GAMS van, Brakenhoff RH, Bree R de, Gerretsen M, Quak JJ, Snow GB. Progress in radioimmunotherapy of head and neck cancer. Oncology Reports 1994; 1: 259-64.

Bree R de, Quak JJ, Roos JC, Hollander W den, Snow GB, Dongen GAMS van. The feasibility of radioimmunotherapy with monoclonal antibody E48 in patients with head and neck cancer. (abstract) Presented on the ninth international conference on monoclonal antibody immunoconjugates 1994, San Diego USA. Antibody Immunoconj Radiopharm 1994; 7: 79.

Bree R de, Roos JC, Quak JJ, Hollander W den, Brakenhoff RH, Snow GB, Dongen van GAMS. MAb U36, a novel monoclonal antibody with potential for therapy of head and neck cancer. (abstract) Presented on the 9th annual IRIST meeting 1994, Velden Austria. Nucl Med 1994; 33: 65.

Bree R de, JC Roos, Quak JJ, Brakenhoff RH, Snow GB, Dongen GAMS van. The feasibility of radioimmunotherapy with monoclonal antibody E48 in patients with head and neck cancer. (abstract) Head Neck 1994; 16: 475.

Bree R de, Roos J, Quak JJ, Hollander W den, Brekel MWM van den, Wal JE van der, Snow GB, Dongen GAMS van. Clinical imaging of head and neck cancer with  $^{99m}\text{Tc}$ -labeled monoclonal antibody E48 IgG or F(ab')<sub>2</sub>. J Nucl Med, 1994; 35: 775-83.

Bree R de, Roos J, Quak JJ, Hollander W den, Snow GB, Dongen GAMS van. Clinical evaluation of monoclonal antibodies 323/A3, cSF25, and K928 in patients with head and neck cancer. Nucl Med Commun 1994; 15: 613-27.

Bree R de, Roos J, Quak JJ, Hollander W den, Wilhelm AJ, Snow GB, Dongen GAMS van. Biodistribution of radiolabeled monoclonal antibody E48 IgG and F(ab')<sub>2</sub> in patients with head and neck cancer. Clin Cancer Res 1995; 1: 277-86.

Bree R de, Quak JJ, Roos JC, Hollander W den, Dongen GAMS van, Snow GB. De toepasbaarheid van het monoklonale antilichaam E48 bij de behandeling van patienten met hoofd/hals kanker. Suitability of monoclonal antibody E48 in the treatment of patients with head and neck cancer. (abstract) Presented on 181e KNO-vergadering 1994, Utrecht. Ned Tijdschr Geneesk 1995; 139: 858.

Bree R de, Roos J, Quak JJ, Hollander W den, Snow GB, Dongen GAMS van. Radioimmunosintigraphy and biodistribution of  $^{99m}\text{Tc}$ -labeled monoclonal antibody U36 in patients with head and neck cancer. Clin Cancer Res 1995; 1: June.



---

## Other publications

Tilanus CC, Bree R de, Clemens A. Klinische toepassingsmogelijkheden van oto-acoustische emissies.(abstract) Ned Tijdschr Geneesk 1990; 134: 2416. Clinical applications of oto-acoustic emissions.(abstract) Clin Otolaryngol 1991; 16: 107.

Bree R de, Wit JM, Gils JF van, Tjabbes T, Brande JL van den. Succesful bromocriptine treatment of a large prolactinoma presenting in adolescence. J Pediatr Endocrinol 1991; 4: 139-43.

Bree R de, Vloten WA van. Tungiasis. Ned Tijdschr Geneesk 1992; 136: 1359-62.

Bouvy LA, Bree R de. Primair navelcarcinoom van de navel, na ogenschijnlijk onschuldige en jarenlange navelafscheiding. Ned Tijdschr Geneesk 1993; 137: 1358-60.